University of Nottingham
UK | CHINA | MALAYSIA

The Role of Airway Epithelial Derived Extracellular Vesicles in Allergic Sensitisation

Thesis submitted to the University of Nottingham for the degree of Doctor of Philosophy

September 2025

William Browne, BSc, MSc

14340382

Supervisors: Professor Lucy Fairclough, Dr David Onion, Dr Victoria James and Dr Stella Cochrane

School of Life Science

University of Nottingham

List of Content

Acknowledgements

Firstly, I would like to thank Professor Lucy Fairclough, to whom I am immeasurably grateful for both the opportunity to undertake a PhD in her laboratory as well as for her support, guidance and unwavering positivity, which has had a profound impact on both my professional and personal development.

Additionally, I am extremely thankful to Dr Stella Cochrane, Dr David Onion and Dr Victoria James as my co-supervisor and these thanks are further extended to Professor Patrick Tighe for their invaluable support and advice over the course of my PhD journey. My time in the Fairclough lab has been made memorable by all the kind and helpful students and staff that have made this tough process that bit easier. I particularly would like to thank our technical staff Tyler and Sophie, without whom the lab could not function as well as it does.

I would also like to thank Unilever and the BBSRC for providing the funding of this research, ultimately allowing me to undertake this PhD.

It has been a joy to undertake my PhD with the other Life Science friends I have made along the way; Alec and Jorge as well as all the other lovely individuals who work in and occupy the offices of B99 and B109.

Finally, I could not have completed this PhD journey without the unwavering support of my family and friends. I am extremely grateful to Oli for his friendship and support as well as his extensive and valuable insight into how “mitochondria are the powerhouse of the cell”. There is no adequate way to thank both my parents, Jane and Jerry as well as my sister Katie who have always been there to support and push me to achieve all my goals, I truly would not be where I am today without them. To my partner Rute thank you for your unshakeable tolerance, support, love and understanding, I couldn’t have done this without you.

Publications

W. Browne, G. Hopkins, S. Cochrane, V. James, D. Onion and L.C. Fairclough (2025). The Role of Epithelial-Derived Extracellular Vesicles in Allergic Sensitisation: A Systematic Review. *International Journal of Molecular Sciences* (https://dx.doi.org/10.3390/ijms26125791)

D. Tucis, G. Hopkins, **W. Browne**, V. James, D. Onion and L.C. Fairclough (2024). The Role of Extracellular Vesicles in Allergic Sensitization: A Systematic Review. *International Journal of Molecular Sciences* (https://dx.doi.org/10.3390/ijms25084492)

G. Hopkins†, **W. Browne**†, D. Tucis†, S. Cochrane, V. James, D. Onion and L.C. Fairclough. Evaluation of Conventional, Imaging and Nanoscale Flow Cytometry Technologies for Extracellular Vesicle Analysis. (In Preparation)

Abstract

The prevalence of allergies has drastically increased over the past 50 years, with an estimated 30% of adults sensitised to an environmental allergen. While this represents a growing public health concern, the mechanisms which underpin allergic sensitisation are poorly understood. Recently, it has been suggested that the airway epithelium can influence allergic outcome through the secretion of extracellular vesicle (EVs). These are small lipid bound vesicles, capable of extracellular communication through the simultaneous delivery of different categories of biomolecules to a recipient cell. While EVs provide an exciting new avenue for better understanding the role of the airway epithelium in allergic sensitisation, the existing research is limited and primarily in patient samples and 2D cultures. Consequently, this research aimed to develop and optimise a 3D culture model and mechanism for its stimulation with the indoor allergens Der p 1 and Can f 1, as well as the novel profiling of EV responses with imaging flow cytometry.

A systematic review of the literature regarding the role of epithelial-derived EVs in allergic sensitisation was conducted, showing that epithelial-derived EVs can both promote tolerance or allergic sensitisation through the delivery of mRNAs that promote Th2 polarisation and cytokine secretion or promote tolerance through the induction of Tregs (miR34a, miR92b, miR146a-5p and miR210). Additionally, this review highlighted a significant gap in the literature, with only one study using a 3D culture model.

Initially, different transformed airway epithelial cell lines were assessed in 2D to identify a suitable candidate for a 3D culture model. Calu-3 cells were selected due to their high expression of key epithelial markers which will be used for the downstream profiling of EVs, as well as their ability to differentiate and form tight junctions when cultured at air liquid interface (ALI). Stimulation of ALI cultures was optimised by assessing submerged exposure, the addition of stimulant to the basal chamber and nebulised exposure. In parallel, a high throughput method for the analysis of EVs using imaging flow cytometry was developed and optimised, allowing for quantification and profiling of markers on EVs. Ultimately, Calu-3 were

cultured at ALI and exposed to either nebulised proteolytically active Der p 1, inactive Der p 1 or Can f 1, for 24 and 48 hours. The effects of exposure on epithelial tissues were assessed using confocal microscopy and tight junction staining, as well as scanning electron microscopy. Additionally, alarmin and inflammatory cytokine responses were profiled using ELISA and EV responses were profiled using imaging flow cytometry.

Nebulised exposure of active Der p 1 was shown to disrupt epithelial barrier function by reducing tight junction expression. Furthermore, Der p 1 and Can f 1 exposure was shown to induce an increase in basal EV secretion. Additionally, Der p 1 exposure was observed to significantly alter the distribution of tetraspanins CD9, CD63 and CD81, as well as upregulate the expression of the epithelial marker E-Cadherin on EVs. Finally, transcriptomic analysis revealed the upregulation of previously identified miRNA, miR92b, as well as miR101-3p, mir103-3p, miR107, miR148a and miR224a-5p, which could play an important role in early development of Th2 responses.

Taken together, the data presented here shows that allergen exposure of epithelial cells can modulate EV responses, increasing secretion of EVs and altering tetraspanin distribution, as well as upregulating miRNA cargos which can promote or prevent sensitisation.

Abbreviations

ABC	Antibody Binding Capacity
AD	Atopic Dermatitis
AJC	Apical Junction Complex
ALI	Air Liquid Interface
AR	Allergic Rhinitis
bae-EVs	Bronchial/Alveolar Epithelial derived Extracellular Vesicles
Calcein-AM	Calcein Acetoxymethyl Ester
Can f	*Canis familiaris*
CD	Cluster of Differentiation
DAMPs	Damage Associated Molecular Patterns
DC	Dendritic Cells
Der p	*Dermatophagoidies pteronyssinus*
EE	Early Endosome
ELISA	Enzyme-Linked Immunosorbent Assay
EpCAM	Epithelial Cell Adhesion Molecule
ESCRT	Endosomal Sorting Complex Required for Transport
EV	Extracellular Vesicle
FBS	Foetal Bovine Serum
FcεR1	High Affinity Fc Receptor
FcεR2	Low Affinity Fc Receptor
FSC	Forward Scatter
FTC-Casein	Fluorescein Thiocarbamoyl-Casein
GWAS	Genome-Wide Association Study
HBECs	Human Bronchial Epithelial Cells
HDM	House Dust Mite
HLA	Human Leukocyte Antigen
HS	Human Serum
ie-EVs	Intestinal Epithelial derived Extracellular Vesicles
IgE	Immunoglobulin E
IgG	Immunoglobulin G
IgM	Immunoglobulin M
IL	Interleukin

IL-4R	**Interleukin 4 Receptor**
ILC2	Type 2 Innate Lymphoid Cells
ILV	Intraluminal Vesicles
ISEV	International Society for Extracellular Vesicles
ISX	ImageStream X MKII
JAK	Janus Kinases
LDH	Lactate Dehydrogenase
LE	Late Endosomes
LoD	Limit of Detection
LPS	Lipopolysaccharide
LPS-BP	Lipopolysaccharide Binding Protein
MC	Mast Cells
MEM	Minimal Essential Medium
MHC	Major Histocompatibility Complex
miRNA	microRNA
MISEV	Minimal Information for Studies of EVS
MSCs	Mesenchymal Stromal Cells
MVB	Multivesicular Body
ne-EVs	Nasal Epithelial derived Extracellular Vesicles
NFκB	Nuclear Factor κ B
NIST	National Institute of Standards and Technology
NTA	Nano particle Tracking Analysis
PAMPs	Pathogen Associated Molecular Patterns
PARs	Protease Activated Receptors
PBS	Phosphate Buffer sailine
PI	Propidium Iodine
Poly(I:C)	polyinosinic-polycytidylic
PRR	Pattern Recognition Receptor
RPM	Replicates Per Million
SCC	Side Scatter

SDS	**Sodium Dodecyl Sulphate**
SEC	Size Exclusion Chromatography
SEM	Scanning Electron Microscopy
TEM	Transmission Electron Microscopy
TGF-β	Transforming Growth Factor β
Th1	T Cell Subset 1
Th2	T Cell Subset 2
TJ	Tight Junction
TLRs	Toll Like Receptors
TNF-α	Tumour Necrosis Factor α
Tregs	T Regulatory Cells
Tspan8	Tetraspanin 8
TSLP	Thymic Stromal Lymphopoietin
VSSC	Violet Side Scatter
ZO-1	Zonula Occludin 1

Chapter 1: General Introduction

1.1.Allergy

1.1.1. What is Allergy?

"Allergy" from the Greek "*allos*" meaning other or different and "*ergia*" meaning energy or action, was first described in 1906 by Austrian paediatrician Clemens von Pirquet (Pirquet, 1906, Igea, 2013). He first used "Allergy" to describe the accelerated responses observed in specific individuals upon the administration of secondary doses of smallpox vaccines (Shulman, 2016). Now, allergy, also referred to as hypersensitivity, is defined as an exaggerated immune response to an inert or innocuous substance.

Hypersensitivity reactions can be split into four types, first defined in 1963 by Coombs and Gell. These categories define hypersensitivity reactions by their varying pathophysiology, considering both the type of immune response generated and the processes by which cell/tissue damage is caused (Coombs and Gell, 1968, Kaufmann, 2019). Type 1 hypersensitivity, sometimes referred to as immediate or Immunoglobulin E (IgE)-mediated hypersensitivity (Type I), are characterised by the binding of allergen-specific IgE to immune effector cells, such as mast cells and basophils, via the high-affinity FcεR1 receptor. Type 1 hypersensitivity responses typically encompass allergies triggered by aeroallergens, such as allergic asthma and hay fever, food-based allergies and also some topical allergies, such as urticaria. Type II hypersensitivity, also known as cytotoxic or IgG/IgM-mediated hypersensitivity, classifies allergies such as haemolytic anaemia. Type III hypersensitivity, sometimes called immune complex-mediated hypersensitivity, is characterised by the formation of antigen-antibody complexes in blood, which leads to disorders such as systemic lupus erythematosus and serum sickness. Finally, type IV hypersensitivity, or delayed or T cell-mediated hypersensitivity, is characterised as T cell mediated immune responses that typically develop around 48 – 72 hours post exposure (Uzzaman and Cho, 2012, Momtazmanesh and Rezaei, 2022).

1.1.2. Epidemiology of IgE-mediated Allergy

Allergic diseases are a significant global public health concern, with the incidence of allergies seeing a drastic increase over the past 50 years. This epidemic, in turn, has seen a significant rise in the prevalence of type 1 hypersensitivity disorders, which has occurred in two major waves. The first wave was observed around 50 years ago and saw a surge in the prevalence of sensitisation to aeroallergens and the development of asthma and allergic rhinitis (AR) in industrialised countries. A second wave, starting around 20 years ago, has now seen an increase in the prevalence of food allergies, mainly in western countries, particularly those with high incidence of asthma and other aeroallergen sensitisations (Wong, 2024, Pawankar, 2014, Warren *et al.,* 2020). It is estimated that around 30% of adults are sensitised to some form of environmental allergen, such as dust, pollen or food (Pawankar, 2014). Recent studies have also shown that around 40% of primary school-aged children (ages: 6-10) suffer from a type 1 hypersensitivity disorder, with a third of these children having multiple allergic diagnoses (Peters *et al.,* 2024, Warren *et al.,* 2020). The ever-increasing rate at which type 1 hypersensitivity disorders appear places a significant physiological, clinical and financial burden on both patients and healthcare systems. Consequently, understanding of the underlying mechanisms that facilitate allergic sensitisation is crucial and will allow for better therapeutic intervention and control of these diseases.

1.1.3. Aetiology of IgE-mediated Allergy

The underlying mechanisms that give rise to type 1 hypersensitivity disorders and the sensitisation of an individual are poorly understood. However, factors such as the environment, genetics, route of allergen exposure and the microbiome are known to contribute to and influence allergic outcome and the development of an allergy. It is likely that changes to these variables, as society has become more industrialised and westernised, have led to the observed increase in allergic disease.

The influence of genetics on the development IgE-mediated allergies was first established in 1916 in a study by Cooke and Veer. The study showed that there was a strong heritability to allergies, with around 50% of allergic

individuals having a familial history of allergy, as opposed to 15% in non-allergic individuals (Cooke and Veer, 1916). Subsequently, a study looking at the inheritance of peanut allergies in pairs of twins showed a concordance rate of 64.3% in monozygotic twins as opposed to 6.5% in dizygotic twins and estimated that the heritability of peanut allergy was up to 81.6% (Sicherer *et al.,* 2000). The understanding of genetic influence on the development of allergies was then further enhanced with the use of Genome-Wide Association Studies (GWAS). These studies allow for a hypothesis-free method to search full genomes for common variants between populations of healthy and allergic individuals (Portelli *et al.,* 2015). GWAS reproducibility, while poor, has led to the identification of a number of genes which influence key processes, such as immune and epithelial barrier function. Key genes identified are involved in T helper 2 (Th2) responses and proinflammatory cytokines (STAT6, IL10, IL4, IL13, TSLP, TNFA and RANTES), IgE receptor affinity (FCER1A and B), innate pattern recognition (CD14, TLR-7 and -9), genes in MHC Class II clusters (HLAG, HLA-DRB1 and HLA-DQB1) and epidermal differentiation and adhesion (PCDH1, FLG and SPINK5) (Arnau-Soler *et al.,* 2025, Gilles *et al.,* 2018, Portelli *et al.,* 2015, Ober and Yao, 2011). Identification of these genes and their dysregulation in the epithelium highlighted the importance of epithelial barrier function and how its dysfunction can facilitate allergic sensitisation.

The environment and its symbiosis with genetically predisposed individuals also play an important role in the development of allergies. Changes to our environment over the past century, associated with the industrialisation and westernisation of countries, such as contact with microbes, air pollution, airborne allergens, food allergens and pathogens, are believed to be a significant contributing factor (Gilles *et al.,* 2018, Rutkowski *et al.,* 2014, Douwes and Pearce, 2002). One hypothesis that reflects this thinking is the “hygiene hypothesis”. Initially proposed by Strachan in 1989, the hygiene hypothesis aimed to explain the observed inverse correlation between family size and the prevalence of AR and hay fever (Strachan, 1989). Here it was suggested that the acquisition of early childhood infections from older siblings could provide protection against the development of allergic

diseases. The counter-regulatory interplay between Th1 and Th2 cells provided the initial explanation for this. The importance of this interplay was emphasised when studies showed that initial atopic sensitisation could occur *in utero* due to the Th2-polarised immune system of a foetus. In healthy infants, this Th2-polarised environment is attenuated over the first year of their lives, through the stimulation of their Th1 response by intracellular microbes and pathogens. However, in infants that go on to develop IgE-mediated disease, this does not occur, and their Th2 response is further promoted (Prescott *et al.,* 1999). The improvement of public health practices resulting from the industrial revolution, such as the decontamination of water, pasteurisation of milk, sterilisation of food products, vaccinations and antibiotics, has all limited infectious disease burden and spread. This reduced burden of disease has drastically improved quality of life but has also resulted in less stimulation of the Th1 responses during early development, weakening Th1 drive in individuals and resulting in Th2 overactivity. In countries where these public health measures are not commonplace, allergic prevalence is markedly lower (Pfefferle *et al.,* 2021, Okada *et al.,* 2010, Rautava *et al.,* 2004). In addition to decreased microbial burden, westernized lifestyles have seen a rise in obesity, diets rich in processed food, reduced exercise and migration to more urbanised environments. These changes have had a significant impact on the predisposition of individuals to allergies, creating an environment that has promoted reduced microbiome diversity and dysbiosis on key protective epithelial barriers. Epidemiologic studies identified that growing up in rural environments in contact with farm animals ("farming effect"), diets rich in fibre with high diversity and contact with siblings or peers were essential for the formation of diverse microbiota on skin, lung and intestinal epithelium (Ober *et al.,* 2017, Roduit *et al.,* 2014). This early interaction of commensal and environmental microbiota is instrumental in determining the threshold for epithelial pattern recognition receptors (PRRs) and downstream signalling pathways. This, in turn, can influence the establishment of immune homeostasis and peripheral tolerance during early childhood and lead to the development of type 1 hypersensitivity later in life (Gilles *et al.,* 2018).

Pollution is another factor contributing to the growing prevalence of allergic disease. Rapid economic and industrial growth, as well as the surging volume and density of automotive transport in urban areas, have facilitated a significant increase in anthropogenic pollutants such as ozone, nitrogen dioxide (NO_2), and fossil fuel CO_2-based emissions (Kim *et al.,* 2025b). Industrialised countries, such as China, are seeing increases in the incidence of respiratory allergies, such as allergic asthma and AR, with early exposure to these pollutants contributing significantly (Wang *et al.,* 2025a, Li *et al.,* 2024b). Anthropogenic pollutants have been shown to influence allergic sensitisation through two key mechanisms. Firstly, they can influence allergic sensitisation directly by promoting allergic inflammation, triggering inflammasome pathways and enhancing allergic sensitisation when exposed in parallel with allergens (Martin *et al.,* 2013, Jenerowicz *et al.,* 2012, Miyabara *et al.,* 1998). In addition, they are able to influence allergic sensitisation as 'biogenic modifiers' (Gilles *et al.,* 2018). Flora and fauna situated in urban areas has been shown to produce more allergenic pollen due to metabolic stress and changes to its microbiome. One study found that birch trees found in ozone-rich environments were shown to upregulate the allergen Bet v 1. Furthermore, the microbial variation on birch pollen was also found to be reduced in NO_2-rich areas (Obersteiner *et al.,* 2016). The microbiome on pollen has been shown to be immunogenic, triggering T-cell responses as a result of dendritic cell (DC) activation (Heydenreich *et al.,* 2012). Changes in the expression of key allergens, coupled with changes to their microbiome as a result of increases in anthropogenic pollution, ultimately increase allergenic potency, promoting sensitisation.

Lastly, the route of allergen exposure also plays an important role in the development of allergies. Initially, it was suggested that the exposure of oral allergens via the gut was a key mechanism in allergic sensitisation. However, evidence now indicates that oral allergen exposure via the skin can result in allergic sensitisation, while oral allergen exposure via the gut induces peripheral tolerance. This observation has also been noted for aeroallergens, such as house dust mite (HDM) and pollen, where exposure can occur orally due to the tendency for young children to put toys and their hands in their

mouths, as well as play on the floor (Custovic, 2015, Calabrese *et al.,* 1989). This early oral exposure to allergens, leading to tolerance and exposure through damaged epithelial barriers, is referred to as the "dual exposure hypothesis" (Kulis *et al.,* 2021). Impaired skin barrier function resulting from environmental damage has been shown to facilitate allergen penetration and presentation to underlying antigen presenting cells (APCs), promoting allergic sensitisation. Notably, loss or dysregulation of filaggrin (FLG gene identified in GWAS studies) has been shown to significantly increase sensitisation in early life (Brough *et al.,* 2014). Furthermore, recent studies have shown that exposure to food allergens via the airway can also facilitate allergic sensitisation. One study showed that dust not only acts as a vector for the inhalation of intact food allergens, but also as a key adjuvant promoting sensitisation (Smeekens *et al.,* 2019), further emphasising the importance of allergen exposure route on sensitisation.

1.1.4. Mechanisms of IgE-Mediated Allergy

1.1.4.1. Allergic Sensitisation

The mechanism of IgE-mediated allergy is comprised of two phases, sensitisation and elicitation. Sensitisation describes the exposure of an allergen which triggers the induction of allergen-specific IgE. This exposure is therefore referred to as a sensitising dose/exposure. Subsequent exposures to the same allergen will trigger degranulation of the primed mast cells and is referred to as allergic elicitation. These exposures are therefore referred to as a shocking dose/exposure. Figure 1.1 depicts the two phases which underly IgE-mediated allergies.

An immune response to an allergen that ultimately results in IgE synthesis is comprised of two key groups of signals. The initial group of signals stimulate the differentiation of naïve $CD4^+$ T cells that have been newly activated by dendritic cells (DCs) of the sub-epithelium. Epithelial barriers such as the skin, gut and airway act as the first line of defence against allergens. While initially thought of as an inert physical barrier, it has been shown that the epithelium plays a key role in immune regulation and allergic outcome. The expression of a diverse array of PRRs on the epithelium

facilitates the recognition of allergens, activating and recruiting APCs, such as DCs, through the secretion of cytokines (Figure 1.1A) (Jakwerth *et al.,* 2022). These sub-epithelial DCs are initially activated by IL-13, secreted by Type 2 innate lymphoid cells (ILC2), and TSLP, secreted by epithelial cells. IL-13 and TSLP are cytokines that suppress the development of Th1 and Th17-inducing DCs, preferentially generating DCs that facilitate the development of Th2 cells. Once these pro-Th2 DCs are activated, they typically take up and process antigens from invading parasitic infections, or in the case of allergies, allergens, and present them on their surface, through the use of the Major Histocompatibility Complex (MHC) Class II (Figure 1.1B). The DCs then migrate to regional lymph nodes, where they encounter and stimulate naïve $CD4^+$ T cells through the interaction of loaded MHC class II complexes and the T cell receptors (TCRs) on the surface of the naïve $CD4^+$ cells (Figure 1.1C).

This stimulation is enhanced through the action of co-stimulatory molecules expressed on DCs, such as B7.1 and B7.2, which interact with the CD28 receptor on naïve $CD4^+$ T cells. This co-stimulatory action induces the allergen-specific T cell to enter the G1 phase of the cell cycle. In addition, it facilitates the induction and secretion of IL-2 and its receptor (IL-2R), which function to enhance the proliferation and survivability of the allergen-specific naïve $CD4^+$ T cells (Murphy *et al.,* 2022). While this stimulation is essential for the activation of antigen-specific naïve $CD4^+$ T cells, it is not enough to push them towards a Th2 phenotype. The final signal required in this initial group of signals is the cytokine IL-4 (Figure 1.1D). IL-4 binds to its receptor (IL-4R) on the surface of activated naïve $CD4^+$ T cells, resulting in the phosphorylation of conserved tyrosine residues on the receptor by associated Janus Kinases (Jak). Cytoplasmic STAT6 then binds to the phosphorylated receptor through an SH2 domain, allowing for the phosphorylation of STAT6's conserved tyrosine- 641 (Krishnamurthy and Kaplan, 2016). Once phosphorylated STAT6 forms heterodimers that translocate to the nucleus and regulate the expression of the transcription factor GATA3. GATA3 is essential for Th2 cell differentiation, stabilising their differentiation by promoting the secretion of more IL-4 and IL-13 and driving the activated naïve CD4 T cells

towards a Th2 phenotype (Figure 1.1D) (Murphy *et al.,* 2022, Krishnamurthy and Kaplan, 2016). Th2 cells are essential in the coordination and generation of a type 2 immune response. Type 2 immune responses are normally induced against infiltrating parasites and helminths, but also allergens.

The second group of signals come from the newly differentiated Th2 cells. This second group consist of the cytokines IL-4, IL-5, IL-9 and IL-13 secreted by Th2 cells, as well as the interaction of CD40L on T cells with its receptor CD40 on B cells (Figure 1.1E). This combination of signals ultimately simulates B cells to undergo heavy chain class switching, changing the secreted antibody from IgM to IgE (Figure 1.1F). The newly secreted IgE then binds to the FcεRI receptors on effector cells, such as mast cells and eosinophils, completing sensitisation (Figure 1.1G&H). As previously stated, IgE production requires class switching recombination. The antibody class is defined by its constant region. Class switching describes the substitution of constant regions of an antibody in the immunoglobulin heavy chain locus. This alters the 'stem' of the antibody, while maintaining the antigen-specific variable, or VDJ, region of the antibody, conferring a new effector function to the antibody. The most common heavy class chain switching seen in type 1 hypersensitivity is the substitution of Cμ (IgM's constant region) with Cε (IgE's constant region) (Murphy *et al.,* 2022, Gould and Sutton, 2008). This recombination is induced by the cytokines IL-4 and IL-13, which bind with Jak1 and Jak3, resulting in the phosphorylation and activation of STAT6, a key transcription factor required for IgE class switching (Krishnamurthy and Kaplan, 2016). IL-4 and IL-13 secretion, coupled with the costimulatory action of CD40/40L, also results in the expression and secretion of soluble CD23. Soluble CD23 forms trimers that interact with the receptor CD21, resulting in the upregulation of IgE synthesis, further facilitating the priming of immune cells against an antigen (Gould and Sutton, 2008). The allergen-specific IgE then binds, via the high-affinity receptor for IgE (FcεRI), to the surface of mast cells.

1.1.4.2.Allergic Elicitation

Allergic elicitation is initiated on subsequent exposure to the same allergen, when allergens bind to and cross-link allergen-specific IgE on the surface of mast cells (Figure 1.1I). The activation of these effector cells results in the promotion of an inflammatory response through the secretion of preformed granules containing key immunomodulatory chemicals, such as histamine (Figure 1.1J). It is the secretion of these chemical mediators that generates the unpleasant allergic pathology (Figure 1.1K). Allergic symptoms and severity of response have been shown to be dependent on route of exposure, as well as dose (Bax *et al.,* 2012). Symptoms can range from irritation of the eye and rhinitis to circulatory collapse as a result of anaphylaxis. Responses to allergens can also be divided into two phases: an immediate response, denoted by the degranulation of mast cells, and a late phase response in which a more sustained inflammation is induced through the recruitment of effector leukocytes such as Th2 cells, eosinophils, and basophils.

Mast cells are divided into two phenotypically distinct subclasses, namely MCt and MCtc. The difference in these mast cells is primarily observed when looking at the 'natural' proteases they release when degranulating. MCt cells only release tryptase, while MCtc cells release both tryptase and chymase. This variation in 'natural' proteases affects the key function of each mast cell subclass, with MCt cells playing a more immune system-focused role, while MCtcs have a more tissue remodelling and angiogenic function (Zhao *et al.,* 2022, Church and Levischaffer, 1997). It should be noted, however, despite their primary functions, both subclasses still express the FcεRI receptor and play a role in IgE-mediated responses to allergens and pathogens. In addition, mast cells located in different tissues also exhibit functionally distinct heterogeneity. A good example of this is seen in mast cells found in the skin. These mast cells express CD88, which is a receptor for anaphylatoxin C5a, allowing these mast cells to also be activated via the complement system (Oskeritzian *et al.,* 2005).

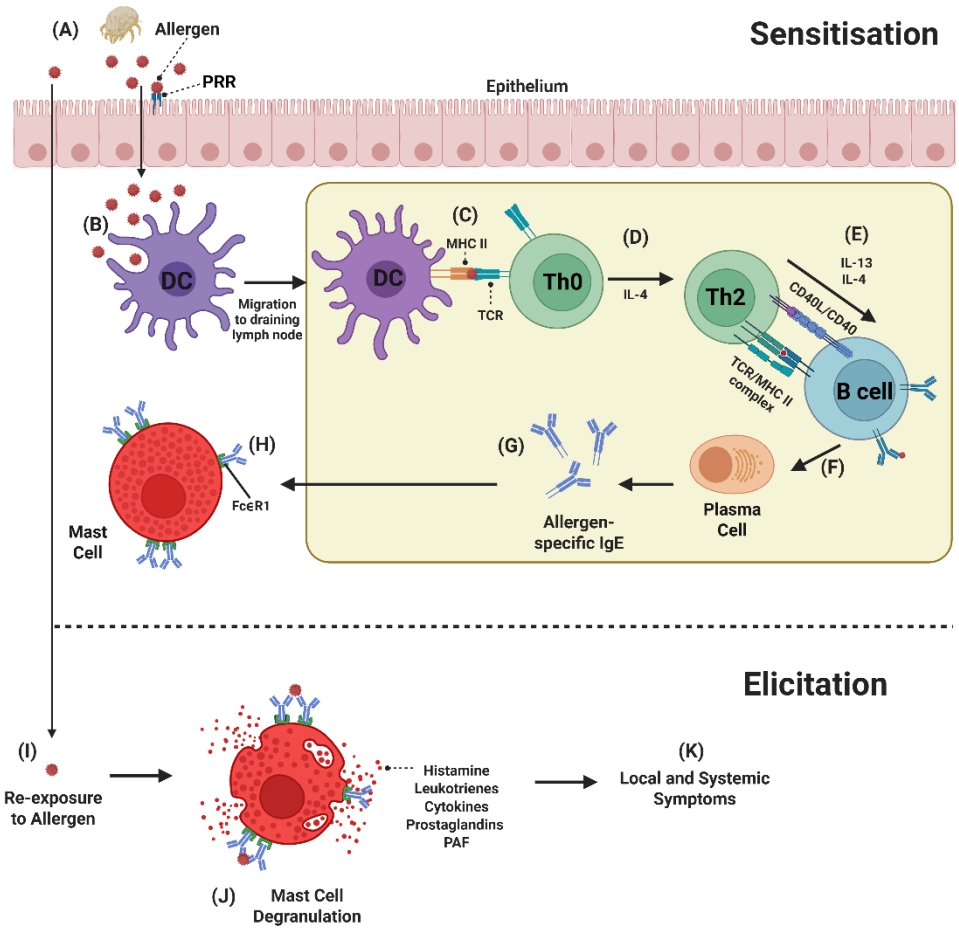

Figure 1.1. The two mechanisms of IgE mediated allergy, Sensitization and Elicitation. Sensitisation: **A)** Allergens interact with PRRs and penetrate the epithelium. **B)** ILC2 induced Pro-Th2 DCs are recruited to the site of allergen infiltration where they internalise and process allergens. **C)** Pro-Th2 DCs migrate to the draining lymph nodes and presents processed allergen via MHC class II to naïve CD4+ Cells. **D)** allergen presentation stimulates IL-4 secretion and differentiation of Th0 to Th2 cells. **E)** Activated Th2 cells also recognise B cell MHC class II allergen complexes promoting IL-4 and IL-13 secretion. **F)** B cell Th2 interactions also promotes class switching form IgM to IgE. **G)** Plasma cells secrete allergen specific IgE. **H)** Allergen specific IgE binds to effector cells such as mast cells via the high affinity receptor FCεR1 "priming" them to allergen. **Elicitation: I)** Subsequent allergen penetration of the epithelium. **J)** Crosslinking of FCεR1 bound allergen specific IgE on mast cells triggers degranulation and the release of inflammatory mediators. **K)** Secretion of inflammatory mediators induce the traditional allergic phenotype.

Mast cells secrete a vast array of chemical mediators, and due to their ubiquitous dispersal throughout tissue, these mediators can exert their effect on a large variety of cell types. Accordingly, mast cells are believed to play a role in a multitude of diseases ranging from allergy to the promotion of tumour development (Lichterman and Reddy, 2021). Mast cell mediators can be broken down into two groups, preformed mediators, like histamine, which exist in granules prior to activation, and synthesised mediators, such as chemokines, cytokines, and eicosanoids (prostaglandins, leukotrienes, lipid mediators and thromboxanes), whose production isn't triggered until activation (Murphy *et al.,* 2022, Lundequist and Pejler, 2011).

Preformed granules consist of a crystalline complex of preformed inflammatory mediators bound to proteoglycans. Upon activation, the granules lose their crystalline structure as it solubilises. Preformed mediators, such as histamine, proteases, and proteoglycans, are subsequently released into the extracellular environment via exocytosis.

Histamine is a key mediator released by mast cells. It plays a central role in the development of allergic pathology, particularly during the immediate phase of an allergic response. Histamine exerts its effects through its interaction with one of four G protein-coupled receptors. The key interaction is between histamine and its receptor H1. This receptor is found on blood vessels, and the interaction of histamine with H1 triggers increased local blood flow and vessel permeability, leading to localised inflammation and oedema. Histamine is also responsible for other key allergic symptoms, such as bronchial and intestinal smooth muscle contraction and increased mucus secretion, as well as itching and sneezing, as it can also activate neural receptors (Simons and Simons, 2011).

The major mast cell protease common to all mast cell subtypes is tryptase. Upon its release into the extracellular environment, it becomes enzymatically active due to the shift towards a neutral pH. Tryptase performs a variety of functions, the most notable are the cleavage of broncho- and vaso-dilatory peptides (contributing to bronchial hyperresponsiveness in conditions such as asthma), the sensitisation of bronchial smooth muscle to contractile

agents, the stimulation of fibroblasts and epithelial cells to proliferate and the triggering of chemo-attractant synthesis (such as IL-8), which recruit granulocytic cells, such as neutrophils and eosinophils (Ramu *et al.,* 2021, Church and Levischaffer, 1997). Chymase is present in only MCtc mast cells and is found in the same secretory granules as tryptase, where it is found in its fully activated form. While MCtcs aren't believed to play a central role in allergy, their secreted chymase has been shown to have a downregulatory or protective function in allergic inflammation, degrading pathogenic cytokines. This protective function was further observed in clinical studies, where chymase-positive MCtcs preserved lung function in severe asthma. Further to this, there is data that also demonstrates that Th2 asthma is associated with a chymase low phenotype (Zhao *et al.,* 2022, Waern *et al.,* 2013).

Mediators that are synthesised post-activation contribute to both acute and chronic inflammation. Lipid mediators notably have both immediate and persistent effects, causing the contraction of smooth muscle, increases in vascular permeability and mucus secretion, and facilitation of the recruitment and activation of granulocytes, which further contribute to allergic pathogenesis. Eicosanoids are synthesised through the cleavage of membrane-derived arachidonic acid via phospholipase A2, which is activated as a result of mast cell activation and degranulation. The resulting substrate is then either oxidised through cyclooxygenase (COX) to form prostaglandin D2, or 5-1ipoxygenase to form leukotriene C4. Prostaglandin D2 is the main prostaglandin synthesised by mast cells and further facilitates the recruitment of Th2 cells and granulocytes, such as eosinophils, to the site of activation through interaction with their PTGDR receptor. Prostaglandin D2 has been shown to play a critical role in allergic pathogenesis, particularly asthma, with PTGDR polymorphisms being strongly linked with disease risk (Schauberger *et al.,* 2016). Two distinct COX enzymes, COX1 and 2, have also been identified, and both are responsible for mediating different parts of the allergic response. COX1, which is constitutively expressed in mast cells, is responsible for the initial generation of prostaglandin D2 upon activation, while COX2 is synthesised post activation and is responsible for the protracted synthesis of

prostanoids, such as prostaglandin D2, later in the allergic response (Morita, 2002).

Leukotrienes, especially C4, D4 and E4, help to sustain the inflammatory responses in tissues. When mast cells are activated, 5-1ipoxygenase translocates from the cytoplasm to the nuclear envelope, where it binds to 5-1ipoxygenase-activating protein. The locus of this oxidising agent and its activating peptide can be found on the long arm of chromosome 5q. This chromosome also encodes the genes for the key cytokines in type 2 immune responses, such as IL-3, IL-4, IL-5, IL-13, as well as granulocyte-macrophage colony-stimulating factor, whose upregulation is highly associated with allergic disease pathogenesis. 5-1ipoxygenase is inducible in a wide range of inflammatory cells situated in the lung, particularly granulocytes, such as mast cells and eosinophils, and the presence of the activated oxidising enzyme in urine is used as an indicator of active allergic disease. Leukotrienes are highly potent mediators controlling contraction of the bronchial and vascular smooth muscle as well as enhancing permeability of postcapillary venules. In addition to this, they upregulate bronchial mucus secretion and eosinophil chemoattraction. TNF-α is another unique mediator secreted by mast cells. It exists in both preformed granules and is also synthesised following mast cell activation. TNF-α activates endothelial cells, stimulating the upregulation in expression of adhesion molecules, such as platelet activating factor (PAF). This upregulation in PAF promotes the incursion of pro-inflammatory leukocytes and lymphocytes into tissue through the upregulation of CD18 on target cells, improving rolling and cell adhesion (Bebo *et al.,* 1996). This further emphasises the importance of these mast cell mediators and their pivotal role in elicitation and the pathogenesis of allergies, particularly asthma.

1.1.4.3.Phases of Allergic Elicitation Response

The allergic elicitation response can be subdivided into two phases: the immediate response and the late phase response. Upon continuous allergen exposure, the numbers of sensitised (IgE-coated) mast cells increase. Post activation of these sensitised mast cells, degranulation takes place, releasing a vast array of inflammatory mediators into the tissue at the sight of activation.

As previously discussed, these mediators are released in two waves, the first wave being the mediators that exist in a preformed active state within the granules of mast cells (histamine, tryptase and chymase), resulting in a rapid increase in vascular permeability. During this phase of an allergic response there is oedema and reddening of the skin. This can be easily observed in the skin, which presents with lesions called a 'wheel and flare reaction' (Figure 1.2). In the airways, smooth muscle constricts, reducing air flow to the lungs, resulting in shortness of breath, wheezing and tightness in the chest. The second wave is the release of synthesised *de novo* mediators (prostaglandin D2 and leukotrienes C4, D4 and E4).

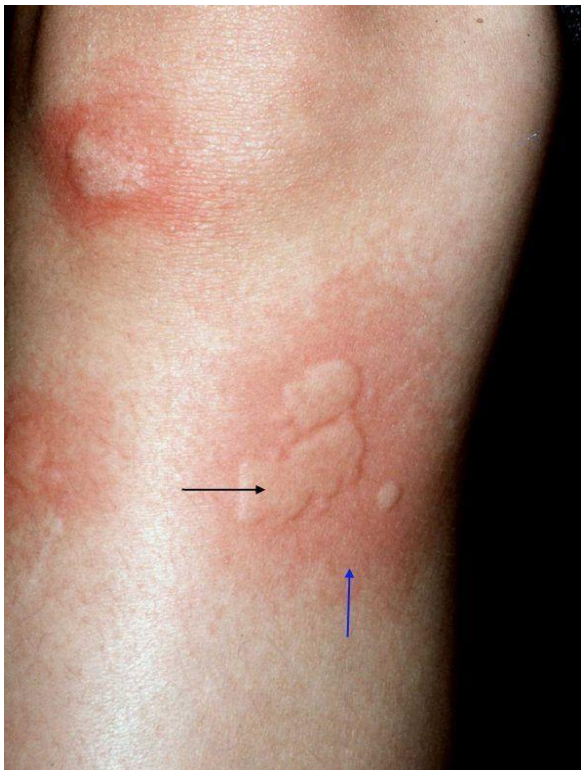

Figure 1.2: Example of a wheel and flare response. Individual with chronic continuous urticaria. The black arrow points to the localised swelling 'wheel' and the blue to the reddened skin or 'Flare' image taken from primary care dermatology society's (PCDS) website; https://www.pcds.org.uk/clinical-guidance/urticaria-spontaneous-syn-chronic-ordinary-urticaria (Accessed 2022).

The likelihood of a late-phase reaction is mainly contingent on the dose of allergen and the individual exposed. The late reaction typically peaks

at about 3-9 hours post allergen exposure, however, it can persist for 24 hours or longer. The late phase reaction is generated through the continuous synthesis of inflammatory mediators by mast cells, particularly vasoactive mediators, such as calcitonin gene-related peptide (CGRP) and vascular endothelial growth factor (VEGF). These mediators contribute to symptoms like oedema through increasing vasodilation and vascular leakage, as well as the recruitment of granulocytes (Pastwińska *et al.,* 2017, Shaik-Dasthagirisaheb *et al.,* 2013). Mast cell derived mediators can influence endothelial cells to upregulate expression of key adhesive molecules during the immediate response. Molecules, such as E-selectin, facilitate the adhesion of circulating leukocytes to the endothelial cells. Subsequent chemoattractants, such as IL-5, are also secreted by activated mast cells and stimulate the infiltration of the activation site with granulocytes, T lymphocytes, and macrophages (Hansen *et al.,* 2004, Bascom *et al.,* 1988, Naclerio *et al.,* 1985). These newly recruited cells, such as neutrophils, have been shown to act as APCs for local allergen-specific T cells, subsequently stimulating them to proliferate and secrete cytokines, reactivating the immediate phase proinflammatory responses (Polak *et al.,* 2019). This continued response is what gives rise to the late-phase allergic pathology, such as a more diffuse oedematous response in skin allergy.

In asthmatic individuals, the allergic response can be nicely mapped through the measurement of peak expiratory flow rate (PEFR) (Figure 1.3). As can be seen in Figure 1.3**,** at around 15 minutes post inhalation of an allergen, a rapid decline in the PEFR is observed (immediate response). This is caused by the constriction of the bronchial smooth muscle. Over time this response starts to attenuate as secreted mediators are metabolised. However, after a few hours, a second drop in PEFR can be seen again. This second drop in PEFR is the late phase response and is triggered by the continued secretion of mediators recruiting granulocytes and other immune cells to the site of inflammation, which in turn activate and release their own mediators.

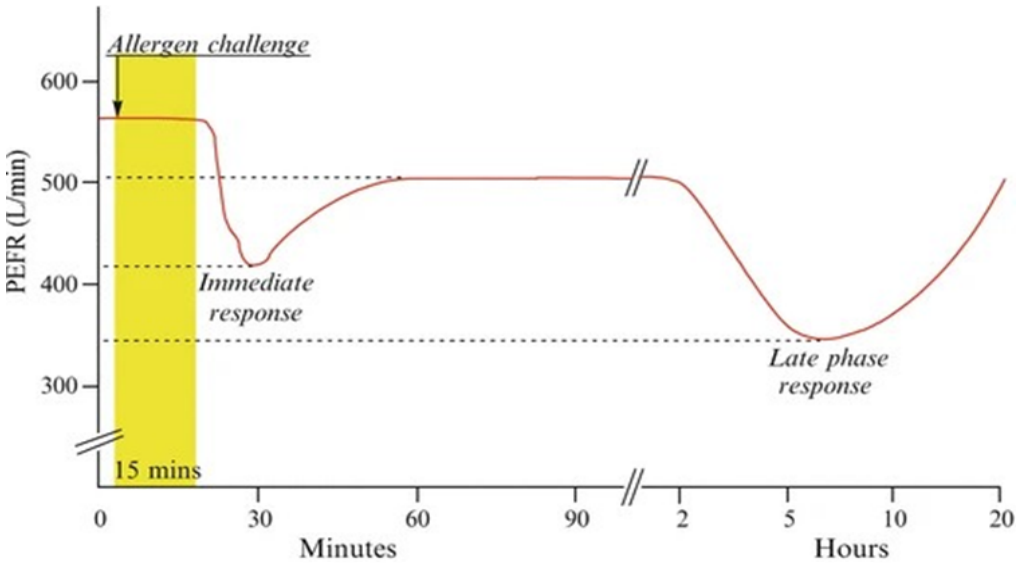

Figure 1.3: Changes in peak expiratory flowrate (PEFR) over time in response to allergen exposure. Changes in PEFR demonstrate the immediate and late response experience by an individual during an allergic response. Image taken from (Baldo and Pham, 2013).

1.1.5. The Airway Epithelium

As previously stated, the airway epithelium was initially thought of as just a physical barrier which acts to protect the underlying mesenchyme from the external environment. However, it has now been shown that the epithelial barrier is an amalgamation of highly specialised cell types, capable of assisting in host defence through immune cell interactions and maintaining homeostasis in response to microbes, noxious stimuli and allergens (Hewitt and Lloyd, 2021). The respiratory tract itself is a complex organ system divided into multiple regions, the upper respiratory tract comprising the nasal cavity, pharynx, larynx. The lower respiratory tract consisting of the "conducting" airways, such as the trachea, bronchi and bronchioles. Lasty, the respiratory zone, which is made up of respiratory bronchioles and alveoli (Figure 1.4A). Each of these regions has a specific function and consequently regional differences in cellular composition, which have been extensively profiled using microscopy and morphological studies (Widdicombe, 2019). Traditionally, the airway epithelial barrier is believed to consist of basal cells tightly surrounded by ciliated cells and secretory cells, such as club (surfactant-secreting) and goblet (mucus-secreting) cells (Figure 1.4Bi)

(Domingo *et al.,* 2025). Ciliated and secretory cells facilitate the clearance of pathogens and other particulate matter, such as allergens, through mucociliary action. While the basal cells they surround are multipotent progenitor cells, they can generate all other major subpopulations found in the epithelium, ultimately, facilitating robust regeneration of the epithelium (Basil *et al.,* 2020). However, with the adoption of advanced sequencing techniques, the epithelial barrier has been shown to be a more significantly dynamic structure, consisting of a variety of different cell types and states capable of responding to environmental change, interacting with commensal microbial communities and communicating with other specialised cellular systems, such as neural and immune (Badaoui and Chanson, 2023).

Single-cell RNA-sequencing (ScRNA-seq) has revolutionised our understanding of the epithelium, revealing a level of cellular diversity that microscopy cannot. This has enabled the comprehensive profiling and characterisation of individual cells and populations of cells within the epithelial barrier. While the basal, ciliated and secretory cells (goblet and club) cells still make up the majority of the airway epithelium, the identification of new cell types, such as tuft cells, which are believed to have sensory and immune functions (synthesising leukotrienes) and ionocytes, which facilitate ion transport and pH regulation, has revealed another level of complexity and function (Figure 1.4Biii). Not only has ScRNA-seq revealed new cell types, but it has also identified intrapopulation variation and new cell states. For example, analysis of air liquid interface (ALI) cultures, allowed for the identification of a precursor subset of multiciliate cells termed “deutrosomal cells”, high in expression of DEUP1, CDC20B and FOXN4, which are involved in the upregulation of centriole and cilia genesis. This population was later identified in healthy human airways (Deprez *et al.,* 2020, Ruiz García *et al.,* 2019). Furthermore, these new cell states are linked to regional locations within the airways, fulfilling similar, but more specific functions. For example, one study showed that goblet cells can be subdivided into two separate classes: goblet 1 and 2. These subclasses are both present in the upper airway epithelium, while only goblet 2 cells can be found in the lower airway epithelium, such as the bronchioles. This goblet 2 subset has a more

immunologically focused function than its counterpart, helping to coordinate innate immune responses through the upregulation of genes CXCL10, IL19 and CSF3, involved in the recruitment of neutrophils, monocytes, DCs and T cells. This variation in heterogeneous cell types is not just linked to location, but also to environmental changes, with cell states varying as a result of environmental changes such as smoking, pollution and allergen exposure. Comparisons of the airways of healthy and mild asthma sufferers lead to the identification of epithelial cell states unique to patients. A "mucous ciliated cell" expressing both ciliated markers (FOXJ1) and goblet cell markers (MUC5AC) is believed to be a transitionary state that results from IL-4 and IL-13 signalling in asthma (Vieira Braga *et al.,* 2019). This further emphasises the dynamic state of the epithelial barrier and its ability to adapt and to coordinate with the immune system to ensure a more robust defence against inhaled pathogens and allergens.

1.1.6. Epithelial Tight Junctions

As explored in the previous section, the airway epithelium is made up of a diverse community of cells which enable the epithelium to fulfil a variety of functions. While the airway epithelium contributes to both sensory and immune pathways, its primary function is still to act as a physical barrier to the external environment. Apical junctional complexes (AJCs) facilitate this barrier function, tightly connecting epithelial cells together to form a continuous barrier. AJCs consist of tight junctions (TJs), adherens junctions, desmosomes and hemidesmosomes (Figure 1.4Bii) (Nur Husna *et al.,* 2021b). TJs are the most apically situated junctions and primarily function to regulate the homeostasis of ions, water and other macromolecules. Consequently, TJs play a central role in the generation of limiting barrier to pathogens (Citi *et al.,* 2024). Adheren junctions are situated below TJs and facilitate cell adhesion, proliferation and differentiation (Campbell *et al.,* 2017, Brüser and Bogdan, 2017). Desmosomes are situated close to adheren junctions and play a similar role in maintaining cellular adhesion and integrity. Finally, hemidesmosomes, facilitate the adhesion of basal epithelial cells to the basement membrane (Nur Husna *et al.,* 2021b).

TJs are comprised of three transmembrane proteins, namely occludin, claudin and junctional adhesion molecules (JAMs). Occludin was the first TJ protein identified and is comprised of two extracellular loops (Figure 1.4 Bii). The C-terminal of occludin interacts directly with zonula occludin (ZO-1), creating barrier integrity, while the N-terminus facilitates paracellular permeability, allowing for the maintenance of homeostasis (Citi *et al.,* 2024). Dysregulation of the epithelial barrier is often linked to the reduced expression of occludin in the epithelium. Downregulation of occludin allows for easier allergen and pathogen penetration of the airway epithelium. This has been observed in the nasal epithelium, where reduced occludin mRNA was detected in AR patients when compared to healthy controls (Steelant *et al.,* 2018). Furthermore, reduced occludin expression allows for HLA-DR- and CD11c-postive-DCs to extend further into the epithelium, closer to the epithelial surface, allowing DCs to experience environmental agents that haven't passed through the TJ (Takano *et al.,* 2005). The Claudin family of proteins consists of 25 members. These proteins have four transmembrane domains, 2 cytoplasmic and 2 extracellular (Figure 1.4 Bii), which allows them to act as gates regulating the movement of molecules paracellularly through the formation of pores (Citi *et al.,* 2024). Like occludin, the C-terminal of claudin also interacts with ZO-1 to provide stability and barrier integrity (Nur Husna *et al.,* 2021b). Additionally, reduced expression of claudins is also linked to dysregulation of epithelial barrier and has been observed in AR patients when compared with healthy controls (Steelant *et al.,* 2018).

As discussed previously, the environment plays a significant role in the development of allergies, through barrier dysregulation. This barrier dysregulation is predominantly the result TJ disruption. This has been observed in HDM-sensitised individuals, where reduced expression of both occludin and claudin-7 mRNA was linked with pollution in urban areas and second-hand cigarette smoke (Nur Husna *et al.,* 2021a). Other studies have identified that diesel exhaust particles (DEPs) and other fine particulate around 2.5µm in diameter (PM2.5) significantly impact TJ integrity and consequently epithelial barrier function (Zeng *et al.,* 2024, Park *et al.,* 2019). One example was a study looking at nasal ALI cultures, which identified significant

reductions in the expression of TJ proteins, occludin, claudin-1 and Z0-1, as well as increased epithelial permeability, upon DEP exposure (Zhao *et al.,* 2018). Additionally, DEP was shown to influence TJ stability through reactive oxygen species (ROS). ROS were shown to suppress TJ protein expression through p38 MAPK and p68 NF-κB, and Akt pathways independently of IL-8 through inhibition of tyrosine phosphate (Kim *et al.,* 2018). Lastly, allergens are also able to disrupt barrier function though TJ dysregulation. This is partially seen with the respiratory allergen HDM. The major allergenic species of HDM are *Dermatophagoidies pteronyssinus* (Der p) and *Dermatophagoides farina* (Der f). Of these species, Der p, particularly the allergen Der p 1, is highly associated with epithelial barrier disruption. Der p 1 is a cysteine protease and its proteolytic activity is capable of cleaving TJ proteins occluidn and claudin-1, facilitating the allergens' penetration of the epithelial barrier and subsequent exposure to the immune system (Nur Husna *et al.,* 2021b)

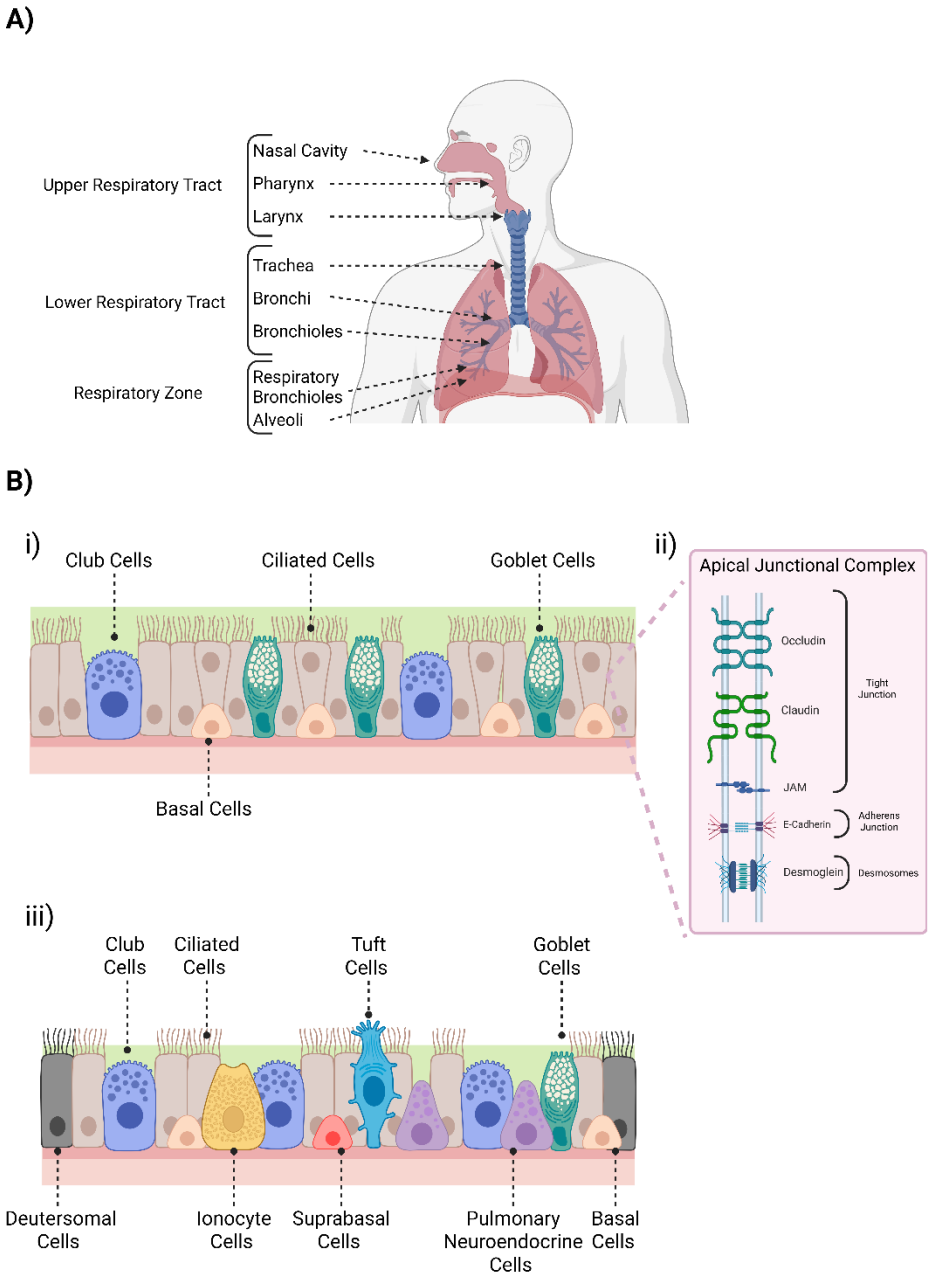

Figure 1.4: Airway regions and epithelial barrier composition: A) The three main divisions of the airways. **B)** Epithelial barrier composition. **Bi)** Simplified traditional view of the epithelial barrier consisting of four cell types: ciliated cells, goblet cells, club cells and basal cells. **Bii)** Epithelial barrier AJC comprised of TJs, adherens junctions and desmosomes which all work to facilitate barrier integrity and impermeability. **Biii)** Current understanding of the epithelial landscape consisting of multiple cell types and states, whose regional expression creates functional specific zones within the divisions of the airway.

1.1.7. Airway Epithelial – Immune Crosstalk in Allergy

Due to the diverse and versatile nature of the airway epithelium composition, it is capable of immune cross-talk via a number of different mechanisms. One of these mechanisms previously alluded to is the expression of a variety of transmembrane or intracellular receptors termed PRRs. These receptors are able to recognise structural motifs unique to bioaerosols, such as allergens, bacterial endotoxins and fungal spores, called pathogen-associated molecular patterns (PAMPs) and damage-associated molecular patterns (DAMPs) (Nabipur *et al.,* 2025). Additionally, as part of facilitating innate immune responses, PRRs have also been shown to act as helper proteins for transmembrane receptors, opsonise targets for phagocytosis and trigger innate and sometimes adaptive immune responses. PRRs are split into two groups, secreted receptors, consisting of toll-like receptors (TLRs), C-type Lectin receptors (CLRs), and protease-activated receptors (PARs) and intercellular cytosolic receptors, such as NOD-like receptors (NLRs) and RIG-I-like receptors (RLRs) (Whetstone *et al.,* 2022). Activation of these receptors triggers epithelial cell cytokine secretion (IL-1β, IL-6, IL-10, IL-13, TNF-α and TGF-β) that ultimately helps to activate and coordinate both the innate and adaptive branches of the immune system (Xu *et al.,* 2025, McClure and Massari, 2014).

TLRs were the first described human PRRs (Medzhitov *et al.,* 1997). These receptors are now one of the most extensively researched PRRs and have been shown to be central in a number of processes, from inflammation, bridging between innate and adaptive immunity, to cancer cell proliferation and survival (Maeda *et al.,* 2019). In humans, currently 10 different functionally active TLR receptors have been identified (TLR1 through TLR10). These receptors are classified by their location of expression, as well as by the PAMPs and DAMPs they recognise. TLR1, TLR2, TLR4, TLR5, TLR6 and TLR10 are expressed on the surface of cells where they predominantly recognise lipid and protein motifs, while TLR3, TLR7, TLR8 and TLR9 are expressed within endosomes and bind to specific nucleic acid ligands, such as viral double-stranded DNA and sense single-stranded RNAs (Xu *et al.,* 2025). TLR downstream signalling is divided into two pathways,

either Myeloid Differentiation factor 88 (MyD88)-dependent or MyD88-independent. All TLRs, with the exception of TLR3, utilise MyD88-dependent signalling. The MyD88-dependent pathway activates mitogen-activated protein kinase (MAPK) and nuclear factor-κB (NF-κB), which in turn allows for the production of proinflammatory cytokines. Alternatively, TLR3 and sometimes TLR4 signalling is mediated by TIR-domain-containing adapter inducing interferon-β (TRIF), which stimulates the synthesis of type 1 IFN to combat viral infection (Luo *et al.,* 2024).

The expression of TLRs in the airway epithelium is well documented. While the expression of TLR mRNA is more generally observed in the airway epithelium, the expression of protein is more variable, being dependent on tissue site and condition of an individual (healthy vs allergic). TLR activation of epithelial cells can induce an array of different responses dependent on tissue location within the respiratory tract. One such response is the production of mucus, which TLRs can induce both directly and indirectly through the stimulation of IL-8 and TNF-α production (McClure and Massari, 2014). While the airway epithelium expresses the majority of TLR receptors, TLR2 and TLR4 are of particular importance. These receptors are typically expressed in low levels on basal epithelial cells and have been shown to be significantly upregulated in inflamed tissue (Regueiro *et al.,* 2009).

TLR2 functions through the formation of heterodimers with TLR1 or TLR6, giving it both a broader range for PAMP recognition and effector function (Oliveira-Nascimento *et al.,* 2012). TLR2 is believed to alleviate allergic inflammation, with its activation being shown to inhibit Th2 responses, prevent antibody class switching and promote anti-inflammatory cytokines such as IL-10 (Xu *et al.,* 2025). Consequently, polymorphisms of this TLR receptor are strongly associated with allergic sensitisation. For example, the TLR2/-16934 T allele has been associated with a lower risk of allergic sensitisation in the children of European farmers (Eder *et al.,* 2004).

TLR4's specific ligand is a component of gram-negative bacteria termed lipopolysaccharide (LPS). TLR4 signal transduction can occur via both the MyD88 or TRIF pathways, inducing different downstream effects.

Triggering the MyD88 pathway results in the upregulation of expression of proinflammatory genes such as TNF-α, IL-6 and IL-1β, through the nuclear translocation of NF-κB factors (Wu *et al.,* 2022). Whereas stimulation through the TRIF pathway is linked to exacerbation of respiratory diseases such as asthma (Xu *et al.,* 2025). TLR4 expression on the airway epithelium has been shown to play an important role in the triggering of type 2 inflammation, as well as granulocytic responses, in allergy. The structural homology between known allergens, such as the HDM allergen Der p 2 and LPS, allows for the triggering of TLR4 receptors directly. Allergenic stimulation of TLR4 facilitates the induction of Th2 responses through the modulation of DC function and the recruitment of effector cells such as mast cells, via the secretion of epithelial-derived alarmins IL-25, IL-33 and TSLP, promoting allergic sensitisation and exacerbating elicitation (McAlees *et al.,* 2015, Trompette *et al.,* 2009, Whetstone *et al.,* 2022).

Epithelial-derived mediators termed alarmin cytokines have been shown to have a central mechanism in the pathogenesis and exacerbation of allergic disease. The release of alarmins such as IL-25 (IL17E), IL-33 and thymic stromal lymphopoietin (TSLP) by the airway epithelium has been shown to influence the production of an array of type 2 cytokines such as IL-4, IL-5 and IL-13 from multiple different effector cells. Upregulation of these type 2 cytokines ultimately promotes the allergic mechanism, such as IgG to IgE class switching, B cell proliferation, eosinophilic inflammation and mucus secretion.

IL-25, sometimes referred to in the literature as IL-17E, was initially identified as a Th2-producing cytokine involved in the polarisation of Th2 responses. IL-25 is a member of the IL-17 family, which is composed of 6 members (A through F). However, IL-25 has a differing biological function from its other family members (Fort *et al.,* 2001). IL-25 is secreted by numerous cell types, including some involved in type 2 immune responses, including epithelial cells, activated Th2 cells, mast cells, alveolar macrophages and fibroblasts. Despite the extensive expression of IL-25, its receptor, IL-25R, is more limited. Currently, IL-25R expression has been identified on ILC2s, mast cells, eosinophils, basophils, invariant natural killer (iNKT) cells

and APCs (Whetstone *et al.,* 2022). This receptor is comprised of two dimer subunits IL-17RA and IL-17RB. IL-25 binds directly to the IL-17RB subunit, which in turn allows for the association of IL-17RA. The engagement of IL-25 and the formation of the IL-17RA/B complex, alongside co-stimulatory signals CD3 and CD28, promotes the upregulation of key pathways, such as NF-κB, MAPK p38 and GATA3. Upregulation of these pathways promotes IL-4, IL-5, IL-6 and IL-13 cytokine secretion as well as CXCL9, CXCL10 and CCL5 chemokines. Within the airway epithelium, IL-25 is expressed as a preformed cytokine, allowing for the immediate secretion upon stimulation by environmental agents, such as allergens (Cheng *et al.,* 2014). In addition to the upregulation of pro-Th2 cytokines and chemokines, airway epithelial secreted IL-25 induces the proliferation of ILC2 (Han *et al.,* 2017). The importance of IL-25 in the pathogenesis of respiratory allergies was emphasised in a study by Ballantyne *et al.,* who demonstrated the inhibition of IL-25 attenuates allergic hyperresponsiveness in the airway, making IL-25 an attractive target for therapeutic intervention (Ballantyne *et al.,* 2007).

IL-33 is a member of the IL-1 family of cytokines, whose role in the regulation of immune inflammation is well established (Dinarello, 2018). IL-33 is constitutively expressed in the nuclei of a number of different cells, including keratinocytes, fibroblasts, recirculating cells from secondary lymphoid tissue, and airway epithelial cells (Whetstone *et al.,* 2022). Uniquely, IL-33 is synthesised with a nuclear localisation sequence and chromatin binding domain, which gives it both the ability to function as a cytokine and a transcription factor (Drake and Kita, 2017). To trigger its downstream effects, IL-33 interacts with its heteromeric receptor, suppression of tumorigenicity 2 (ST2). This receptor is expressed in two forms, the first being ST2L, which is IL-33's active receptor and transduces IL-33 signalling. The second form of ST2 is sST2, which is an inactive form of the receptor and acts as a comparative inhibitor, ultimately blocking IL-33 activity (Hayakawa *et al.,* 2007). The receptor ST2L is highly expressed on an array of mature leukocytes, such as mast cells, Th2 lymphocytes, ILC2s, basophils, eosinophils and macrophages. Engagement of IL-33 with ST2L induces conformational changes in the receptor, allowing for the recruitment of

IL1RAcP. Formation of a IL33/ST2/IL1RAcP complex facilitates activation of key type 2 immune response pathways, such as NF-κB, MAPK p38, JAK2 and PI3K. Triggering of these pathways induces the synthesis and release of proinflammatory mediators IL-6, IL-8, MCP-1 and MCP-3 (Whetstone *et al.,* 2022). The pathways and consequently the downstream effects that IL-33 activates are cell-specific. For example, in ILC2 cells, IL-33 signalling activates p38 MAPK, which in turn promotes subsequent GATA3 signalling, resulting in the production of IL-5 and IL-13. In contrast, IL-33 signalling in basophils and eosinophils activates NF-κB, promoting type 2 inflammation (Liew *et al.,* 2016). Within the airway epithelium, IL-33 is highly expressed, particularly by bronchial epithelial cells. This expression is known to be further upregulated by exposure to environmental agents, such as allergens. In addition to the expression of IL-33, bronchial epithelial cells also express the functional receptor ST2L. Expression of this receptor creates a positive feedback loop, which further promotes Th2 responses in the airway (Yagami *et al.,* 2010). IL-33 is one of the first cytokines to be secreted by the airway epithelium in response to allergen challenge. A primary target of this fast cytokine response are ILC2s, inducing IL-5 and IL-13 secretion as previously stated. This activation is potent, and has been shown to induce almost 10-fold more cytokine secretion than ILC2s activated by type 2 T cells (Chen *et al.,* 2017). In addition to ILC2 signalling, IL-33 can also induce IgE-dependent and independent release of inflammatory mediators, such as histamine, IL-4, IL-5, IL-6, IL-8 and 13 in basophiles, further emphasising the importance of IL-33 in the pathogenesis of hypersensitivity disorders (Whetstone *et al.,* 2022).

Initially, TSLP was identified as a pre-B cell growth factor. TSLP has two main isoforms in humans. A short isoform that is expressed under basal conditions and a long isoform whose expression is induced as a result of contact with environmental stimuli such as allergens (Dong *et al.,* 2016). TSLP is expressed by a diverse range of immune and epithelial cells, including airway epithelial cells and keratinocytes, as well as monocytes, basophils, macrophages and myeloid DCs. Of the three key alarmin signals involved in the development of Th2 responses, TSLP has the most diverse range of targets.

CD4+, CD8+, myeloid cells, T regulatory cells (Tregs), monocytes, mast cells, basophils, eosinophils, B cells, NKT cells and airway smooth muscle cells all express TSLP's receptor TSLPR (IL-7Ra) (Whetstone *et al.,* 2022). TSLP, alongside TLR stimuli, such as LPS, promotes DC maturation and the upregulation of MHC class II, as well as key co-stimulatory molecules CD40, CD56, CD80, CD83 and CD-LMAP (Froidure *et al.,* 2014). TSLP does not directly stimulate the production of pro-inflammatory cytokines like the other alarmins, but instead inhibits Th1-polarising cytokines such as IL-12 and type 1 IFNs. TSLP primes DCs promoting the expression of OX40L, which facilitates the skewing and polarisation of naïve T cells towards a Th2 phenotype. These Th2 cells subsequently produce IL-4, IL-5, IL-13 and TNF-α, further promoting a type 2 immune response (Watanabe *et al.,* 2004). TSLP has also been shown to promote DCs, facilitating the induction and expansion of Th2 memory cells, further exacerbating allergic disease (Wang *et al.,* 2006). In addition to DCs, TSLP has a potent effect on granulocytic cells, facilitating their recruitment into the airways through the upregulation of the adhesion molecule CD18 and the chemokines CXCL8, CXCL1 and CCL2. The interaction of TSLP with mast cells, in conjunction with other signals such as IL-1β and TNF-α, has also been shown to further promote the secretion of pro-Th2 cytokines IL-5, IL-13, IL-6 and IL-8. Furthermore, studies have shown TSLP signalling with mast cells can act as a positive feedback loop, with TSLP mast cells being shown to directly upregulate the expression of epithelial-derived TSLP (Allakhverdi *et al.,* 2007, Miyata *et al.,* 2008).

The airway epithelium also expresses both the high and low affinity receptors for IgE, FcεR1 and FcεRII, respectively (Campbell *et al.,* 1998, Campbell *et al.,* 1994). Both receptors play an important role in the pathogenesis of allergic inflammation and have been shown to be upregulated in patients with allergic asthma when compared with healthy participants (Domingo *et al.,* 2025). Expression of the high affinity receptor for IgE, FcεRI, on airway epithelial cells has also been shown to enhance allergic sensitisation and elicitation. In addition, cross-linking of FcεRI-IgE complexes on the epithelium promotes barrier dysfunction, disrupting tight junction formation by down-regulating key junction proteins, such as zonula

occludens-1 (ZO-1), E-Cadherin and claudin-18. Furthermore, the IgE doesn't have to be allergen specific, with microbial colonies, particularly staphylococci populations, being shown to produce "superantigens" capable of facilitating class switching in local B cells to IgE (Huvenne *et al.,* 2010, Gould *et al.,* 2007). This IgE synthesis in turn upregulates the expression of FcεRI receptors on epithelial cells, resulting in the formation of IgE- FcεRI complexes on epithelial cells. Consequently, IgE crosslinking then downregulates junction proteins, increasing transepithelial permeability and facilitating allergen immune interactions, thereby promoting allergen challenge and sensitisation. Additionally, airway epithelial FcεRI-IgE engagement upregulates the expression of epithelial growth factor receptor (EGFR), whose activation plays an important role in the secretion of key Th2 response-inducing alarmin cytokines IL-25, IL-33 and TSLP (Weng *et al.,* 2023).

FcεRII (CD23), the low affinity receptor for IgE, has also been shown to play an important role in airway epithelial allergen interactions and subsequent immune response. This receptor acts as a bidirectional transporter, facilitating the movement of IgE from the basolateral side of the epithelium to the apical luminal side, and vice versa. Allergen-specific IgE released into the lumen can subsequently bind to inhaled allergen. The IgE–allergen complex is then transported back across the epithelial barrier, via CD23, to the lamina propria, where it allows for direct communication of the epithelium with key effector cells, such as mast cells, crosslinking allergen-specific IgE-FcεRI complexes, triggering degranulation and the induction of a hypersensitivity response (Domingo *et al.,* 2025, Palaniyandi *et al.,* 2011).

1.1.8.Extracellular vesicles

Extracellular vesicles (EVs) are defined as particles secreted by all cells, delimited by a lipid bilayer, and cannot replicate on their own (Welsh *et al.,* 2024). These particles act as a mechanism for extracellular communication due to their immense functional variability. This functional variability is due to the fact that an EV is capable of containing any biomolecule category, such as proteins, lipids, nucleic acids, and sugars, that are synthesised within the cell of origin. These lipid-bound vesicles act as both a protective and targeted way to deliver multiple signals simultaneously to cells in the immediate extracellular environment, as well as to sites further removed within an organism. EVs are classified based on three key factors, their biogenesis (exosomes, microvesicles, apoptosomes and autophagic EVs), their inferred role (oncosome, matrix vesicles, stress EVs and migrasomes), and lastly their size (small EVs and large EVs) (Sheta *et al.,* 2023).

Exosomes are secreted by all cell types and have been identified in a vast array of biological fluids, such as bronchial fluid, breast milk, urine, amniotic fluid, tears and gastric acid, emphasising the vast potential and functionality of EVs (Doyle and Wang, 2019). The term “exosome” is an amalgamation of the terms used to describe their biogenesis and secretion, endosome and exocytosis. Exosomes are formed from the inward budding of the limiting membrane of endosomes and are typically considered to be 30-150nm in diameter (Bebelman *et al.,* 2018). It is experimentally difficult to distinguish exosomes from other EV subtypes, as it requires the confirmation of exocytosis for an accurate identification. Currently, a lot of literature uses the tetraspanin markers CD9, CD63 and CD81 as a mechanism for the positive identification of exosomes. However, the universality of these markers is not fully understood and consequently is not suitable alone for the accurate identification of exosomes. This is often overlooked in the literature, and so consequently it is now suggested that exosomes be called “small EVs” unless exocytosis is confirmed (Sheta *et al.,* 2023, Welsh *et al.,* 2024). Furthermore, it has also been suggested that the subtype of exosomes should be further divided into small exosomes (Exo-S), ranging from 30-80nm and large exosomes (Exo-L), ranging from 80-150nm. The biogenesis, sorting and

subsequent release of exosomes involves a sequence of highly regulated processes. Firstly, the formation of early endosomes (EEs), then the maturation of these EEs into late endosomes (LEs), coupled with inward budding and the formation of multivesicular bodies (MVBs) containing intraluminal vesicles (ILVs). These MVBs are then subsequently transported to and then fused with the plasma membrane, facilitating their release into the extracellular space. ILVs expelled into the extracellular space via exocytosis are termed exosomes (Figure 1.5) (Wang *et al.,* 2025b). EEs are formed by the invagination and endocytosis of ubiquitinated regions of the plasma membrane (Figure 1.5A). After internalisation, EEs undergo additional invagination, producing vesicles within the complex called ILVs (Figure 1.5B). This process is highly regulated and is primarily driven by the Endosomal Sorting Complex Required for Transport (ESCRT) (ESCRT-dependent pathway). Additionally, other proteins also play a central role in the biogenesis of exosomes in an ESCRT-independent pathway, such as cholesterol, sphingomyelinase 2 (nSMase2) and tetraspanins. The ESCRT-dependent pathway is regulated by five sequential proteins, ESCRT-0, ESCRT-I, ESCRT-II, ESCRT-III and VPS4-VTA1. ESCRT-0 fulfils two roles in the biogenesis of exosomes. Initially, ESCRT-0 acts as a clustering protein for exosome cargo, engaging and binding ubiquitinated cargo molecules designated for exocytosis (Figures 1.5Bi). Additionally, it also segments the plasma membrane of EEs, binding to ubiquitinated sites and recruiting clathrins and ubiquitin ligases. ESCRT-I also binds with and clusters ubiquitinated cargo molecules as well as forming complexes with both ESCRT-0 and ESCRT-II. Formation of ESCRT-0-I-II complexes invaginates the EEs plasma membrane around these cargo rich microdomains (Figure 1.5Bii). Additionally, the formation of the ESCRT-0-I-II complexes recruits ESCRT-III, maturing these domains into vesicles attached to the limiting membrane by a constricting neck region (Figure 1.5Biii). ECRT-III additionally recruits deubiquitinating machinery to the vesicle, removing cargo ubiquitin markers. Lastly, VPS4-VTA1 scissions off the mature bud into the intraluminal space, creating ILVs (Figure 1.5BiV&BV**)** (Wang *et al.,* 2025b). The repetition of this process transitions EEs into LEs and ultimately into MVBs, which contain vast numbers of synthesised ILVs (Figure 1.5C).

MVBs are then transported to the plasma membrane of cells, binding and releasing their ILVs into the extracellular space, where they are termed exosomes (Figure 1.5D).

Knockout of ESCRT ultimately led to the identification of the ESCRT-independent pathway, with the identification of secreted exosomes expressing CD63 (Trajkovic *et al.,* 2008). Studies identified that exosome release is also facilitated by the enzyme nSMase2. This metabolises sphingomyelin into ceramides, which are lipids that play an important role in the organisation of the plasma membrane, creating lipid raft microdomains which contain flotillins and cholesterol, which play a central role in forming ILVs. Tetraspanins also play an important role ESCRT-independent biogenesis, acting as membrane scaffold proteins that recruit cargo to the microdomains like ESCRT-0-I-II complexes. This was demonstrated in APCs, where the recruitment of MHC-Class II was shown to be ubiquitin independent, relying on CD9-enriched areas of the plasma membrane for its recruitment (Buschow *et al.,* 2009). Within the tetraspanin family, CD9, CD63 and CD81 are core components in the biogenesis of vesicles, hence why the literature often uses them as exosome-specific markers.

Microvesicles are another subpopulation of small EVs, ranging from 100-500nm (Sheta *et al.,* 2023). Experimentally, these EVs are hard to distinguish from exosomes and other EV subtypes due to their overlapping size ranges. Consequently, there has been a recent push in the literature, particularly by the International Society of Extracellular Vesicles (ISEV), to discourage this term in reporting, preferring small EVs as an umbrella term, unless biogenesis is confirmed (Welsh *et al.,* 2024, Théry *et al.,* 2018). Microvesicles differ from exosomes, not just in their maximum size, but also in biogenesis, shedding or blebbing from the membrane of cells (D'Souza-Schorey and Clancy, 2012). Due to the heterogeneity of microvesicles, the mechanisms underlying their biogenesis are not fully understood, however, several mechanisms have been outlined (Sedgwick and D'Souza-Schorey, 2018, Bebelman *et al.,* 2018, Abels and Breakefield, 2016, D'Souza-Schorey and Clancy, 2012). Initially, ADP-ribosylation factor 6 (ARF6) triggers a cascade which activated phospholipase D. This is followed by the recruitment

of the extracellular signal-regulated kinase (ERK) to the plasma membrane at the site of budding, where it is phosphorylated and, in turn, activates myosin light chain kinase (MLCK). Subsequent phosphorylation of MLCK tiggers the shedding of microvesicles (Bebelman *et al.,* 2018). ARF6 has also been identified to play a role in the selective trafficking of cargo to sites of budding (Tricarico *et al.,* 2017). Additionally, ESCRT-I, in conjunction with protein TSG101 and arrestin domain-containing protein 1 (ARRDC1), has been shown to play a role in their biogenesis, facilitating the recruitment of VPS4-VTA1, which scissions off buds, releasing them into the extracellular environment. (Nabhan *et al.,* 2012).

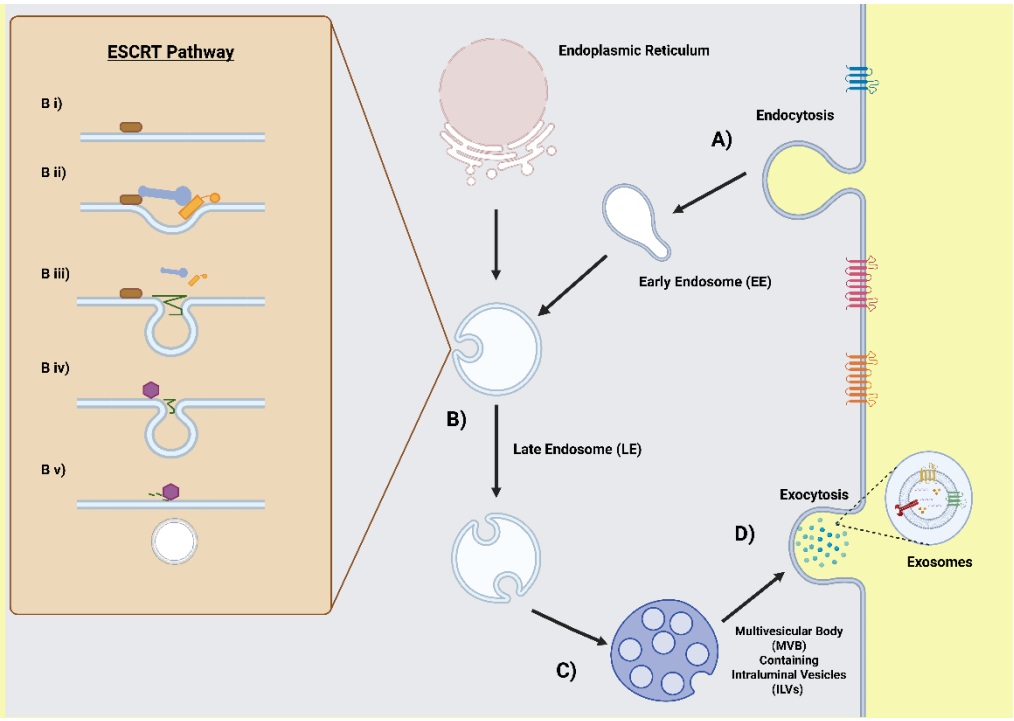

Figure 1.5: **Biogenesis and budding and exosomes. A)** Invagination and endocytosis of the cell's plasma membrane, leading to the formation of an EE. **B)** Loading ubiquitinated cargo and budding of EEs regulated primarily by the ESCRT pathway. **Bi)** Binding of ESCRT-0 to the EE plasma membrane, recruiting and clustering ubiquitinated cargo molecules. **Bii)** Formation of an ESCRT-0-I-II complex, tiggering the initial invagination of the EE plasma membrane around cargo rich microdomains. **Biii)** ESCRT-0-I-II facilitates the recruitment of ESCRT-III and the subsequent binding of deubiquitinating machinery. **BiV)** ESCRT-III promotes the maturation of the cargo rich domains into vesicles pinching the two sides of the domain together and forming a neck region. **BV)** VPS4-VTA1 binds to the ESCRT-III and scissions off the vesicle creating an ILV within the EE. **C)** Formation of multiple ILVs within an EE sees it mature into an LE and ultimately into an MVB. **D)** MVBs are transported to the plasma membrane where they bind and release their ILVs into the extracellular space. Exocytosis ILVs are termed "Exosomes".

1.1.9. Extracellular Vesicles as Immune Modulators

The diversity of EV cargo resulting from their ability to package and transmit any category of biomolecule from within the cell of origin makes them a potent mechanism for intercellular communication. Consequently, over the last decade, research into EVs and the role they play in the regulation and maintenance of homeostasis is a rapidly developing field, with EVs being shown to play an important role in a wide range of mechanisms, including – angiogenesis, tissue repair and re-modelling, endogenous regeneration, anti-apoptosis and immunomodulation to name but a few (Mohammadipoor *et al.,* 2023).

Within the immune system, EVs and their secretion from all types of immune cells play an important role in the initiation, maintenance and attenuation of immune responses, both of the innate and adaptive branches of the immune system (Buzas, 2023). During innate immune responses EVs play a key role in the generation of inflammation. One mechanism through which this is achieved is the secretion of inflammatory mediators by DCs and macrophages. These DC and macrophage-derived EVs, contain lipid mediators such as eicosanoids as well as functional enzymes involved in the biogenesis of leukotrienes, facilitating the recruitment of granulocytes (Boilard, 2018, Esser *et al.,* 2010). Additionally, necroptotic-derived EVs were shown to be able to induce the secretion of TNF-α and CCL2 in macrophages, promoting inflammation (Shlomovitz *et al.,* 2021). Furthermore, activation of the inflammasome during pyroptosis results in a significant increase in EV secretion, as well as the selective loading of pro-inflammatory miRNAs (hsa-miR-124-3p, has-miR155-5p and miR-126-3p). Neutrophil-derived EVs also play an important role in either regulating inflammation, either promoting or inhibiting depending on the environment at the time of biogenesis. Complement receptor Mac1 on neutrophils is central to this functioning as a switch for the production of pro- or anti-inflammatory EVs (Szeifert *et al.,* 2021, Kolonics *et al.,* 2020).

Within adaptive immunity, EVs have been shown to play an important role in all stages of the development of antigen-specific responses. Starting with T cell development, where it has been demonstrated that EVs can contribute to the negative selection of T cells specific to self-antigens, through their secretion in the thymic microenvironment. These EVs are predominantly secreted by thymic epithelial cells and deliver tissue-restricted antigens to conventional DCs (Skogberg *et al.,* 2015). Furthermore, thymic epithelial-derived EVs have also been shown to carry an array of proteins that promote the maturation of CD4+ and CD8+ T cells, such as sphingosine-1-phosphatase lysase (SGPL1) and p21-protein-activated kinase-2 (PAK2). EVs have also been linked to B cell development and differentiation. Antibody mediated engagement of CD24 on immature bone marrow B cells induced secretion of CD24+ EVs, facilitating B cell selection and development (Ayre *et al.,* 2015). One of the most important and well-established mechanisms through which EVs can modulate adaptive immunity is through the presentation of antigens. EVs were first shown to carry MHC in 1996 by Rapose *et al.,* where they demonstrated that B cell-derived EVs carried functional MHC-antigen complexes (Raposo *et al.,* 1996). Subsequent studies have further demonstrated this, with DCs pulsed with antigen/MHC class 1 complexes being able to prime naïve CD8+ T cells. Additionally, the synaptic transfer of EVs between donor and recipient DCs has also been shown to facilitate the cross-priming of CD8+ cells (Balan and Bhardwaj, 2020).

EVs don't just play a role in the activation of immune responses, they are also involved in the regulation and suppression of immune responses. Immunoregulatory molecules such as cytotoxic T lymphocyte antigen 4 (CTLA-4), programmed death ligand 1(PDL1) and ectoenzymes CD39 and CD73 have all been shown to be expressed on the surface of EVs (Buzas, 2023). T regulatory cells (Tregs) have specifically been shown to produce CD73-expressing EVs, these EVs contribute to immune suppression by facilitating the production of adenosine, suppressing T cells and NK cells (Smyth *et al.,* 2013). Treg-derived EVs have also been shown to modulate DCs. Delivery of miR150-5p and miR142-3p by EVs to LPS-activated DCs has been shown to promote IL-10 secretion and downregulate IL-6, suggesting

a possible role for EVs in the generation of tolerogenic DCs (Tung *et al.,* 2018).

1.1.10.Extracellular Vesicles in Allergic Sensitisation

The role that EVs play in the development of allergies is extensive, ranging from acting as inhaled carriers of allergens (pollenosomes), to modulators of the immune system promoting both allergic sensitisation and tolerance (Tucis *et al.,* 2024, Prado *et al.,* 2015). Host-derived EVs play a central role in allergic sensitisation. These EVs are secreted by immune cells such as DCs, B cells and TfH cells, as well as epithelial cells. DC-derived EVs play an important role in the development of Th2 responses. A study by Huang *et al.* demonstrated that EVs isolated from TSLP stimulated DCs promoted the proliferation of CD4+ T cells as well as the elevation of IL-4 and differentiation towards a Th2 phenotype (Huang *et al.,* 2019). Additionally, DC-derived EVs also act as a vector for the presentation of allergens, inducing the production of pro-Th2 cytokines, such as IL-4 (Vallhov *et al.,* 2015). Conversely, DC-derived EVs have also been shown to have a tolerogenic effect, promoting a Th1-like response and the generation of allergen specific IgG, as well as the proliferation of ovalbumin (OVA) specific CD8+ T cells (Wahlund *et al.,* 2017). DCs cultured with OVA and IL-2 were also able to induce tolerance through the secretion of EVs containing IL-2 and OVA-MHC complexes. These EVs bind to the surface of allergen-specific CD4+ T cells inducing their differentiation into Treg cells and the subsequent suppression of Th2 responses (Yu *et al.,* 2020). T follicular (Tfh) cell derived EVs also facilitate allergic sensitisation, through the secretion of miR142-5p-containing EVs. These EVs promote the maturation of DCs through the inhibition of CDK5. The maturation of these DCs promoted the polarisation of Th2 responses in naïve mice, elevating IL-13 and IgE secretion while also supressing the secretion of IFN-γ and IL-17 (Teng *et al.,* 2022). A study investigating the role of B cell derived EVs in allergy, demonstrated that they could promoted allergic sensitisation through the presentation of allergen-MHC complexes to T cells. Presentation of these complexes induced the proliferation of allergen specific T cells as well as the secretion of Th2-like cytokines IL-5 and IL-13 (Admyre *et al.,* 2007). Lastly, EVs isolated from the

plasma of individuals with allergic rhinitis were shown to contain higher amounts of Der p 1 relative to healthy donors. As observed with B cell derived EVs, these plasma membrane derived EVs were also capable of allergen presentation, promoting T cell differentiation and increased secretion of IL-13 (Fang *et al.,* 2021).

In addition to the promotion of sensitisation, host derived EVs can promote tolerance. Mesenchymal stromal cells (MSCs)-derived EVs in particular appear to have an important role in the development of immune tolerance (Tucis *et al.,* 2024). One mechanism through which they induce tolerance is through the release of miR146a-5p-containing EVs. These EVs were shown to inhibit Th2 differentiation through the miR146a-5p inhibition of SERPINB2, preventing allergic sensitisation (Zhou *et al.,* 2021). Additionally, MSC-derived EVs can directly modulate DCs. A study by Peng *et al.* demonstrated that MSC-derived EVs were able to inhibit the differentiation of monocytes into immature DCs, down regulating the expression of CD40, CD80, CD86 and HLA-DR. Furthermore, mature DCs when cultured with these MSC-derived EVs suppressed Th2 responses, down regulating the production of IL-4, IL-9 and IL-13 through the upregulation of IL-10 and Treg cells (Peng *et al.,* 2022). Finally, MSC-derived EVs containing OVA were shown to have a prophylactic effect in mice, preventing sensitisation to OVA and inducing tolerance through decreasing the expression of IL-4 and IgE (Asadirad *et al.,* 2023). Epithelial-derived EVs have also been shown to significantly influence both allergic sensitisation and tolerance. The role of epithelial-derived EVs in allergic sensitisation is included in the systematic review presented in the first results chapter of this thesis (Browne *et al.,* 2025).

Exogenous EVs can also influence allergic sensitisation. This occurs primarily through one mechanism, the disruption of the skin epithelium by commensal and pathogenic bacterial-derived EVs (Tucis *et al.,* 2024). EVs secreted by *staphylococcus aureus* were shown to induce the expression of key pro-inflammatory mediators such as IL-6 and TSLP in dermal fibroblasts. Furthermore, when *S. aureus* EVs were applied to damaged epidermis *in vivo* enhanced production of IL-4, IL-5, IFN- γ and IL-17 was observed alongside

the recruitment of granulocytes such as mast cells (Hong *et al.,* 2011). Further review of the *S. aureus* colonies found on patients with atopic dermatitis (AD) revealed increased levels of α-hemolysin in comparison to colonies on healthy individuals. Secretion of α-hemolysin in EVs demonstrated a more cytotoxic effect on keratinocytes than solubilise forms, suggesting α-hemolysin-containing EVs play an important role in epithelial barrier disruption, facilitating allergen penetration and promoting sensitisation (Hong *et al.,* 2014). Lastly, EVs derived from resistant strains of *S. aureus* have been shown to act as immunostimulants, promoting Th2 inflammatory responses and the upregulation of Th2-like cytokines IL-4 and IL-5, promoting IgE-mediated hypersensitivity (Asano *et al.,* 2021).

1.1.11. Study Aims

The presented work aimed to assess the role of airway epithelial-derived small EVs in the promotion of allergic sensitisation. A humanised 3D cell culture model of bronchial epithelium was developed and stimulated with a traditional respiratory allergen, Der p 1, and a non-traditional respiratory allergen, Can f 1. Subsequently, Th2-promoting cytokine secretion was evaluated to indicate epithelial stimulation. EV responses were quantified and characterised using optimised imaging flow cytometry and EV cargo was evaluated using transcriptomic analysis.

Chapter 2: Materials and Methods

2.1. Materials

2.1.1. Epithelial Cell Lines

Transformed bronchial epithelial cell lines BEAS-2B (Cat.no. CRL-3588) and Calu-3 (Cat.no. HTB-55) were purchased from the American Type Culture Collection (ATCC). While the cells lines A549 (ATCC, Cat.no. CCL-185) and primary bronchial epithelial cells (kindly donated by Professor Ian Sayers (University of Nottingham, UK) in (June 2022)) were sourced from within the university.

2.1.2. 2D Cell Culture

All cells were cultured in either Corning T25 (Cat.no. 430639, Corning, UK) or T75 Flasks (Cat.no 430641, Corning, UK).

BEAS-2B cells were cultured in un-supplemented LHC-9 serum-free culture media (Cat.no. 12680013, Thermofisher, UK).

Initial Calu-3 passages were cultured in Advanced Dulbecco's Modified Eagle Medium (DMEM) (Cat.no. 12491015, Thermofisher, UK) supplemented with 4mM GlutaMAX (Cat.no. 35050-038, Thermofisher, UK) and Penicillin (100IU)-Streptomycin (100µg/mL) (Cat.no. P0781, Merk, UK)

Due to advanced DMEM's pre-supplementation with bovine AlbuMAX, cultures were ultimately transferred into Minimal Essential Media (MEM) culture media (Cat.no. 51200046, Thermofisher, UK), supplemented with 4mM GlutaMAX (Cat.no. 35050-038, Thermofisher, UK), 1% Sodium Pyruvate (Cat.no.S8636, Merk, UK), 1% non-essential amino acids (Cat.no. M7145, Merk, UK), Penicillin (100IU)-Streptomycin (100µg/mL) (Cat.no. P0781, Merk, UK) and 5% heat inactivated human AB serum (Cat.no. H5667, Merk, UK).

Cell counting was conducted using Trypan Blue (Cat.no. T10282,ThermoFisher, UK) and disposable Countess cell counting chamber

slides (Cat.no. C10283) on a Countess 3 Automated Cell Counter (Cat. no. A49862, ThermoFisher, UK).

2.1.3. 3D Air Liquid Interface Culture

Calu-3 Cells were grown on Costar 6.5mm, 0.4µm pore polyester ALI Inserts (Cat.no. 3413, Merk, UK). After submerged culture set up, inserts were cultured in MucilAirTM Culture Medium (Epithelix, Switzerland).

2.1.4. Flow Cytometry

Multiple flow cytometry machines provided by the University of Nottingham's Flow Facility were utilised. Epithelial cell staining experiments were performed on either the CytoFLEX S (Beckman Coulter, UK) or ID7000 (Sony, UK) spectral cytometer. Antibodies used for epithelial cell characterisation are shown in Table 2.1.

Table 2.1. Antibodies used for the profiling of 2D and 3D epithelial cell cultures, listing: target, fluorophore, brightness, manufacturer, category number and staining volume used.

Antibody Target	Fluorophore	Manufacturer	Cat.no.	Staining Volume (µl)
βIV- Tubulin	AlexFlour488	Abcam	Ab237201	0.5
Tspan8	PE-Vio770	Miltenyi	130-106-865	10
EpCAM	PE-Cy7	Biolegend	369816	5
E-Cadherin	APC	Biolegend	324107	5
CD66	BV605	Biolegend	342323	5
CD271	PE	Biolegend	345105	5

EV quantification and Tetraspanin characterisation was performed on an ImageStreamX MKII (ISX) (Luminex Corporation, UK). The antibody panel to profile both general EV markers and tissue specific EV markers are shown in Table 2.3

Table 2.2. Fluorescent antibodies used for the comparison of REAaffinity and conventional antibodies, their fluorophore, manufacturer and antibody type.

Target	Fluorophore	Brightness	Manufacturer	Cat.no.	Type	Conc. Used (µg/mL)
CD9	APC	4	Miltenyi	130-118-808	REAffinity	2.5
CD63	PE	5	Miltenyi	130-118-077	REAffinity	2.5
CD81	PE-Vio615	5	Miltenyi	130-131-387	REAffinity	2.5
CD63	APC	4	Miltenyi	130-119-787	REAffinity	2.5
CD81	APC	5	Miltenyi	130-118-078	REAffinity	2.5
CD9	APC	4	Biolegend	312017	Conventional	2.5
CD63	PE	5	Biolegend	353004	Conventional	2.5
CD81	PE-Vio615	5	Biolegend	349520	Conventional	2.5
CD63	APC	4	Biolegend	353008	Conventional	2.5
CD81	APC	5	Biolegend	349510	Conventional	2.5

Table 2.3 Antibodies used in the final assay EV characterisation, listing: target, fluorophore, brightness, manufacturer, category number and staining concentration used.

Antibody	Fluorophore	Brightness	Manufacturer	Cat.no.	Conc. Used (µg/mL)
CD9	APC	4	Miltenyi	130-118-808	2.5
CD63	PE	5	Miltenyi	130-118-077	2.5
CD81	PE-Vio615	5	Miltenyi	130-131-387	2.5
EpCAM	PE	5	Miltenyi	130-110-999	2.5
E-Cadherin	PE-Vio615	5	Miltenyi	130-125-732	2.5
Tspan8	APC	4	Miltenyi	130-128-391	2.5
REA Control Antibody Human IgG1	APC	4	Miltenyi	130-113-434	2.5
REA Control Antibody Human IgG1	PE	5	Miltenyi	130-113-450	2.5
REA Control Antibody Human IgG1	PE-Vio615	5	Miltenyi	130-113-439	2.5

Cells were washed with phosphate buffer albumin (PBA) as part of intracellular and extracellular staining. PBA was made in-house, comprising of 1X phosphate buffered saline (PBS) (Cat.no. BP399-4, Fisher Scientific, UK) with 30% bovine serum albumin (BSA) (Cat.no. A7284, Merk, UK) and 20% Sodium Azide (Cat.no. S2002, Merk, UK).

4% paraformaldehyde fixation buffer was purchased from Biolegend (Cat.no.420801, UK) and permeabilisation buffer was purchased from Thermofisher (Cat.no.00-8333-56, UK) for the fixation and permeabilization of cells for intracellular staining, respectively.

2D Cell Culture viabilities were assessed using an Annexin V and PI Staining kit (Cat. No 120-092-052, Miltenyi,UK). Annexin V/PI Kits required the use of Annexin binding buffer (Cat.no. 130-092-820, Miltenyi, UK).

The limit of detection (LoD) for fluorophores was assessed on ISX and CytoFLEX using Anti-Human (Cat.no. 816B, Bangs Laboratories, US) and Anti-Mouse (Cat.no. 815B, Bangs Laboratories, US) IgG Quantum™ Simply Cellular microspheres according to the manufacturer's instructions (Bangs Laboratories, Fishers, IN, USA).

Sizing sensitivity was assessed on the ISX and CytoFLEX using NIST beads (60 nm, 80 nm, 101 nm, 125 nm, 151 nm,) (ThermoFisher 3060A, 3080A, 3125A, 3100A and 3150A). Additionally, sizing on the sizing on the ISX was performed with a the vFC™ EV analysis assay kit (Cellarcus Biosciences, US)

Calcein -AM 1mM stock solutions were prepared by dissolving 1 vial of lyophilized Calcein-AM dye (Cat.no. 42520, Biolegend, UK) in 50µl DMSO (Cat.no. D8418, Merk, UK).

2.1.5. Confocal and Scanning Electron Microscopy

0.5% Triton-X permeabilisation buffer was prepared by dissolving 50µl of 100% Triton-X (Cat.no. 10671652, Fisher Scientific) in 9.5 ml of 1X PBS (as above). Immunofluorescence buffer was prepared by dissolving 833.3µl of 30% BSA, 100µl of 100% TritonX and 25µl of 100% Tween-20 in 9ml of 1x PBS. Fluorescent conjugated antibodies for ZO-1 (Cat.no. MA3-

39100-A647, Thermofisher, UK) and Occludin (Cat.no. 331588, Thermofisher, UK) were used to stain tight junctions.

2.1.6. Lactate Dehydrogenase (LDH) Viability

Promega's RealTime-Glo™ MT cell viability assay (Cat.no.G9711) was utilised to assess 3D culture viability. A 2x RealTime-Glo™ reagent was prepared prior to assay, by adding 2µl of MT cell viability substrate (1000x) and 2µl if NanoLuc® Enzyme (1000x) (components of kit) to 996µl of culture media. Assays were performed in opaque non-binding surface 384 well plates (Cat.no. CLS3574, Merk, UK) and samples analysed using a GloMax Explorer Microplate Reader (Promega, US).

2.1.7. Allergens

Low-endotoxin Der p 1 (Cat.no. LTN-DP1-1) and low-endotoxin Can F 1 (Cat.no. LTN-CF1-1) were purchased from Indoor Biotechnologies, UK, for stimulation of epithelial cells. Der p 1's proteolytic activity was activated using L-Cysteine (Cat.no. A10435.18, Thermo scientific, UK) and inhibited when relevant with E-64 (Cat.no. E3132, Merk, UK). Proteolytic activity of Der p 1 was evaluated using a Calbiochem protease assay kit (539125, Merk, UK). As part of the proteolytic activity assay, 5% Trichloroacetic acid (TCA) was produced by dissolving 1.634g of TCA (Cat.no. T/3000/50, Fisher Scientific, UK) in deionised water to create a 1m solution. A 5% stock was prepared by subsequently diluting further (1:20) in deionised water.

2.1.8. Positive Control Stimulants

Polyinosinic-polycytidylic acid (Poly(I:C)) (Cat.no. P1530, Merk, UK) was utilised as a positive control for stimulating epithelial cells. Lipopolysaccharide (LPS) from *Escherichia Coli* O111:B4 purified using gel-filtration chromatography (L4391, Merk, UK) and purified using phenol extraction (L2630, Merk, UK) were also assessed. Carrier free LPS binding Protein (LPS-BP) (Cat.no. 870-LP-025/CF) was also utilised to enhance LPS stimulations.

2.1.9. *Bacillus* Protease Assay

Bacillus protease activity was measured using a EnzChek™ Protease Assay Kit (Cat.no. E6639, ThermoFisher, UK). BODIP TR-X solution was prepared by adding 0.2ml of 0.1M sodium bicarbonate (8.3 pH) to a lyophilized substrate vial. 1x digestion buffer was prepared by diluting 20x digestion buffer in deionised water to a final volume of 50ml. 10μg/ml BODIPY casein working solution was prepared by adding 0.2ml of BODIP TR-X solution to 19.8ml of 1x digestion buffer. Samples analysed using a GloMax Explorer Microplate Reader (Promega, US).

2.1.10. Cytokine ELISAs

Cytokine secretion was profiled using R&D systems DuoSet ELISA kits; IL-1β (DY201), IL-6 (DY206), IL-8 (DY208), IL-17E (DY1258-05), IL-33 (DY3625B) and TSLP (DY139). To prepare standards, 1X reagent diluent was made in house by diluting 10X reagent diluent concentrate 2 (Cat.no. DY995, R&D systems) in PBS to ensure absorbance could be measured. Samples were assessed with an Agilent BioTek Epoch Microplate Spectrophotometer (Aglient, UK)

2.1.11. Nebuliser

A Cloud Alpha AX12 Vitrocell Chamber (Vitrocell, Germany) was utilised for nebulisation experiments. The nebuliser used was an Aerogen Pro-Nebulsier (2.6-6.0 vMD) (Cat.no 90-002, Aerogen, Ireland).

2.2. Methods

2.2.1. Cell Culture

2.2.1.1. 2D Epithelial Cell Culture and Subculture

25cm^2 Corning flasks containing 7ml of supplemented MEM culture media (Section 2.1.2.) were seeded with 1x10^6 Calu-3 cells and incubated at 37ºC and 5% CO_2 (2x10^6 cells in 75cm2 flasks). Culture media was changed every two days until cultures reached 80-90%, where they were then subcultured. At confluence, culture media was aspirated from flasks and cultures were washed three times with 5ml of 37°C PBS. Washed cultures were subsequently incubated in 7ml of 37ºC TrypLE Express (10ml in 75cm^2

flasks). Cultures were incubated in TyrpLE until cells had fully detached from flasks, which was assessed using a brightfield microscope. 8ml of 37ºC was then added to the culture flask, and the content was then transferred into 15ml Falcon tubes, which were subsequently centrifuged at 150g for 10 minutes. After centrifugation, the supernatant was aspirated and the pellets were resuspended in 2ml of culture media. Cell counts were performed on cell suspensions, and flasks were seeded appropriately. Cells used for experiments were seeded into 96-well plates at a density of 50,000 cells per well and incubated at 37ºC and 5% CO_2. Cells not utilised were frozen and stored in liquid nitrogen.

2.2.1.2. Cell Count

Cell counts were performed using Trypan blue staining and analysed using a Countess 3 Automated Cell Counter. 10µl of cell suspension was mixed with 10µl of Trypan Blue and pipetted into a disposable Countess slide. Slides were inserted into the Countess 3 and counts were performed automatically.

2.2.1.3. 2D Epithelial Stimulation

Cells were cultured in 96-well plates until 80% confluence, which was assessed using a brightfield microscope (37ºC and 5% CO_2). Upon reaching the desired confluence, media was changed to serum-free LHC-9 and incubated for three days. To stimulate, media was aspirated from wells and replaced with 200µl LHC-9 media supplemented with relevant stimulant concentration. Cells were incubated at 37ºC and 5% CO_2 until samples were collected after 24- or 48- hours.

2.2.1.4. 3D Epithelial Cell Culture

The apical side of 6.5mm (0.4µm pore and 0.33cm^2 culture surface) trans wells inserts were seeded with 200µl of 5% HS-supplemented MEM culture media (Section 2.1.2.) containing $7x10^4$ Calu-3 cells. 0.5ml of 5% HS-supplemented MEM culture media was also added to the basolateral side (500µl). Cells were cultured under submerged conditions, changing basal media every two days until confluence was reached (37ºC and 5% CO_2). Apical media was aspirated after reaching confluence and basal media was

replaced with MucilAir^{TM} Culture media (500µl). Inserts were cultured at ALI for 21 days before use, replacing media every 2 days (37ºC and 5% CO_2).

For submersion experiments, stimulation stocks were made up to final stimulation concentration by diluting stimulants in 0.22µm sterile filtered PBS. Basal chamber media (MucilAir^{TM} culture media) was changed prior to stimulation (500µl per chamber) and 50µl of stimulation stock was added to the apical chamber for relevant exposure durations (37ºC and 5% CO_2). Following 24- and 48-hour exposure, the 50µl of stimulation stock was removed and placed into Eppendorf's. Apical surfaces were then washed with 200µl of 37ºC sterile filtered PBS for 3 minutes and this was added to Eppendorf's. This was repeated and Eppendorf's were topped up with a further 50µl to give a total volume of 500µl. This allowed for direct comparison of apical and basal concentrations.

For 2- and 8-hour exposure, stimulation preparation was conducted as previous. However, after relevant exposure durations, the stimulants were aspirated and inserts were left to incubate for 24- and 48- hours post initial addition of stimulant (37ºC and 5% CO_2). Apical samples were collected as previous with two 3-minute 200µl sterile PBS washes (37ºC), which was topped up with 100µl of PBS to create a total volume of 500ul.

ELISAs were conducted as outlined in Section 2.2.11. All Cytokines were run on neat sample with the exception of IL-8 which was analysed using samples diluted 1:10 in PBS.

2.2.1.5. Nebulisation of 3D Inserts

ALI Cultures generated as above, were used as soon as possible to ensure low mucus cover of the inserts. ALI inserts were apically washed with 200µl of 37ºC 0.22µm filtered sterile PBS for 10 minutes at 37ºC and 5% CO_2 to clear any mucus on inserts two days prior to exposure. Samples were nebulised using a Cloud Alpha AX12 control chamber and Aerogen Pro-Nebuliser (2.6-6.0 vMD). Prior to exposure, concentrations required for nebulisations were calculated using the equations below, as per manufacturer's instructions.

The following equation determines the mass of test substance introduced into the chamber. M = Mass, C = Concentration added to the nebuliser and Vneb is the volume of stimulant added to the nebuliser.

$$m = C \times Vneb$$

The following equation determines the mass deposition on the cross-sectional area of the aerosol chamber (assuming 100% nebulisation of liquid reaches the bottom of the chamber). Dep= Deposition of nebulised liquid (μg/cm^2), Ac = Cross-sectional area of the chamber (200.54cm^2).

$$Dep = \frac{C \times Vneb}{Ac}$$

The following equation determines the mass deposited in a cross-sectional area of an individual ALI insert. Dep_{insert} = mass deposited in insert (μg) , A_i = area of inserts (0.33cm^2) and Dep is previously calculated.

$$dep_{insert} = dep \times A_i$$

Typically, 80% of nebulised mass reaches the bottom of the chamber, and so M is factored accordingly. However, with the configuration available, deposition was shown to be 35% (Chapter 5).

After calculating concentrations of stimulant required (compensating for 35% deposition) for nebulisation, individual stocks were produced, Table 2.4 shows final volumes and concentrations added to the nebuliser for each stimulant. Der p 1 was activated 20 minutes prior to nebulisation through the addition of 5mM L-Cysteine. Additionally, inactive Der p 1 was produced by adding 10μM of E-64 to the Der p 1 stock 20 minutes prior to nebulisation. The nebuliser was loaded with relevant stimulant, and 24-well plates containing inserts in culture media (37ºC) were placed in the chamber. The chamber was sealed to prevent leaking of nebulised simulant, and the nebuliser was run until the liquid was fully nebulised. The Chamber was left sealed for 10 minutes to allow for full deposition of stimulants. The chamber was then opened and inserts were transferred into new 24-well plates with 500μl of 37ºC culture media and incubated for 24 or 48 Hours (37ºC and 5% CO_2). Between stimulations, both the nebuliser and chamber were cleaned

with ethanol as per manufacturer's instructions to ensure inserts were only exposed to relevant stimulants.

Table 2.4. Stimulants added to nebuliser in final experiment, Concentration added to the nebulised, volume added to the nebuliser and the deposition on ALI inserts.

Stimulant	Concentration added to Nebuliser (mg/ml)	Vneb (ml)	Deposition (μg/cm^2)
PBS (Unstimulated)	Neat	0.3	-
Poly(I:C)	2.0	0.3	1.0
Active Der P 1 (Der P 1 and L-Cysteine)	1.0	0.2	0.35
Inactive Der P 1 (Der p 1 and E-64)	1.0	0.2	0.35
Can F 1	1.0	0.2	0.35

2.2.2. 3D Insert Microscopy

2.2.2.1. Tight Junction Staining

Culture media was aspirated from wells of inserts randomly selected for staining. To remove any debris, cells were washed with 200μl of room temperature 0.22μm filtered sterile PBS for 5 minutes. This PBS was aspirated and washes were repeated four more times for a total of five washes per insert. Cells were then fixed by adding 4% formaldehyde to the apical chamber (200μl) and basal chamber (750μl) for 30 minutes at room temperature. Fixation buffer was removed and cells were permeabilised by adding 0.5% TritonX in PBS to the apical (200μl) and basal (750μl) chambers for 30 minutes at 4^{o}C. Inserts were then washed for 5 minutes with PBS at room temperature, 200μl in the apical chamber and 1ml in the basal chamber. This was repeated two times for a total of three washes. Cells were blocked with the addition of 100μl of 5% BSA in immunofluorescence buffer (Section 2.2.20) to the apical chamber. Inserts were subsequently stained with 50μl of 5μg/ml Occludin AF488 and ZO-1 AF647-conjugated antibodies in

immunofluorescence buffer. Samples were incubated overnight in the dark at 4ºC. Cells were then washed with 1ml of room temperature immunofluorescence buffer for 5 minutes before aspiration. Insert membranes were cut using a scalpel and placed on to coverslips. Coverslips were placed in 24 well plates and submerged in 2ml of PBS and stored at 4ºC. Samples were analysed on a Zeiss LSM9000 with AiryScan, Objective: Plan-Apochromat 20x, numerical aperture: 0.8, Lasers used: AlexaFlour488 and AlexaFlour647, pixel size: 0.074x0.074µm, Z step size: 0.7µm. Images were analysed using Zen3.5 software.

2.2.2.2. Scanning Electron Microscopy

Inserts were initially washed and fixed as previously described (see above). Membranes of selected inserts were subsequently cut out using a scalpel and placed into individual wells of a 24 well plate. Cells were then dehydrated using 200µl of a graded series of ethanol dilutions; 50, 70, 90 and 100% for 10 minutes per dilution. 100% ethanol dehydration was repeated for 10 minutes. After dehydration cells were submerged in 100µl of hexamethryldisilazane and left until the solution had evaporated. Samples were mounted on to aluminium stubs and sputter coated with platinum before analysis with a JEOL JSM IT-200 LV SEM using a voltage of 5 kV and a working distance of 10 mm.

2.2.3. Cellular Flow Cytometry

Cells were isolated from culture wells using 200µl Accutase (Thermofisher, UK) before staining with fluorescently conjugated antibodies. Detachment was assessed using a brightfield microscope. All antibodies were added at manufacturer's recommended concentrations. Analysis was either performed on either Kaluza Analysis 2.1 (conventional and spectral flow cytometry) or on Ideas6.2 (Imaging flow cytometry) software.

2.2.3.1. Extracellular staining

200µl of cell suspensions were harvested into FACS tubes, 1ml of PBA was added and centrifuged at 300xg for 5 minutes. Supernatants were aspirated and pellets were tapped to resuspend. Appropriate antibody volumes (Table 2.1) were added to the cell suspension and incubated in the dark for 30

minutes at 4ºC. 2ml of PBA was then added to the cells and centrifuged at 300g for 5 minutes. Supernatants were aspirated and pellets resuspended through tapping. Cells were fixed in 300µl of fixation buffer (4% formaldehyde fix in 1X PBS) and analysed using flow cytometry or stained for intracellular markers (see below).

2.2.3.2. Intracellular Staining

After Extracellular Staining (see above), cells were left in fixation buffer for a minimum of 30 minutes. Cells were then centrifuged at 300g for 5 minutes. Supernatant was aspirated and pellets were resuspended through tapping. 2ml of permeabilisation buffer was added to cells and incubated in the dark for 30 minutes 4ºC. Cells were again centrifuged for 5 minutes at 300g and supernatants were aspirated, and pellets resuspended through tapping. Appropriate antibody volumes (Table 2.1) were added and incubated in the dark for 30 minutes at room temperature. Finally, cells were centrifuged at 300g for 5 minutes, supernatants were aspirated and pellets resuspended through tapping. 300µl of fixation buffer was added to suspensions and cells were subsequently analysed using flow cytometry.

2.2.4. Calibration of Flow Cytometry

Evaluation of two flow cytometry techniques were assessed for their EV quantification and characterisation suitability. A Cytoflex S (conventional flow cytometry) and an ImageStream X MKII (ISX, Imaging flow cytometry) were compared.

2.2.4.1. Sizing Limit of Detection

National Institute of Standards and Technology (NIST) certified polystyrene size standards (60 nm, 80 nm, 101 nm, 125 nm, and 151 nm, (ThermoFisher 3060A, 3080A, 3125A, 3100A, and 3150A)), were utilised on ISX, CytoFLEX S, and NTA. Beads were diluted in 0.22 µm sterile-filtered PBS accordingly for each machine; 1:10,000 and 1:100,000 for ImageStream X MkII and 1:100,000 for CytoFLEX S. Additionally, NIST certified polystyrene size standards (80 nm, 101 nm, 200 nm, 300 nm, and 450 nm, (Thermo Fisher 3080A, 30100A, 3200A, 3300A, and 3450A)) were used and diluted at 1:100,000. Light scattering signals of NIST bead populations run on

the CytoFLEX S were then fitted with Mie theory using FCMPASS software (Welsh *et al.,* 2020). The refractive index of each bead (specified by the manufacturer) was input into the software. Scattering cross sections of the calibration beads were calculated by integrating the amplitude scattering matrix elements over 576 collection angles. Data and theory were log_{10}-transformed to scale the data into the theory using a least-square-fit. Transformation of this data provides trigger threshold in the context of EV size, giving the limit of detection.

Sizing was also performed using a vFC™ EV analysis assay kit run on the ISX. The ISX was first calibrated using vCal™ nanoRainbow beads and the manufacturer's provided IDEAS layout. 5 µL of a synthetic vesicle size standard, Lipo100™, or 5 µL primary epithelial cell supernatant, were then stained with vFRed™ at 1x concentration in vFC™ staining buffer, in a total volume of 50 µL for 60 minutes at room temperature, in the dark. Samples were then diluted 1:30 in staining buffer before running on the ImageStream X MkII. Files were imported into IDEAS software and exported as FCS files, before analysing in FCS Express (DeNovo software) using the manufacturer's provided layouts. Using the Lip100™ size standard, vFRed-positive events were selected and calibrated using FCS Express transformations tool and inputting a surface area equation generated by the manufacturer's layout. This size calibration was then applied to samples from primary epithelial cells to size the EVs.

2.2.4.2. Fluorescent Limit of Detection

Anti-Human and Anti-Mouse IgG Quantum™ Simply Cellular fluorescent standardisation beads (Bangs Laboratories, Fishers, IN, USA) were used to assess antibody binding capacity on ImageStream X MkII and CytoFLEX S. 50µl of PBS was added to five different bead populations of differing binding capacity. Four of these bead populations were stained with double the recommended staining concentration of the antibody (defined by antibody manufacturer), ensuring saturation. The blank population remained unstained. Samples were incubated in the dark for 30 minutes at room temperature. 1ml of PBS was added to the samples and centrifuged at 2500g

for 5 minutes. Supernatants were aspirated and samples were resuspended in 1ml of PBS and centrifuged again at 2500g and resuspended in 500µl for Cytoflex S and 50µl for ImageStream X MKII to ensure all unbound antibody was washed away. LoDs were determined using product-specific templates provided by the manufacturer. All instrument lasers were set to max power for LoD analysis (unless stated otherwise).

2.2.5. Extracellular Vesicle Calcein-AM and Tetraspanin Staining

20µl of culture supernatant was isolated from stimulated samples at relevant time points and was stained and run immediately to prevent EV degradation in samples. 20µl of sample was stained with 10µm calcein-AM (Section 2.1.4) and 2.5µg/ml of antibody (Table 2.1) and incubated for 60 minutes (37^{o}C & 5% CO_2). EV staining was done in duplicate using 2 different antibody panels. A general EV tetraspanin panel stained for CD9, CD63 and CD81 and an Epithelial marker panel stained for EpCAM, Tspan8 and E-Cadherin (Table 2.1 shows all antibodies used, their staining concentration and fluorophore). Samples were then diluted 1:5 in 0.22µm filtered PBS and analysed using an ISX imaging flow cytometer (settings listed below).

2.2.6. ImageStream X MKII Acquisition Settings

ImageStream X Mk II (ISX) was equipped with 405nm (120mW) 488 nm (400mW), 561 nm (200 mW) 642 nm (2 mW) and 785 nm (100mW) lasers. All lasers were run at their maximum power unless specified. The sample flow rate was set to 44mm/sec (Setting: Speed to Low and Sensitivity to High). High Gain was turned on and magnification was set to 60x. Both camera 1 and 2's sensitivities were set to 32 for all channels and both camera's gains were 1. Eppendorf's containing a minimum of 20µl were loaded into the autosampler for analysis.

2.2.7. Size Exclusion Chromatography

Before analysis of EVs with Transmission Electron Microscopy (TEM), Transcriptomics cargo analysis and Nanoparticle Tracking Analysis (NTA), EVs were isolated and concentrated. Cell supernatants were removed

from wells and centrifuged for 5 minutes at 300g to remove cell debris. EVs were then isolated by size exclusion chromatography (SEC) using qEV original 35 columns with an automated fraction collector (Izon Science). Fractions 1-7 of 500 µL were collected, pooled, and concentrated by centrifuging at 4000g for 10 minutes using 10 kDa Amicon columns (Merck, UK).

2.2.8. Transition Electron Microscopy of Extracellular Vesicles

SEC isolated EVs were placed on carbon-coated 300 Cu mesh TEM grids (Cat.no. AGG2300C, Agar Scientific, UK) for 15 minutes and then fixed with 2% paraformaldehyde for 10 minutes. The grids were washed 5 times with deionised water before incubating with 4% Uranyl Acetate for 10 minutes. Excess stain was removed before allowing to dry completely, and then grids were imaged using a Tecnai BioTwin TEM, operating at 80kV, and images were recorded on a Gatan Orius camera.

2.2.9. Nanoparticle Tracking Analysis

SEC isolated EVs were diluted 1 in 1000 in 0.22 µM filtered PBS and inserted into an Analytik Zetaview mono (Analytik LtD, UK) to determine particle size distribution and quantification. Prior to analysis, a 1:10 dilution of 100 nm carboxylated polystyrene (IZON) and a 1:1000 dilution of 200 nm polystyrene (Malvern Panalytical) nanoparticles were used to calibrate the sensitivity of the instrument. Automatic settings were applied for the minimum expected particle size, minimum track length, and blur settings. Sensitivity was set at 78, gain at 26.88, and temperature set at 21 °C. National Institute of Standards and Technology (NIST) beads were run at a sensitivity of 65. Data processing and analysis of particle size distribution were performed using ZetaView Software (8.05.16.SP7) (Analytik LtD, UK).

2.2.10. Viability Assays

In accordance with MISEV recommendations viability of samples was assessed at sample collection time points (24 and 48 hours).

2.2.10.1. Annexin-PI

Annexin V and Propidium Iodide (PI) staining was used in 2D optimisation to assess culture viability. 10x Annexin binding buffer was diluted to 1x in deionised water. 200µl detached cell suspensions were harvested into FACS tubes, 1ml of 1x annexin binding buffer and centrifuged for 10 minutes at 300g. Supernatants were aspirated and pellets resuspended in 50µl of 1x binding buffer. 5µl Annexin V (FITC) as per manufacturer's instructions was added to cells and incubated at room temperature for 15 minutes. 1ml of 1x annexin binding buffer was added to the samples and centrifuged at 300g for 5 minutes. Supernatants were aspirated and pellets were resuspended in 200µl of binding buffer. 0.33µl of 1mg/ml PI staining solution was added to samples which were analysed immediately using flow cytometry.

2.2.10.2. Lactate Dehydrogenase (LDH) Assay

LDH assays were used to profile 3D culture viability. Culture media was isolated from stimulated culture at sampling time points (24 and 48 hours) and diluted in LDH storage buffer (1:5 dilution). Diluted samples were kept at -20^{o}C until assayed. Diluted samples were thawed prior to assays and 20µl of dilutions were transferred into opaque 384-well plates in duplicate. LDH standard was diluted in LDH storage buffer (as per manufactures instructions) and 20µl of serially diluted standard was plated in duplicate. 20µl of LDH detection reagent was added to all samples after preparation (Section 2.1.5.). Plates were sealed and incubated for 60 minutes at room temperature. Luminescence was measured using a GloMax Explorer Microplate Reader (Promega, US) with an integration of 1 second per well. The standard's known concentrations were plotted against luminesce scores (subtracted from blank sample) and fitted with a hyperbola curve using Graphpad Prism (10.5.0 software version). Sample LDH concentration (mU/ml) were interpolated from standards curves.

Percentage viability was calculated using the following equation:

$$Percentage\ Viability = 100 - \left(100\ \times \frac{Sample\ LDH\ Comcentration}{TritonX\ LDH\ Concentration}\right)$$

2.2.11. Cytokine ELISAs

Culture supernatant was harvested after incubation with different stimuli and concentration of cytokines IL-1β, IL-6, IL-8, IL-17E, IL-33 and TSLP were assessed by ELISA (R&D, UK) following manufacturer's instructions.

In brief, 384 well plates were coated with appropriate concentrations of capture antibody dissolved in PBS, as per manufacturer's instructions (Table 2.5) for relevant cytokines. Plates were sealed and incubated overnight at 4^{o}C. Capture antibody was the aspirated from wells and plates were washed three times with wash buffer (PBS-0.05%Tween-20) using a Biochrom ASYA Atlantis plate washing robot. Plates were then blocked with 100µl of 1X reagent diluent (Section 2.1.8.) and incubated for 1 hour at room temperature. Plates were then washed again as previous. Samples were diluted appropriately depending on cytokines evaluated (neat sample for all cytokines except IL-8, which was measured with 1:10 and 1:20 dilutions) and 20µl of dilutions was plated into 384 well plates in duplicate (unless stated otherwise). Standards were diluted in 1X reagent diluent and serially diluted in concentration ranges specified by manufacturers (Table 2.5). 20µl of standards was plated into 384 well plates in duplicate, with final wells of standards containing just 1x reagent diluent so background could be subtracted during analysis. Samples and standards were incubated at room temperature for 2 hours. Plates were washed again as previously and 20µl of appropriate detection antibodies diluted in 1X reagent diluent as per manufacturer's instructions (Table 2.5) were added to plates. Plates were incubated for 2 hours at room temperature and washed again as pervious. 20µl of 40-fold diluted Streptavidin-HRP was added to 384-well plates and incubated for 20 minutes at room temperature before washing as previously. 50µl of ultra TMB substrate solution was added to wells and incubated in the dark for 20 minutes at room temperature. Finally, 50µl of stop solution was added to plates and absorbance of samples was measured at 570nm (Reference wavelength) and 450nm (test wavelength) using an Agilent BioTek Epoch Microplate Spectrophotometer. Absorbance of known standard concentrations (Table 2.5) was plotted and fitted with a hyperbola curve to generate standard curves,

from which sample concentrations could be interpolated (pg/ml) (Graphpad Prism 10.5.0 Software).

Table 2.5. Table showing working concentrations of capture and detection antibodies for each cytokine assessed as well as the standard curve ranges.

Cytokine	Capture Antibody working Concentration (µg/ml)	Detection Antibody working Concentration (ng/ml)	Standard Curve Range (pg/ml)
IL-1β	4.0	75	3.91-250
IL-6	2.0	50	9.38-600
IL-8	4.0	10	31.2-2000
IL-17E (IL-25)	2.0	15	11.7-750
IL-33	1.0	30	23.4-1500
TSLP	0.8	3	31.2-2000

2.2.12. Der p 1 Cysteine Protease Activity

To assess the functionality of Lotox Der p 1 allergen stocks (Indoor Biotechnologies, UK), proteolytic activity was confirmed using a cysteine protease activity kit (Calbiochem®, UK). Test samples were made by diluting 20µg/ml Der p 1 to a final concentration of 10µg/ml in either 0.22µm sterile filtered PBS or 0.22µm sterile filtered PBS combined with 5mM L-cysteine (active Der p 1) or 5mM L-cysteine and 10µM E-64 (Inactivated Der p 1). 10µl of test samples and 1mg/ml trypsin control were separately plated into 96-well plates and combined with 25µl of FTC-casein and 25µl incubation buffer and incubated for 24 hours (37^{O}C). 120µl of 5% TCA (Section 2.1.7.) was added to each well and incubated for 20 minutes at 37ºC. Plates were centrifuged at 400xg and 4ºC for 15 minutes. 40µl of supernatant was isolated from samples and plated into a 96-well flat bottom plate. Each sample was mixed with 160µl of assay buffer and absorbance of samples was measured at 492nm using an Agilent BioTek Epoch Microplate Spectrophotometer.

2.2.13. *Bacillus* Protease Activity

An EnzChek® Protease Assay Kit (Invitrogen, UK) was used to assess the protease function after nebulisation. 500µl of sample was isolated from all

wells of a 24-well plate, nebulised with protease, diluted in 500µl 1X digestion buffer (Section 2.1.9). 100µl of dilution of each sample was plated in duplicate into 384-well microplates and 100µl of 10µg/ml BODIPY TR-X casein (Section 2.1.9) was added to the samples. A standard was prepared by performing 1:2 serial dilutions of protease stock and subsequently were prepared and plated as previously described. Samples were incubated in the dark at room temperature for 60 minutes. Sample florescence was read at 645nm and standard sample fluorescence was plotted against known concentration and fitted with a curve to allow for interpolation of unknown sample concentrations.

2.2.14. Transcriptomic Analysis

To ensure enough EVs were present in samples to get robust data, 70µl of 48-hour basal samples was collected from each of the six repeats. These six samples were combined in pairs to create three samples and EVs were isolated and concentrated as described (Section 2.2.7). Samples were stored at -80°C until being shipped to TAmiRNA (Austria) for RNA isolation and transcriptomic analysis.

2.2.14.1. RNA Isolation of EVs

RNA isolations were performed by TAmiRNA on SEC isolated EV samples. Total RNA was extracted from EV suspension using the miRNeasy Mini Kit (Qiagen, Germany, Cat. 217004). Each sample was treated with 1ml of Qiazol. Additionally, a synthetic RNA oligonucleotide mix obtained from the miRCURY Spike-In kit (Qiagen, Germany, Cat. 339390) was added to each sample at equimolar amounts to monitor RNA extraction efficiency. After incubation at room temperature for 15 minutes, 200 µL chloroform were added to the lysates followed by cooled centrifugation at 12,000g for 15 minutes at 4°C. Precisely 650µL of the upper aqueous phase were mixed with 7µL glycogen (5mg/mL) to enhance precipitation. Samples were transferred to a miRNeasy mini column, and RNA was precipitated with ethanol followed by automated washing with RPE and RWT buffer in a QiaCube liquid handling robot. Finally, total RNA was eluted in 30 µL nuclease free water and stored at -80°C until further analysis.

2.2.14.2. Small RNA Sequencing Analysis

For all samples, 4,25 µL of total RNA was used as an input for small RNA sequencing library preparation. To each RNA sample 1µL of miND spike-in standards (TAmiRNA, Austria) were added prior to small RNA library preparation using the RealSeq Biofluids library preparation kit (RealSeq Biosciences / BioCat Cat.600-00048-SOM). Adapter-ligated libraries were amplified with 20 PCR cycles using barcoded Illumina reverse primers in combination with the Illumina forward primer. Library quality control was performed using an Agilent Small Fragment Kit (Cat. DNF-476-0500). An equimolar pool consisting of all sequencing libraries was prepared and sequenced in single read mode with 100 cycles on an Illumina NextSeq 2000 P2 Flowcell.

2.2.14.3. Transcriptomic Analysis

Transcriptomic analysis was conducted by TAmiRNA. Their analysis methodology is as follows: Next-generation sequencing (NGS) data was analysed using the miND® analysis pipeline (Diendorfer *et al.,* 2022): Overall quality of the NGS data was evaluated automatically and manually with fastQC v0.12 (Andrews, 2010) and multiQC v1.14 (Ewels *et al.,* 2016). Reads from all passing samples were adapter trimmed and quality filtered using cutadapt v3.3 (Martin, 2011) and filtered for a minimum length of 17nt. Mapping steps were performed with bowtie v1.3.0 (Langmead *et al.,* 2009) and miRDeep2 v2.0.1.2 (Friedländer *et al.,* 2012), whereas reads were mapped first against the genomic reference GRCh38.p12 provided by Ensembl (Zerbino *et al.,* 2018) allowing for two mismatches and subsequently miRBase v22.1 (Griffiths-Jones, 2004), filtered for miRNAs of hsa only, allowing for one mismatch. For a general RNA composition overview, non-miRNA mapped reads were mapped against RNAcentral v23.0 (Sweeney *et al.,* 2019) and then assigned to various RNA species of interest. Statistical analysis of preprocessed NGS data was done with R v4.3 and the packages pheatmap vNA, pcaMethods v1 and genefilter v1. Differential expression analysis with edgeR v4.0 (Robinson *et al.,* 2010) used the quasi-likelihood negative binomial generalized log-linear model functions provided by the package. The independent filtering method of DESeq2 (Love *et al.,* 2014) was

adapted for use with edgeR to remove low abundance miRNAs and thus optimize the false discovery rate (FDR) correction. Additional NGS QC and absolute quantification of miRNAs was done using miND® spike-ins (Khamina *et al.,* 2022) based on a linear regression model.

2.2.15. Statistical Analysis

All statistical analysis was performed using GraphPad Prism 10.5.0. p-values of <0.05 were considered significant fort all experiments. All data was analysed for normality using Shapiro-Wilk tests. Where normally distributed, One-way ANOVA with Dunnett's multiple comparison tests were used. If data was non-parametric, a Kruskal-Wallis test with Dunnett's multiple comparison was used instead. The majority of tests used were One or Two-way ANOVA's with Dunnett's multiple corrections tests. Figure legends outline specific tests and corrections used to calculate shown significances.

Chapter 3: The Role of Epithelial-Derived Extracellular Vesicles in Allergic Sensitisation: A Systematic Review

3.1. Introduction

IgE-mediated allergy, also known as Type 1 hypersensitivity or atopic allergy, is a subtype of allergy involving immunoglobulin E (IgE) and is characterised by the rapid onset of symptoms after contact with an allergen. This type of allergy has seen an increase in prevalence over the past decades, with up to an estimated 30% of adults and 40% of children now being sensitised to at least one allergen, such as pollen, dust or food (Pawankar, 2014). In conjunction with this, there has also been an increased burden on healthcare systems (Pawankar, 2014, Warren *et al.,* 2020). Sensitisation is the first stage in the development of an IgE-mediated allergy. It occurs after initial allergen exposures and results in an individual's mast cells and basophils becoming primed with IgE-specific antibodies to a given allergen. Once sensitised, individuals can progress to being symptomatic with further exposures to an allergen leading to cross-linking of IgE and release of chemical mediators from mast cells and basophils that cause symptoms such as rhinitis, asthma, urticaria and in rare cases anaphylaxis. Proteins are the predominant triggers of allergic sensitisation and the most common target of the triggered IgE response, however recent research has also implicated both lipids (Hopkins *et al.,* 2022, Hopkins *et al.,* 2023, Tordesillas *et al.,* 2017) and carbohydrates (Hils *et al.,* 2020, Keumatio Doungstop *et al.,* 2021, Royer *et al.,* 2010) as other molecules that can influence allergic sensitisation.

The epithelium serves as the first barrier to the external environment and allergens. Once thought of as just a physical barrier, the epithelium has now been shown to have a more complex relationship with the immune system, interacting with and helping to orchestrate immune responses through its communication with dendritic cells, effector T cells and macrophages (Jakwerth *et al.,* 2022). Dysfunction and penetration of the physical barrier are frequently observed in allergic diseases, representing one of the initial steps in

allergic sensitisation. Some allergens have been shown to cleave tight junctions (TJ) between cells, facilitating allergen entry and driving subsequent allergic sensitisation (Georas and Rezaee, 2014, Hellings and Steelant, 2020, Jakwerth *et al.,* 2022, Wan *et al.,* 1999). This forms the basis of the epithelial barrier hypothesis, where penetration of these TJs has been shown to facilitate induction and polarisation of the immune system towards a Th2 response through the secretion of cytokine mediators, such as Interleukin (IL)-25, IL-33 and Thymic Stromal Lymphopoietin (TSLP) (Akdis, 2021, Grotenboer *et al.,* 2013, Michaudel *et al.,* 2018, Sugita and Kabashima, 2020, Ziegler, 2012). Moreover, the route of allergen exposure is believed to in-fluence allergic sensitisation. The dual allergen exposure hypothesis suggests that early oral exposure to peanuts promotes tolerance, while exposure through the skin, without concurrent oral exposure, leads to allergy (Du Toit *et al.,* 2018). Additionally, more recent studies have updated the initial hypothesis to also include the airway as an alternative route of sensitisation to peanut leading to food allergy (Kulis *et al.,* 2021). Consequently, it is now well-established that epithelial cells play a key role in IgE-mediated allergic sensitisation, though details of the mechanisms involved are still to be fully elucidated.

Recent research has started to shed light on a new potential mediator, extracellular vesicles (EVs), secreted by epithelial cells, that could influence the development of an allergic phenotype (Hovhannisyan *et al.,* 2021). EVs are defined as membrane-bound particles released from cells, including epithelial cells, fibroblasts, mesenchymal cells, dendritic cells, B cells, T cells, mast cells and tumour cells, among others. They have an inability for self-replication and can serve as intercellular communicators (Welsh *et al.,* 2024). The presence of EVs has also been shown in multiple body fluids, including saliva, plasma, breast milk, urine, bronchoalveolar lavage and malignant effusions. EVs vary significantly in size, ranging from 30nm to 10μm, and are currently divided into the subtypes: microvesicles, exosomes, apoptosome and autophagic EV. This classification reflects their size, biogenesis, method of re-lease and function (Doyle and Wang, 2019, Jeppesen *et al.,* 2019, Johnson *et al.,* 2020, Sheta *et al.,* 2023). EVs can facilitate intercellular communication through the transmission of various biomolecules (lipids, proteins, sugars and

nucleic acids) (Johnson *et al.,* 2020, Yáñez-Mó *et al.,* 2015). The transmission of these biomolecules or "cargo" to other cells, or simply receptor-mediated binding of EVs at the cell surface, results in the downstream influence of essential cellular processes required for the maintenance of homeostasis (El Andaloussi *et al.,* 2013, Mohammadipoor *et al.,* 2023), with EVs being shown to influence processes such as immune surveillance (Raposo *et al.,* 1996), tissue repair (Gatti *et al.,* 2011), and blood coagulation (Del Conde *et al.,* 2005).

Epithelial-derived EVs have recently been highlighted in the pathogenesis of allergies, with roles in type 1 hypersensitivity disorders, such as asthma and allergic rhinitis (AR) being reported (Fang *et al.,* 2021, Harvey-Seutcheu *et al.,* 2024, Hovhannisyan *et al.,* 2021, Sangaphunchai *et al.,* 2020). Although the literature is limited, research into epithelial-derived EVs and their facilitation of immune communication could provide the potential to better understand the mechanisms that underpin allergic sensitisation. In addition, this may lead to an insight into new therapeutic strategies, as well as interventions, to help mitigate the ever-increasing prevalence of Type 1 hypersensitivities. Thus, this systematic review aims to investigate the current understanding of the potential role of epithelial-derived EVs in IgE-mediated allergic sensitisation, whether indirectly (e.g. through affecting epithelial barrier integrity) or more directly through alteration of the immune environment (e.g. promoting a Th2-dominant milieu).

3.2. Materials and Methods

3.2.1. Search Strategy

This review was conducted following the Preferred Reporting Item for Systematic Re-views and Meta-Analyses (PRISMA) 2020 guidelines. Relevant articles were identified using three databases: EMBASE, PubMed and Web of Science up to 30th January 2025. A search for grey literature was also conducted with no relevant articles being found. Databases were filtered for the removal of review articles as well as articles not published in English.

The search terms used, constructed around the two key terms 'epithelial vesicles' and 'allergy', were: "Epithelial," "Epithelium," "BALF," " Bronchoalveolar Lavage Fluid," "Lavage" and "Extracellular Vesicles," "EVs," "Microvesicle," "Exosome," "Ectosome," "Shedding Vesicle," "Microparticle" and "Allergic Response," "Allergy," "Allergen," "Sensitisation," "Type 1 Hypersensitivity," "IgE," "Tolerance" using the advanced search settings for each database, as per Supplementary Document 1.

The search yielded a total of 608 articles: 284 from PubMed, 213 from Embase and 111 from Web of Science. Articles from the searches were imported into EndNote where duplicates were removed and the remaining articles were screened initially by title and then subsequently by abstract to remove articles not relevant to the potential role of epithelial-derived EVs in IgE-mediated allergic sensitisation. This initial screening was subsequently validated by an independent reviewer. The remaining articles then had their full texts screened and were evaluated by WB, and independently by GH, for inclusion in the study using the inclusion/exclusion criteria outlined in Table 3.1. A PRISMA 2020 diagram outlines the process followed for the identification and inclusion of relevant articles in this systematic review (Figure 3.1).

Table 3.1: The inclusion and exclusion criteria used to determine eligibility.

Inclusion	Exclusion
IgE-mediated allergy	Non-original research paper, e.g. reviews, commentary, case report, etc.
Epithelial-derived EVs	Non-IgE-mediated allergies
Allergic sensitisation	Non-English language publications
Clinical data	Conference abstract
Experimental data	Research involving nanoparticles but not extracellular vesicles from a cell source
Healthy subjects	Pre-prints
Allergic subjects	correspondence
Human studies	
Animal models	
Research involving the extraction, identification, or production of EVs or their contents, such as DNA, miRNA, or protein	
Isolation method of EVs included	

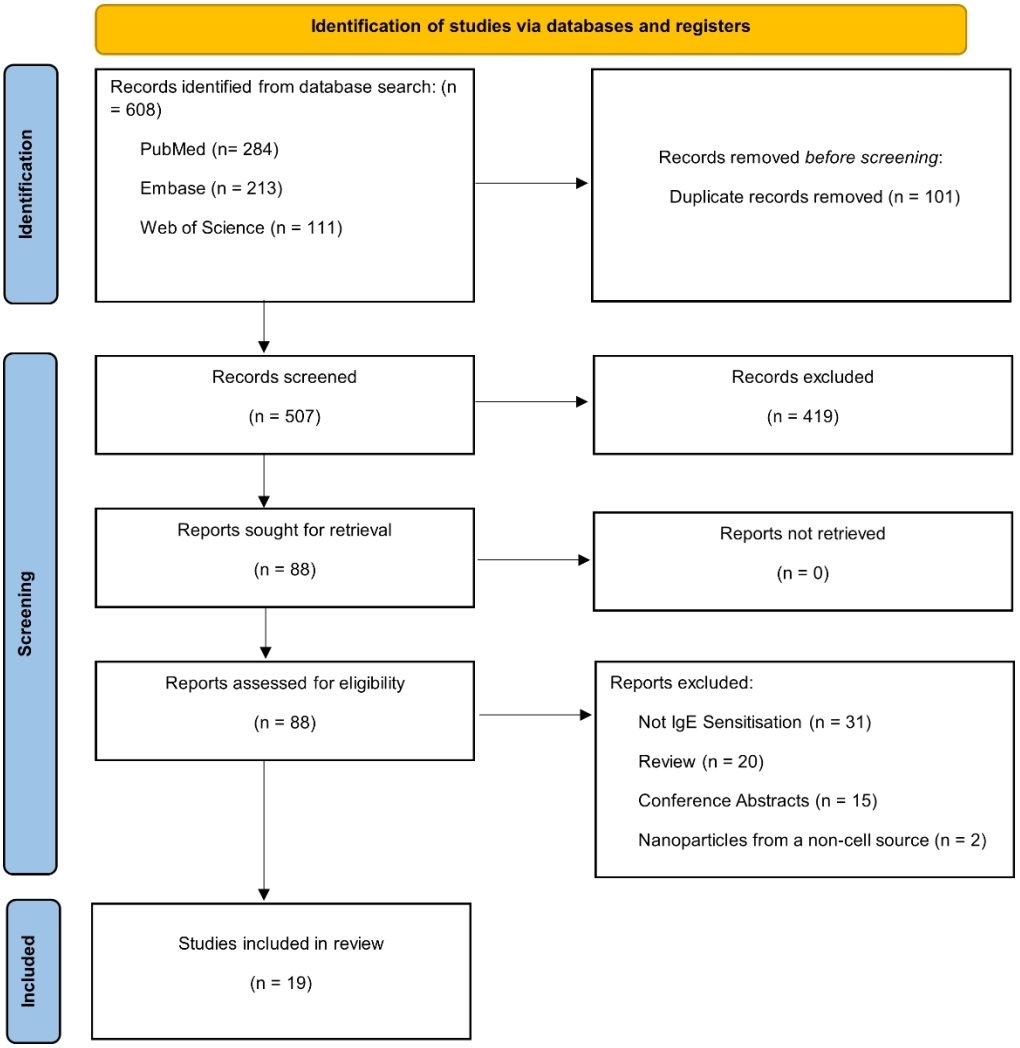

Figure 3.1. A PRISMA 2020 Flow diagram summarising the process for the selection of article within the study.

3.2.2. Data extraction and quality assessment:

Ultimately, 18 papers were found to provide information on the potential role of epithelial-derived EVs in IgE-mediated allergic sensitisation and so were eligible for inclusion. Data regarding the design of the research was subsequently reviewed and the studies' quality was scored based on a set of criteria outlined in Table 3.2. Scores were attributed to each paper under the following sections: Model used, Allergen Characterisation, Robustness of the model, Sample size, EV isolation and EV characterisation. Due to the variety of different models utilised in the papers, it is possible for studies to receive multiple scores relating to the models, their robustness, and sample size. Consequently, a paper's final score is reflected as a percentage of the aggregate total marks for all models. The aim of this scoring system was to allow for a comprehensive evaluation of research by the current guidelines for EV research, with low scores not reflecting a study's validity and reliability but lacking factors that could further strengthen the study.

Table 3.2: Criteria used to derive study quality scores.

Category	Scoring Criteria
Model: If multiple models used a combined score is given	- Cell Culture (*In Vitro* - murine) (1) - Animal Model (*In Vivo*) (2) - Cell Culture (*In Vitro* - human) (3) - Human (*Ex Vivo*) (4)
Material Used for sensitisation: Summative score of all points	- Allergen used to sensitize clearly defined (1) - Endotoxin measurements performed (1) - Protein content measurements performed (1)
Robustness of Model: If multiple models used a combined score is given	Human studies (*Ex Vivo*): - Allergic Status not specified or not clearly defined (0) - Allergic Patients were sought from a Clinical Setting (1) - Allergic patients were sought from Clinical Setting AND had a positive testing to allergen (Specific IgE, skin test or challenge) (2) - Allergic patients were sought from a Clinical Setting with a non-sensitised control group (3) - Allergic patients were sought from Clinical Setting AND had a positive testing to allergen (Specific IgE or Positive allergen Challenge) with a healthy control group (4) Animal Model (In Vivo): - Sensitisation of animals not specified or defined (0) - Sensitisation of animals partially defined (Discloses some but NOT all the following: exposure method, dosing, and duration) (1) - Sensitisation of animals fully defined outlining (exposure method, dosing, and duration) (2) - Sensitisation of animals partially defined (Discloses some but NOT all the following: exposure method, dosing, and duration) with a negative control group (3) - Sensitisation of animals fully defined outlining (exposure method, dosing, and duration) with a negative control group (4) Cell Culture (*In Vitro*): - Transformed Cell Line using partially defined exposures (Discloses some but NOT all the following: exposure method, dosing, and duration) (1) - Transformed Cell Line using fully defined exposures (exposure method, dosing, and duration) (2) - Primary Cells using partially defined exposures (Discloses some but NOT all the following: exposure method, dosing, and duration) (3) - Primary Cells using fully defined exposures (exposure method, dosing, and duration) (4)

Sample Size: If multiple models used a combined score is given:	Human studies (*Ex Vivo*): - Number of participants not defined (0) - 5 or less participants per group (1) - 6 to 10 participants per group (2) - 11 or more participants per group (3) Murine Model (*In Vivo*): - Number of animals per group not defined (0) - 5 or less animals per group (1) - 6 to 10 animals per group (2) - 11 or more animals per group (3) Cell Culture (*In Vitro*): - n not specified (0) - n = 1 (1) - n = 3 (2) - n > 3 (3)
EV Isolation	No Isolation - precipitation only techniques Studies looking direct in a liquid with no isolation applied (usually done on very low volume samples). (0) Poor – ultra centrifugation at one speed or serial UC without sucrose cushion. (1) Fair - size exclusion chromatography (without a precipitation or concentration step) or Immuno- capture beads for investigation of non-specific populations. (2) Good - Size exclusion chromatography with a precipitation or concentration step or the use of a specific isolation method such as exosome EV isolation, purification kits or Immuno-capture beads utilizing a unique marker. (3)
EV characterisation	No Characterisation – No attempt made to profile or characterise EVs or Exosomes. (0) Poor – Use of Just one characterisation technique (Quantification, sizing, biomarkers, cargo analysis) (1) Fair – The use of multiple complimentary characterisation techniques and at least 1 biomarker. (2) Good – Everything mention prior as well as appropriate controls (E.g. robust profiling of culture conditions such as media, inclusion of positive and negative controls such as those recommended by MISEV2018) (3) Very Good – Everything mentioned in prior as well the addition of extra biomarkers (3+) or the utilization of any other novel techniques. (4)

3.1.Results

3.1.1. PRISMA and Publication Selection:

A total of 18 publications fulfilling the criteria for inclusion were identified in this review (Tables 3.3, 3.5 and 3.7). The earliest study was published in 2008 and from this point onwards there has been a relatively consistent publication rate (Figure 3.2A). The results indicate that currently, all research in this area focuses on three epithelial EV sources, namely the nasal, bronchial/alveolar and intestinal epithelia (Figure 3.2B). In this review, results have been divided by these three sources of EVs, with details of their potential role in allergic sensitisation reported.

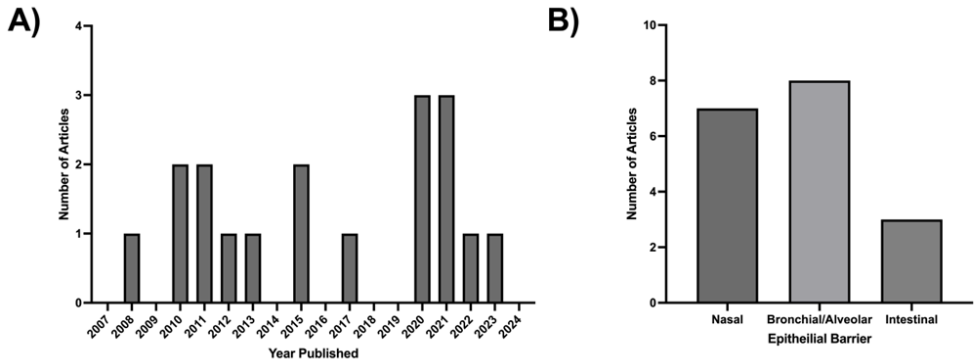

Figure 3.2. Metrics on publications identified for inclusion in the review **(A)** Number of publications over time **(B)** Number of publications concerning each epithelial barrier.

3.1.2. Nasal Epithelial-Derived Extracellular Vesicles (ne-EVs)

In total, seven publications with information on the potential role of EVs derived from the nasal epithelium in IgE-mediated allergic sensitisation were identified (Table 3.3) (Li *et al.,* 2023, Luo *et al.,* 2015, Qiu *et al.,* 2011, Qiu *et al.,* 2012, Wang *et al.,* 2021, Wu *et al.,* 2015, Zhu *et al.,* 2020). Two of the publications appeared to contain repeat data and raised questions regarding controls and methodologies used. As a result, these are not described in detail here but are included in Table 3.3 as they met the search and screening criteria described (Qiu *et al.,* 2011, Qiu *et al.,* 2012). Of the five other publications identified, four described effects of ne-EVs on Th1/Th2 polarisation, which could influence IgE-mediated allergic sensitisation. In one paper, IL-10-

secreting monocytes were shown to be induced by nasal epithelial EVs containing mRNA-146α. These IL-10+ monocytes exhibited an immunosuppressive effect on CD4+ effector T cells and subsequent Th2 polarisation (Luo *et al.,* 2015). In another, the examination of variation in epithelial EV cargo between healthy patients and individuals with AR revealed significant differences in the expression of a wide variety of mRNAs. Specifically, these mRNAs were involved in key pathways associated with allergic development, such as c-fos, Lyn and MUC7 (Wu *et al.,* 2015). Investigation into the relative expression of microRNA-146α-5p (miR-146α-5p) in the nasal epithelial-derived EVs revealed significant downregulation in AR patients. The expression of miR-146α-5p was shown to play an important role in the Th1/Th2 differentiation, with lower expression being demonstrated to promote Th2 differentiation and IL-4 cytokine secretion from naïve CD4+ T cells (Li *et al.,* 2023). Two studies examined the influence of Long non-coding RNA (lncRNA) cargo in ne-EVs (Wang *et al.,* 2021, Zhu *et al.,* 2020) . Growth arrest specific 5 (GAS5) was identified as a cargo of ne-EVs. GAS5 was shown to influence Th1/Th2 differentiation through the downregulation of T-bet and the enhancer of Zeste 2 polycomb repressive complex 2 subunit (EZH2), suppressing Th1 differentiation and promoting Th2 polarisation (Zhu *et al.,* 2020). Ne-EVs containing LncRNA Nuclear Paraspeckle Assembly Transcript 1 (NEAT1) were shown to facilitate the pathogenesis of AR through the induction of IL-13 mediated inflammatory response, as well nasal epithelial cell apoptosis. The ne-EV-induced damage to the epithelium facilitates allergen barrier penetration ultimately allergic sensitisation (Wang *et al.,* 2021).

Table 3.3. Studies involving Nasal epithelial-derived EVs (ne-EVs).

First Author	Title	Allergen	Cells Responding	Model	Isolation	Characterisation	Reported Findings
Qiu et al, 2011 and 2012	**2011** Cytotoxic T lymphocytes mediate chronic inflammation of the nasal mucosa of patients with atypical allergic rhinitis (Qiu *et al.,* 2011) **2012** Antigen-specific activities of CD8+T cells in the nasal mucosa of patients with nasal allergy (Qiu *et al.,* 2012)	Der P 1	Dendritic Cells and CD8+ T cells	Cell Line (RPMI2650) and Human Patients	**Serial Ultracentrifugation**: 300× g 10min, 1200× g 20min, 10,000× g 30min, 100,000× g 1h.	EM, Western Blot and Bradford Assay	Staphylococcal enterotoxin B (SEB) & Der p 1 pulsed EVs , (and those pulsed with LPS), induced dendritic cell maturation. DCs matured with SEB & Der p 1 pulsed generated allergen specific granzyme B and perforin secreting $CD8^+$ cytotoxic T Cells (Qiu *et al.,* 2011) A higher frequency of CD8+ T cells in patient samples compared to controls (Qiu *et al.,* 2012)
Luo et al 2015 (Luo *et al.*, 2015)	Epithelial cell-derived microRNA-146a generates interleukin-10-producing monocytes to inhibit nasal allergy	N/A	Monocytes	Human Patients, Cell Line (RPMI 2650) and Mouse Model (BALB/c)	**Serial Ultracentrifugation**: 300× g 10min, 1200× g 20min, 10,000× g 30min, 100,000× g 1h.	Western Blot and RTq-PCR	Reduced expression of mRNA-146α in EVs of patients with AR compared to healthy controls prevents the induction of IL-10^+ monocytes were shown to have a suppressive effect $CD4^+$ effector T cells and Th2 Polarisation
Wu et al 2015	Altered microRNA Expression Profiles of Extracellular Vesicles in Nasal Mucus from Patients with Allergic Rhinitis	N/A	N/A	Human Patients	**Serial Ultracentrifugation**: 3000× g 15min, 10,000× g 30min, 50,000× g 1h, 100,000× g 1h.	FACS and RTq-PCR	Cargo analysis of EVs from patients with AR compared to healthy controls showed changes in expression of a wide variety of mRNAs involved in key pathways associated with allergic development such as the c-fos, Lyn and MUC7

Zhu et al 2020	Exosomal long non-coding RNA GAS5 suppresses Th1 differentiation and promotes Th2 differentiation via downregulating EZH2 and T-bet in allergic rhinitis	Ovalbumin	Naïve CD4+ T cells	Human Patients and Cell Culture (RPMI 2650)	**Serial Ultracentrifugation**: 12,000× g 45min, 110,000× g 2h, 110,000× g 70min	TEM, Western Blot and RTq-PCR	GAS5 can influence Th1/Th2 differentiation downregulating T-bet ultimately suppressing Th1 differentiation and promoting Th2 polarisation
Wang et al 2021	Exosomal lncRNA Nuclear Paraspeckle Assembly Transcript 1 (NEAT1)contributes to the progression of allergic rhinitis via modulating microRNA-511/Nuclear Receptor Subfamily 4 Group A Member 2 (NR4A2) axis	N/A	N/A	Human patients and Cell Culture (Primary Cells)	**Precipitation** - EXOQuick Kit	TEM, Western Blot and RTq-PCR	EVs containing LncRNA NEAT1 induce IL-13 mediated inflammatory responses and nasal epithelial cell apoptosis.
Li et al 2023	ESP-B4 promotes nasal epithelial cell-derived extracellular vesicles containing miR-146a-5p to modulate Smad3/GATA-3 thus relieving allergic rhinitis ESP-B4/miR-146a-5p in AR	Ovalbumin	Naïve CD4+ T cells	Human Patients, Rat Model (Wistar Rats) and Cell Culture (RPMI2650)	**Serial Ultracentrifugation**: 12,000× g 45min, 110,000× g 2h, 110,000× g 70min	TEM, Western Blot, NTA and RTq-PCR	Down regulation of miR-146α-5p in AR patients compared to healthy controls was shown to play an important role in the Th1/Th2 differentiation

With regards to quality scores, all publications reporting information related to the potential role of ne-EVs in allergic sensitisation utilised human AR patient samples. In general, all studies received good human study robustness scores, with all studies seeking allergic patients from a clinical setting (Li *et al.,* 2023, Luo *et al.,* 2015, Qiu *et al.,* 2011, Qiu *et al.,* 2012, Wang *et al.,* 2021, Wu *et al.,* 2015, Zhu *et al.,* 2020). Five publications also included defined healthy control patient samples (Li *et al.,* 2023, Luo *et al.,* 2015, Qiu *et al.,* 2012, Wang *et al.,* 2021, Wu *et al.,* 2015, Zhu *et al.,* 2020). Six studies describe using a diagnostic test such as serum-IgE measurement or skin testing to identify allergen-sensitised or allergic patients (Li *et al.,* 2023, Luo *et al.,* 2015, Qiu *et al.,* 2011, Qiu *et al.,* 2012, Wu *et al.,* 2015, Zhu *et al.,* 2020). Only one study did not perform such a test (Wang *et al.,* 2021). Five studies used more than 11 participants per group receiving maximum sample size scores (Li *et al.,* 2023, Luo *et al.,* 2015, Qiu *et al.,* 2011, Wang *et al.,* 2021, Zhu *et al.,* 2020), however, one publication did not include a control group (Qiu *et al.,* 2011). Two studies received lower sample size scores with one study utilising 10 participants per group (Luo *et al.,* 2015) and the other study, whilst having more than 11 participants in their allergic groups, only had 10 controls, consequently receiving a lower score (Qiu *et al.,* 2012). Five studies also utilised a cell line model (Li *et al.,* 2023, Qiu *et al.,* 2011, Qiu *et al.,* 2012, Wang *et al.,* 2021, Wu *et al.,* 2015), two of these using the transformed cell line RPMI2650 (Li *et al.,* 2023, Qiu *et al.,* 2011, Qiu *et al.,* 2012, Wu *et al.,* 2015) and one using primary cells (Wang *et al.,* 2021). Reporting on the exposure of these cell lines was generally poor and only two studies fully defined their exposure (Li *et al.,* 2023, Wang *et al.,* 2021). Two studies also implemented animal models (Li *et al.,* 2023, Luo *et al.,* 2015) and received identical robustness and sizing scores, fully defining exposure and using 6-10 animals per group. Defining the sensitisation material used was poor across all papers. While not all papers used allergens in their models, those that did only reported the allergen used and provided no further information, such as protein or endotoxin measurements (Li *et al.,* 2023, Qiu *et al.,* 2011, Qiu *et al.,* 2012, Wu *et al.,* 2015).

Concerning EVs, six of seven studies used sequential ultracentrifugation stages for the isolation of EVs (Li *et al.,* 2023, Luo *et al.,* 2015, Qiu *et al.,* 2011, Qiu *et al.,* 2012, Wu *et al.,* 2015, Zhu *et al.,* 2020), with one study utilising an ExoQuick EV precipitation kit (Wang *et al.,* 2021). EV characterisation varied between the papers, however, six of the seven studies utilised western blots (Li *et al.,* 2023, Luo *et al.,* 2015, Qiu *et al.,* 2011, Qiu *et al.,* 2012, Wang *et al.,* 2021, Zhu *et al.,* 2020) to characterise either EV Cargo (Qiu *et al.,* 2011, Qiu *et al.,* 2012) or surface proteins (Li *et al.,* 2023, Luo *et al.,* 2015, Wang *et al.,* 2021, Zhu *et al.,* 2020). Five studies used microscopy techniques, two using immunogold electron microscopy (Qiu *et al.,* 2011, Qiu *et al.,* 2012) and three imaged using conventional TEM (Li *et al.,* 2023, Wang *et al.,* 2021, Zhu *et al.,* 2020). RTq-PCR was also used for cargo analysis and quantification by five papers (Liu, 2002, Luo *et al.,* 2015, Wang *et al.,* 2021, Wu *et al.,* 2015, Zhu *et al.,* 2020). Two studies used nano tracking analysis (NTA) to profile EV sizing (Li *et al.,* 2023, Wang *et al.,* 2021). Lastly, one paper used flow cytometry to profile tetraspanin biomarkers on EVs (Wu *et al.,* 2015). In general, none of the studies received a characterisation score lower than 'Poor' and made an attempt to characterise isolated EVs. Two studies received 'poor' characterisation scores despite using multiple complimentary techniques due to a lack of EV biomarker characterisation (Qiu *et al.,* 2011, Qiu *et al.,* 2012), the remaining 5 studies all profiled at least one EV biomarker alongside complimentary techniques (Li *et al.,* 2023, Luo *et al.,* 2015, Wang *et al.,* 2021, Wu *et al.,* 2015, Zhu *et al.,* 2020). The characterisation scores were also observed to improve with publishing date. The lowest scores received by studies were 52% (Luo *et al.,* 2015) and 53% (Qiu *et al.,* 2011), with all other studies scoring 56% and above (Li *et al.,* 2023, Qiu *et al.,* 2012, Wang *et al.,* 2021, Wu *et al.,* 2015, Zhu *et al.,* 2020). One study received a score of 76% due to its robust use of human, murine and cell line models coupled with its comprehensive characterisation EV characterisation with this study being the only one of the seven to receive the maximum characterisation score (Li *et al.,* 2023). All scores attained by these studies are fully outlined in Table 3.4.

Table 3.4: Scoring of paper involving Nasal epithelial derived EVs (ne-EVs).

Author	Model (n/10)	Robustness of Model			Sample Size			Sensitisation Material (n/3)	EV Isolation (n/3)	EV Characterisation (n/4)	Total Score	Bias Score
		Murine Model (n/4)	Cell Culture (n/4)	Human Studies (n/4)	Murine Model (n/3)	Cell Culture (n/3)	Human Studies (n/3)					
Qiu et al, 2011	Human Patient samples (4) Cell Culture - Human (3)		Immortalized cell line, partially defined exposure (1)	From Clinical setting and positive skin prick test (2)		3 repeats (2)	11 or more participants per group (3)	Allergen Defined (1)	Serial UC (1)	One Method Utilized (1)	18/34	53%
Qiu et al, 2012	Human Patient samples (4) Cell Culture - Human (3)		Immortalized cell line, partially defined exposure (1)	Allergic Patients from clinical setting with serum IgE, IgG, skin prick test and non-allergic but chronic rhinitis controls (4)		3 repeats (2)	6-10 participants per group (2)	Allergen Defined (1)	Serial UC (1)	One Method Utilized (1)	19/34	56%
Luo et al, 2015	Human Patients samples (4), Cell Culture - Human (3), Animal Model (2)	Sensitisation fully defined (4)	Immortalized cell line, partially defined exposure (1)	Allergic Patients from clinical setting with serum IgE, IgG, skin prick test and healthy controls (4)	6 -10 animals per group (2)	3 repeats (2)	6-10 participants per group (2)	Allergen Defined (1)	Serial UC (1)	Multiple complimentary Techniques (2)	28/41	66%
Wu et al, 2015	Human Patient samples (4)			Allergic Patients from clinical setting with serum IgE, IgG, skin prick test and healthy controls (4)			11 or more participants per group (3)		Serial UC (1)	Multiple complimentary Techniques (2)	14/27	52%
Zhu et al, 2020	Human Patient samples (4)			Allergic Patients from clinical setting with serum IgE, IgG, skin prick test and healthy controls (4)			11 or more participants per group (3)		Serial UC (1)	Multiple Complementary techniques and suitable controls (3)	15/27	56%

Wang et al, 2021	Human Patient samples (4) Cell Culture - Human (3)		Primary Cell line and fully defined exposures (4)	Allergic Patients from a clinical setting and a control group (3)		3 repeats (2)	11 or more participants per group (3)		Precipitation - EXOQuick-TC (3)	Multiple Complementary techniques and suitable controls (3)	25/34	74%
He-Li et al, 2023	Human Patients samples (4), Cell Culture - Human (3), Animal Model (2)	Sensitisation fully defined (4)	Transformed cell line and fully defined exposure (2)	Allergic Patients from clinical setting with serum IgE, IgG, skin prick test and healthy controls (4)	6 -10 animals per group (2)	3 repeats (2)	11 or more participants per group (3)	Allergen Defined (1)	Serial UC (1)	Multiple Complementary techniques and suitable controls and additional biomarkers (4)	32/41	78%

3.1.3. Bronchial/Alveolar Epithelial-Derived Extracellular Vesicles (bae-EVs)

Eight publications reporting data on the potential role of bae-EVs in allergic sensitisation were identified (Table 3.5). Two publications investigated the influence of EVs isolated from the bronchial alveolar lavage fluid (BALF) of mice tolerised to the allergen Ole e 1 (ExoTol). The first study revealed that these Exotol were able to inhibit a Th2 response through the suppression of IgE and IgG1 and upregulation of TGF-β (Prado *et al.,* 2008) . A follow-on study investigated Exotol's impact on sensitisation to other antigens. In this study a 'bystander suppression' was observed with Exotol inhibiting sensitisation to the allergen Bet v 1, suppressing IgE and IgG1, as well as the Th2 cytokines IL-5 and IL-13 (Prado *et al.,* 2010). One study demonstrated that LPS exposure enhanced bae-EVs production and that the LPS-induced bae-EVs enhanced sensitisation to ovalbumin in mice, as well as promote TNF-a and IL-6 secretion in macrophages (Shin *et al.,* 2010). Enhanced bae-EV secretion and cargo changes were also noted in Th2 cytokine-stimulated epithelial cells in another study. These bae-EVs were subsequently shown to induce monocyte proliferation and suppression of their secretion was shown to alleviate asthmatic symptoms (Kulshreshtha *et al.,* 2013). A study focussed on miRNA expression, reported that there were increased amounts of bae-EVs in BALF from HDM-exposed mice compared to sham-controlled exposed mice and that the miRNA cargo was significantly changed. Analysis of the miRNA cargo suggested selective sorting of miRNA including Th2 inhibitory miRNAs, including those with IL-13 and IL-5Ra as putative targets, into bae-EVs with HDM exposure (Gon *et al.,* 2017). Three further publications reported on the influence of bae-EVs on DCs, with one study that evaluated the miRNA cargo of EVs derived from primary normal human bronchial epithelial cells treated with IL-13 to induce an asthma-like phenotype, and EVs isolated from nasal lavages of children with asthma. Analysis of the EVs from the IL-13 treated NHBE cells revealed changes in the expression of 16 miRNAs, and miR-34a, miR-92b and miR-210 levels in EVs from the nasal lavages correlated with lung function parameters. Subsequent pathway analysis predicted these miRNAs could help regulate Th2 polarisation and DC

maturation (Bartel *et al.,* 2020). Another study, examining the effect of ovalbumin (OVA) allergen challenge on mice airway epithelium revealed the enhanced secretion of bae-EVs carrying OVA. These OVA induced bae-EVs promoted the infiltration of neutrophils, monocytes and DCs into the lung, as well as inducing macrophages to secrete proinflammatory cytokines IL-6, TNF-a and IL-1β (Yu *et al.,* 2021). Lastly bae-EVs secreted after HDM stimulation were shown to facilitate the recruitment of DCs in the lung and to activate DC through the cargo contactin-1 (CNTN1), as well as upregulating the expression of CD40, ultimately promoting Th2 differentiation (Zhang *et al.,* 2021b).

Table 3.5: Studies involving airway epithelial-derived EVs.

First Author	Title	Allergen	Cells Responding	Model	Isolation	Characterisation	Outcome
Prado et al 2008	Exosomes from bronchoalveolar fluid of tolerized mice prevent allergic reaction	Ole e 1	T Cells	Mouse Model (BALB/c) & Cell Culture	**Ultracentrifugation**: 100,000× g for 18h	EM, Western Blot and FACS	EVs isolated from the BALF of mice tolerised to the allergen Ole e 1 were able to inhibit a Th2 responses, suppressing IgE and IgG1 and upregulating TGF-β
Prado et al 2010	Bystander suppression to unrelated allergen sensitisation through intranasal administration of tolerogenic exosomes in mouse	Ole e 1 & Bet v 1	T Cells	Mouse Model (BALB/c) & Cell Culture	**Ultracentrifugation**: 100,000× g for 18h	EM, Western Blot and FACS	Bystander suppression was observed after nasal administration of BALF-derived EVs from tolerised mice inhibiting sensitisation to other allergens, supressing IgE and IgG1 as well as the Th2 cytokines Il-5 and IL-13
Shin et al 2010	Extracellular vesicles are key intercellular mediators in the development of immune dysfunction to allergens in the airways	Ovalbumin	T Cells and Dendritic Cells	Mouse Model (BALB/c)	**Sucrose Cushion Serial Ultracentrifugation**: 500× g 10min, 3000× g 20min, **Cushioned:** 100,000× g 2h 100,000× g 2h.	TEM, Western Blot, FACS and Bradford Assay	LPS exposure enhanced airway epithelial derived-EVs (ae-EVs) production. These LPS-induced EVs were shown to enhanced sensitisation to allergens and promote TNF-a and IL-6 secretion in macrophages
Kulshreshtha et al 2013	Proinflammatory role of epithelial cell-derived exosomes in allergic airway inflammation	Ovalbumin	Monocytes	Mouse Model (BALB/c) Cell culture (BEAS-2B)	**Serial Ultracentrifugation**: 300x g 5min, 800x g 5min, 2000x g 10min, 10,000x g 30min, 70,000x g 60min	TEM, Western Blot and FACS	Th2 cytokine stimulated epithelial cells had increased EV secretion and cargo changes. These EVs induce monocyte proliferation

Gon et al 2017	Selective release of NAs via extracellular vesicles is associated with house-dust mite allergen-induced airway inflammation	House Dust Mite	CD4+ T helper cells	Mouse Model (C57BL/6J)	**Precipitation** - EXOQuick Kit	TEM, Western Blot and qNano Counter	EVs used to remove Th2 inhibitory miRNAs that down regulate IL-5 and Il-13 receptors on epithelial cells
Bartel et al 2020	Human airway epithelial extracellular vesicle miRNA signature is altered upon asthma development	N/A	N/A	Human Patients & Cell Cell Culture (Primary Cells)	**Precipitation** - EXOQuick Kit	TEM, Western Blot, NTA and SeramiR miRNA	Changes in expression of miR-34a, miR-92b and miR-210 predicted by pathway analysis to promote DC induced Th2 polarization of CD4+ T cells regulate Th2 polarisation and DC maturation
Yu et al 2021	Increased airway epithelial cell-derived exosomes activate macrophage-mediated allergic inflammation via CD100 shedding	Ovalbumin	Macrophages	Mouse Models (C57BL/6J) & Cell Culture (Primary Cell and BEAS-2B)	**Serial Ultracentrifugation**: 300× g 10min, 3000× g 15min, 10,000× g 30min 100,000× g 70min, 100,000x g 70min.	TEM, Western Blot and NTA	OVA containing EVs promote infiltration of neutrophils, monocytes and DCs into the lung and induce macrophages to secrete IL-6, TNF-a and IL-1β
Zhang et al 2021	Epithelial exosomal contactin-1 promotes monocyte-derived dendritic cell-dominant T-cell responses in asthma	House Dust Mite	Dendritic Cells	Human Patient, Mouse Model (C57BL/6N) & Cell Culture (Primary cells)	**Serial Ultracentrifugation**: 2000× g 10min, 10,000× g 30min 100,000× g 70min, 100,000x g 70min.	TEM, Western Blot and NTA	HDM stimulation relesed EVs that recruit DCs in the lung. These EVs can activate DC though the catgo CNTN1 and upregulate the expression of CD40

With regards to quality scores, of the eight studies looking at the influence bae-EV on allergic sensitisation seven utilised mouse models (Gon *et al.,* 2017, Kulshreshtha *et al.,* 2013, Prado *et al.,* 2010, Prado *et al.,* 2008, Shin *et al.,* 2010, Yu *et al.,* 2021, Zhang *et al.,* 2021b). Reporting of the sensitisation protocol in these models was generally good, with all seven studies clearly defining this (Gon *et al.,* 2017, Kulshreshtha *et al.,* 2013, Prado *et al.,* 2010, Prado *et al.,* 2008, Shin *et al.,* 2010, Yu *et al.,* 2021, Zhang *et al.,* 2021b). The robustness of the models was variable, with two studies using more than 11 mice per group (Gon *et al.,* 2017, Prado *et al.,* 2008), one using 6-10 mice per group (Kulshreshtha *et al.,* 2013) and four studies using 5 or less mice (Prado *et al.,* 2010, Shin *et al.,* 2010, Yu *et al.,* 2021, Zhang *et al.,* 2021b). Five of the seven studies utilising mouse models also implemented a cell culture model (Kulshreshtha *et al.,* 2013, Prado *et al.,* 2010, Prado *et al.,* 2008, Yu *et al.,* 2021, Zhang *et al.,* 2021b) with three using murine primary cells (Prado *et al.,* 2010, Prado *et al.,* 2008, Zhang *et al.,* 2021b) and two using an transformed cell line (Kulshreshtha *et al.,* 2013, Yu *et al.,* 2021). Only two studies utilised human patient samples, with just 6-10 participants per group (Bartel *et al.,* 2020, Zhang *et al.,* 2021b), and whilst both studies identified patients from a clinical setting, only one provided information regarding their allergic status performing a skin test and measuring serum IgE (Bartel *et al.,* 2020).

Concerning EVs, five studies isolated EVs using either ultracentrifugation (UC) or serial UC (Kulshreshtha *et al.,* 2013, Prado *et al.,* 2010, Prado *et al.,* 2008, Yu *et al.,* 2021, Zhang *et al.,* 2021b) and one study implemented a sucrose cushion as part of UC (Shin *et al.,* 2010) . Two studies isolated EVs using ExoQuick precipitation kit (Bartel *et al.,* 2020, Gon *et al.,* 2017, Shin *et al.,* 2010). EV characterisation in all the studies was suitable, with the eight studies receiving a score of 'good' or better. All eight studies used western blot analysis to characterize exosome biomarkers as well as TEM to confirm the presence of isolated EVs. Four studies profiled EV cargo using RTq-PCR (Bartel *et al.,* 2020, Gon *et al.,* 2017, Yu *et al.,* 2021, Zhang *et al.,* 2021b), with one also using a sermiR miRNA exosome profiling kit (Bartel *et al.,* 2020). Three studies profiled sizing using NTA (Bartel *et al.,*

2020, Yu *et al.,* 2021, Zhang *et al.,* 2021b). Lastly, two studies also used flow cytometry to analyse EV biomarker expression (Prado *et al.,* 2010, Prado *et al.,* 2008). The highest scoring paper (79%) (Bartel *et al.,* 2020), utilised two high scoring robust model systems, as well as an ExoQuick precipitation kit for isolation, followed by comprehensive EV characterisation (Bartel *et al.,* 2020). The lowest score received by a study was 52% (Shin *et al.,* 2010), this was mainly due to the use of just one model with a small sample size. All scores are outlined in Table 3.6.

Table 3.6: Scoring of paper involving airway epithelial-derived EVs.

Author	Model (n/10)	Robustness of Model			Sample Size			Sensitisation Material (n/3)	EV Isolation (n/3)	EV Characterisation (n/4)	Total Score	Bias Score
		Murine Model (n/4)	Cell Culture (n/4)	Human Studies (n/4)	Murine Model (n/3)	Cell Culture (n/3)	Human Studies (n/3)					
Prado et al, 2008	Animal Model (2), Cell culture - Murine (1)	Sensitisation fully defined (4)	Primary Cell line and fully defined exposures (4)		11 or more mice per group (3)	more than 3 repeats (3)		Allergen Defined (1)	UC (1)	Multiple Complementary techniques and suitable controls and additional biomarkers (4)	23/34	68%
Prado et al, 2010	Animal Model (2), Cell culture - Murine (1)	Sensitisation fully defined (4)	Primary Cell line and fully defined exposures (4)		5 or less mice per group (1)	more than 3 repeats (3)		Allergen Defined (1)	Serial UC (1)	Multiple Complementary techniques and suitable controls and additional biomarkers (4)	21/34	62%
Shin et al, 2010	Animal Model (2)	Sensitisation fully defined (4			5 or less mice per group (1)			Allergen Defined (1)	Sucrose Cushioned UC (2)	Multiple Complementary techniques and suitable controls and additional biomarkers (4)	14/27	52%
Kulshreshtha at al, 2013	Cell culture - Human (3), Animal Model (2)	Sensitisation fully defined (4)	Transformed cell line and partially defined exposure (1)		6 -10 mice per group (2)	3 repeats (2)		Allergen Defined (1)	Serial UC (1)	Multiple Complementary techniques and suitable controls (3)	19/34	56%
Gon et al, 2017	Animal Model (2)	Sensitisation fully defined (4)			11 or more mice per group (3)			Allergen Defined (1)	Precipitation - EXOQuick-TC (3)	Multiple Complementary techniques and suitable controls (3)	16/27	59%

Bartel et al, 2020	Human Patient samples (4), Cell Culture - Human (3)		Primary Cell line and fully defined exposures (4)	Allergic Patients from clinical setting with serum IgE, IgG, skin prick test and healthy controls (4)		3 repeats (2)	6-10 participants per group (3)		Precipitation - EXOQuick-TC (3)	Multiple Complementary techniques and suitable controls and additional biomarkers (4)	27/34	79%
Yu et al, 2021	Cell Culture - Human (3), Animal Model (2)	Sensitisation fully defined (4)	Immortalised cell line and fully defined exposure (2)		5 or less mice per group (1)	Not specified (0)		Allergen Defined (1)	Serial UC (1)	Multiple Complementary techniques and suitable controls (3)	17/34	50%
Zhang et al, 2021	Human Patient samples (4), Animal Model (2) Cell Culture - Murine (1)	Sensitisation fully defined (4)	Primary Cell line and partially defined exposures (3)	Allergic Patients from a clinical setting and a control group (3)	5 or less mice per group (1)	Not specified (0)	6-10 participants per group (3)	Allergen Defined (1)	Serial UC (1)	Multiple Complementary techniques and suitable controls (3)	26/41	63%

3.1.4. Intestinal Epithelial-Derived Extracellular Vesicles (ie-EVs)

Only three studies evaluating the role of intestinal epithelial-derived EVs (ie-EVs) were identified (Table 3.7). All three of these studies generated data on the potential role of ie-EVs in food allergy. One study showed intestinal epithelial cells (IECs) post OVA uptake secrete ie-EVs containing integrin αvβ6 and OVA. These αvβ6/OVA ie-EVs induced antigen-specific tolerogenic Tregs and TGF-β+ DCs suppressing Th2 responses in the gut (Chen *et al.,* 2011). Another study using vasoactive intestinal peptide deficient (VIPd) and wild-type mice showed that VIPd mice failed to induce type 1 regulatory T cells in the intestine, and that exposure to VIP in culture induced IL10 expression in IECs. Exosomes derived from OVA/VIP-primed IECs carried allergen-MHC II complexes, as well as IL-10, and these OVA/VIP-primed ie-EVs were able to induce Tr1 differentiation in OVA-specific CD4+ cells (Zeng *et al.,* 2020). Administration of OVA/VIP-primed ie-ECs also suppressed experimental food allergy. Lastly, ie-EVs isolated from the lamina propria of OVA-fed mice, which containing OVA were characterised and reported to have increased expression of MHCII compared to those from naïve mice. OVA was also detected in the EVs from the OVA-fed mice. EVs from OVA fed mice were also reported to induce CD4+Foxp3+T cell differentiation, as well as promote the secretion of Treg-promoting cytokines IL-10 and TGF-β in macrophages (Shin *et al.,* 2022).

Table 3.7: Studies involving intestinal epithelial-derived EVs.

First Author	Title	Allergen	Cells Responding	Model	Isolation	Characterisation	Outcome
Chen et al 2011	Intestinal epithelial cell-derived integrin αβ6 plays an important role in the induction of regulatory T cells and inhibits an antigen-specific Th2 response	Ovalbumin	Dendritic Cells	Mouse Model (Balb/c) Cell Culture (IEC4.1)	**Serial Ultracentrifugation**: 300x g 10min, 1200x g 20min, 10,000x g 30min, 100,000x g 1h	EM, Western Blot and Bradford Assay	Intestinal epithelial cells post OVA uptake secrete EVs containing integrin αvβ6 and OVA. These EVs induced antigen-specific Tregs and TGF-β+ DCs
Zeng et al 2020	Exosomes carry IL-10 and antigen/MHC II complexes to induce antigen-specific oral tolerance	Ovalbumin	Tregs and Tr1 Cells	Cell Culture (Mode K cells) and Mouse Models (VIPd and BALB/c)	**Serial Ultracentrifugation**: 300x g 10min, 1200x g 20min, 10,000x g 30min, 100,000x g 1h	Western Blot and Bradford Assay	VIPd mice fail to induce Tr1 cells in the intestine. EVs from OVA/VIP primed IECs carry allergen-MHC II complexes and IL-10 which are able to induce Tr1 differentiation in OVA-specific $CD4^+$ cells and administration of these suppressed experimental food allergy.
Shin et al 2022	Extracellular vesicles derived from small intestinal lamina propria reduce antigen-specific immune response	Ovalbumin	Tregs	Mouse Model (C57BL/6)	**Sucrose Cushion Serial Ultracentrifugation**: 500× g 10min, 3000× g 20min, **Cushioned:** 100,000× g 2h 100,000× g 2h.	TEM, Western Blot, Bradford Assay and Dynamic light scattering (sizing)	EVs containing OVA and MHCII induce $CD4^+Foxp3^+$ T cell differentiation and promote the secretion of Treg-promoting cytokines IL-10 and TGF-β in macrophages

With regards to quality scores, all three studies examining ie-EVs utilised mouse models (Chen *et al.,* 2011, Shin *et al.,* 2022, Zeng *et al.,* 2020), with two studies fully defining sensitisation protocols (Chen *et al.,* 2011, Zeng *et al.,* 2020) and one study not disclosing the stimulation concentration, ultimately receiving a lower score (Shin *et al.,* 2022). Furthermore, the same study also didn't define its sample size (Shin *et al.,* 2022) , with the other two studies using 6-10 mice per group (Chen *et al.,* 2011, Zeng *et al.,* 2020). In addition to the use of mouse models, two studies also used cell models (Chen *et al.,* 2011, Zeng *et al.,* 2020). Both models utilised received low robustness scores due to the use of immortalised cell lines, however definition of exposure of the models was fully detailed.

Concerning EVs, isolation methods used in all three studies were generally 'poor' with all three using UC. One study, however, did use a sucrose cushion receiving a slightly higher score (Shin *et al.,* 2022). Characterisation of EVs in the studies was variable and poor. Two of the three papers used microscopy to confirm the presence of isolated EVs (Chen *et al.,* 2011, Shin *et al.,* 2022) with one using TEM (Shin *et al.,* 2022) and one using immunogold EM (Chen *et al.,* 2011). One study sized EVs using dynamic light scattering (Shin *et al.,* 2022) . Two studies used western blots to profile EV biomarkers lacked suitable controls. Consequently, no study scored more than a score of 'Fair' for characterisation, despite using multiple complementary techniques. The lowest score received by a study was 37% (Shin *et al.,* 2022), this was the result of using just one model as well as the poor disclosure regarding sensitisation and the absence of sample sizes used. While the study used TEM, western blot and dynamic light scattering to profile the EVs, the lack of appropriate controls meant the study also received a low characterisation score. The highest score achieved by a study was 53% (Zeng *et al.,* 2020). This study utilised multiple models and had good model robustness, as well as reasonable sample sizes. While using multiple techniques for EV characterisation, the lack of suitable characterisation controls resulted in a low score. All scores are outlined in Table 3.8.

Table 3.8: Scoring of paper outlining intestinal epithelial-derived EVs.

Author	Model (n/10)	Robustness of Model			Sample Size			Sensitisation Material (n/3)	EV Isolation (n/3)	EV Characterisation (n/4)	Total Score	Bias Score
		Murine Model (n/4)	Cell Culture (n/4)	Human Studies (n/4)	Murine Model (n/3)	Cell Culture (n/3)	Human Studies (n/3)					
Chen et al, 2011	Animal Model (2), Cell culture - Murine (1)	Sensitisation fully defined (4)	Transformed cell line and fully defined exposure (2)		6 -10 mice per group (2)	3 repeats (2)		Allergen Defined (1)	Serial UC (1)	Multiple complimentary Techniques (2)	17/34	50%
Zeng et al, 2020	Animal Model (2), Cell culture - Murine (1)	Sensitisation fully defined (4)	Transformed cell line and fully defined exposure (2)		6 -10 mice per group (2)	more than 3 repeats (3)		Allergen Defined (1)	Serial UC (1)	Multiple complimentary Techniques (2)	18/34	53%
Shin et al, 2022	Animal Model (2)	Sensitisation of mice partially defined (3)			Number not defined (0)			Allergen Defined (1)	Sucrose Cushioned UC (2)	Multiple complimentary Techniques (2)	10/27	37%

3.1.5. Discussion

Allergies are a significant global issue with their prevalence and burden continuing to increase (Gutowska-Ślesik *et al.,* 2023, Pawankar, 2014, Warren *et al.,* 2020). Despite this, the underlying mechanisms leading to the development of allergies are poorly understood. The recent and ever-growing research into extracellular vesicles provides a new avenue to further understand these mechanisms. In this systematic review, we analyse the current research suggesting the potential roles of epithelial-derived extracellular vesicles in facilitating allergic sensitisation or tolerance.

A total of 18 publications were identified that indicate that epithelial-derived EVs can cause effects with the potential to promote tolerance or allergic sensitisation. Some of the studies identified indicate that epithelial-derived EVs are able to drive sensitisation through the altered expression of miRNAs delivered to immune cells, ultimately facilitating the differentiation and polarisation of T cells into Th2 cells, as well as promoting Th2 cytokine secretion (Bartel *et al.,* 2020, Li *et al.,* 2023, Luo *et al.,* 2015, Wang *et al.,* 2021, Wu *et al.,* 2015, Zhang *et al.,* 2021b, Zhu *et al.,* 2020). Yet in other studies Epithelial-derived EVs were shown to induce tolerance, promoting Treg and Tr1 differentiation by inducing the secretion of the cytokines TGF-β and IL-10 and suppressing the secretion of Th2 cytokines IL-5 and IL-13 (Chen *et al.,* 2011, Prado *et al.,* 2010, Prado *et al.,* 2008, Shin *et al.,* 2022, Zeng *et al.,* 2020). This review therefore highlights that epithelial EVs can either pro-mote tolerance or sensitisation depending on which epithelial barrier they are derived from and the status of the patient, cell or animal model used.

Regarding potential mechanisms, the studies suggest a number could be at play. One key mechanism identified is that ne-EVs are capable of promoting Th2 differentiation of naïve CD4+ T cells, achieving this either directly or indirectly (Li *et al.,* 2023, Luo *et al.,* 2015, Zhu *et al.,* 2020). For example, reduced expression of the miRNA146a-5p observed in allergic patients was shown to prevent down-regulation of Smad3/GATA-3 (Li *et al.,* 2023), as well as preventing the induction of Th2 sup-pressing IL-10+ monocytes (Luo *et al.,* 2015), ultimately facilitating Th2 polarisation and

allergic sensitisation (Mowen and Glimcher, 2004, Ouyang *et al.,* 2000). Furthermore, upregulated lncGAS5 in allergic patients ne-EVs was shown to down-regulate EZH2 expression in CD4+ cells promoting Th2 differentiation as well the production of Th2 cytokine such IL-4, again promoting sensitisation (Zhu *et al.,* 2020). In contrast, another mechanism identified was the promotion of Th2 differentiation via DCs (Bartel *et al.,* 2020, Wu *et al.,* 2015, Zhang *et al.,* 2021b). Pathway analysis suggested that observed downregulation of miR34a,miR92b, miR210, as well as down-regulation of Lyn, could play an important role in the early development of allergy by promoting Th2 polarisation (Bartel *et al.,* 2020, Beavitt *et al.,* 2005, Wu *et al.,* 2015). CNTN1 bearing bae-EVs were also shown to activate DCs, as well as upregulate the expression of CD40, again promoting Th2 differentiation. The current understanding of how polarisation of naïve T cells are induced is incomplete (Lamiable *et al.,* 2020), however the studies reviewed here suggest that EVs released from the epithelium can as act as a signal to further promote Th2 differentiation. Another method by which epithelial EVs can influence sensitisation is though recruitment and induction of IL-6, TNF-a and IL-1β secreting macrophages, promoting type 2 inflammation (Kulshreshtha *et al.,* 2013, Shin *et al.,* 2010, Yu *et al.,* 2021). Ne-EVs were also shown to induce barrier damage and dysfunction as another mechanism for promoting sensitisation (Qiu *et al.,* 2011, Qiu *et al.,* 2012, Wang *et al.,* 2021), an example being the finding that EVs containing lncRNA NEAT1 were also able to damage the epithelial barrier through the promotion of IL-13 secretion and apoptosis (Wang *et al.,* 2021). Epithelial barrier dysfunction can play a major role in facilitating increased allergen penetration and immune cell exposure, promoting sensitisation (Pothoven and Schleimer, 2017). A study by Kortekaas et al demonstrated that maintenance of the nasal epithelial barrier was essential in the prevention of allergic sensitisation (Kortekaas Krohn *et al.,* 2020). This further emphasises the role that epithelial EVs can play in the development of allergy.

As previously stated, epithelial-derived EVs are also capable of promoting immune tolerance. In particular, it is worth noting that, despite the small number of papers, all three identified studies on ie-EVs reported a

tolerizing influence and identified similar mechanisms through which ie-EVs can induce tolerance. All three studies suggest that OVA-induced ie-EVs facilitate the induction of Tr1 and Treg responses, suppressing Th2 responses and ultimately resulting in tolerance to the allergen (Chen *et al.,* 2011, Shin *et al.,* 2022, Zeng *et al.,* 2020). One mechanism suggested that ie-EVs generated from OVA stimulation had upregulated expression of αvβ6 which stimulated TGF-β secretion in DCs, suppressing sensitisation (Chen *et al.,* 2011). Furthermore, it was suggested that ie-EVs generated from OVA challenge can also activate macrophages to secrete Treg polarising cytokines IL-10+ and TGF-β further promoting Treg differentiation and promoting tolerance (Shin *et al.,* 2022). Additionally, ie-EVs carrying IL-10, as well as MHC II/OVA peptide complexes, were shown to be able to recognise and trigger the differentiation of OVA-specific CD4+ T cells into Tr1 cells (Zeng *et al.,* 2020). The role of the intestinal epithelium in the generation of oral tolerance, as well as the central role played by Tregs and other T regulatory cell subsets is well established (Battaglia *et al.,* 2004, Hadis *et al.,* 2011, Miranda-Waldetario and Maria, 2024). A study by Mucida *et al.* demonstrated the necessity of peripheral induced antigen specific Treg cells for oral tolerance (Mucida, 2005), highlighting the importance of ie-EVs in the suppression of sensitisation. Another mechanism for the suppression of Th2 responses was identified in bae-EVS (Prado *et al.,* 2010, Prado *et al.,* 2008). One study reported the induction of exosomes in Ole e 1 tolerised mice were shown to have a prophylactic effect on the sensitisation and challenge of naïve mice, inhibiting the production of an IgE response, as well as the production of Th2 cytokines (Prado *et al.,* 2008). This prophylactic effect was shown to also suppress sensitisation to an unrelated allergen Bet v 1 through the suppression of IL-5 and 13 suggesting EVs can induce 'bystander tolerance' (Prado *et al.,* 2010).

It is important to draw attention to the generally low-quality scores attained by the studies in this review. These low scores can mainly be attributed to poor EV isolation methods. The studies concerning intestinal EVs had an average score of 47%, this was 14 points lower than the studies looking at ne-EVs which had the next lowest (with an average score of 61%),

potentially questioning the reliability of the mechanisms identified. The highest scoring section was the bae-EV studies, which had an average score of 62%, this was only 1 point higher than the nasal studies suggesting better reliability and robustness in the mechanisms identified in both these sections. This highlights the need for further high-quality studies investigating ie-EVs. The quality of EV isolation scores also emphasises the need for the implementation of more robust isolation methods that ensure better purity without the risk of EV damage or rupturing. Of the 18 studies identified 72% of the studies received the minimum score for EV isolation (Chen *et al.,* 2011, Kulshreshtha *et al.,* 2013, Li *et al.,* 2023, Luo *et al.,* 2015, Prado *et al.,* 2010, Prado *et al.,* 2008, Qiu *et al.,* 2011, Qiu *et al.,* 2012, Wu *et al.,* 2015, Yu *et al.,* 2021, Zeng *et al.,* 2020, Zhang *et al.,* 2021b, Zhu *et al.,* 2020), with only three studies getting the maximum score (Bartel *et al.,* 2020, Gon *et al.,* 2017, Wang *et al.,* 2021). Characterisation of EVs across the studies was better than isolation, with only 16% of paper receiving the minimum possible characterisation score (Chen *et al.,* 2011, Qiu *et al.,* 2011, Qiu *et al.,* 2012), while 28% received the maximum characterisation score (Bartel *et al.,* 2020, Li *et al.,* 2023, Prado *et al.,* 2010, Prado *et al.,* 2008, Shin *et al.,* 2010). Moving forward, future research should employ techniques that minimize damage to EVs while ensuring high-purity isolation. Additionally, it is crucial to exclude other potential mediators, such as cytokines, which could obscure the downstream effects of EVs. In addition to this, the use of more comprehensive characterisation would allow for better identification and differentiation of EV sub-populations allowing for more robust investigation into the different signals released by epithelial cells as a part of allergic sensitisation.

The robustness of model scores was significantly higher, with 50% of studies using samples from human participants. Additionally, 67% of these studies received the maximum score for characterising allergic participants, identifying them from a clinical setting, and performing skin prick tests and serum IgE level tests (Bartel *et al.,* 2020, Li *et al.,* 2023, Luo *et al.,* 2015, Qiu *et al.,* 2012, Yu *et al.,* 2021, Zhu *et al.,* 2020). The use of human samples gives a much more biologically relevant model for furthering the under-standing of

allergic sensitisation. 67% of the papers utilised animal models (mouse models) (Chen *et al.,* 2011, Gon *et al.,* 2017, Kulshreshtha *et al.,* 2013, Li *et al.,* 2023, Luo *et al.,* 2015, Prado *et al.,* 2010, Prado *et al.,* 2008, Shin *et al.,* 2010, Shin *et al.,* 2022, Yu *et al.,* 2021, Zeng *et al.,* 2020, Zhang *et al.,* 2021b). Notable differences in human relevance include IL-10 being induced in both Th1 and Th2 responses in humans, but only in Th2 responses in mice. Addition-ally, mice express only CD1d receptors on dendritic cells, whereas humans express CD1a, b, c, d, and e. Furthermore, murine models require artificial methods to induce allergies (Aun *et al.,* 2017, Krieger *et al.,* 2013, Mestas and Hughes, 2004). Lastly, despite good model robustness scores, no study performed any endotoxin measurement to ensure their sensitisation material was endotoxin-free. Endotoxins have been shown to promote inflammatory responses when exposed simultaneously with allergen (Liu, 2002, Trivedi *et al.,* 2003), consequently providing measurements of endotoxin levels in the allergen preps used provides further credibility to observed downstream immune responses.

Moving forward, EVs provide an exciting and rapidly growing area of research for further understanding the mechanisms through which epithelial cells influence allergic out-comes. It is evident from the studies identified in this review that EVs can play a role in both the induction of sensitisation and tolerance to allergens and this role is affected by the epithelial barrier of origin, as well as changes in EV cargo as a result of patient health status and allergen challenge. More research into epithelial-derived EVs and the changes to cargo associated with allergen exposure is still needed to create a more comprehensive understanding of how epithelial-derived EVs can influence allergic sensitisation and tolerance. In addition, there was a notable gap in the current literature with the lack of any articles studying the effect of EVs derived from the skin epithelium. The skin is the largest organ and is the first barrier to interact with environmental stimuli and consequently is a location where sensitisation can occur (Janssen *et al.,* 2024). Furthermore, skin epithelial-immune cross-talk plays a role in allergic sensitisation and responses, secreting cytokines such as TSLP to influence Th2 polarisation (He *et al.,* 2008, Simmons and Gallo, 2024). Currently, there is a lot research

focusing on the role of EVs in the development of skin allergy and atopic dermatitis, however, these all focus on the effect of EVs derived from the skin microbiome or from immune cells rather than from the skin epithelium itself (Harvey-Seutcheu *et al.,* 2024, Lambring *et al.,* 2019, Tucis *et al.,* 2024). Future research on the role of skin epithelial-derived EVs in allergic sensitisation could uncover new mechanisms and potential therapeutic interventions. Finally, only one of the identified articles used a 3D cell culture model (Bartel *et al.,* 2020). The adoption of more biologically relevant human cell culture models, such as air liquid interface (ALI) culture, would further enhance model robustness and provide a more biologically relevant model for investigating the role of epithelial-derived EVs in allergic sensitisation. As these techniques become more widely adopted, the evaluation of these models, as well as the mechanisms through which they are stimulated, could pro-vide a more appropriate way to differentiate and score article robustness.

In conclusion, this systematic review provides some evidence of the effects that epithelial-derived extracellular vesicles can have on immune responses to allergens. The studies identified here suggest that epithelial EVs could play a pivotal role in influencing the allergic outcome via both direct and indirect mechanisms. Mechanisms identified that facilitate allergic sensitisation include: The promotion of naïve CD4+ T cell Th2 differentiation, the promotion of Th2 cells via DCs, recruitment and induction of IL-6, TNF-a and IL-1β secreting macrophages and the induction of barrier damage and dysfunction. Conversely, some mechanisms were identified that showed epithelial derived EVs promote allergic tolerance through the induction of Tr1 and Treg responses. The limited number of published studies and the lack of research on the skin epithelium highlight the need for dedicated research in these areas to enhance our understanding of epithelial-derived EVs and their role in promoting allergies.

Chapter 4: Optimisation of 2D Cell Culture

4.1. Introduction

The airway epithelium acts as the first line of defence against inhaled agents such as pathogens and allergens. The airway epithelium fulfils this defensive function through two key mechanisms. Firstly, the epithelium acts as a physical barrier comprised of a diverse range of cells, such as ciliated and goblet cells, which are compactly arranged and held together by tight junctions to prevent penetration of inhaled agents. These cells subsequently expel inhaled agents through muco-ciliary action. The second function of the airway epithelium is triggered through its direct interaction with inhaled agent. This interaction triggers epithelial-immune cell cross-talk and coordination of innate and adaptive immune responses. The direct interaction of the epithelium and inhaled agents is facilitated by pattern recognition receptors (PRRs), such as Toll-like receptors (TLRs). These TLRs recognise damage associated molecular patterns (DAMPS) and pathogen associated molecular patterns (PAMPs), such as lipopolysaccharide (LPS) and polyinosinic:polyctidylic acid (Poly(I:C)). Triggering of TLR on airway epithelial cells induces secretion of epithelial cytokines, such as alarmins IL-25 (IL-17E), IL-33 and TSLP, and EVs (Wenger *et al.,* 2023). In the context of IgE mediated allergy, these signals act as the initial triggers for allergic sensitisation and elicitation, promoting the recruitment of immune cells to regions of allergen challenge and promoting skewing of Th2 immune responses (Browne *et al.,* 2025, Whetstone *et al.,* 2022).

Due to their vast potential, EVs have emerged as an exciting new avenue for the better understanding of biological mechanisms. This has resulted in a recent surge in EV interest and, by extension, a need for standardisation of practices and their reporting to facilitate robust and comparable research (Demkow and Stelmaszczyk-Emmel, 2021, Van Deun *et al.,* 2017). To this end, the International Society of Extracellular Vesicles (ISEV) published a set of guidelines termed the “Minimal Information for Studies of Extracellular Vesicles” (MISEV) focusing on the collecting and

processing of EVs, as well as their identification, quantification and characterisation (Welsh *et al.,* 2024, Théry *et al.,* 2018, Lötvall *et al.,* 2014).

To ensure robust downstream analysis of EVs, these guidelines need to be considered in the initial optimisation of cultures. A major recommendation of the MISEV's guidelines is limiting the introduction of exogenous EVs into the culture and subsequent analysis. Core culture supplements such as serum, growth factors and antibiotics are known sources of exogenous EVs and can also influence EV production and composition, conflating downstream analysis (Zhou *et al.,* 2017, Németh *et al.,* 2017, Burger *et al.,* 2017). Consequently, identification of a cell line capable of serum-free culture, or optimisation of serum-free stimulation conditions, are essential. Additionally, for downstream characterisation of EVs, MISEV recommends the use of multiple bio markers, including general EV markers such as tetraspanins (CD9, CD63 and CD81), coupled with origin cell-specific markers (EpCAM, Tspan8 and E-Cadherin). EpCAM and Tspan8 are MISEV recommended epithelial origin markers, with EpCAM being strongly recommended due to its expression being highly restricted to epithelial cells (Théry et al., 2018, Trzpis et al., 2007). EpCAM, Tspan8 and E-Cadherin are all extracellularly expressed on epithelial cells and play and important role in the adhesion of epithelial cells and epithelial barrier integrity, with E-cadherin, forming adherens junctions below tight junctions in the apical junction complex (Figure 1.4B). Finally, the assessment of culture viability, preferably apoptotic and necrotic populations at sample collection, is also recommended as increases in cell death result in the release of cell membrane fragments and apoptotic bodies, obscuring downstream assessment of the EVs.

In this chapter, 2D experiments were used to identify and profile a suitable epithelial cell line to be used subsequent in 3D cultures. In addition, MISEV-compliant conditions for initial evaluations of positive control stimulants were tested.

4.2. Materials and Methods

4.2.1. Epithelial Cell Characterisation

Full methods can be found in Section 2.2 Methods. In brief, characterisation of epithelial cells was performed after cells were isolated from flasks during subculture (Section 2.2.1.1). Initial Calu-3 passages were cultured in Advanced Dulbecco's Modified Eagle Medium before optimal media composition was assessed (Section 2.2.1). Initial characterisation aimed to identify a suitable cell line expressing relevant downstream analysis markers, to be used in a 3D model. The cell lines Calu-3 and BEAS-2B, A549 (ATCC, Cat.no. CCL-185) and primary bronchial epithelial cells (kindly donated by Professor Ian Sayers (University of Nottingham, UK) in (June 2022)) were all assessed for potential model suitability. Cells were stained with the manufacturer's recommended concentration of fluorescent antibodies (Table 4.1) and analysed using conventional flow cytometry. Section 2.2.3 outlines the intra- and extracellular staining processes utilised.

Table 4.1. Fluorescent antibodies used for characterisation of airway epithelial cell lines, their fluorophore and manufacturer.

Antibody Target	Fluorophore	Manufacturer	Cat.no.
EpCAM	PE-Cy7	Biolegend	369816
E-Cadherin	APC	Biolegend	324107
βIV- Tubulin	AlexFlour488	Abcam	Ab237201
Tspan8	PE-Vio770	Miltenyi	130-106-865

4.2.2. Optimised Culture Media Composition

To optimise Human Serum supplementation, Minimal Essential Media (MEM), supplemented with 4mM GlutaMAX, 1% Sodium Pyruvate, 1% non-essential amino acids and Penicillin (100IU)-Streptomycin (100µg/mL) was used as a base (Section 2.1.2). Additional supplementation with either 3, 5 or 10% heat inactivated human AB serum (Cat.no. H5667, Merk, UK) was assessed to see the effect on marker expression and culture time.

4.2.3. Optimisation of 2D Positive control stimulants

Cells were cultured to 80% confluence in 96 well plates (37ºC and 5% CO_2). At 80% confluence, media was swapped to serum-free LHC-9 two days prior to stimulations. Stimulation stocks of Poly(I:C) and LPS were made by dissolving stimulants in LHC-9 media to final stimulation concentrations. Culture media was aspirated from wells and replaced with 200µl of relevant media/stimulant stock. 200µl supernatants were isolated after 24- and 48- hour incubations (37ºC and 5% CO_2) and ELISAs were run as outlined in Section 2.2.11. Additionally, cells were isolated from wells using Accutase (Section 2.2.3) and viability was assessed using annexin-V/PI staining and flow cytometry (Section 2.2.10.1). Gating strategy and localisation of quadrants is outlined in Section 4.3.3.1. Cells negative for both markers were considered viable and this percentage of the total sample is given as the sample's viability.

4.3. Results

4.3.1. Selection and Characterisation of Transformed Airway Epithelial Cells Line

This research project initially investigated the bronchial epithelial cell line BEAS-2B as a potential cell line for the airway model due to its being optimised for serum-free culture. BEAS-2B were initially profiled for the expression of epithelial cell markers (Table 4.2) using conventional flow cytometry to confirm cellular identity and suitability.

Table 4.2. Epithelial cell markers used to confirm the BEAS-2B phenotype and suitability. Epithelial markers and corresponding target.

Epithelial Marker	Target Function	Location
E-Cadherin	Epithelial Adheren junction protein	Cell Surface
βIV-Tubulin	Axonemes	Cell Cytoskeleton
EpCAM (CD326)	Epithelial Adhesion molecule	Cell Surface

Figure 4.1A presents representative flow plots outlining the gating strategy for BEAS-2B cells. BEAS-2B cells were initially gated according to their size (forward scatter (FSC)) and granularity (side scatter (SCC)) (Figure 4.1Ai). Subsequently, a plot of FSC-Height (peak signal intensity) against FSC-Area (total integrated signal) was used to select single cells (Figure 4.1 Aii). Figure 4.1Bi&ii shows that the expression of in-house BEAS-2B cells previously cultured in FBS did not express the marker E-Cadherin (Figure 4.1Bii) and additionally showed low expression of βIV-Tubulin (Figure 4.1Bi). Literature suggested that knocked out expression of E-Cadherin in BEAS-2B could be the result of FBS culture, and consequently, a new cell line was purchased, exclusively cultured in unsupplemented serum-free media (LHC-9). Figure 4.1Ci&ii show the expression of both βIV-Tubulin and E-Cadherin on BEAS-2B cultured exclusively in serum-free conditions. This emphasised the importance of selected culture conditions on epithelial marker expression.

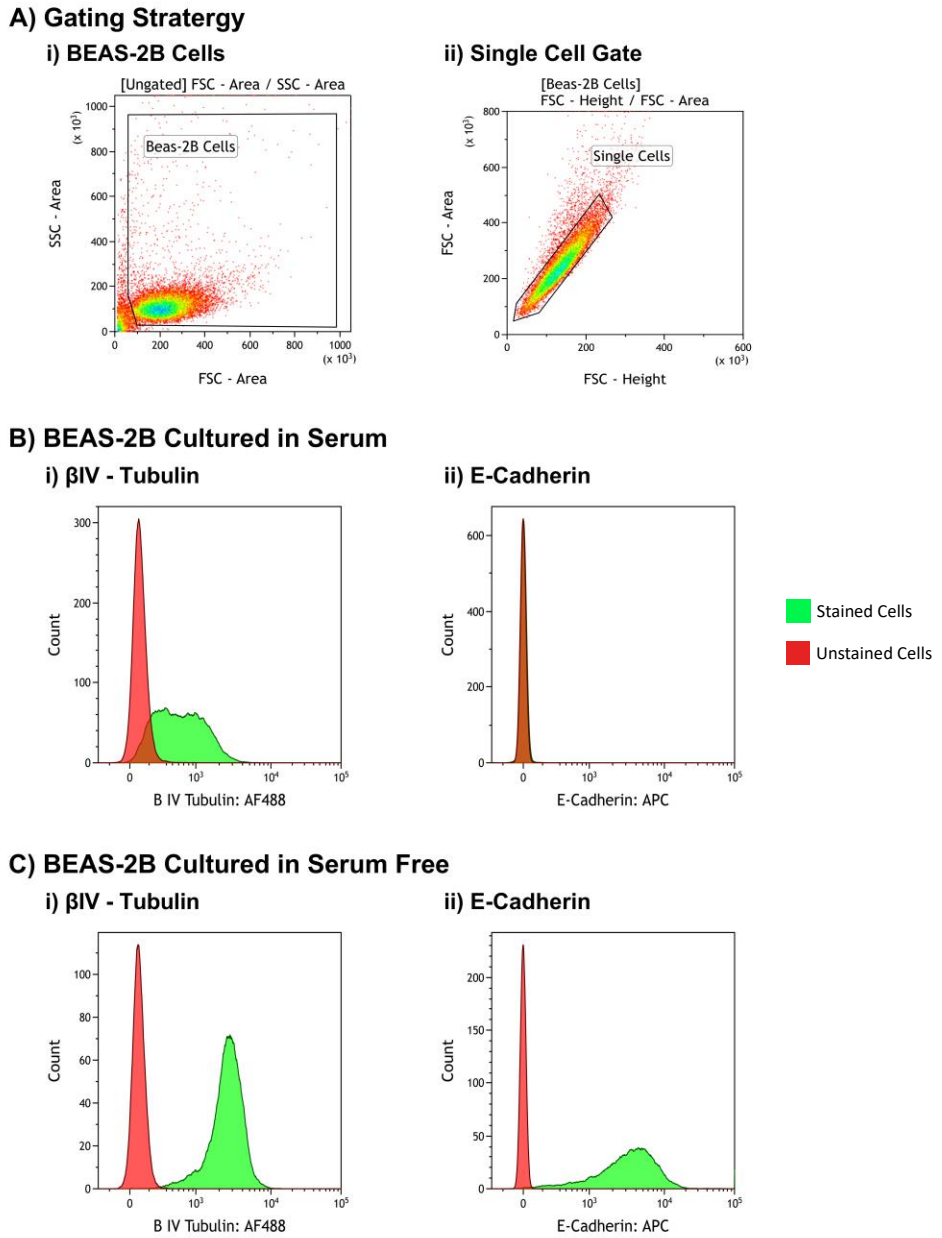

Figure 4.1. Phenotyping of BEAS-2B Cells. A) Gating strategy for the selection of BEAS-2B cells. **Ai)** Initial gating of BEAS-2B cells. **Aii)** Isolation of single cell events. **B)** Histogram overlays of fluorescent intensity, for BEAS-2B cells previously cultured in FBS **(Bi)** βIV-Tubulin and **(Bii)** E-Cadherin. **C)** Histogram overlays of fluorescent intensity, for BEAS-2B cells in LHC-9 **(Ci)** βIV-Tubulin and **(Cii)** E-Cadherin.

To further assess the suitability of BEAS-2B for use in the airway model, the cell line was also checked for the expression of EpCAM, using both conventional and imaging flow cytometry (Figure 4.2). EpCAM will be used as an EV marker to define epithelial origin, as recommended by MISEV,

so its extracellular expression is necessary. Extracellular staining of BEAS-2B for EpCAM showed no expression of the marker (Figure 4.2Ai). However, further staining revealed partial intracellular expression (Figure 4.2Aii), which was subsequently re-confirmed using imaging flow cytometry, which again showed intracellular localisation of EpCAM expression (Figure 4.2 Bi&ii).

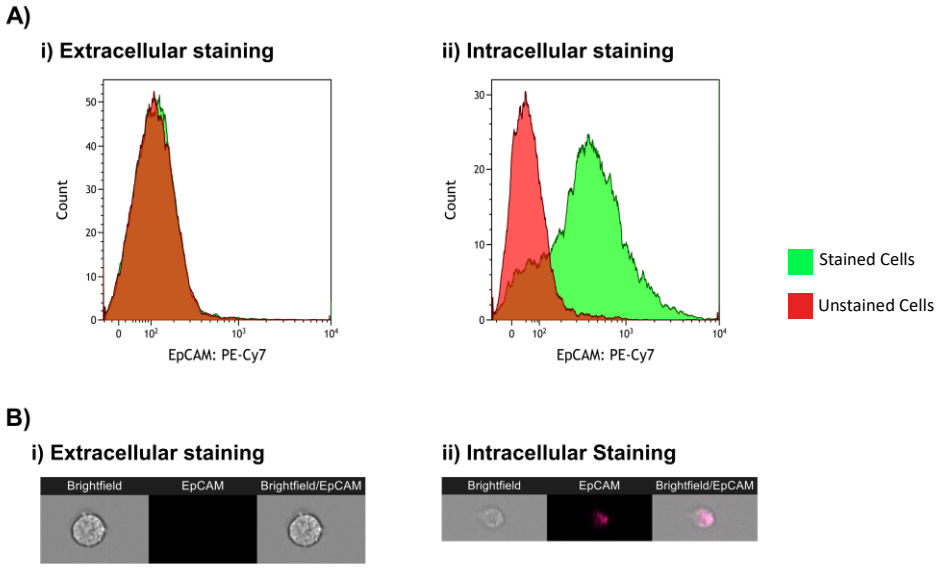

Figure 4.2. BEAS-2B EpCAM Expression Assessment. A) Conventional flow cytometry histograms of EpCAM fluorescent intensity. **Ai)** Extracellular stained BEAS-2B cells. **Aii)** Intracellular stained BEAS-2B. **B)** Imaging flow cytometry, internalisation overlays. **Bi)** Extracellular stained BEAS-2B cells. **Bii)** Intracellular stained BEAS-2B cells.

Lack of extracellularly expressed EpCAM on BEAS-2B confirmed their unsuitability for the airway model. Consequently, the alveolar epithelial cell line A549, bronchiole epithelial cell line Calu-3, and human primary bronchial epithelial cells (HBECs) were evaluated for model suitability, screening initially for EpCAM expression using conventional flow cytometry (Figure 4.3). No extracellular EpCAM expression was observed on A549 cells (Figure 4.3A) with minimal being observed on HBECs (Figure 4.3B). Conversely, the expression of EpCAM on Calu-3 was observed to be much higher with around 90% of cells showing positive expression of the marker (Figure 4.3C).

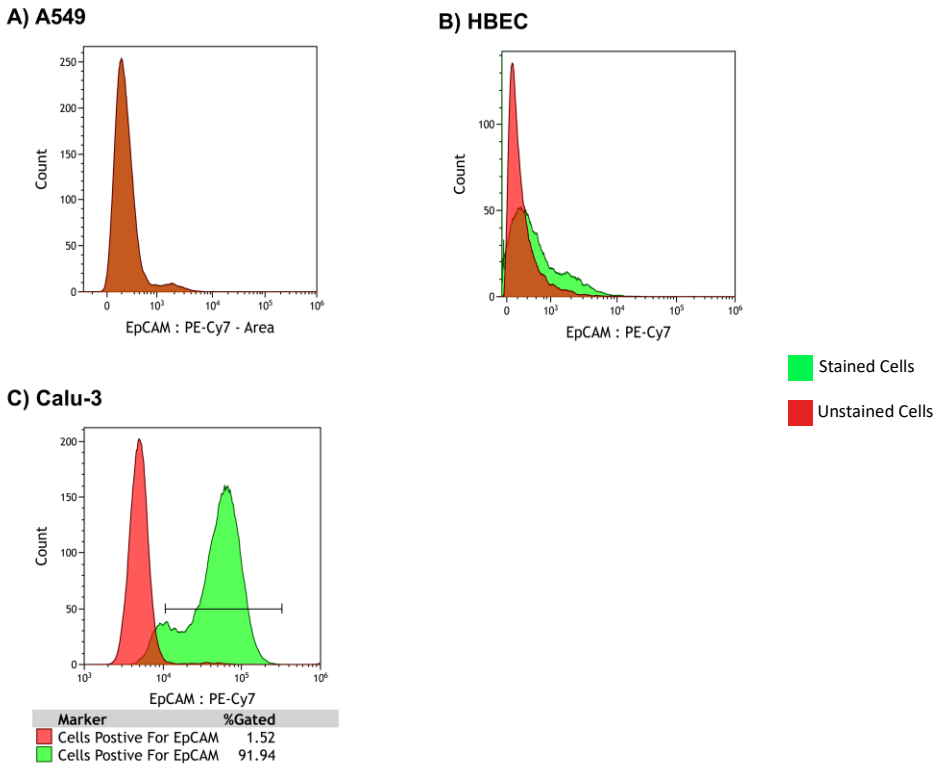

Figure 4.3. Histograms Overlays of Extracellular EpCAM Fluorescent Intensity. A) A549 **B)** Primary Human Bronchial Epithelial Cells (HBEC) **C)** Calu-3.

Calu-3 cells were subsequently screened for the remaining markers (Table 4.2) as well as for the marker Tspan8 (Figure 4.4). Tspan8 will be an additional maker to denote EV origin as recommended by MISEV. Strong expression of markers βIV-Tubulin (Figure 4.4A), E-Cadherin (Figure 4.4B) and Tspan8 (Figure 4.4C) confirmed epithelial identity and Calu-3 suitability. Consequently, Calu-3 cells were utilised moving forward.

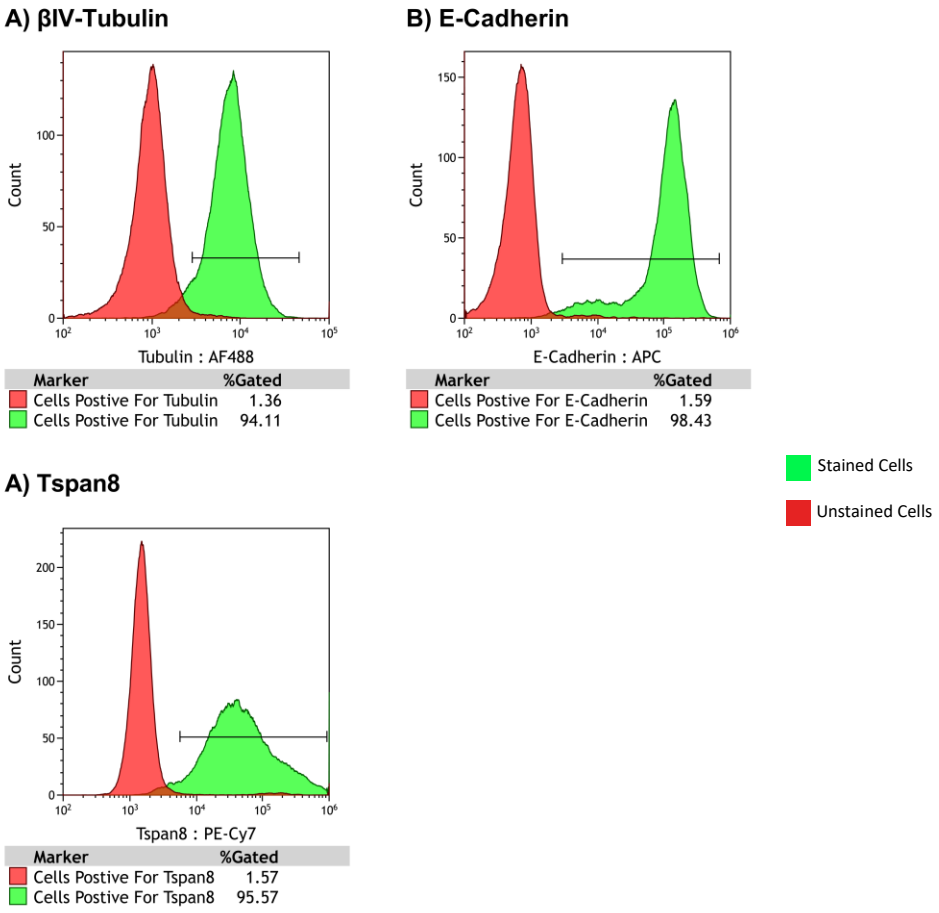

Figure 4.4. Histograms of Epithelial Marker Fluorescent Intensity. A) βIV-Tubulin **B)** E-Cadherin **C)** Tspan8.

4.3.2. Optimisation of Cell Culture Conditions

Having profiled and subsequently identified a suitable cell line for the airway epithelial model, optimisation of its culture was required. Previous observations of media composition affecting epithelial markers expression on BEAS-2B (Figure 4.1) made it necessary to establish the effect of a serum-free culture on Calu-3 and its marker expression. To do so, two cultures were established from the previously profiled Calu-3 culture, with one culture receiving un-supplemented LHC-9 and the other culture's conditions remaining unchanged, receiving advanced DMEM supplemented with 4mM GlutaMAX and 100µg/ml penicillin and streptomycin (Pen/Strep), as per manufacturers specification. Cultures were incubated at 37$^{\circ C}$ and 5% CO_2 and passaged twice before re-profiling the expression of epithelial markers E-Cadherin and EpCAM using conventional flow cytometry. Figure 4.5 shows expression of EpCAM and E-Cadherin on cells cultured in advanced DMEM (Figure 4.5A) and in serum-free LHC-9 (Figure 4.5B). As can be seen in Figures 4.5Ai & Bi, the expression of EpCAM did not change between the two conditions and remained consistent with the initial EpCAM profiling (Figure 4.3C). However, a noticeable shift in signal intensity was observed when comparing the expression of E-Cadherin in both culture conditions (Figure 4.5Aii & Bii). As can be seen in Figure 4.5Aii the expression of the of E-Cadherin is almost 100%, which was consistent with initial profiling of cell line (Figure 4.4B). However, E-Cadherin expression in serum-free culture can be seen to have decreased relative to both the initial sample and its advanced DMEM counterpart (Figure 4.4B and Figure 4.5Aii), with there being a left shift in stain intensity. Additionally, a proportion of cells in the stained sample are negative for the marker, with overlap between the unstained and stained signals. Consequently, to ensure marker expression remained high, it was decided to culture Calu-3s in serum-containing conditions and subsequently transition them to serum-free for the duration of stimulation to allow for subsequent EV analysis.

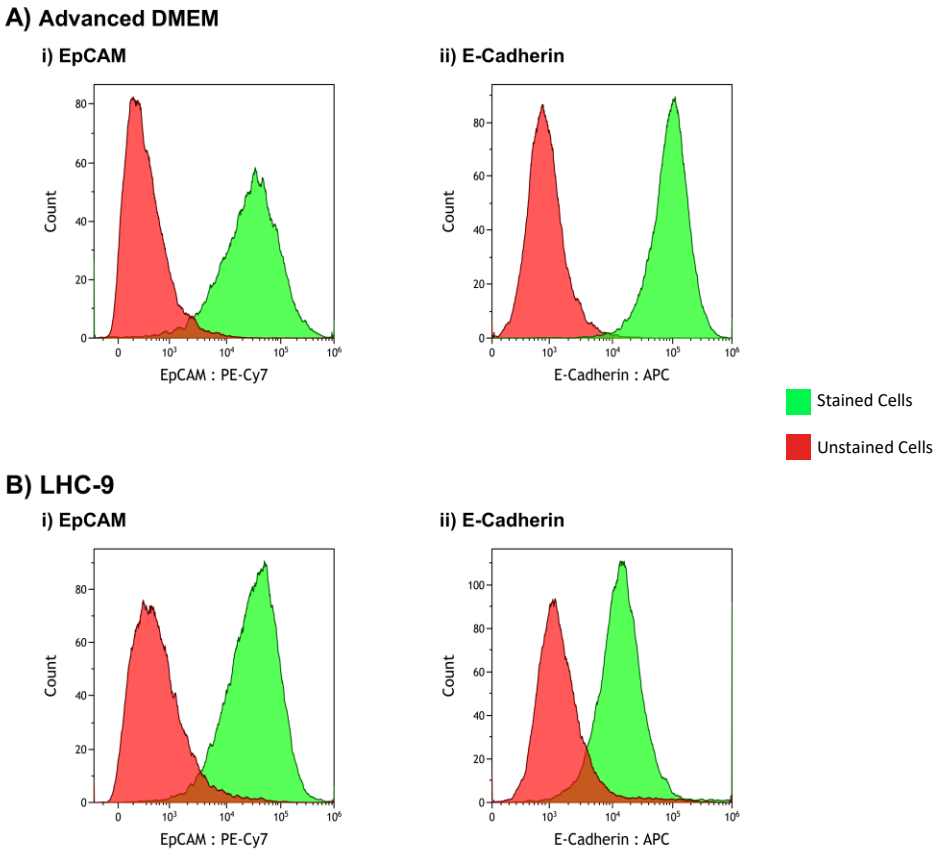

Figure 4.5. Histograms of EpCAM and E-Cadherin Florescent Intensity in Different Culture Conditions. A) Calu-3 cells cultured in Advanced DMEM, **Ai)** EpCAM **Aii)** E-Cadherin. **B)** Calu-3 cells cultured in Advanced DMEM, **Bi)** EpCAM **Bii)** E-Cadherin.

Unilever funding guidelines require minimal use of animal-derived products. Due to serum-free culture not being viable and advanced DMEM being pre-supplemented with AlbuMAX^{TM} (a bovine-derived supplement), a variety of different humanised culture media compositions were assessed. Three 25cm^2 flasks were each incubated with 1x10^6 cells and cultured in either minimal essential medium (MEM), supplemented with 4mM glutaMAX, 1% sodium pyruvate, 1% non-essential amino acids (n-EAA), 100µg/ml Pen/Strep, and either 3%, 5% or 10% heat-inactivated human AB serum. Cultures were observed and imaged every two to three days (Figure 4.6A) and percentage confluence for each image was scored (Figure 4.6B). All three cultures survived and grew; however, the rate of culture growth was observed to slow with increased supplementation of Human AB serum. As can be seen in Figure 4.6Aiii and Figure 4.6B, cells supplemented with 10% human AB

serum only reached around 50% confluence after 16 days, as opposed to both 3% and 5% which reached around 80% confluence at the same time point (Figure 4.6 Ai and Aii and Figure 4.6B).

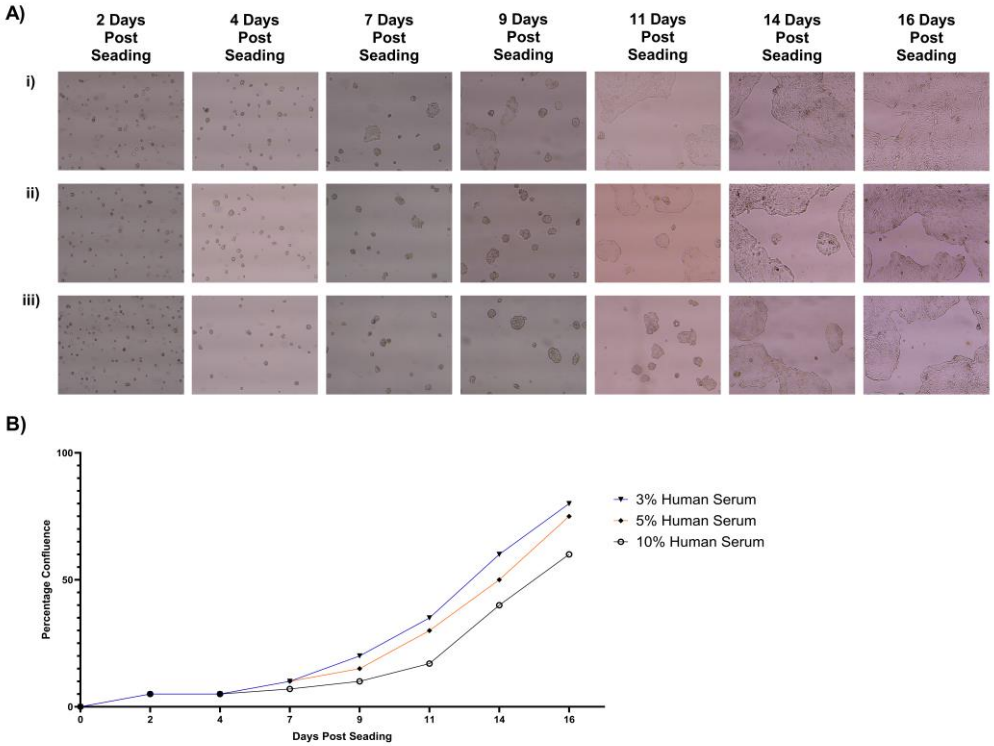

Figure 4.6. Assessment of 3%, 5% and 10% Human AB Serum Supplementation. A) Images of culture growth over time, **Ai)** 3% Human AB Serum **Aii)** 5% Human AB serum **Aiii)** 10% Human AB Serum. **B)** Percentage confluence of cultures overtime.

In addition to monitoring culture success and growth rate, extracellular expression of the epithelial markers Tspan8 and EpCAM was also assessed for each of the three conditions (Figure 4.7). No change in expression of either marker was observed under the different culture conditions, and expression of both markers remained consistent with previous profiling of their expression (Figures 4.3C, 4.4A and 4.5Bi). Due to there being little difference between culture time and marker expression, 5% human AB serum supplementation was selected as the standard culture composition and was used for all remaining 2D cultures of Calu-3 cells.

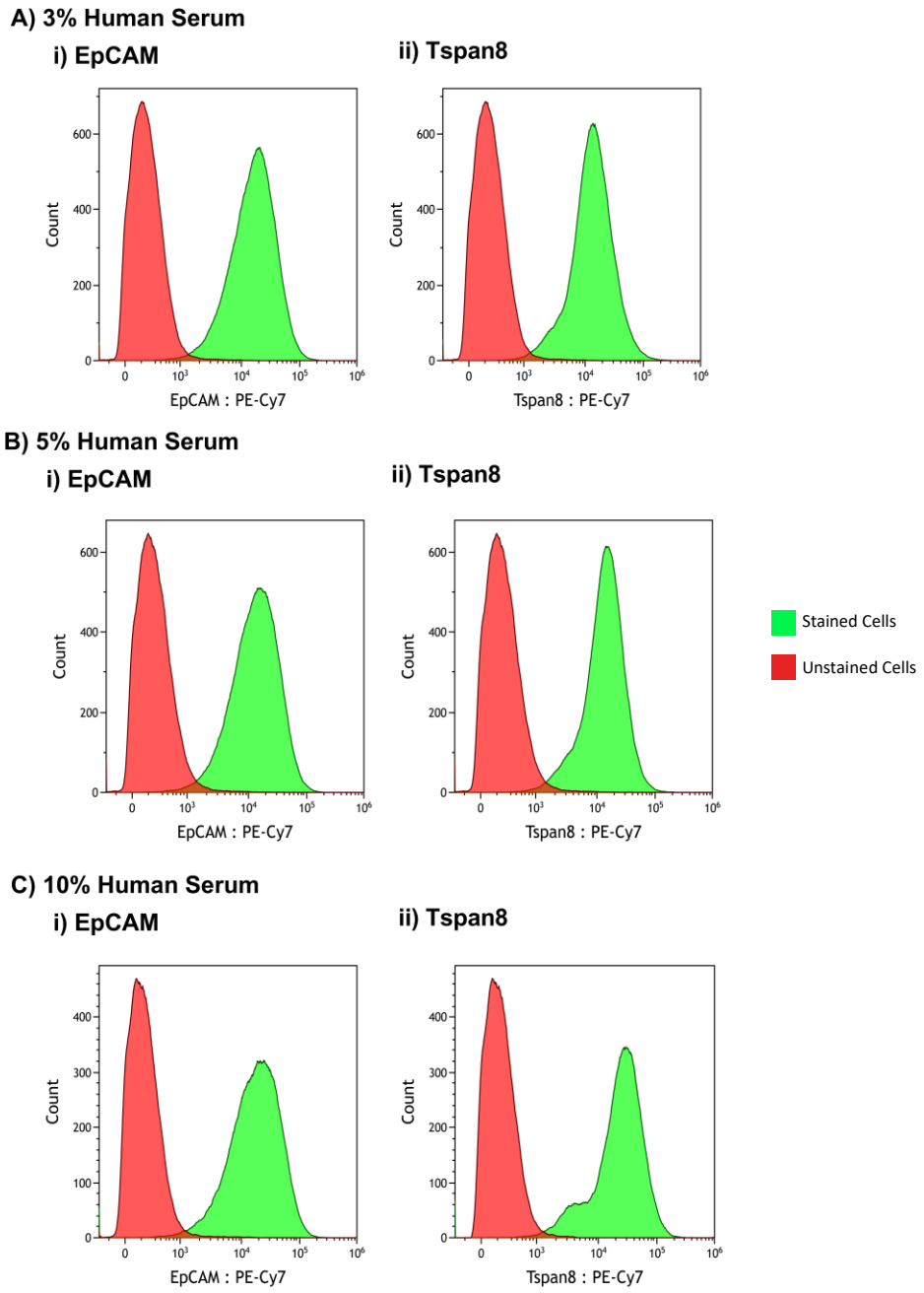

Figure 4.7. Histograms of EpCAM and Tspan8 Florescent Intensity in Different Culture Conditions. A) 3% Human Serum **Ai)** EpCAM **Aii)** Tspan8. **B)** 5% Human serum **Bi)** EpCAM **Bii)** Tspan8. **C)** 10% Human serum C**i)** EpCAM **Cii)** Tspan8.

4.3.3. 2D Assessment of Control Stimulations

2D cultures were utilised to initially profile Calu-3's IL-6 and IL-8 cytokine response to positive control stimulants Poly(I:C) (TLR-3 agonist) and LPS (TLR-4 agonist). Additionally, as 3D culture is serum-free, variation in stimulation response between the two conditions was assessed. Analysis of IL-6 and IL-8 cytokine responses was performed by ELISA. Standard curves were generated for each cytokine and used to interpolate cytokine concentration (Figure 4.8). Limit of detection (LoD) of the assays was also calculated using the mean background optical density (OD) +3S.D.

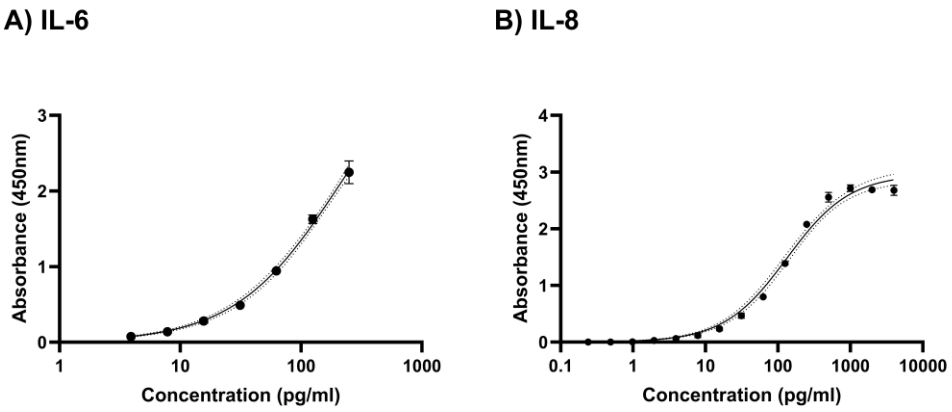

Figure 4.8. IL-8 and IL-8 Standard Curves. A) IL-6 and **B)** IL-8 standard curved produced to interpolate cytokine concentration (pg/ml).

4.3.3.1. LPS Stimulation

The TLR-4 agonist LPS was evaluated as a positive control stimulant. Literature indicated that a 24-hour exposure of LPS between 0.5 – 1µg/ml should stimulate bronchial epithelial cells (Schulz *et al.,* 2002). Cells were seeded into 96-well plates and cultured up to 80% confluence in MEM+5% HS as established previously. Subsequently, media was changed to serum-free LHC-9 three days prior to stimulation. Cells were subsequently stimulated with either 0.5µg/ml or 1.0µg/ml LPS for 24 and 48 hours at 37°C and 5% CO_2. Changes in IL-6 and IL-8 secretion were measured in duplicate via ELISA as previously described (Figure 4.8).

IL-6 secretion increased with 24 hour, 0.5µg/ml LPS exposure, seeing an increase from an average of 14.37pg/ml basal unstimulated secretion to an average 45.2pg/ml (Figure 4.9Ai). This increase wasn't observed for 1µg/ml. After 48-hour exposure an increase in IL-6 secretion was observed for 1µg/ml, increasing to 66pg/ml. Additionally, this increase in IL-6 secretion was also observed with 0.5µg/ml stimulation (Figure 4.9Aii). This increase in IL-6 response was further emphasised when comparing 24- and 48-hour secretion. As can be seen in Figure 4.9Aiii there was a slight increase in the secretion of IL-6 in unstimulated samples; however there was a significant increase in secretion between 24- and 48-hour samples for both stimulation concentrations, suggesting further exposure to LPS maintains the response (Figure 4.9Aiii).

Despite the observed increase in response to IL-6, IL-8 resulted in no change in secretion after either 24 or 48 hours of exposure for either concentration. Due to the intention to transition to a 3D model, successful IL-6 stimulation in line with the literature was deemed proof of principle and both concentrations were taken forward. As literature indicates differences in monolayer (2D culture) and 3D response, these concentrations were assessed in 3D in the subsequent chapter.

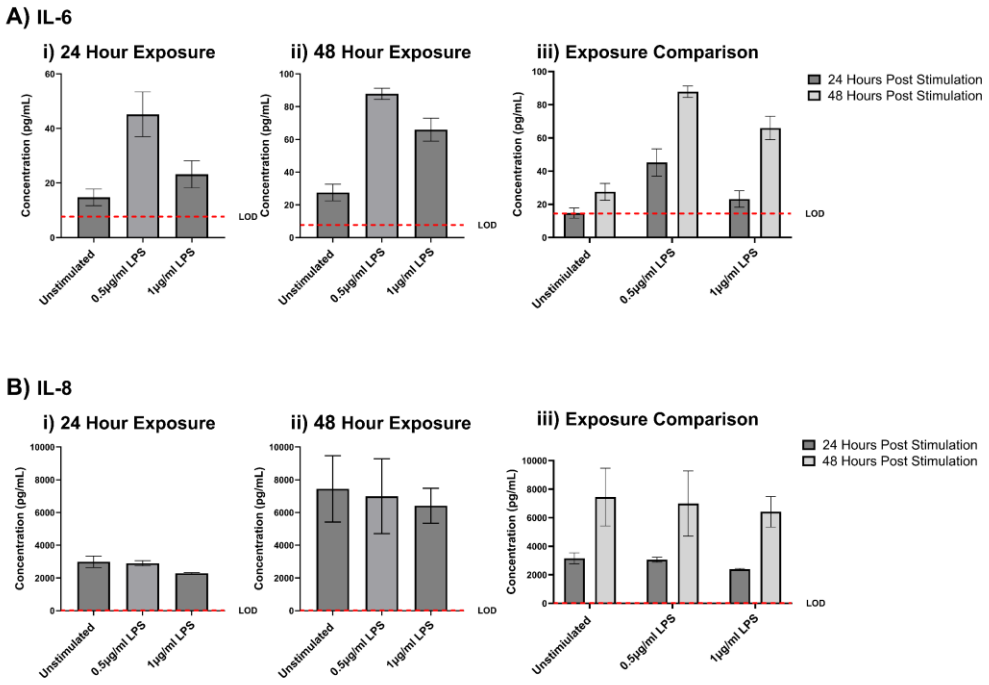

Figure 4.9. IL-6 and IL-8 Response to 0.5 and 1.0µg/ml LPS Stimulation. A) Changes in IL-6 secretion as a result of **Ai)** 24 hours exposure and **Aii)** 48-hour exposure to LPS. **Aiii)** comparison of 24- and 48-hour responses. **B)** Changes in IL-8 secretion as a result of **Bi)** 24 hours exposure and **Bii)** 48-hour exposure to LPS. **Biii)** comparison of 24- and 48-hour responses. LoD is indicated by doted red line ; 7.69pg/ml - IL-6 and 14.5pg/ml – IL-8. Columns represent mean and error bars represent standard deviation. (N=2) .

In addition to profiling cytokine response, viability of stimulated cultures was also assessed after 24- and 48-hour exposure to 0.5 and 1.0µg/ml LPS. Viability was profiled via flow cytometry, using annexin V and PI staining. Figure 4.10 outlines the gating strategy for the identification of cells by size (FSC) and granularity (SSC) (Figure 4.10Ai), as well as the subsequent selection of single cells from a FSC height by area plot (Figure 4.10Aii). Single Colour stains for both PI (Figure 4.10Bi) and annexin V (Figure 4.10Bii) were then used to locate quadrant gates. Cells that are double negative in the lower left quadrant are considered viable.

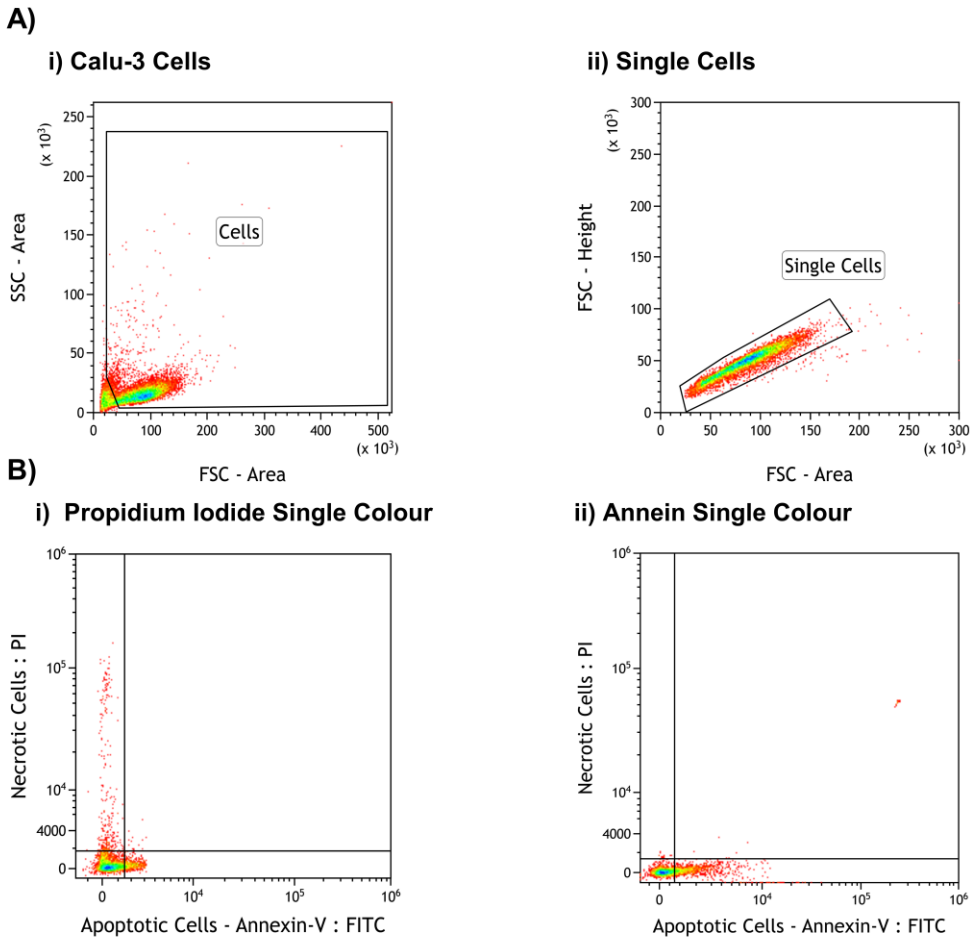

Figure 4.10 Exemplar Gating Strategy for Annexin-V/PI staining. Cells were initially gated for using a SSC vs FSC plot **Ai)**. Single Cell events were subsequently isolated using a FSC-Height Vs FSC Area plot **Aii)**. Single Colour stains for PI **Bi)** and Annexin-V were **Bii)** were used to position quadrant gate for analysis.

The gating strategy outline above was used to analyse Calu-3 cell viability after 24- and 48-hour exposure to 0.5 and 1.0µg/ml LPS in serum-free culture, 37°C and 5% CO_2. Representative dot plots displaying cell viability for unstimulated, 0.5 and 1.0µg/ml LPS-stimulated cells for 24 and 48 hours are presented Figure in 4.11. Unstimulated cells stained with annexin-V FITC and PI after 24 hours and 48 hours can be seen in Figures 4.11Ai and 4.11Bi respectively, adjacent to these plots are presented 24- and 48-hour 0.5 and 1.0µg/ml LPS stimulations (Figure 4.11Aii, Aiii, Bii and Biii). Figure 4.11C shows average viability of stimulated and unstimulated cultures after 24 (N=3) and 48-hour (N=2) exposure to 0.5 and 1.0µg/ml LPS. Two-way ANOVA analysis revealed no significant difference in culture viability

between stimulated and unstimulated cultures after 24-hour exposure. 48-hour time viability also appeared to mirror 24-hour observations. This data further supported the selection of 0.5 and 1.0µg/ml LPS as suitable concentrations for Calu-3 stimulation.

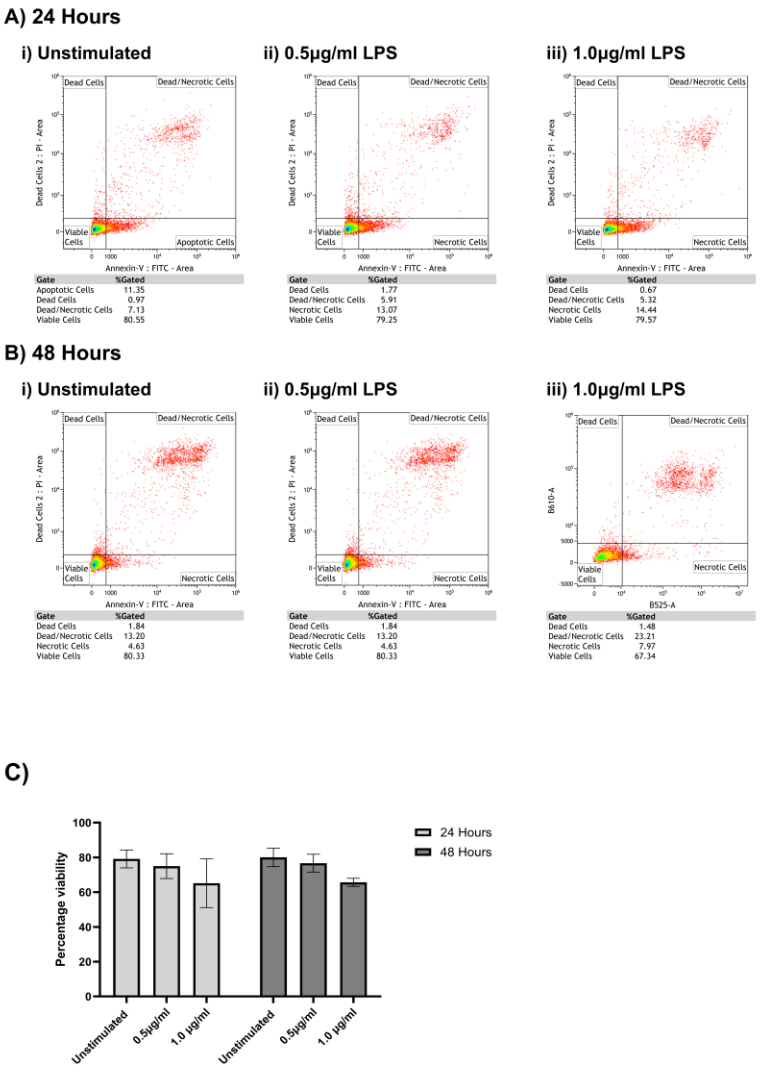

C)

Figure 4.11. 24- and 48- Hour Annexin-V/PI Viability Staining Plots for Unstimulated, 0.5 and 1.0µg/ml Stimulated Cultures. A) representative viability plots of **Ai)** unstimulated **Aii)** 0.5µg/ml **Aiii)** 1.0 µg/ml cultures after 24-hour exposure. **B)** Representative viability plots of **Bi)** unstimulated **Bii)** 0.5µg/ml **Biii)** 1.0 µg/ml cultures after 48-hour exposure. **C)** Comparison of 0.5 and 1.0µg/ml LPS stimulated and unstimulated viability after 24- (N=3) and 48-hour exposure (N=2). Columns represent means and error bars indicate standard deviation. One-way ANOVA tested significance between unstimulated and stimulation conditions after 24-hour exposure.

3D exposure experiments showed variable and poor response to LPS (See Chapter 5). It was hypothesised that one potential cause of this could be due to the serum-free nature of the 3D-culture. Serum naturally contains LPS binding protein (LPS-BP), consequently, it was decided to evaluate the effect of supplementing serum-free conditions with LPS-BP on IL-6 and IL-8 secretions. This was initially done in 2D cultures for proof of principle. Cells were seeded into 96-well plates and cultured up to 80% confluence in MEM+5% HS. Media was changed to serum-free LHC-9 three days prior to stimulation for relevant samples. Cells were subsequently stimulated with 0.5µg/ml LPS supplemented with or without 2.5ng/ml LPS-BP (as per manufacturer's instructions). Samples were exposed for just 24 hours as both literature and previous data indicated this exposure duration would be sufficient to generate a response. Samples were incubated at 37°C and 5% CO_2.

Changes in IL-6 secretion are shown in Figure 4.12A. Surprisingly, cultures with human serum showed no significant increase in the secretion of IL-6 when stimulated with 0.5µg/ml LPS (Figure 4.12Ai) compared to the unstimulated control, and this response was not enhanced with the addition of 2.5ng/ml LPS binding protein (Figure 4.12Ai). Serum-free cultures also didn't significantly increase IL-6 secretion (Figure 4.12Aii), however, when serum-free cultures were stimulated with 0.5µg/ml LPS supplemented with 2.5ng/ml LPS-BP, stimulation was enhanced, with a significant increase in IL-6 secretion observed (Figure 4.12Aii). Comparison of serum and serum-free culture responses showed a significantly reduced IL-6 secretion in serum-free culture, even in the presence of LPS-BP (Figure 4.12Aiii). This response was significantly reduced in all conditions, including unstimulated samples, providing an initial indication of culture condition on cytokine response.

IL-8 secretion was enhanced with the addition of LPS-BP for both serum and serum-free culture (Figure 4.12B). Stimulation of both cultures with just 0.5µg/ml LPS saw no significant increase in IL-8 secretion. In human serum cultures the addition of LPS-BP saw an increase in IL-8 secretion from an average of 1599.2pg/ml in unstimulated samples to an average of 2592.5pg/ml (Figure 4.12Bi). Serum free cultures saw a similar increase in

response, with an unstimulated average of 934.0pg/ml increasing to 1565.9pg/ml (Figure 4.12Bii). Comparison of IL-8 responses for both culture conditions again showed significantly reduced cytokine secretion for all conditions in serum-free media (Figure 4.12Biii), consistent with IL-6 observations.

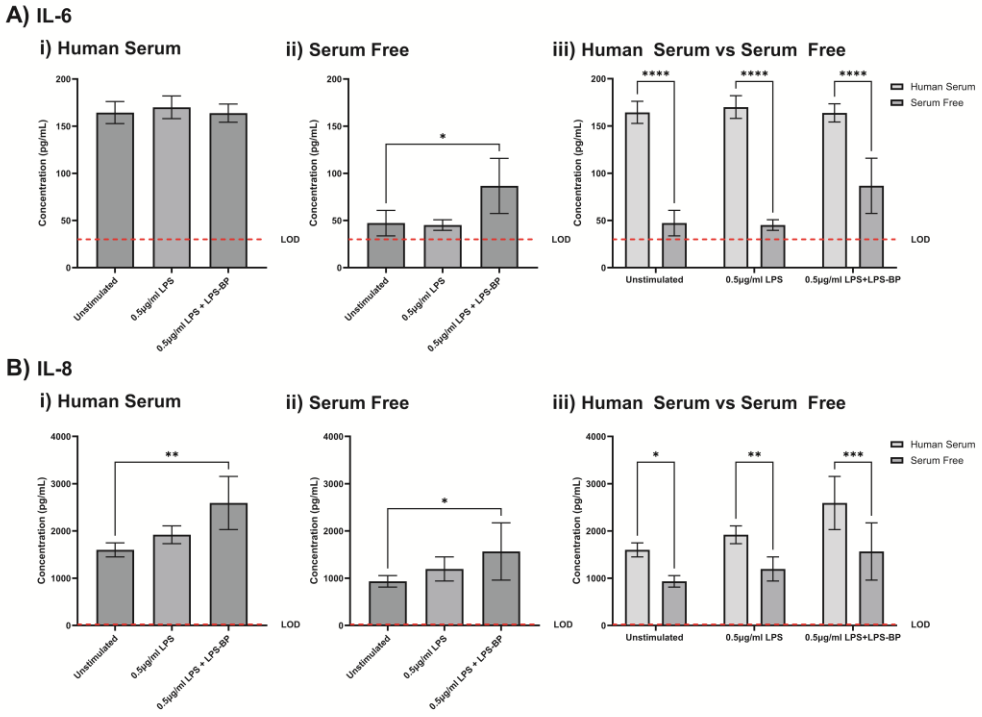

Figure 4.12. IL-6 and IL-8 Response of Human Serum and Serum Free Cultures to 24- Hour Exposure of 0.5µg/ml LPS with and Without LPS-BP. A) Changes in IL-6 secretion as a result of 24 hours exposure to 0.5µg/ml LPS with and without LPS-BP in **Ai)** Human serum Cultures and **Aii)** Serum Free Cultures. **Aiii)** Comparison of Human serum and serum free culture IL-6 responses. **B)** Changes in IL-8 secretion as a result of 24 hours exposure to 0.5µg/ml LPS with and without LPS-BP in **Bi)** Human serum Cultures and **Bii)** Serum Free Cultures. **Biii)** Comparison of Human serum and serum free culture IL-8 responses. LoD is indicated by doted red line ; 30.1pg/ml - IL-6 and 22.0pg/ml – IL-8. Columns represent mean and error bars represent standard deviation. One way ANOVA with Dunnett's multiple comparison test compared stimulation concentrations and Two-way ANOVA with Sidak's multiple comparison test compared culture conditions. *p≤0.05, **p≤0.01, ***p≤0.001, ****p≤0.0001.

Having established the enhancing effect of LPS-BP on cytokine responses, a series of LPS concentrations were assessed in both serum and serum-free conditions. Cells were seeded into 96-well plates and cultured up to 80% confluence in MEM+5% HS. Media was changed to serum-free LHC-9 three days prior to stimulation for relevant samples. Cells were subsequently stimulated with either 0.125, 0.25, 0.5, 0.75 and 1μg/ml LPS supplemented with 2.5ng/ml LPS-BP for 24 hours at 37°C and 5% CO_2. Additionally, both medias were profiled to assess any cytokine background.

24-hour exposure of LPS induced significant upregulation of IL-6 in serum cultures when exposed to 0.5, 0.75 and 1.0μg/ml LPS. While increases were significant, the upregulation of cytokine was small (Figure 4.13Ai). As can be seen in Figure 4.13Ai, unstimulated samples secreted an average of 18.24pg/ml, which significantly increased to 25.7, 24.8 and 27.5pg/ml when exposed to 0.5, 0.75 and 1.0μg/ml LPS, respectively. Serum-free stimulation also saw significant increases in samples exposed to 0.5 and 0.75μg/ml LPS (Figure 4.13Aii). As with serum-stimulated cultures, increases in cytokine secretion of IL-6, while significant, were small, with unstimulated samples increasing from 14.4pg/ml to 19.8 and 21.1pg/ml with 0.5 and 0.75μg/ml LPS, respectively. Comparison of culture conditions revealed significant differences in response to LPS (Figure 4.13Aiii). Unstimulated samples showed no significant difference in basal secretion of cytokine over 24 hours. However, responses to 0.25, 0.5 and 1.0μg/ml showed that serum-free responses were significantly lower than serum-containing, as previously observed. Lastly, profiling of IL-6 in the media alone revealed no detectable level of IL-6, indicating variation in the response is not due to media composition.

IL-8 secretion in response to 24-hour exposure to LPS showed significant upregulation only when stimulated with 0.5μg/ml (Figure 4.13Bi). Unstimulated samples saw a more pronounced cytokine increase than observed in IL-6, with unstimulated samples increasing from 882.3pg/ml to 1246.1pg/ml when stimulated with LPS. Stimulation of serum-free cultures also saw a significant increase in IL-8 secretion after 24-hour exposure to 0.5μg/ml stimulation compared to unstimulated samples, increasing from an average of 307.4pg/ml to 483pg/ml (Figure 4.13Bii). Additionally, as can be

seen Figure 4.13Bii, there was also a significant increase in IL-8 secretion when samples were stimulated with 0.75 and 1.0µg/ml. Comparison of IL-8 responses in both serum and serum-free culture also revealed significantly lower levels of IL-8 secretion in response to all stimulation conditions, as well as significantly lower basal secretion in unstimulated samples in the serum-free culture (Figure 4.13Biii), as previously observed. Lastly, profiling IL-8 content in the media alone revealed no detectable levels of IL-8, again indicating variation in the response is not due to media composition.

Re-assessment of LPS concentrations in 2D with LPS-BP supplementation re-affirmed that 0.5µg/ml LPS was a suitable stimulation concentration for cultures.

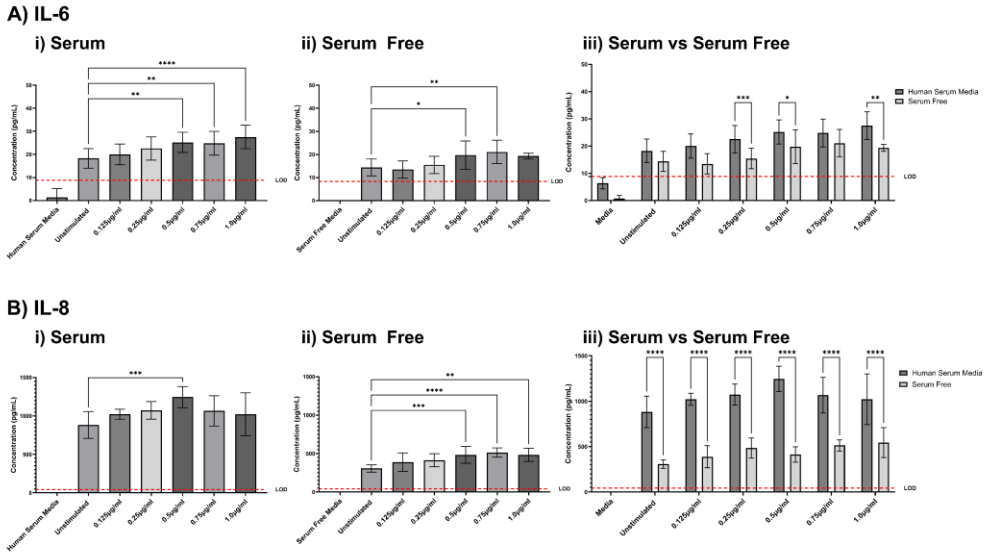

Figure 4.13. IL-6 and IL-8 response to 0.125, 0.25, 0.5, 0.75 and 1.0µg/ml LPS stimulation in Serum and Serum Free Cultures. A) IL-6 Secretion 24 Hours post stimulation in **Ai)** Serum and **Aii)** Serum Free cultures. **Aiii)** comparison of Culture IL-6 secretion. **B)** IL-8 Secretion 24 Hours post stimulation in **Bi)** Serum and **Bii)** Serum Free cultures. **Biii)** comparison of Culture IL-8 secretion. LoD is indicated by doted red line ; 8.34pg/ml - IL-6 and 43.32pg/ml – IL-8. Columns represent mean and error bars represent standard deviation. One way ANOVA with Dunnett's multiple comparison test compared stimulation concentrations and Two-way ANOVA with Sidak's multiple comparison test compared culture conditions. *p≤0.05, **p≤0.01, ***p≤0.001, ****p≤0.0001.

4.3.3.2.Poly(I:C) stimulation

The TLR-3 agonist Poly(I:C) was also assessed as a possible positive control. Cells were seeded into 96-well plates and cultured up to 80% confluence in MEM+5% HS as established previously. Subsequently, media was changed to serum-free LHC-9 three days prior to stimulation for relevant samples. Cells were subsequently stimulated with 5, 10 or 15µg/ml Poly(I:C) for 24 or 48 hours at 37°C and 5% CO_2. Changes in IL-6 and IL-8 secretion are shown in Figure 4.14. To establish significant changes in cytokine secretion between unstimulated samples and different conditions, normality was assessed using Shapiro-Wilk tests. If normally distributed, One-Way ANOVA with Dunnett's multiple comparison tests were used. If not normally distributed, a Kruskal-Wallis test with Dunnett's multiple comparison was used. Significant changes between serum and serum-free conditions were assessed with a Two-Way ANOVA.

IL-6 secretion 24 hours post stimulation significantly increased in response to 5, 10 and 15µg/ml Poly(I:C) for samples cultured exclusively in human serum (Figure 4.14Ai). This response was also shown to be dose dependent, with significance increasing with stimulant concentration. Unstimulated cells secreted an average of 82 pg/ml of cytokine over 24 hours, with this increasing to an average of 243.1 pg/ml, 362.2 pg/ml and 447 pg/ml with 5, 10 and 15 µg/ml respectively. Significance and a dose dependent response was also observed in serum-free conditions; however, unlike with serum cultures, this significance was just for stimulations with 10 and 15µg/ml Poly(I:C) (Figure 4.14Aii). Despite this variation between the two conditions, there was no significant difference in IL-6 secretion between serum and serum-free stimulation at any concentrations 24 hours post stimulation (Figure 4.14Aiii). This significant increase in IL-6 secretion persisted to 48 hours. Significant increases were observed for all stimulation concentrations for both media conditions (Figure 4.14Bi and Bii). This response was again observed to be dose dependent, with IL-6 response increasing with stimulation concentration. Lastly, again, there was no significant difference between serum and serum-free IL-6 secretion for any stimulation concentration after 48 hours (Figure 4.14Biii).

IL-8 secretion also significantly increased 24 hours post Poly(I:C) stimulation. Significant increases in IL-8 secretion were observed in both culture conditions when stimulated with 10 and 15µg/ml (Figure 4.14Ci and Cii), with IL-8 secretion increasing in a dose-dependent manner. Unstimulated samples were observed to increase from 899.5pg/ml to 1550.2pg/ml and 1797.5pg/ml in serum cultures when stimulated with 10 and 15µg/ml, respectively (Figure 4.14Ci). This significant increase was also observed in serum-free cultures (Figure 4.14Cii), with IL-8 secretion in unstimulated samples increasing from an average 481.8pg/ml to 1045.1pg/ml and 1730.6pg/ml when stimulated 10 and 15µg/ml, respectively. Despite the apparent variation between the 10µg/ml response in serum and serum-free culture, there was no significant difference in culture response between the two conditions for any stimulation concentration (Figure 4.14Ciii). 48-hour stimulation with Poly(I:C) also saw significant increases in IL-8 secretion, with IL-8 significantly increasing for all stimulation concentrations in serum culture (Figure 4.14Di). Unlike with IL-6 secretion, this significant increase was not observed for all stimulations at 48 hours in serum-free cultures, with there being no significant increase observed for both 5 and 10µg/ml stimulations (Figure 4.14Dii). Furthermore, comparison of serum-free and serum IL-8 responses 48 hours post stimulation revealed a significant difference in response between the 10µg/ml stimulations (Figure 4.14Diii). Serum-free responses at 48 hours post-stimulation with 10µg/ml were significantly smaller than in serum cultures. However, there was no significant difference in response to any other stimulation concentration.

Despite slight variation in the observed 48 hour IL-8 response, 10µg/ml was identified as a suitable stimulation concentration for Poly(I:C) and its effect on culture viability was assessed.

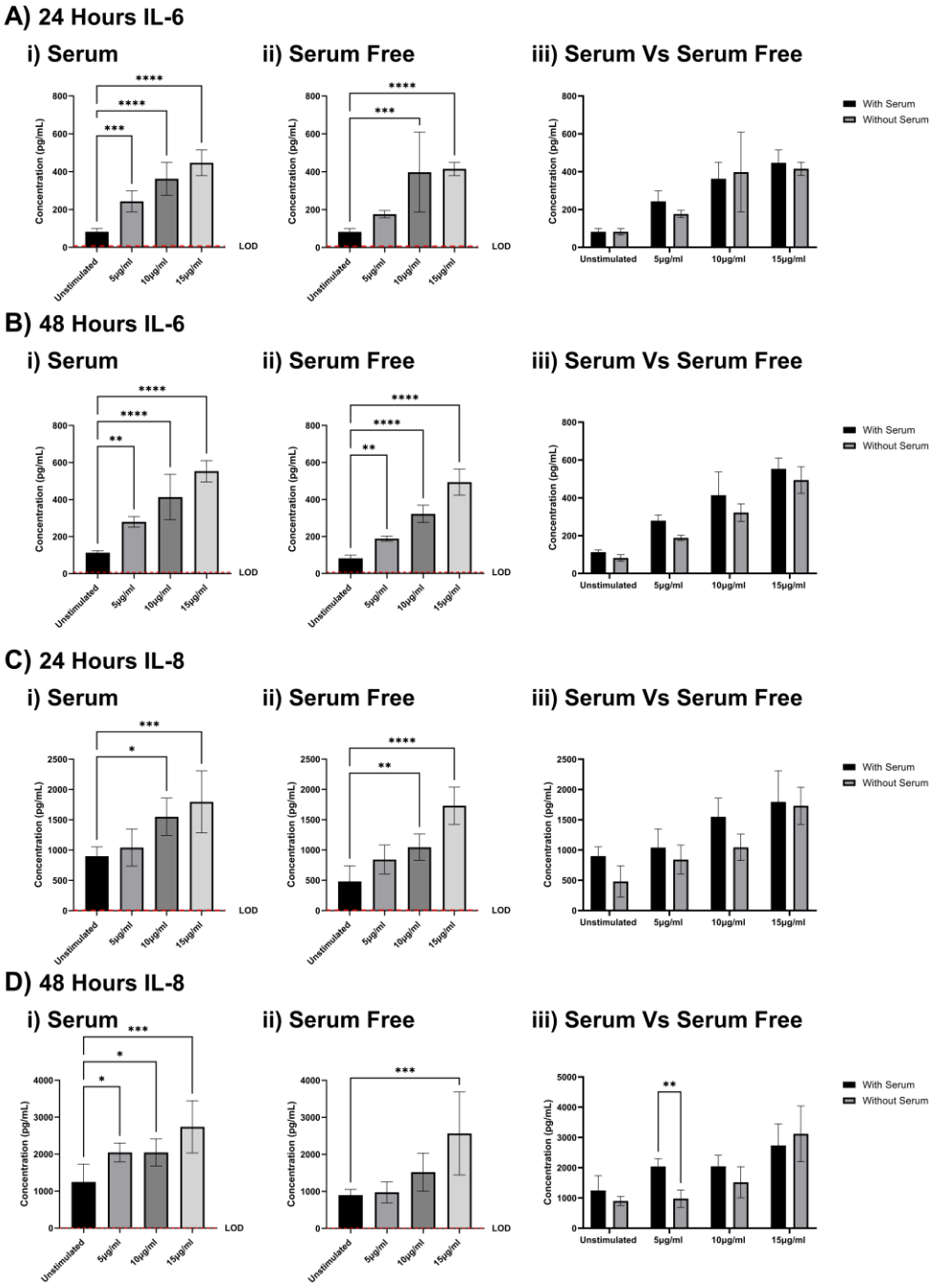

Figure 4.14. IL-6 and IL-8 response to 5, 10 and 15µg/ml Poly(I:C) stimulation in Serum and Serum Free Cultures. A) IL-6 Secretion 24 Hours post stimulation in **Ai)** Serum and **Aii)** Serum Free cultures. **Aiii)** comparison of Culture IL-6 secretion. **B)** IL-6 Secretion 48 Hours post stimulation in **Bi)** Serum and **Bii)** Serum Free cultures. **Biii)** comparison of Culture IL-6 secretion. **C)** IL-8 Secretion 24 Hours post stimulation in **Ci)** Serum and **Cii)** Serum Free cultures. C**iii)** comparison of Culture IL-8 secretion. **D)** IL-8 Secretion 24 Hours post stimulation in **Di)** Serum and **Dii)** Serum Free cultures. **Diii)** comparison of Culture IL-8 secretion. LoD is indicated by doted red line ; 7.17pg/ml - IL-6 and 10.77pg/ml – IL-8. Columns represent mean and error bars represent standard deviation. One way ANOVA with Dunnett's multiple comparison test compared stimulation concentrations and Two-way ANOVA with Sidak's multiple comparison test compared culture conditions. *p≤0.05, **p≤0.01, ***p≤0.001, ****p≤0.0001.

Having assessed the Calu-3 responses to Poly(I:C) in serum and serum-free conditions and identified a potential stimulation concentration of 10µg/ml, its effect on cell viability was assessed. Viability was profiled via flow cytometry, using annexin V and PI staining. The gating strategy outlined in Figure 4.15 was used to analyse Calu-3 cell viability after 24- and 48-hour exposure to 10µg/ml Poly(I:C) in serum-free culture, 37°C and 5% CO_2. Representative dot plots displaying cell viability for unstimulated and 10µg/ml Poly(I:C) stimulated cells at 24 and 48 hours are presented Figure 4.15. Unstimulated cells stained with annexin-V FITC and PI after 24 hours and 48 hours can be seen in Figures 4.15Ai and 4.15Bi respectively, adjacent to these plots are presented 24- and 48-hour 10µg/ml Poly(I:C) stimulations (Figure 4.15Aii and Bii). Figure 4.15C shows average viability of stimulated and unstimulated cultures after 24 and 48-hour exposure to 10µg/ml Poly(I:C) (N=3). Two-way ANOVA analysis revealed no significant difference in culture viability between stimulated and unstimulated cultures at each time point, as well as no significant variation in culture viability between 24- and 48-hour time points. This data further supported the selection of 10µg/ml of Poly(I:C) as a suitable concentration for Calu-3 stimulation.

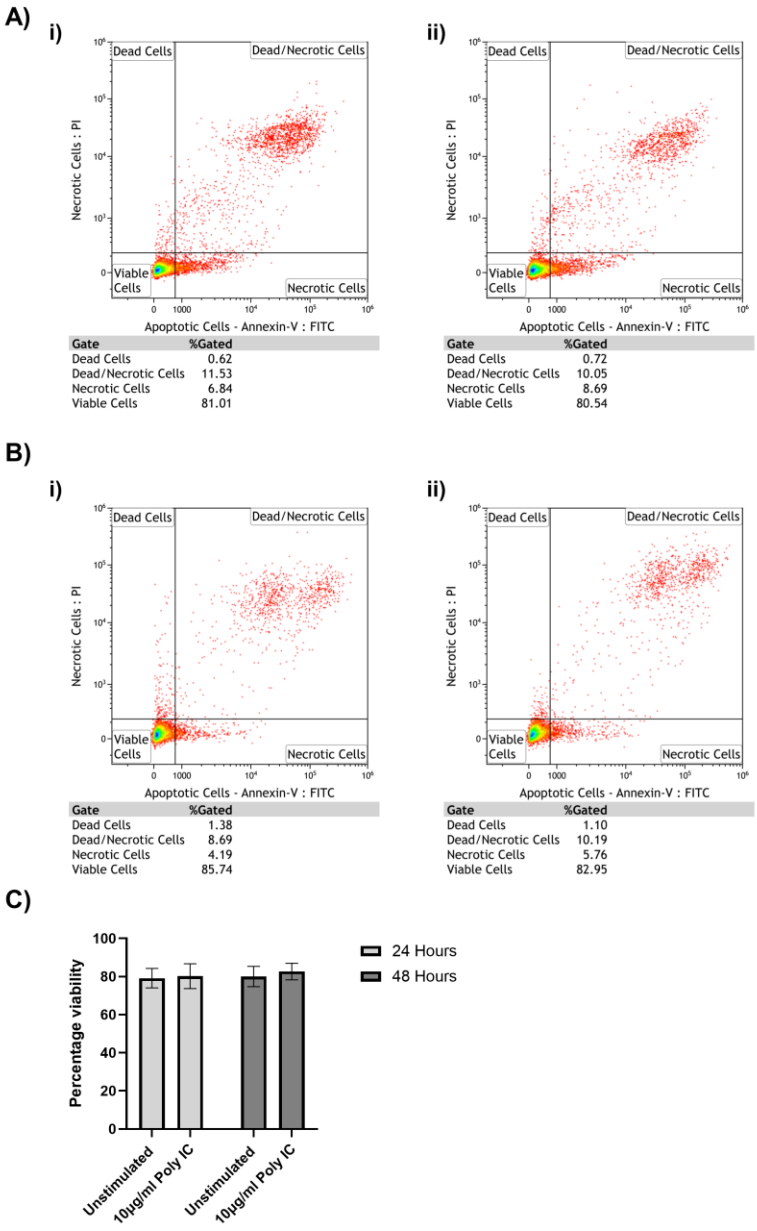

Figure 4.15. 24- and 48- Hour Annexin-V/PI Viability Staining Plots for Unstimulated and 10µg/ml Poly(I:C) Stimulated Cultures. A) Representative viability plots of unstimulated **Ai)** and 10µg/ml Poly(I:C) stimulated cultures after 24-hour exposure **Aii)**. **B)** Representative viability plots viability of unstimulated **Bi)** and 10µg/ml Poly(I:C) stimulated cultures after 48-hour exposure **Bii). C)** Comparison of 10µg/ml Poly(I:C) stimulated and unstimulated viability after 24- and 48-hour exposure (N=3). Columns represent means and error bars indicate standard deviation. Two-way ANOVA with uncorrected Fisher's least significant difference tested significance between stimulation condition and time point *$p \leq 0.05$.

4.4. Discussion

This chapter aimed to create an epithelial model which allows the profiling of EV responses by airway epithelial cells after allergen exposure. The results presented illustrate the process of selecting a suitable cell line, as well as the identification of optimal culture conditions and profiling of relevant controls. Initial profiling of BEAS-2B and Calu-3 phenotype showed expression of epithelial markers (E-Cadherin and βIV-Tubulin) in agreement with previous data (Stewart *et al.,* 2012).

Subsequent characterisation of EVs will look at expression of the MISEV-recommended epithelial markers, EpCAM and Tspan8 (Théry *et al.,* 2018). Thus, their extracellular expression on potential cell lines was also assessed. BEAS-2B lacked extracellular EpCAM expression, contradicting current literature (Han *et al.,* 2020). This disparity might be due to their culture conditions of BEAS-2B in FBS, which was shown by Zhao and Kilmecki to significantly alter the phenotype and gene expression of BEAS-2B cells, particularly E-Cadherin (Zhao and Klimecki, 2015). Conversely, Calu-3 extracellular expression of EpCAM was high, as previously reported (Meier *et al.,* 2009, Frederick *et al.,* 2007). EV biogenesis, particularly exosome biogenesis, is derived from the origin cell's plasma membrane, so a lack of extracellular EpCAM expression on this plasma membrane could affect expression of markers on the surface of secreted EVs and thus influence characterisation via flow cytometry. Consequently, Calu-3 were selected for the model.

Calu-3 cell culture in serum-free conditions showed downregulation of epithelial marker E-Cadherin, thus a 5% human AB serum supplement culture medium was chosen. The selected conditions were supported by confidential information shared by Unilever collaborators and were similar to conditions identified for human serum culture of keratinocytes (Belot, 2017). Importantly, optimised culture composition did not influence expression of epithelial extracellular markers EpCAM and so were used for all subsequent experiments.

Once a cell line and culture conditions were identified, positive control stimulants were assessed by ELISA to establish concentrations capable of inducing a cytokine response. Initial LPS stimulations saw poor cytokine induction in Calu-3, contrary to the literature, which indicated that stimulation of Calu-3 and other epithelial cells with LPS induces strong IL-8 and IL-6 response (Journeay *et al.,* 2008, Schulz *et al.,* 2002). Subsequent review of the literature indicated that serum contains high concentrations of LPS-BP (18.1μg/ml) (Gallay *et al.,* 1994), and supplementation of cultures with LPS-BP yielded improved responses to stimulants, inducing similar responses to previous research in serum-containing cultures (Journeay *et al.,* 2008, Schulz *et al.,* 2002). Thus, it is important to consider the addition of LPS-BP when stimulating cells in serum-free conditions. Additionally, Poly(I:C) stimulation of Calu-3 was assessed. Dose experiments identified induction of significant cytokine responses in IL-6 and IL-8, consistent with results presented in previous literature (Islam *et al.,* 2021, Herbert *et al.,* 2017, Chen *et al.,* 2019). Furthermore, cell viability showed that the positive controls did not induce cell apoptosis, confirming that these were suitable for downstream analysis of EVs.

Here we have shown the considerations in the selection of a suitable epithelial cell line and positive controls, as well as optimisation of culture. Positive control responses were profiled in 2D, and non-lethal cytokine-inducing concentrations were identified to be taken forward into 3D models. The next chapter will outline the optimisation of a 3D model, as well as techniques used for successful stimulation.

Chapter 5: Optimisation of 3D Cell Culture Model

5.1. Introduction

For many years, animal models have been considered the gold standard model and key tool in the research and investigation into the health-related impacts of inhaled substances. However, human-specific differences in the pathogenesis and presentation of disease significantly limit the biological relevance of animal models. This was emphasised by an investigation into the translational potential of therapies identified in animals. This showed that only 5% of therapies confirmed in animal models were successfully translated into humanised treatments (Lam et al., 2025, Ineichen et al., 2024). While *in silico* computer modelling in toxicological studies could prove to be a useful tool in the future, humanised *in vitro* culture systems present a more robust and biologically relevant option.

When generating a human *in vitro* culture model, it is important to consider a variety of key factors, such as the scale, anatomical accuracy and cell populations relevant to the area being modelled (Nichols *et al.,* 2014). Currently, there are numerous lung cell models, with these falling into one of two categories: either 2D or 3D models. 2D lung models are the simplest form of tissue culture, consisting of submerged monolayers comprised of a single cell type. However, the airway epithelium is comprised of a diverse community of different cell types and states held together by tight junctions. Furthermore, localisation of expression of these cell types creates functionally specific regions within the airway epithelium (Hewitt and Lloyd, 2021). Consequently, the simplistic nature of 2D homogenous cell cultures makes them unsuitability for modelling airway epithelial responses in a biologically relevant way. Despite 2D cultures lacking the cellular diversity and structures found in the tissues they aim to model, they have been shown to be useful in profiling basic lung cell function and differentiation (Miller and Spence, 2017).

The ability of 3D cultures to provide greater complexity facilitates the closer replication of the tissue or microenvironment being modelled.

Consequently, these culture models provide an avenue for assays with greater biological relevance.

One method for generating a 3D model is the culture of cells at the air liquid interface (ALI). This describes the process of culturing epithelial cells exposed to air on their apical side and submerged in media on their basal side. Culture of cells in this manner induces epithelial polarisation and the formation of complex structures, such as tight junctions (Lee *et al.,* 2023). Additionally, ALI culture of epithelial cells allows for their differentiation into different epithelial cell types, such as secretory cells and ciliated epithelial cells.

3D experiments presented in this chapter aim to profile and confirm the generation of 3D airway epithelial ALI cultures, as well as optimise a suitable mechanism for the successful stimulation of these cultures with the previously identified positive control stimulants, LPS and Poly(I:C).

5.2. Materials and Methods

5.2.1. 3D Culture Characterisation

ALI Cultures were grown as outlined in Section 2.2.1.4. Characterisation of ALI cultured epithelial cells was performed after cells were isolated from trans wells using Accutase (Section 2.2.3). Initial characterisation aimed to confirm the successful generation of ALI cultures. Cells were stained with the manufacturer's recommended volume (5µl) of fluorescent antibodies (Table 5.1) and analysed using conventional flow cytometry. Section 2.2.3 outlines the intra- and extracellular staining processes utilised.

Table 5.1. Fluorescent antibodies used for characterisation of airway epithelial cell lines, their fluorophore and manufacturer.

Antibody Target	Fluorophore	Manufacturer	Cat.no.
EpCAM	PE-Cy7	Biolegend	369816
E-Cadherin	APC	Biolegend	324107
Tspan8	PE-Vio770	Miltenyi	130-106-865
CD66	BV605	Biolegend	342323
CD271	PE	Biolegend	345105

Tight junction formation was assessed using fluorescent staining (Section 2.1.5) for Z0-1 (AlexaFlour647) and Occludin (AlexaFlour488) as per manufacturer's instructions and assessed using confocal microscopy (Section 2.2.2.1). Additionally, formation of cilia was assessed using scanning electron microscopy. Samples were washed and dehydrated with a graded series of ethanol dilutions before sputter coating with platinum (Section 2.2.2.2.).

5.2.2. 3D Submersion stimulation

Submersion experiments were carried out as specified in Section 2.2.1.4. In brief, 50µl of stimulant diluted in PBS was added to the apical chambers of inserts and left to incubate (37ºC and 5% CO_2). Following 24- and 48-hour exposure, the 50µl of stimulant was isolated into Eppendorfs and

apical surfaces were then washed twice with 200µl of 37ºC sterile filtered PBS for 3 minutes and washes were added to Eppendorfs. This was topped up to a final volume of 500µl to allow for direct comparison of apical and basal concentrations.

2- and 8-hour (Section 2.2.1.4) apical samples were submerged in stimulant (as above) for either 2 or 8 hours. Stimulants were aspirated after exposure and samples were collected 24 and 48 hours after the initial addition of stimulant. Apical samples were collected as above with two 200µl sterile PBS washes (37ºC) and topped up with 100µl of PBS to create a total volume of 500ul.

ELISAs were conducted as outlined in Section 2.2.11. All cytokines were run on neat sample with the exception of IL-8 which was analysed using samples diluted 1:10 in PBS.

5.2.3. Nebulisation Stimulations

Concentrations added to the nebuliser were calculated using the equations outlined in Section 2.2.1.5. As per Section 2.2.1.5. inserts were apically washed with 200µl of sterile filtered 37ºC PBS two days prior to stimulation to ensure mucus cover of the inserts was low. Stimulations were carried out using an Aerogen Pro-nebuliser (2.6 -6.0vMD) (Aerogen, Ireland). Inserts were nebulised until all liquid in the nebuliser was used and were left in the chamber Cloud Alpha AX12 (Vitrocell, Germany) for 10 minutes to allow for deposition (full method in Section 2.2.1.5). Samples were then incubated for 24 and 48 hours at 37ºC and 5% CO_2. Apical sample collection was conducted as above (see 2- and 8-hour exposure).

ELISAs were conducted as outlined in Section 2.2.11. All Cytokines were run on neat sample with the exception of IL-8 which was analysed using samples diluted 1:10 in PBS.

5.3. Results

5.3.1. Profiling of 3D cultures

To create a more robust and biologically relevant model of the airway than 2D submersion cultures, cells were cultured at air liquid interface (ALI). Culturing airway epithelial cells this way allows for differentiation of cells and the formation of tight junction complexes. ALI inserts were cultured as specified (Method section reference). ALI cultures were initially profiled using flow cytometry, confocal microscopy and scanning electron microscopy (SEM). The markers used for profiling epithelial cells are detailed in table 5.2.

Table 5.2. Epithelial cell markers used to profile ALI Cultures. Epithelial markers and corresponding target.

Epithelial Marker	**Target Function**	**Location (Target Cell)**
E-Cadherin	Epithelial Adheren junction protein	General Epithelial marker
Tspan8	Axonemes	Goblet Cells (Epithelial cancer marker)
EpCAM (CD326)	Epithelial Adhesion molecule	General Epithelial marker
CD271	Involved in Cell Survival, differentiation and Migration	Basal Cells
CD66	Immune Adhesion molecule	Secretory Cells

Figure 5.1. shows the expression of epithelial cell markers. Samples were analysed using ID7000 spectral flow cytometer. Compensation bead single stains were used for unmixing (Data not shown). Unmixed samples were analysed as previously shown (Figure 4.1A). High expression of both E-Cadherin and Tspan8 was observed (Figure 5.1A&B), consistent with 2D cultures, further affirming their selection as epithelial-derived EV markers for EV characterisation. EpCAM expression (Figure 5.1C), while present in cultures, was lower than the expression in 2D cultures. Additionally, a shift in signal between CD66-stained and unstained cells denoted the presence of secretory cells within the population, indicating the successful differentiation of ALI cultures (Figure 5.1 D). CD271 staining was negative and showed no basal cell population (Figure 5.1E).

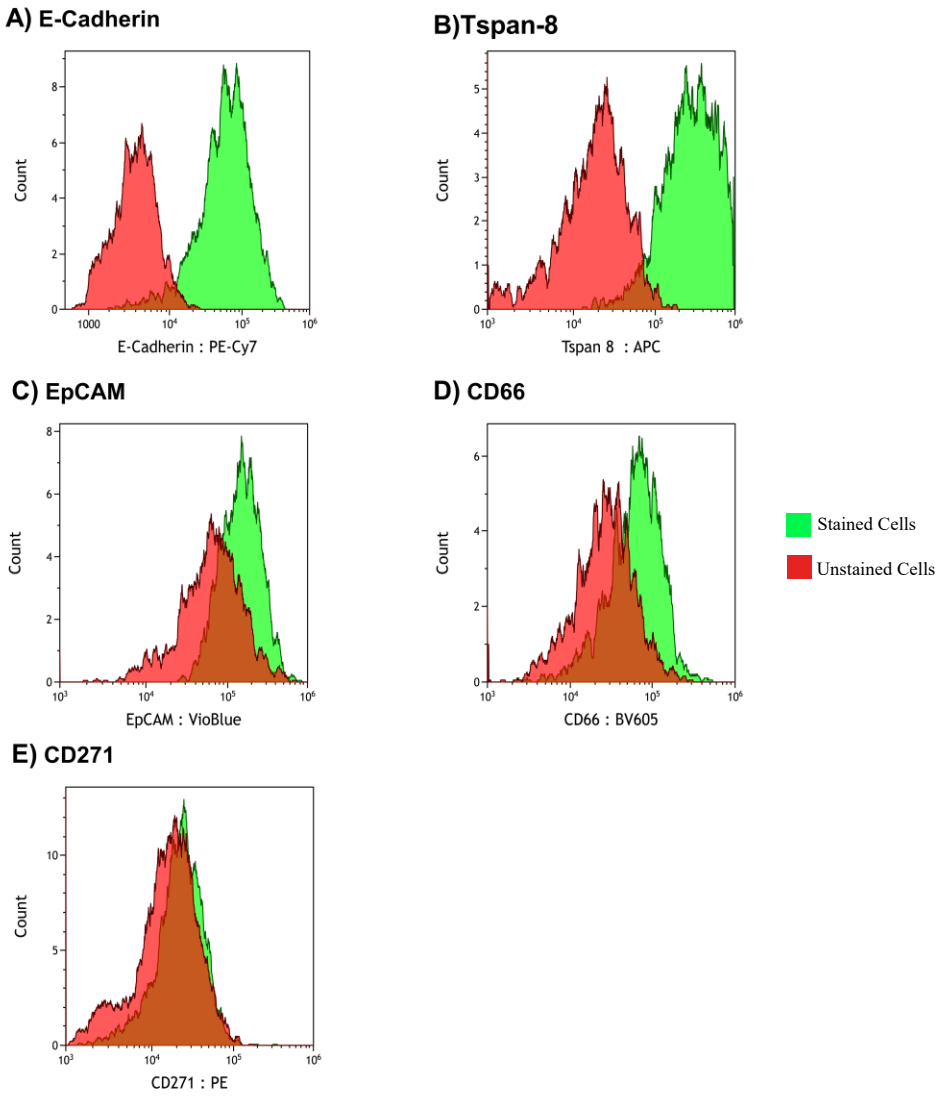

Figure 5.1. Histograms Overlays of Epithelial Cell Markers Fluorescent Intensity. Fluorescent intensity histograms of unstained and stained samples analysed using a Sony ID7000 spectral flow cytometer. **A)** E-Cadherin, **B)** Tspan8, **C)** EpCAM, **D)** CD66 and **E)** CD271. Red histograms represent unstained samples and green represent strained samples.

In addition to profiling cell populations within 3D cultures, the tissue structure and tight junctions were evaluated using confocal microscopy. Inserts were fluorescently stained for tight junction markers ZO-1 and Occludin and imaged on a Zeiss LSM 9000 microscope. Figure 5.2 shows single colours for ZO-1 (Figure 5.2A) and Occludin (Figure 5.2B), as well as the combined final stain (Figure 5.2C). Staining revealed the presence of both markers localised to cell boundaries, confirming the formation of tight junctions during the ALI culture process.

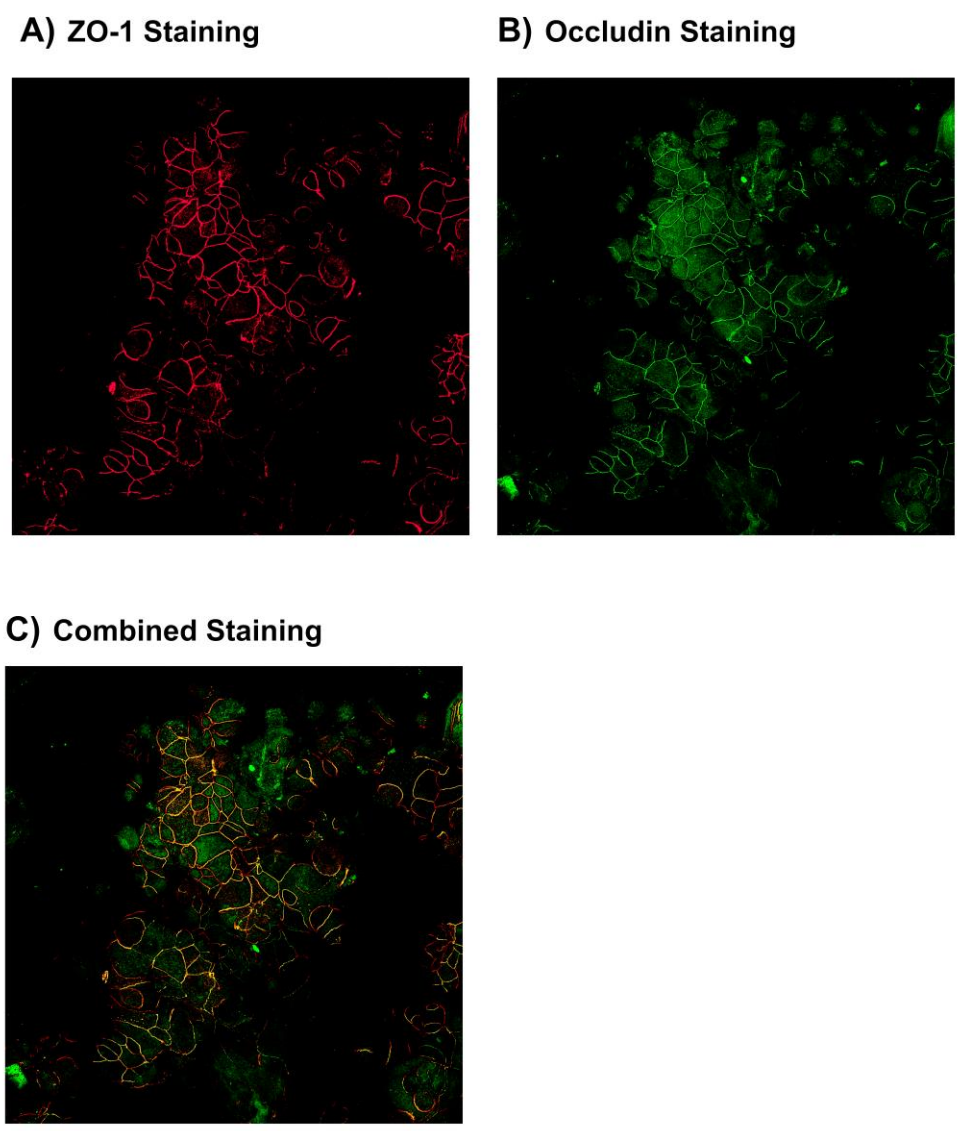

Figure 5.2. 3D Epithelial culture ZO-1 and Occludin Tight Junction Staining. ALI Culture stained with fluorescently tagged antibodies for ZO-1 and Occludin. Samples analysed using ZeissLSM9000. Objective: Plan-Apohcromat 20x, numerical aperture 0.8. A) Alexa647 laser, ZO-1. B) Alexa488 laser, Occludin. C) Alexa647 and Alexa488 laser, ZO-1 and Occludin.

Final profiling conducted on ALI inserts was imaging of cilia using scanning electron microscopy (SEM). Inserts were prepared as described in section (Methods insert) and imaged using a Zeiss Crossbeam 550. Figure 5.3 shows images of inserts increasing in magnification. Figure 5.3A shows 1.0K magnification of ciliated epithelial cells. Increasing in magnification to 2.50Kx (Figure 5.3B) allowing for the identification of cilia on the surface of

cells. Further increases in magnification to 15.58Kx allowed for a more focused view of the cilia (Figure 5.3C). Confirmation of cilia, along with the previous profiling of tight junctions (Figure 5.2) and cell populations (Figure 5.1), showed successful generation of a more biologically and physiologically relevant culture, which will be utilised instead of 2D monocultures moving forward.

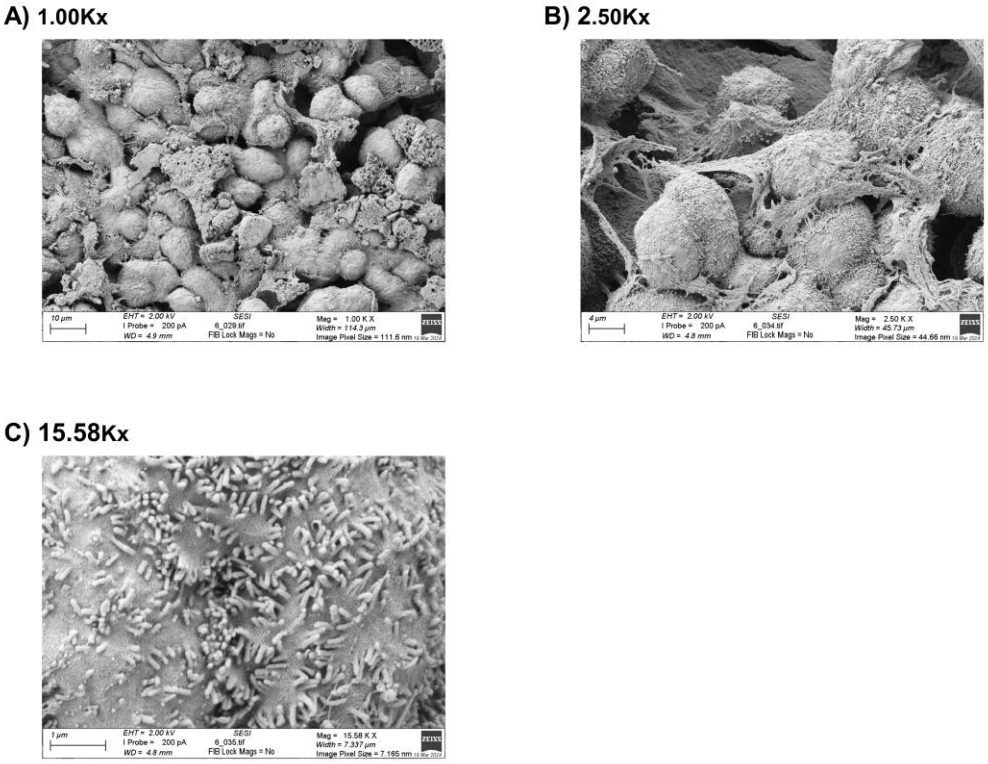

Figure 5.3. SEM Images of ALI cultured Calu-3 Cilia . ALI Cultured Calu-3 cells imaged at **A)** 1.0Kx, **B)** 2.5Kx and **C)** 15.58Kx magnification, on Zeiss Crossbeam550.

5.3.2. Submersion Stimulations

Having profiled and confirmed the successful generation of a 3D model of the airway epithelium (Section 4.3.4), control stimulations were re-assessed. Previously identified concentrations of 10µg/ml Poly(I:C), as well as 0.5 and 1.0µg/ml LPS, were used to stimulate 3D cultures. An initial test stimulation of 3D cultures was conducted (N=1) for each of the three identified stimulation conditions. To mirror initial 2D proof of concept stimulations (sections 4.3.3.1&2), cultures were apically submerged in 50µl of either 10µg/ml Poly(I:C), 0.5µg/ml or 1.0µg/ml LPS, and unstimulated controls were submerged in 50µl of PBS, for 24 and 48 hours. The effect of stimulant exposure on secretion of IL-1β, IL-6, IL-8, IL-17E (IL-25), IL-33 and TSLP was measured using ELISAs. Figure 5.17 shows exemplar standard curves for IL-1β (Figure 5.17A), IL-17E (Figure 5.17B), IL-33 (Figure 5.17C) and TSLP (Figure 5.17D). Exemplar standard curves for IL-6 and IL-8 are shown in Chapter 4.

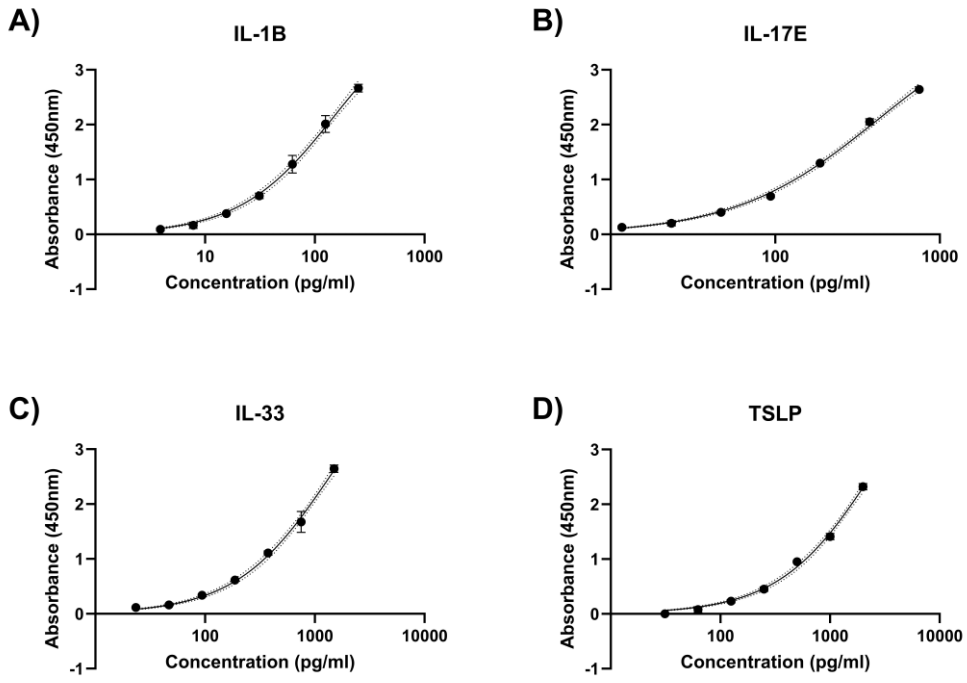

Figure 5.4. IL-1β, IL-17E, IL-33 and TSLP Standard Curves. A) IL-1β, **B)** IL-17E, **C)** IL-33 and **D)** TSLP standard curves produced to interpolate cytokine concentration (pg/ml).

No apical or basal cytokine secretion was detected for IL-1β, IL-17E, IL-33 and TSLP after 24 or 48 exposures (data not shown). However, both IL-6 and IL-8 were detected (Figure 5.5). Initial stimulations saw an increase in apical IL-6 when stimulated with 0.5 and 1μg/ml LPS for 24 hours (Figure 5.5Ai). Additionally, Poly(I:C) apical IL-6 decreased relative to the unstimulated control. After 48 hours exposure, increases in apical IL-6 were seen with 0.5μg/ml LPS and 10μg/ml Poly(I:C) (Figure 5.5Aii). However, comparison of 24- and 48-hours responses showed IL-6 concentration decreased for all samples, except Poly(IC) (Figure Aiii). Basal IL-6 was not detected at 24 Hours (Figure 5.5Bi), however this changed after 48 hours, with basal IL-6 detected in just unstimulated samples (Figure Bii).

Changes in apical IL-8 concentration were also observed, increasing after 24-hour stimulation with 0.5μg/ml LPS (Figure 5.5Ci). As with IL-6, 24 hour Poly(I:C) stimulation saw a decrease in IL-8. After 48- hour exposure a small increase in apical IL-8 was seen for all stimulants (Figure Cii). However, as with IL-6, comparison of 24- and 48-hour apical IL-8 responses showed a decrease with time, except for Poly(I:C) stimulation (Figure 5.5Ciii). IL-8 basal responses at both 24 and 48 hours for stimulants, decreased relative to unstimulated samples (Figure 5.5Di&Dii). Comparison of 24- and 48- hours showed increased IL-8 concentrations with time (Figure 5.5Diii).

While initial test stimulations appeared to have some effect on cytokine production at 24 and 48 hours, it was observed that submersion of inserts for 24- and 48-hour durations was damaging the cell layer, causing cells to detach from the trans wells. Mechanically damming the epithelial insert would prevent additional analysis of the epithelial barrier post-stimulation.

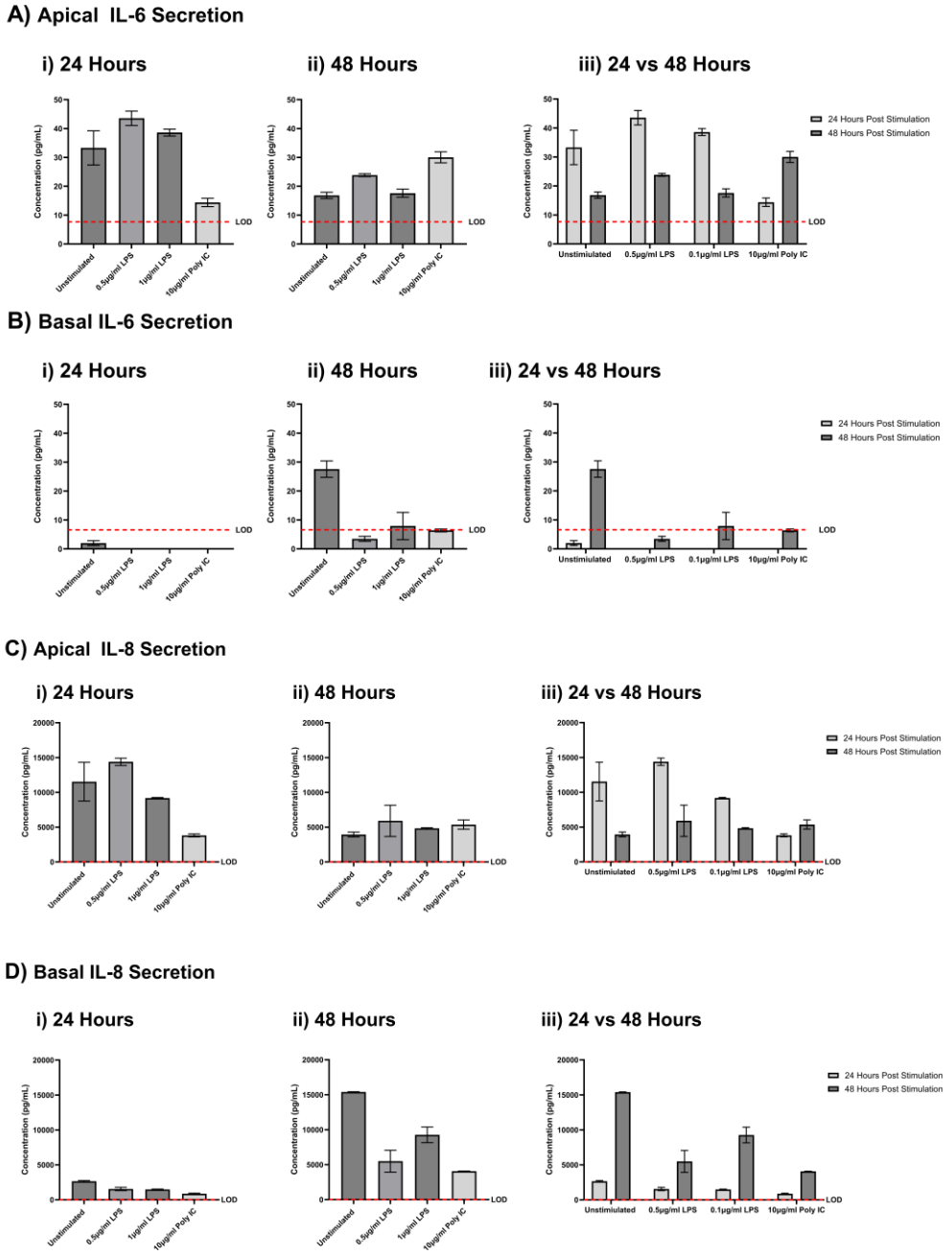

Figure 5.5. IL-6 and IL-8 Response to 24 and 48 submersion stimulation of ALI cultures with 0.5µg/ml LPS, 1.0µg/ml LPS and 10µg/ml Poly(I:C). A) Changes in apical IL-6 secretion as a result of submerged **Ai)** 24 hours exposure and **Aii)** 48-hour exposure . **Aiii)** comparison of 24- and 48-hour apical responses. **B)** Changes in basal IL-6 secretion as a result of submerged **Bi)** 24 hours exposure and **Bii)** 48-hour exposure . **Biii)** comparison of 24- and 48-hour basal responses. **C)** Changes in apical IL-8 secretion as a result of submerged **Ci)** 24 hours exposure and **Cii)** 48-hour exposure. C**iii)** comparison of 24- and 48-hour apical responses. **D)** Changes in basal IL-8 secretion as a result of submerged **Di)** 24 hours exposure and **Dii)** 48-hour exposure. D**iii)** comparison of 24- and 48-hour basal responses. LoD is indicated by doted red line ; 8.0pg/ml - IL-6 and 22.8pg/ml – IL-8. Columns represent mean and error bars represent standard deviation. (N=2) .

Due to the observed damage resulting from 24- and 48-hour submersion of ALI epithelial cultures, reduced submersion durations were assessed. Cultures were apically submerged in 50µl of either PBS (unstimulated control), 10µg/ml Poly(I:C) or 0.5µg/ml for 2 or 8 hours (to mimic a short-term or long-term exposure to allergen) (N=3). After exposure duration, stimulants were aspirated from the trans wells so that the inserts were no longer submerged. Samples were incubated (37ºC and 5%CO_2) for 24- and 48-hours post addition of the stimulant. The effect of stimulant exposure on secretion of IL-1β, IL-6, IL-8, IL-17E (IL-25), IL-33 and TSLP was measured in duplicate via ELISAs.

As with previous stimulations, no apical or basal cytokine secretion was detected for IL-1β, IL-17E, IL-33 and TSLP after 2 or 8 exposures (data not shown). No significant changes in apical IL-6 were observed after 2- or 8-hour exposure with either stimulant for both 24- and 48-hour samples (Figure 5.6Ai&Aii). However, comparison of 24- and 48-hour apical responses saw a significant increase in IL-6 apical cytokine for both exposure durations (Figure 5.6Aiii&Aiv). As observed previously, basal IL-6 secretion was low and undetectable for most conditions, with no significant change in concentration being observed in 24- or 48-hour samples after either exposure duration (Figure 5.6B).

After 24-hour incubation, a significant change was observed in the apical IL-8 secretion of inserts exposed to 10µg/ml Poly(I:C) (Figure 5.6Ci). Additionally, a significant decrease in apical IL-8 was observed in inserts exposed to 0.5µg/ml for two hours. After 48 Hours, no significant differences were observed (Figure 5.6Cii). Comparison of 24- and 48-hour responses saw significant increases in apical IL-8 with time for both exposure durations (Figure 5.6Ciii&iv). Basal IL-8 concentrations didn't see any significant changes after 24 hours for either exposure (Figure 5.6Di). After 48 hours a significant decrease in IL-8 was observed in 2 hour 0.5µg/ml LPS exposures, no other significant changes were observed (Figure 5.6Dii). Comparison of 24- and 48-hour basal IL-8 responses saw no significant changes for either exposure duration (Figure 5.6 Diii&Div).

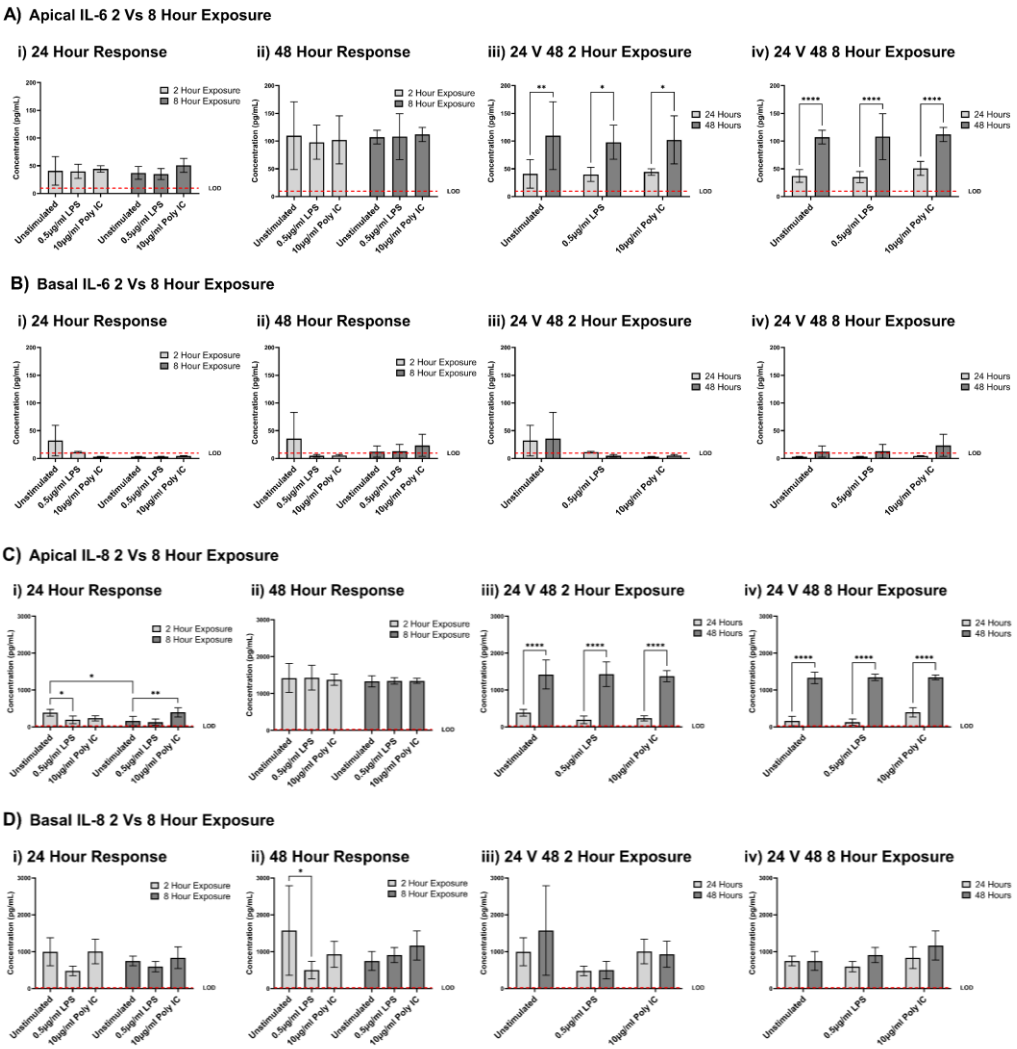

Figure 5.6. Apical and Basal IL-6 and IL-8 Response to 2- and 8-Hour Exposure to 5µg/ml LPS, 10µg/ml Poly(I:C). A) Apical IL-6 Secretion, comparison of 2- and 8-hour exposure, **Ai)** 24 Hours post stimulation **Aii)** 48 Hours post stimulation. **Aiii)** Comparison of 2-hour exposure response at 24 and 48 hours. **Aiv)** Comparison of 8-hour exposure response at 24- and 48-hours. **B)** Basal IL-6 Secretion, comparison of 2- and 8-hour exposure, **Bi)** 24 Hours post stimulation **Bii)** 48 Hours post stimulation. B**iii)** Comparison of 2-hour exposure response at 24 and 48 hours. **Biv)** Comparison of 8-hour exposure response at 24- and 48-hours.**C)** Apical IL-8 Secretion, comparison of 2- and 8-hour exposure, **Ci)** 24 Hours post stimulation **Cii)** 48 Hours post stimulation. **Ciii)** Comparison of 2-hour exposure response at 24 and 48 hours. **Viv)** Comparison of 8-hour exposure response at 24- and 48-hours. **D)** Basal IL-6 Secretion, comparison of 2- and 8-hour exposure, **Di)** 24 Hours post stimulation **Dii)** 48 Hours post stimulation. **Diii)** Comparison of 2-hour exposure response at 24 and 48 hours. **Div)** Comparison of 8-hour exposure response at 24- and 48-hours. LoD is indicated by doted red line; 9.55pg/ml - IL-6 and 25.53pg/ml – IL-8. Columns represent mean and error bars represent standard deviation. Two-way ANOVA with Sidak's multiple comparison test compared was used to test significance. *p≤0.05, **p≤0.01, ***p≤0.001, ****p≤0.0001. (N=6)

While inserts were not damaged with the shorter submersion times, variability in response, as well as a lack of significant response above unstimulated background, suggested stimulation concentrations may need re-evaluation to compensate for reduced exposure time. Literature, utilising nebulisation suggested increasing the concentration of LPS to an equivalent dose of 3µg/ml might induce a larger cytokine response which could induce a response higher than background. Consequently, this stimulation concentration of LPS was evaluated to assess the effect of increasing concentration on cytokine secretion. Cultures (N=3) were stimulated with 50µl of 3µg/ml of LPS for 2 or 8 hours. Stimulants were aspirated after exposure duration and changes in apical and basal IL-1β, IL-6, IL-8, IL-17E (IL-25), IL-33 and TSLP secretion were assessed in duplicate via ELISA 24 hours post-stimulant addition.

As with previous experiments, no measurable concentration of IL-1β, IL-17E, IL-33 and TSLP was detected (Data not shown). Figure 5.7A shows apical and basal IL-6 secretion after 2- and 8-hour exposure to LPS. While not significant, a small increase in apical IL-6 concentration was observed in inserts exposed for 2 hours with 3µg/ml LPS, with average concentration increasing from 95pg/ml in unstimulated controls to 110.5pg/ml. In the 8-hour exposed samples, this increase in secretion was significant, increasing from an average of 132pg/ml to 159pg/ml (Figure 5.7Ai). Comparison of 2- and 8-hour exposure also saw a significant increase in induced response after 8-hour submersion for both unstimulated and stimulated samples. Evaluation of IL-6 basal secretion (Figure 5.7Aii) showed a similar response to apical samples, with a significant increase in IL-6 response being observed in samples exposed to 3µg/ml LPS for 8 hours. However, comparison of 2- and 8-hour basal response showed no significance difference, unlike that observed in apical samples.

In contrast to IL-6, IL-8 apical concentrations did not significantly change for either exposure duration (Figure 5.7Bi). Additionally, there was no significant variation in the response between 2- and 8-hour exposed samples. Evaluation of basal IL-8 responses (Figure 5.7Bii) to 2-hour submersion stimulation also showed no significant difference between stimulated and

unstimulated control samples. 8-hour exposure to 3µg/ml LPS generated a significant increase relative to controls, increasing from an average of 1981pg/ml in unstimulated samples to 3332pg/ml. However, while significant, this response was highly variable. Comparison of 2- and 8-hour exposure showed no significant difference in the response of unstimulated samples, but there was a significantly higher response to stimulants when exposed for 8 hours as opposed to 2 hours.

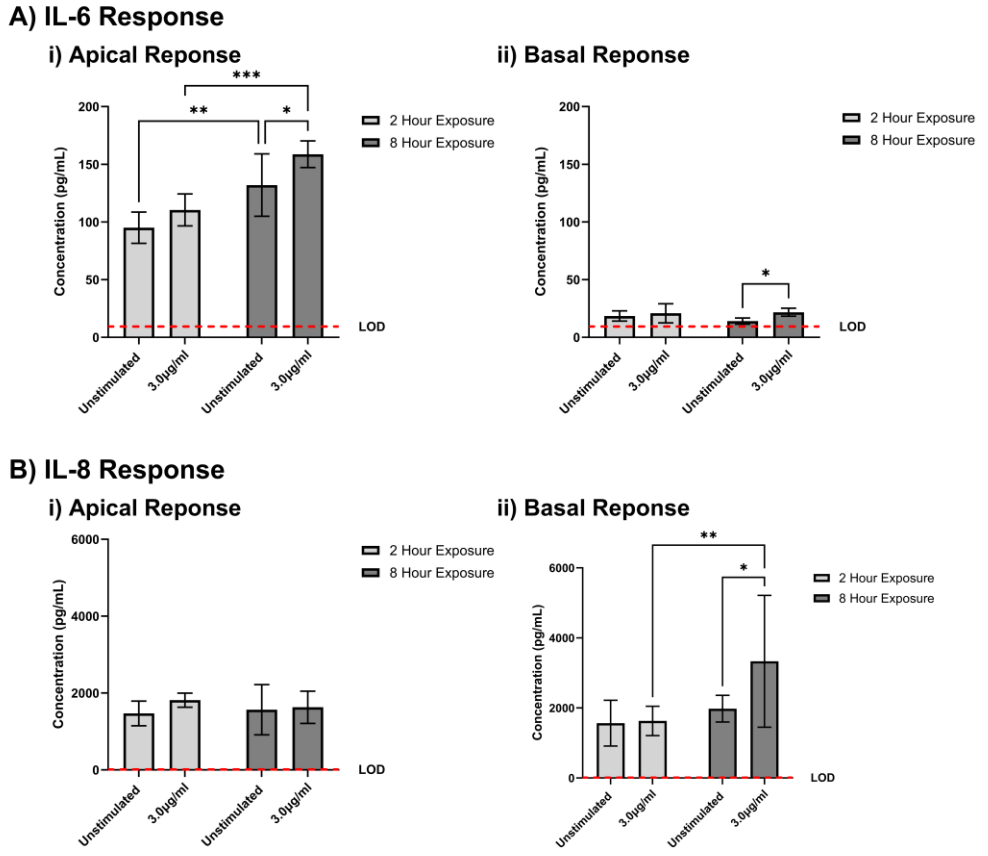

Figure 5.7. Evaluation of ALI 24- Hour Response to 2- and 8-Hour Exposure of 3µg/ml LPS. A) IL-6 response to stimulants **Ai)** Apically and **Aii)** Basally. **B)** IL-8 response to stimulants **Bi)** Apically and **Bii)** Basally. LoD is indicated by doted red line; 9.32pg/ml - IL-6 and 13.6pg/ml – IL-8. Columns represent mean and error bars represent standard deviation. Two-way ANOVA with Sidak's multiple comparison test compared was used to test significance. *p≤0.05, **p≤0.01, ***p≤0.001, ****p≤0.0001. (N=6).

Increasing LPS concentration to 3µg/ml did see some significant stimulation over the unstimulated background, however, this response was inconsistent and variable. Additionally, the significance increases in apical IL-6 response observed between exposure durations indicated the potential impact of the submersion on the observed response. Furthermore, the observed increase in 2-hour exposure response, while not significant, could indicate that a higher concentration and lower submergence may give a clearer and less mechanically influenced response. Consequently, some additional higher concentrations were evaluated to assess if responses could be increased relative to unstimulated controls after 2-hour exposure. Cultures were apically submerged in 50µl of either PBS (unstimulated control), 3, 4.5 or 6µg/ml for 2 or (N=3). After exposure duration, stimulants were aspirated from the trans wells so that the inserts were no longer submerged. Samples were then incubated for 24-hours post addition of the stimulant. The effect of stimulant exposure on secretion of IL-1β, IL-6, IL-8, IL-17E (IL-25), IL-33 and TSLP was measured in duplicate via ELISAs.

As with all previous stimulations, no measurable concentration of IL-1β, IL-17E, IL-33 and TSLP was detected (Data not shown). Figure 5.8A shows IL-6 response to stimulants. Apical IL-6 concentrations did not significantly increase relative to unstimulated controls, with 2-hour exposure to 6µg/ml LPS seeing a significant decrease in IL-6 concentration (Figure 5.8Ai). This lack of significant increase was also seen basally, and again a significant decrease in IL-6 concentration relative to unstimulated controls was observed in 3µg/ml (Figure Bii).

Figure 5.8B shows IL-8 apical and basal responses to the different LPS concentrations. No significant changes were observed in apical concentrations of IL-8 (Figure 5.8Bi). Basal concentrations also did not see a significant increase in IL-8 concentrations. However, there was a significant decrease in 3µg/ml stimulation relative to unstimulated controls, comparable with IL-6 (Figure5.8Bii).

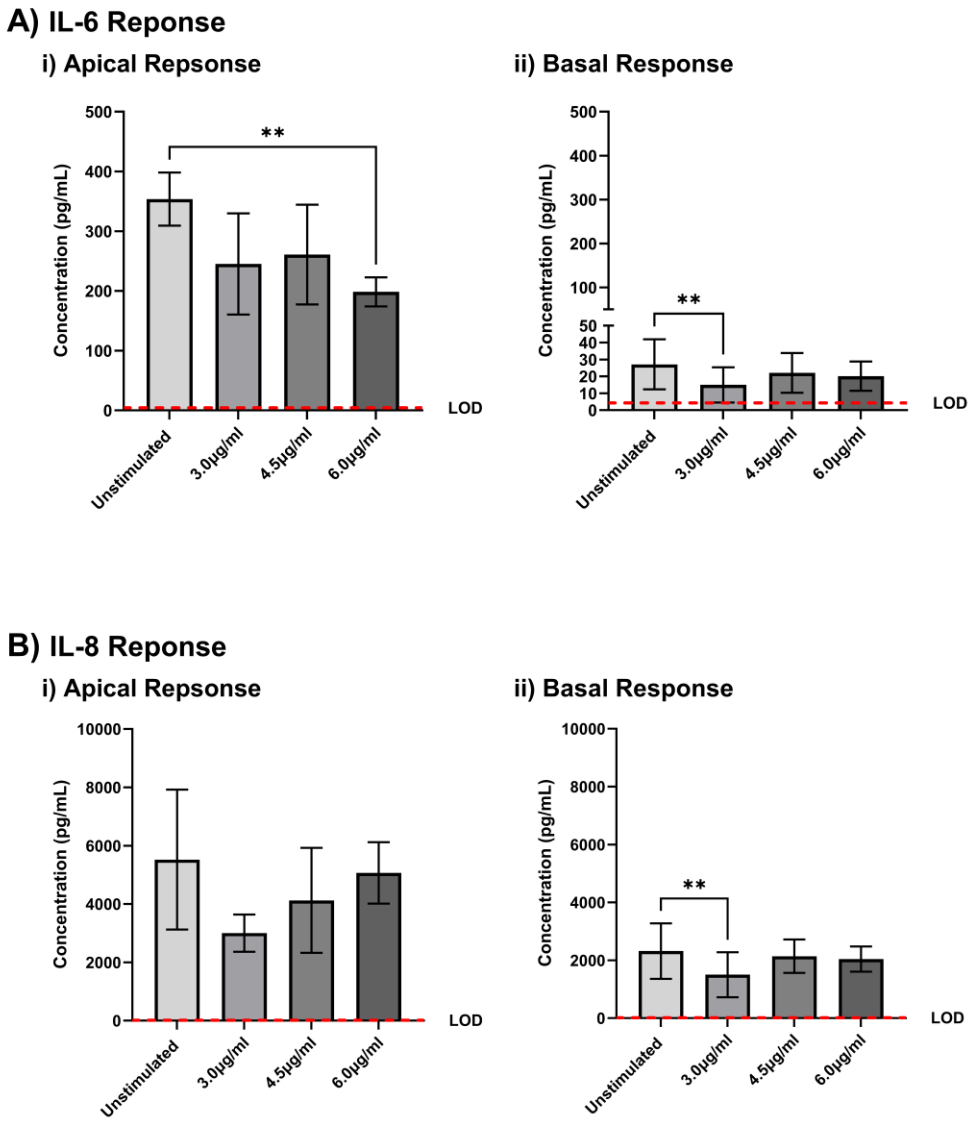

Figure 5.8. Evaluation of ALI 24- Hour Response to 2- Hour Exposure of 3, 4.5 and6µg/ml LPS. A) IL-6 response to stimulants **Ai)** Apically and **Aii)** Basally. **B)** IL-8 response to stimulants **Bi)** Apically and **Bii)** Basally. LoD is indicated by doted red line; 4.38pg/ml - IL-6 and 14.4pg/ml – IL-8. Columns represent mean and error bars represent standard deviation. Two-way ANOVA with Sidak's multiple comparison test compared was used to test significance. *p≤0.05, **p≤0.01, ***p≤0.001, ****p≤0.0001. (N=6).

Lack of significant responses above background indicates that increases in concentration did not offset reduced exposure duration of the cultures. Consequently, submergence stimulations were deemed to not be suitable and alternative stimulation mechanisms were assessed.

5.3.3. Basal Chamber Stimulation Assessment

Having established that apical submersion with stimulants was not a suitable mechanism for model stimulation, the addition of stimulants to the basal chamber of the ALI cultures was assessed. Due to the strong 2D response induced by Poly(I:C) (section 4.3.3.2) in comparison to LPS (section 4.3.3.1), the previously identified concentration of 10µg/ml was selected to assess the suitability of this stimulation mechanism. Cultures (N=2) were incubated for 24 and 48 hours (37ºC and 5% CO_2) with or without 10µg/ml Poly(I:C) added to the basal chamber. Apical and basal IL-6 and IL-8 cytokine secretion changes were assessed in duplicate via ELISA.

IL-6 apical secretion was not observed to significantly change relative to unstimulated controls after either 24- or 48-hour exposure to 10µg/ml Poly(I:C) (Figure 5.9 A). Furthermore, there was no significant change in response between 24- and 48-hour exposed samples. Additionally, there was no basal cytokine for IL-6 detected (Data not shown). While IL-6 responses were muted, there was a significant increase in apical IL-8 samples after 24-hour exposure, with an increase from 470pg/ml in unstimulated samples to 2095pg/ml. This significant increase was not observed after 48-hour exposure, with a significant decrease being observed between the 24- and 48-hour responses (Figure 5.9Bi). Basal IL-8 concentrations were also detected, but no significant difference was observed between stimulated and unstimulated samples as well between exposure durations (Figure 5.9Bii). While this method of stimulation induced significant changes in IL-8 secretion, it was not a physiologically relevant route of exposure, consequently nebulisation of stimulants was assessed.

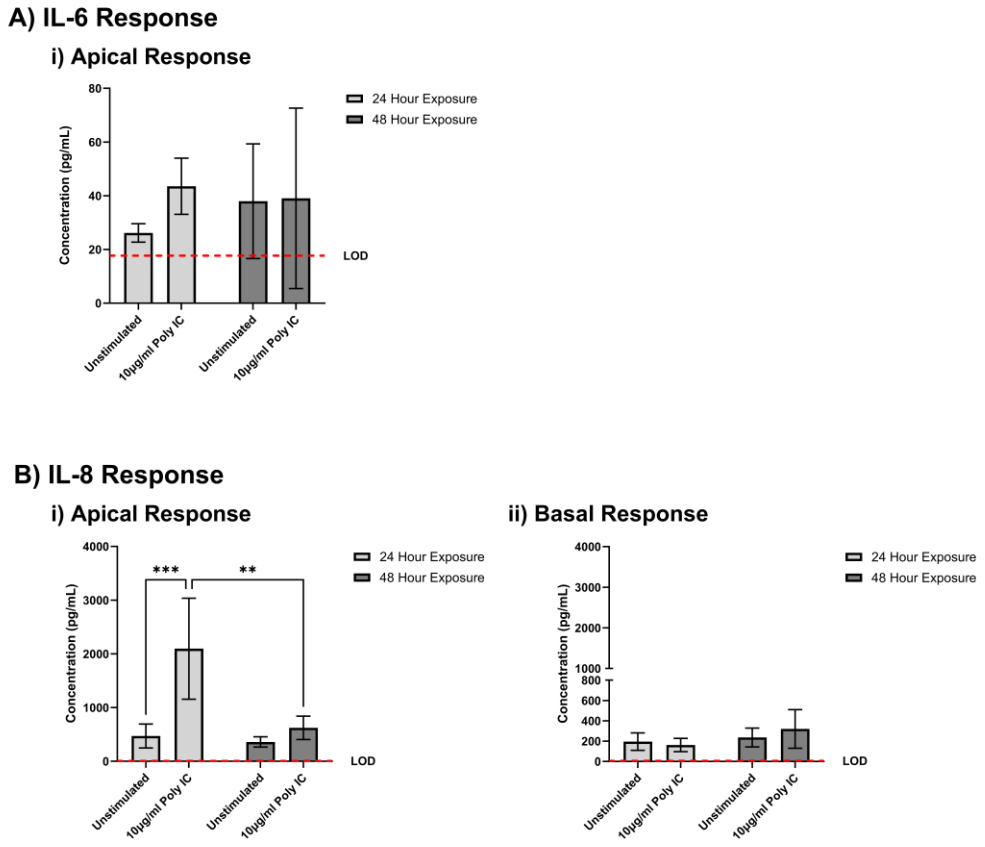

Figure 5.9. Evaluation of 24- and 48-Hour Basal stimulation of ALI With 10 µg/ml Poly(I:C). A) IL-6 response to **Ai)** Apical cytokine. **B)** IL-8 response to stimulants **Bi)** Apical cytokine **Bii)** Basal cytokine. LoD is indicated by doted red line; 17.7pg/ml - IL-6 and 5.51pg/ml – IL-8. Columns represent mean and error bars represent standard deviation. Two-way ANOVA with Sidak's multiple comparison test compared was used to test significance. *p≤0.05, **p≤0.01, ***p≤0.001, ****p≤0.0001. (N=4).

5.3.4. Standardising Nebulisation

In addition to evaluating basal stimulation, nebulisation was also assessed as a mechanism for stimulation, as this is more physiologically relevant. Before nebulisation of ALI inserts, *Bacillus s.p* protease was nebulised and activity assessed to ensure that nebulisation did not damage potential stimulants or affect their functionality. 300µl of 1.76mg/mL protease was nebulised into a 24-well plate containing 500µl of PBS. This concentration was selected to give a target deposition of 4µg and a final concentration of 2000ng/ml per well after factoring in 80% deposition efficiency as per the manufacturer's instructions. Protease activity was measured in each well in duplicate (N=48). *Bacillus s.p* stock was used to generate a standard curve from which concentrations were interpolated (Figure 5.10A). Protease was detected in all wells (Figure 5.10B), confirming that nebulisation did not affect the protease activity. Additionally, deposition per well was 401.3ng/ml with a small degree of variation. This average deposition was 25 % less than the expected 2000ng/ml. Factoring in the initial 80% deposition efficiency adjustment suggested that deposition efficiency was closer to about 20% .

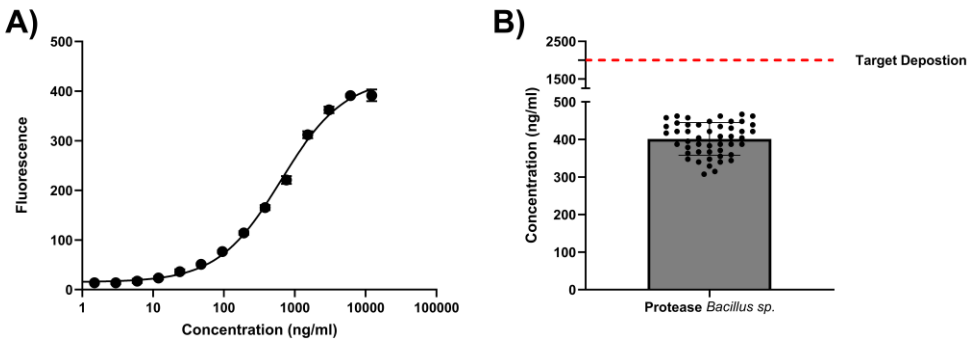

Figure 5.10. Assessment of proteolytic activity post nebulisation. A) Standard curve. **B)** Average protease concentration per well. Column represents the mean and error bars represent standard deviation.

Deposition was affected by the suboptimal configuration of the nebuliser. Unfortunately, the optimal configuration was not available for the duration of the project, however, the manufacturer suggested amending the location of plates within the chamber to get a more efficient deposition. To assess this, IL-6 was nebulised into a 24-well plate containing 500µl of PBS and concentrations were analysed in duplicate via ELISA (N=48). 300µl of 132ng/ml IL-6 was nebulised with a target deposition of 150pg/ml, adjusting for the originally observed 20% deposition efficiency. Figure 5.11 shows the average concentration of IL-6 per well after nebulisation. Deposition was improved, exceeding the expected deposition. The average concentration per well was 260.1pg/ml, suggesting that the deposition efficiency was now about 35% as opposed to 20% observed previously.

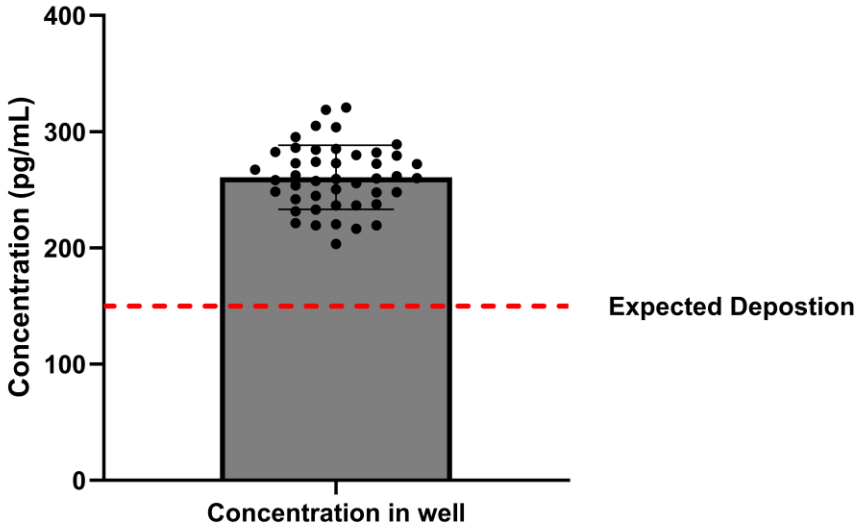

Figure 5.11. Assessment of IL-6 deposition post nebulisation. Average IL-6 concentration per well after nebulisation (expected deposition 150pg/ml). Column represents the mean and error bars represent standard deviation.

5.3.5. Nebulisation of Control Stimulants

Having established that nebulisation didn't affect stimulant activity (Figure 5.10) and having optimised the nebuliser's configuration to get a 35% deposition efficiency (Figure 5.11), concentrations of positive control stimulants were assessed.

5.3.5.1. Nebulisation of LPS

Initially LPS was assessed, since previous concentration of 3µg/ml had been inferred from a nebulisation study. Stimulation of inserts with 50µl of 3µg/ml was delivering a total of 0.145µg per insert, deposition of this into an ALI insert (0.32cm^2) gives a stimulation of 0.45µg/cm^2. This deposition was assessed for suitability as a positive control stimulant. The previous poor LPS response was also thought to be potentially due to the LPS isolation method. Previously, the LPS used was purified using phenol extraction. To assess this impact, an additional new LPS of the same bacterial origin (*Escherichia coli,* O111:B4), but purified via gel-filtration chromatography, was assessed alongside the previous LPS. ALI inserts were nebulised with either PBS (unstimulated controls), 0.45µg/cm^2 of either phenol or gel purified LPS (N=3) and apical and basal responses were profiled using IL-8 ELISAs, 24- and 48-hours post nebulisation (37ºC and 5% CO_2).

After 24 hours, a significant change in apical IL-8 concentrations between the gel-extracted LPS relative to unstimulated controls was observed. Phenol-extracted LPS did not induce a significant response (Figure 5.12A). This significant increase was not observed at 48 hours, and comparison of 24- and 48-hour incubation showed a significant decrease in apical IL-8 between the two time points for both LPS stimulants. Assessment of the basal IL-8 response showed no significant changes in IL-8 cytokine after 24 hours relative to unstimulated controls (Figure 5.12B). However, after 48 hours a significant difference between unstimulated and gel-extracted LPS was observed. This significant increase in IL-8 basal cytokine was not observed for the phenol-extracted LPS. Comparison of 24- and 48-hour basal responses showed significant increases in concentration of IL-8 for unstimulated and both LPSs.

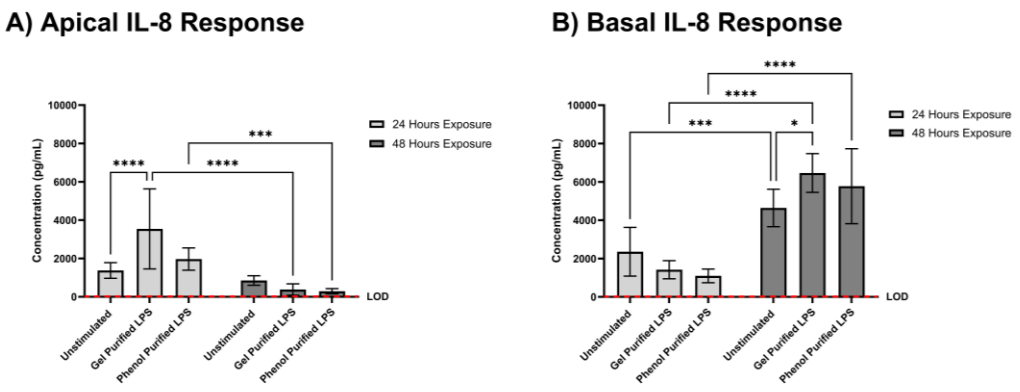

Figure 5.12. Stimulation of ALI Inserts with Nebulised 0.45µg/cm^2 Gel-Chromatography and Phenol Extracted LPS. 24- and 48-hour **A)** apical and **B)** Basal responses to 0.45µg/cm^2 gel-chromatography and phenol extracted LPS stimulations. LoD is indicated by doted red line; 24.1pg/ml – IL-8. Columns represent mean and error bars represent standard deviation. Two-way ANOVA with Sidak's multiple comparison test compared was used to test significance. *p≤0.05, **p≤0.01, ***p≤0.001, ****p≤0.0001. (N=6).

Improved IL-8 response to gel-chromatography purified LPS apically at 24 hours and basally at 48 hours suggested that it would be a more suitable LPS control stimulant than phenol extracted. Consequently, it was decided that moving forward, this LPS would be selected for stimulations. While significance was observed, the IL-8 response observed was variable and not as pronounced as the literature suggested. Due to the serum-free nature of the 3D culture, it was thought that the addition of LPS-binding protein (LPS-BP) might enhance stimulation via nebulisation, as previous experiments in 2D suggested that the addition of LPS-BP enhanced LPS stimulation. To assess if this would enhance the response to LPS (N.B. LPS references in this chapter refer to gel-chromatography purified LPS moving forward) stimulation via nebulisation in 3D, ALI inserts (N=3) were nebulised with either PBS (unstimulated controls),0.45µg/ml LPS or 0.45µg/ml LPS supplemented with an equivalent dose to 2D experiments of 1.56ng/cm^2 LPS-BP (deposition of 0.0005µg per ALI insert). IL-8 secretion was quantified in duplicate using ELISAs 24- and 48-hours post stimulation 37^{o}C and 5% CO_2.

Figure 5.13A shows the apical IL-8 responses at 24- and 28-hours post stimulation. After 24 hours, a significant increase in apical IL-8 cytokine

between unstimulated and 0.45µg/ml LPS-stimulated samples was observed. However, stimulation with 0.45µg/ml LPS supplemented with LPS-BP did not see a significant change in IL-8 concentration. After 48 hours, no difference in apical IL-8 cytokine was observed between stimulated and unstimulated controls. Additionally, there was no significant difference in IL-8 concentrations between 24- and 48-hour exposed samples. Basal IL-8 secretion (Figure 5.13B) saw no significant IL-8 change between stimulated and unstimulated samples after both 24- and 48-hour exposure. Comparison of 24- and 48-hour response did show a significant increase in IL-8 concentration between 24 and 48 hours in 0.45µg/ml LPS simulated samples.

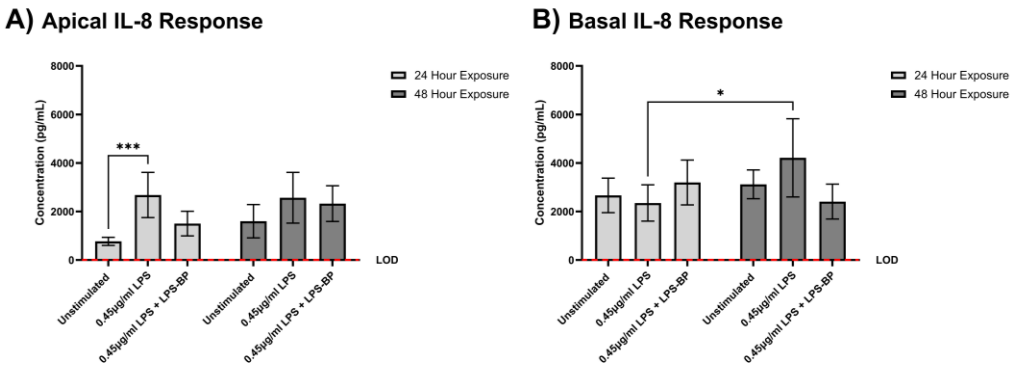

Figure 5.13. Stimulation of ALI Inserts with Nebulised 0.45µg/cm^2 Gel-Chromatography with and without LPS-BP. 24- and 48-hour **A)** apical and **B)** Basal responses to 0.45µg/cm^2 LPS with and without 1.56ng/cm^2 LPS-BP. LoD is indicated by doted red line; 5.71pg/ml – IL-8. Columns represent mean and error bars represent standard deviation. Two-way ANOVA with Sidak's multiple comparison test compared was used to test significance. *p≤0.05, **p≤0.01, ***p≤0.001, ****p≤0.0001. (N=6).

Inconsistency in responses between stimulations and conditions ultimately led to LPS being deemed not to be a suitable positive control moving forward and consequently was not used in future experiments.

5.3.5.2. Nebulisation of Poly(I:C)

As LPS gave inconsistent results, nebulisation of Poly(I:C) was also assessed as a positive control. Initially, a concentration of 0.5µg/cm^2 was assessed. This would deliver 0.168µg of Poly(I:C) to each insert. This was a lower dose than that profiled in 2D stimulation, where 2µg was delivered to each well (200µl of 10µg/ml). However, stimulation was limited by the 35% deposition efficiency and the stock concentration of the Poly(I:C). ALI inserts were stimulated with either nebulised PBS (unstimulated controls) or 0.5µg/cm^2 Poly(I:C) (N=3), and apical and basal responses were profiled in duplicate via IL-8 ELISAs, 24- and 48-hours post nebulisation (37ºC and 5% CO_2).

Evaluation of the apical response to Poly(I:C) (Figure 5.14A) at 24 hours showed no significant increase, however, while not significant, the IL-8 concentrations almost doubled, seeing an increase in average IL-8 concentration from 769pg/ml to 1448pg/ml. However, after 48 hours a significant difference was observed between stimulated and unstimulated samples, with IL-8 concentrations increasing 1600pg/ml to 3044pg/ml. Comparison of 24- and 48-hour responses showed significant increases IL-8 concentrations in both unstimulated and stimulated samples, with a greater increase observed between stimulated samples.

Figure 5.14B shows the basal response to nebulised Poly(I:C) after 24- and 48-hour exposure. After 24 hours, a significant increase in IL-8 concentration was observed in stimulated samples with an increase in average concentration from 2665pg/ml to 3865pg/ml. This significant increase observed at 24-hour hours was even greater at 48 hours, with stimulated samples having an average IL-8 concentration of 5058pg/ml relative to 3121pg/ml in unstimulated samples. Furthermore, comparison of responses between 24- and 48-hour hours showed no change in unstimulated response but a significant increase in stimulated responses, indicating successful stimulation and confirming Poly(I:C) as a suitable positive control stimulant.

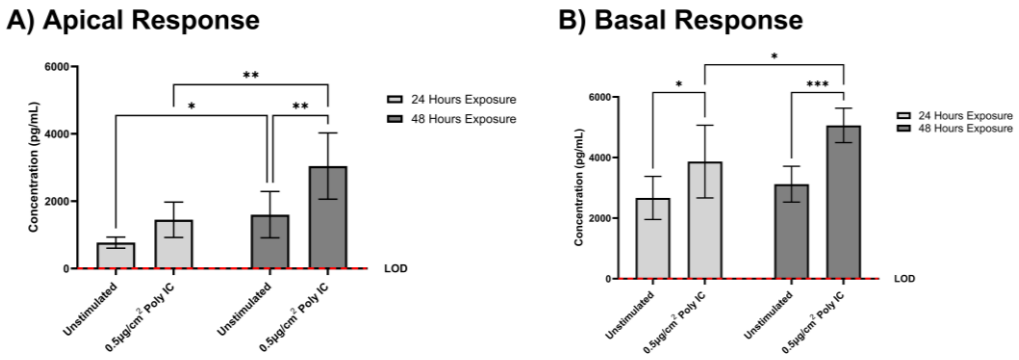

Figure 5.14. Stimulation of ALI Inserts with Nebulised Poly(I:C) at a Dose of 0.5μg/cm² . 24- and 48-hour **A)** Apical and **B)** Basal responses to stimulation with 0.5μg/cm² Poly(I:C). LoD is indicated by doted red line; 5.71pg/ml – IL-8. Columns represent mean and error bars represent standard deviation. Two-way ANOVA with uncorrected fisher's LSD multiple comparison. *p≤0.05, **p≤0.01, ***p≤0.001,

Having seen successful stimulation of ALI cultures with 0.5μg/cm^2, additional concentrations were assessed to attempt to generate a greater response. ALI cultures (N=3) were stimulated with doses of either PBS (unstimulated control) or 0.5, 1.0, 2.5 or 5μg/cm^2 Poly(I:C). Samples were incubated for 24 hours (37ºC and 5% CO_2) and changes in IL-8 concentration were assessed in quadruplets via ELISA.

Figure 5.15A shows the apical response to Poly(I:C) stimulation after 24 hours. Significant increases in apical IL-8 concentrations were observed after 24 hours in samples stimulated with 1.0 and 2.5μg/cm^2 relative to unstimulated controls. Notably, there was no change in apical response when stimulated with 5μg/cm^2, relative to unstimulated controls. Additionally, basal concentrations (Figure 5.15B) saw a dose-dependent significant increase in IL-8 concentration after stimulation with 0.5, 1.0 and 5μg/cm^2 doses relative to unstimulated controls.

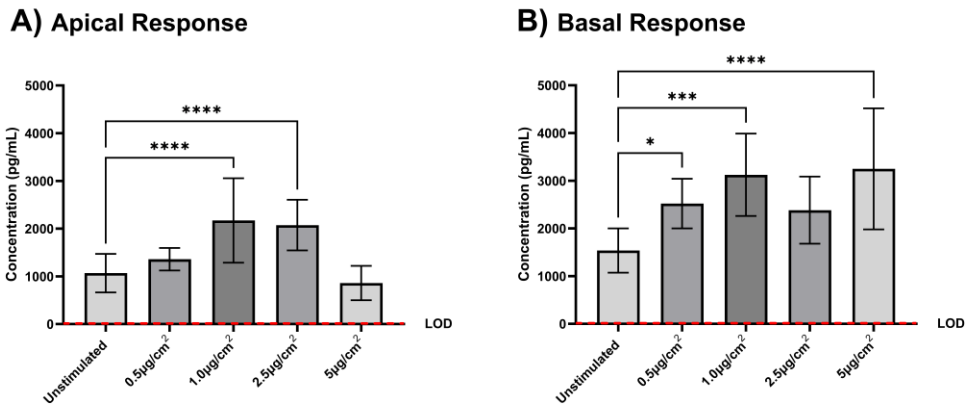

Figure 5.15. Stimulation of ALI Inserts with Nebulised Poly(I:C) at a Dose of 0.5, 1.0, 2.5 or 5µg/cm². A) 24-hour apical IL-8 response relative to PBS stimulated control **B)** 24-hour basal IL-8 response relative to PBS stimulated control. LoD is indicated by doted red line; 13.1pg/ml – IL-8. Columns represent mean and error bars represent standard deviation. One way ANOVA with Dunnett's multiple comparison test compared stimulation concentrations to unstimulated controls. *p≤0.05, **p≤0.01, ***p≤0.001, ****p≤0.0001. (N=12).

Stimulation of 1.0µg/cm^2 nebulised Poly(I:C) was identified as a suitable stimulation concentration for positive control stimulations and was utilised for final experiments.

5.3.6. Co-factor Controls

Having established a mechanism for stimulation and identified a suitable positive control, it was then possible to assess the impact of potentially confounding co-factors. In the final experiment, the allergen Der p 1 was to be used in both its active and inactive form. Der p 1 activation will be achieved through the addition of 5mM L-Cysteine to the Der P 1 stock 20 minutes prior to nebulisation. Additionally, Der p 1 will be inhibited through the addition of the Cysteine protease inhibitor E-64 to the nebulisation stock, at a concentration of 10μM. Consequently, their individual effects on ALI inserts were profiled to ensure these factors don't influence the final assay. ALI inserts were dosed with either nebulised PBS (unstimulated controls), L-Cysteine 5mM stock or E-64 10μM stock (N=5) and apical and basal responses were profiled in duplicate via ELISAs, looking at cytokines IL-1β, IL-6, IL-8, IL-17E (IL-25), IL-33 and TSLP, 24- and 48-hours post-nebulisation (37ºC and 5% CO_2).

ELISAs for IL-1β, IL-6, IL-17E and IL-33 did not detect a measurable concentration of cytokine (Data not shown). However, IL-8 was detected both apically and basally (Figure 5.16). Apical IL-8 responses showed no significant differences in IL-8 concentration for either co-factor relative to unstimulated controls at both 24 and 48 hours (Figure 5.16A). Additionally, there was no change in the apical response over time, with no significant variation being seen between time points. Basal IL-8 responses were also not significantly different to unstimulated controls at either time point (Figure 5.16B). A significant increase between 24 and 48 hours was observed, however this was for all conditions, including the unstimulated control.

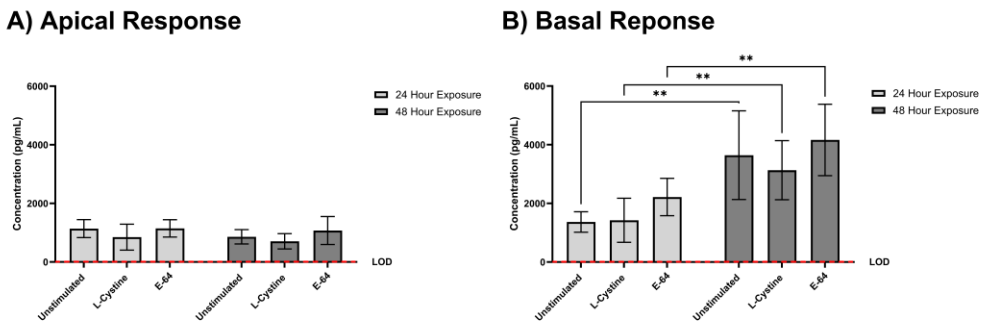

Figure 5.16. Assessment of Co-Factor Variables on ALI Apical and Basal IL-8 Cytokine Secretion After 24 and 48 Hours. A) 24- and 48- hour apical IL-8 response to co-factors relative to PBS stimulated control **B)** 24- and 48- hour basal IL-8 response to co-factors relative to PBS stimulated control. LoD is indicated by doted red line; 16.63pg/ml – IL-8. Columns represent mean and error bars represent standard deviation. One way ANOVA with Dunnett's multiple comparison test compared stimulation concentrations to unstimulated controls. *p≤0.05, **p≤0.01, ***p≤0.001, ****p≤0.0001. (N=10).

In addition to cytokine response profiling, viability was assessed using an LDH assay to ensure the co-factors didn't kill or damage inserts. For LDH analysis, it is first necessary to generate a standard curve, from which LDH luminescence can be interpolated into concentration. Figure 5.17 shows a representative standard curve.

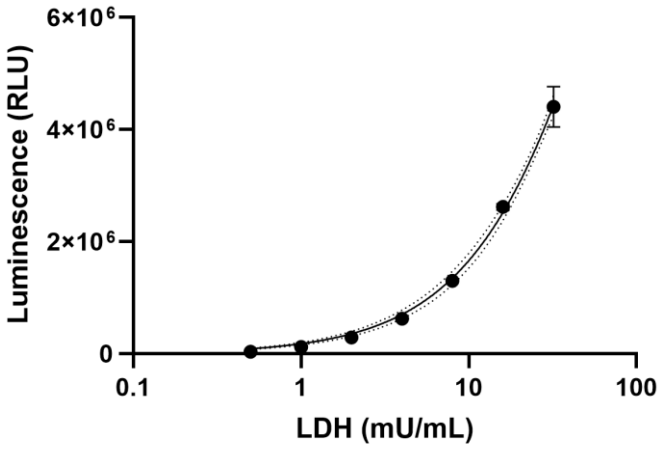

Figure 5.17. LDH Standard Curves. A standard curve was generated to interpolate LDH concentrations from luminescence readings.

10% Triton X was added to inserts for 15 minutes as per manufacturer's instructions, and this LDH response was used as a positive control (Figure 5.18Ai and Aii). Each sample percentage viability was then calculated as a percentage of this positive control and subtracted from 100 to give percent viability (Figure 5.18B). No significant change in viability was observed between unstimulated controls and both co-factor variables at 24 and 48 hours. A significant decrease in viability was seen between 24 and 48 hours for all conditions. However, all viabilities were above 90% at both time points.

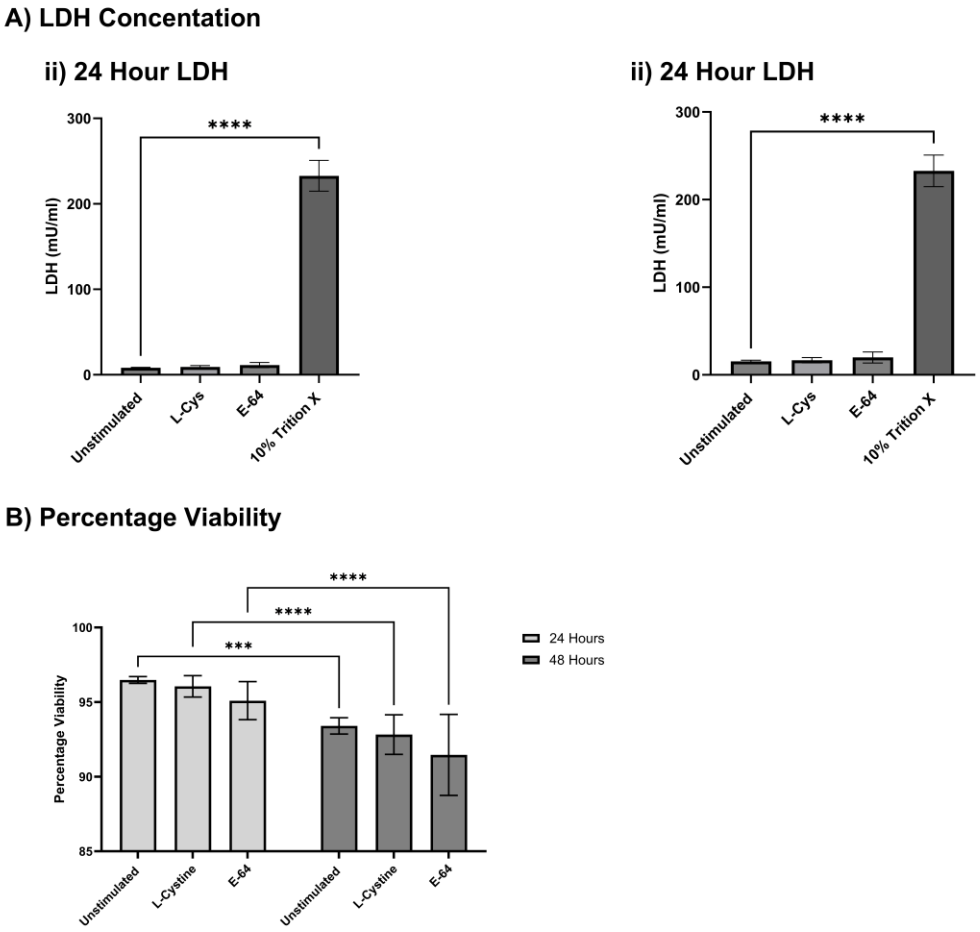

Figure 5.18. Assessment of Co-Factor Variables Effect on ALI Viability. A) Average LDH levels after **Ai)** 24-hour and **Aii)** 48- Hour exposure. **B)** Percentage Viability of cultures after 24- and 48-hour exposure to co-factor variables. One way ANOVA with Dunnett's multiple comparison test compared stimulation concentrations and Two-way ANOVA with Sidak's multiple comparison test compared culture conditions. *p≤0.05, **p≤0.01, ***p≤0.001, ****p≤0.0001. (N=10)

5.3.7. Can f 1 Preliminary Trial

A preliminary trial stimulation was conducted with just Can f 1 prior to the final experiment to assess if 0.35µg/cm^2 would influence the cytokine response and viability in ALI cultures. Inserts were stimulated with nebulised Can f 1 (0.5µg/cm^2) or PBS (N=5) and apical and basal responses were profiled in duplicate via ELISAs looking at cytokines IL-1β, IL-6, IL-8, IL-17E (IL-25), IL-33 and TSLP, 24- and 48-hours post nebulisation (37^{o}C and 5% CO_2).

ELISAs for IL-1β, IL-6, IL-17E and IL-33 did not detect a measurable cytokine concentration (Data not shown). Figure 5.19 shows the IL-8 cytokine response. Profiling of the Apical cytokine response showed a significant increase in IL-8 concentration after 24-hour exposure, increasing from an average of 1138pg/ml in unstimulated samples to 2076pg/ml (Figure 5.19A). However, this significant increase was not observed after 48-hour exposure. Additionally, there was no significant difference in basal cytokine between stimulated and unstimulated samples at either time point (Figure 5.19B). Comparison of 24- and 48-hour responses showed no significant difference in Can f 1 stimulation over time; however, unstimulated controls did have a significant increase in basal IL-8 at 48-hours compared to 24-hours

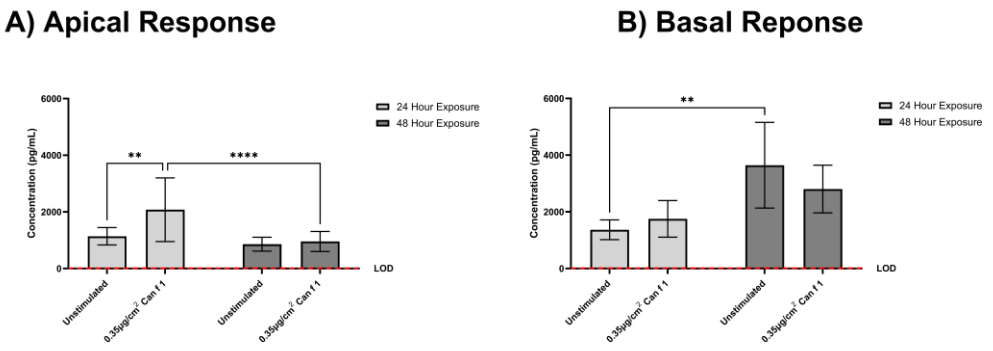

Figure 5.19. Preliminary Assessment of Nebulised Can f 1 (0.35µg/cm^2) on ALI Apical and Basal IL-8 Cytokine Secretion After 24 and 48 Hours. A) 24- and 48- hour apical IL-8 response to Can f 1 relative to PBS stimulated control **B)** 24- and 48- hour basal IL-8 response to Can f 1 relative to PBS stimulated control. LoD is indicated by doted red line; 16.63pg/ml – IL-8. Columns represent mean and error bars represent standard deviation. One way ANOVA with Dunnett's multiple comparison test compared stimulation concentrations to unstimulated controls. *p≤0.05, **p≤0.01, ***p≤0.001, ****p≤0.0001. (N=10).

The effect of Can f 1 nebulisation on viability was also assessed using the LDH assay at both 24- and 48-hours (Figure 5.20). Comparison of viability between unstimulated and stimulated samples after 24 hours showed no significant difference. This changed after 48 hours, where viability was seen to decrease from an average of 93% to 91%. Comparison of 24- and 48-hour viability showed no significant change in unstimulated viability, however, there was a significant change in Can f 1 viability, decreasing from an average of 96% to 91%, but this was still within the limit stated in the MISEV guidelines.

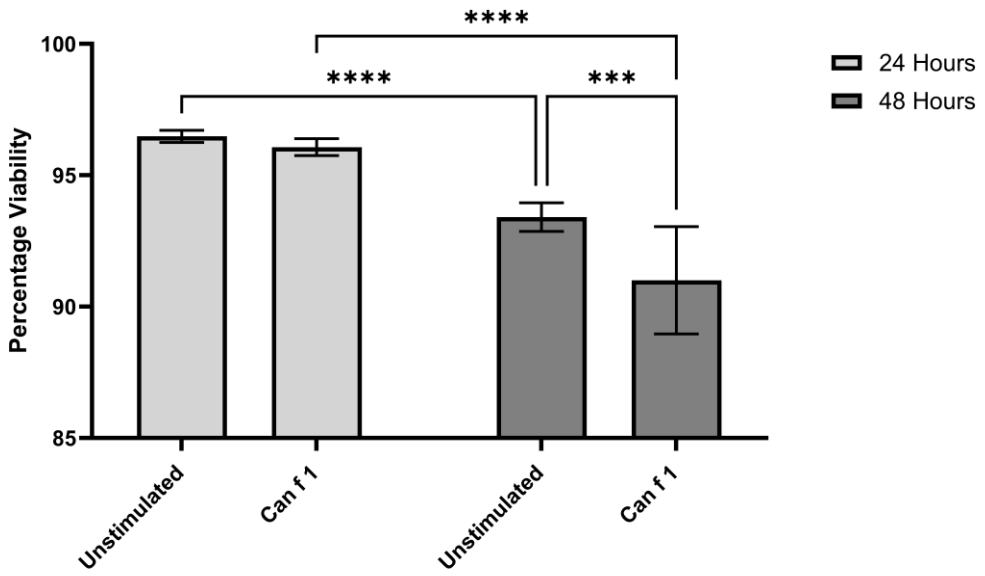

Figure 5.20. Assessment of Can f 1 nebulisation (0.35µg/cm^2) on ALI Viability.
Percentage viability of cultures after 24- and 48-hour exposure to Can f 1 relative to 10% triton X control. Two-way ANOVA with Sidak's multiple comparison test compared culture conditions. *p≤0.05, **p≤0.01, ***p≤0.001, ****p≤0.0001. (N=10)

5.4. Discussion

3D cell models of the airway epithelium provide a more biologically relevant model, allowing for the modelling of direct aeroallergen interaction with the diverse community of epithelial cells and substructures found in the lung. The aim of this chapter was to demonstrate the generation of a representative 3D model of the lower airway epithelium, as well as identify a suitable mechanism for its stimulation using previously identified positive control stimulants.

Consistent with the literature, ALI cultures were able to differentiate into different cell types, as well as form tight junctions and cilia (Wallace *et al.,* 2025, Lee *et al.,* 2023). Having successfully established 3D culture, mechanisms for stimulation were assessed and optimised. Initially, submersion stimulations were assessed, but this resulted in high background levels of cytokines, particularly IL-6 (an inflammatory, hypoxia and drowning-associated marker (Keryakous *et al.,* 2022, Mimasaka *et al.,* 2001)) across all conditions, suggesting cell responses were induced by the stimulation mechanism rather than the stimulant. Consequently, application of the stimulant to the basal chamber was assessed. This method usefully induced stimulation, however, due to its lack of biological relevance in comparison to nebulised stimulation, it was not utilised.

The possibility of utilising a Vitrocell Cloud Alpha AX12 nebulisation chamber arose. The biological relevance of this mechanism of stimulation, coupled with the recent adoption of nebulisers in respiratory research, made optimisation of this process a primary focus. Preliminary nebulisation assessment demonstrated that proteolytic activity was not affected by nebulisation, confirming this as a vector for delivery of active Der p 1 allergen to inserts.

Optimal configuration of the nebulising chamber averages 80% deposition, but due to logistical constraints, the chamber was not used in its optimal configuration. Thus, it was first necessary to assess the effect this had on stimulant deposition. Deposition efficiency of the chamber was optimised to an efficiency of 35%. Factoring in efficiency, positive controls were

assessed, and cytokine responses were profiled. LPS results were inconsistent throughout the experiments, even with LPS-BP supplementation, proving to be unreliable. In contrast, nebulisation of Poly(I:C) resulted in consistent increases in IL-8, with a deposition of 1μg/cm^2 identified as a suitable positive control for the model.

The final experiment of this project will expose Calu-3 ALI inserts to proteolytically active and inactive forms of Der p 1. The different proteolytic states of Der p 1 will be induced through the addition of either L-cysteine or E-64 (referred to as co-factors) (Gough *et al.,* 1999). Therefore, it was necessary to profile the stimulatory effects of these individual co-factors. Nebulisation of these co-factors did not induce a cytokine response or influence cell viability.

Finally, Can f 1 was tested to assess if the maximum concentration available using this model (0.35μg/cm^2), due to reduced deposition efficiency, would elicit any cytokine response. Results showed that short-term exposure to nebulised allergen was able to induce an IL-8 cytokine response, but it also resulted in a slight decrease in cell viability. This concentration was thus deemed to be sufficient and ultimately taken forward.

The data presented in this chapter demonstrates the successful generation of a biologically relevant model of the lower airway epithelium. Exposure of this model to nebulised positive controls showed lower unstimulated background when compared to submersion stimulations and was able to successfully induce a cytokine response. The control tests showed co-factors did not elicit a response, and the control allergen, Can f 1, was able to induce IL-8 secretion. The next phase of optimisation experiments will focus on the development of a high-throughput method for the quantification and characterisation of EVs using flow cytometry.

Chapter 6: Optimisation of Extracellular Vesicle Quantification and Characterisation

6.1. Introduction

The conventional methods for the quantification of EVs currently require their initial isolation from cultures using either ultracentrifugation, density gradients, immunoprecipitation or size exclusion chromatography (SEC). These are followed by nano particle tracking analysis (NTA) to size EVs and transmission electron microscopy (TEM) to visualise EVs. While these methods have high sensitivity, they are time-consuming and low-throughput processes, which don't facilitate the simultaneous characterisation of samples. Techniques such as Single-Particle Interferometric Reflectance (SP-IRIS) and flow cytometry are currently growing in popularity as they offer the potential for multiparametric analysis of samples without the need for prior isolation. While both techniques allow for the investigation of biomarker colocalization on individual events as well as evaluate sample counts and event sizes, flow cytometry is both a cheaper, more accessible and faster technique to use. Consequently, Flow cytometry is emerging as a powerful alternative to low-throughput EV analysis methods (Gul *et al.,* 2022).

Conventional flow cytometry functions through three systems: fluidics, optics and electronics (McKinnon, 2018). The fluidics system consists of a pressurised sheath that facilitates the delivery of the sample to a laser array (optics system). These lasers generate signals by scattering off objects as well as the excitation of fluorophores, which are captured by detectors (photomultiplier tubes) and converted into digital signals by the electronic system. Conventional flow cytometry was initially designed for the analysis of large particles, such as cells, and so typically has a lower resolution and higher levels of electronic noise, which makes small particle analysis challenging. Imaging flow cytometry combines conventional flow cytometry with fluorescent microscopy. This requires lower flow rates of samples (fluidics system) for the capturing of images using a CCD camera (optics system). Consequently, samples have longer exposures times and a higher signal-to-

noise, resulting in greater sensitivity compared to conventional cytometers (Rees *et al.,* 2022).

Fluorescent antibodies and dyes are central components of flow cytometric analysis, allowing the selective staining of markers on populations such as cells or EVs. These positively stained populations then generate signals which allow for their detection from negative fractions, facilitating selective profiling without the need for prior isolation or purification. Calcein acetoxymethyl ester (AM) is a fluorescent probe, composed of a calcein fluorescent dye conjugated with acetoxymethyl ester. In this Calcein-AM state the probe is non-fluorescent, however, when it is internalised through the penetration of intact lipid bilayers, the AM ester group is cleaved by cytosolic esterases, allowing the calcein to fluoresce (L. Miles *et al.,* 2015). This functionality allows the selective staining of intact EVs (Gray *et al.,* 2015, Chuo *et al.,* 2018). This high selectivity makes calcein-AM a more optimal stain than less specific plasma membrane dyes, which can bind to membrane fragments from cells or damaged EVs, conflating analysis. Utilisation of this dye also allows for the gating of intact EVs and subsequent profiling of EV biomarkers, such as tetraspanins CD9, CD63 and CD81 on individual EVs, giving greater insight into tetraspanin expression in a population that current methodologies, such as western blotting, which is only semi-quantitative.

Optimisation experiments in this chapter aim to first identify a suitable cytometer and fluorophore panel for the analysis of small EVs, as well as identify an optimal staining concentration for calcein-AM to facilitate robust and representative EV quantification and characterisation.

6.2. Materials and Methods

6.2.1. Conventional Profiling of EVs Using TEM and NTA

Initial profiling of EVs in culture was performed by first isolating EVs using SEC (Section 2.2.7.). EVs were then sized and quantified using NTA (Section 2.2.9.) and imaged using carbon coated-300 Cu mesh TEM grids run on a Tecni BioTwin TEM (Section 2.2.8).

6.2.2. Optimisation of Small EV Analysis Using Flow Cytometry

Initially, a comparison of the sizing sensitivity for a conventional (CytoFLEX) and imaging (Image) flow cytometer using NIST polystyrene beads ranging from 60-151nm was performed (Section 2.2.4.1.). This was undertaken to identify a machine with adequate sensitivity for the detection of small EVs. CytoFLEX data was analysed using FCMpass (Welsh *et al.,* 2020) to determine LoD. ISX LoD was assessed using a vFC^{TM} EV analysis kit (Cellarcus Bioscienes) (Section 2.2.4.1).

After assessment of the sizing LoD, different calcein-AM concentrations ranging from 0.1-200μM were assessed to find a staining concentration which would both saturate samples and have a high stain index to allow for optimal staining (Section 2.2.5). Additionally, different concentrations of multiple detergents were assessed to find a suitable detergent to deplete optimally stained (Section 2.2.5) EV populations, acting as a control to indicate successful staining of lipid vesicles.

The LoD's of fluorophores PE-Cy5, PE-Cy7, PE, APC and PE-Vio615 were quantified using Quantum^{TM} Simply Cellular beads (Bangs Laboratories, IN,USA) on the ISX (Section 2.2.4.2). LoDs were calculated in terms of antibody binding capacity (ABC) using manufacturer's supplied analysis template. Having identified fluorophores, EVs were stained as outlined in Section 2.2.5 with either REAffinty antibodies or conventional mouse monoclonal antibodies, either using pan-APC or mixed fluorophore panel (Table 6.1) to assess if staining could be improved using the former.

Table 6.1 Fluorescent antibodies used for the comparison of REAaffinity and conventional antibodies, their fluorophore, manufacturer and antibody type.

Target	Fluorophore	Brightness	Manufacturer	Cat.no.	Type
CD9	APC	4	Miltenyi	130-118-808	REAffinity
CD63	PE	5	Miltenyi	130-118-077	REAffinity
CD81	PE-Vio615	5	Miltenyi	130-131-387	REAffinity
CD63	APC	4	Miltenyi	130-119-787	REAffinity
CD81	APC	5	Miltenyi	130-118-078	REAffinity
CD9	APC	4	Biolegend	312017	Conventional
CD63	PE	5	Biolegend	353004	Conventional
CD81	PE-Vio615	5	Biolegend	349520	Conventional
CD63	APC	4	Biolegend	353008	Conventional
CD81	APC	5	Biolegend	349510	Conventional

6.3. Results

6.3.1. Confirmation of EVs in Culture

To optimise the quantification of EVs, it was first necessary to establish their presence in ALI cultures. Media was isolated from basal chambers of ALI cultures and EVs were isolated using size exclusion chromatography (SEC) and concentrated. Figure 6.1Ai shows nano tracking analysis (NTA) sizing histograms of isolated EVs, which ranged in size from 50-300nm. NTA also provided an initial estimate of EVs/ml of around $2.8x10^{10}$ EVs per/ml (Figure 6.1Aii). Analysis of cultures after SEC with transition electron microscopy (TEM) also confirmed the presence of EVs exhibiting standard cup-shaped morphology (Figures 6.1B&C). EVs sized using TEM (Figure 6.1Bii) were consistent with NTA sizing; however, Figure 6.1Ci&ii shows aggregated EVs, which can conflate NTA quantification as they are registered as single events. Additionally, NTA does not differentiate between EVs and any potential contaminants in the preparation. Consequently, the potential of conventional (CytoFLEX S) and Imaging (ImageStream X MKII) flow cytometry for the quantification EVs was assessed.

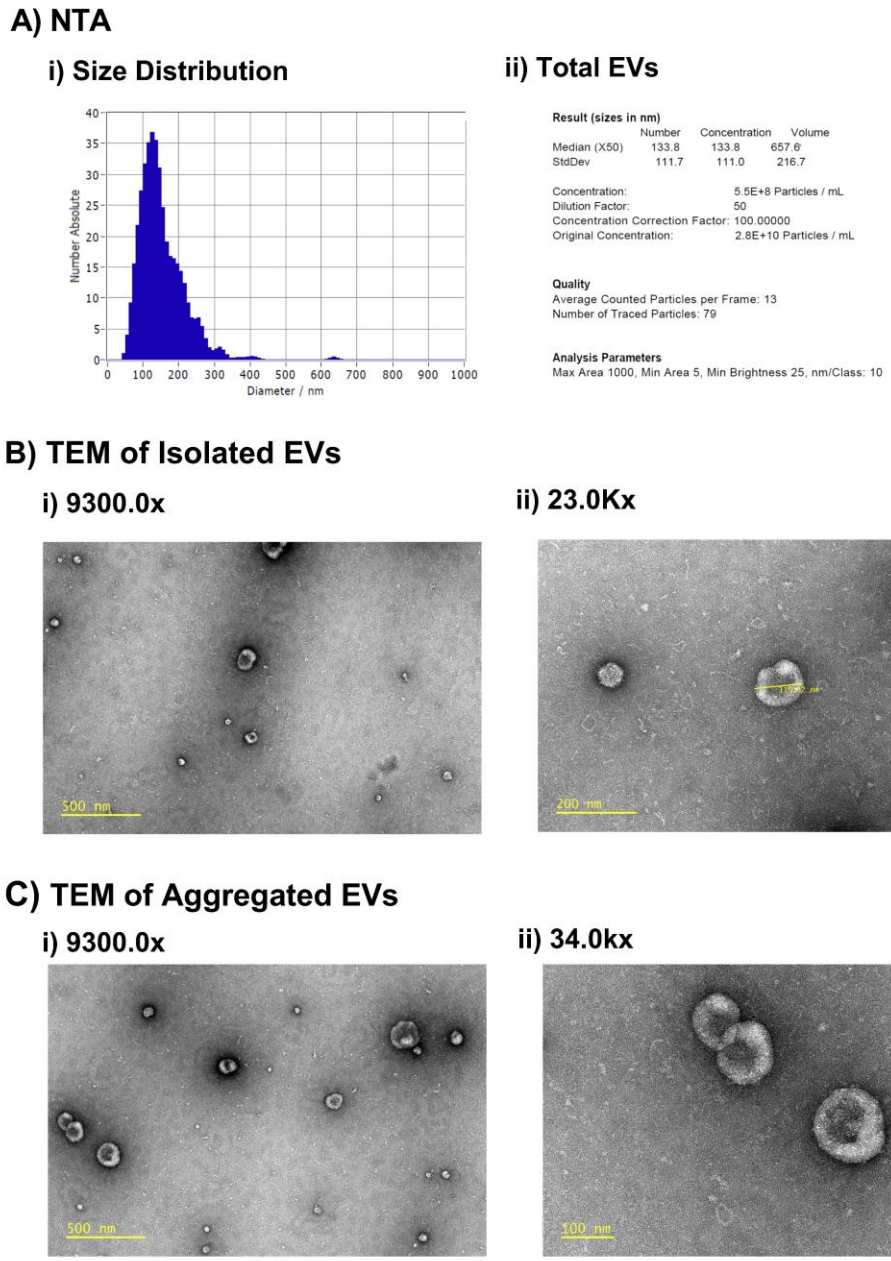

Figure 6.1. Initial Quantification and Imaging of EVs Isolated from Basal Chamber of ALI culture using SEC. A) Analysis of basal chamber EVs using NTA **Ai)** Sizing distribution histogram and **Aii)** Total EV count for sample. **B)** Analysis of basal chamber EVs using TEM **Bi)** 9300x and **Bii)** 23.0kx magnification. **C)** EVs stuck together **Ci)** 9300x and 34.0kx magnification

6.3.2. Conventional and Imaging Flow Cytometry Size Limit of Detection

To initially assess the suitability of the CytoFLEX and ImageStream X MKII (ISX) for EV quantification and characterisation, the sizing limit of detection (LoD) for both cytometers was assessed to ensure they could detect small EVs (40-200nm).

6.3.2.1. CytoFLEX Sizing Limit of Detection

To assess the LoD for the CytoFLEX, National Institute of Standards and Technology (NIST) sizing beads of 60, 80, 101, 121, 151nm were individually run on the CytoFLEX using violet side scatter (VSSC) and a threshold of 40k to allow for profiling of LoD in the machine's optimal configuration for small particle analysis. Figure 6.2A shows the gating strategy used to isolated beads (Figure 6.2Ai) and select for single bead events (Figure 6.2Aii). Figure 6.2B shows an overlay histogram of the 80, 101, 121 and 151nm bead populations and median VSSC intensity of each population (X-Med). 60nm populations were not detectable on of the CytoFLEX (Data not shown) indicating an LoD between (60 and 80nm). This initially indicated that the CytoFLEX might not have the required sizing sensitivity needed for the analysis of small EVs.

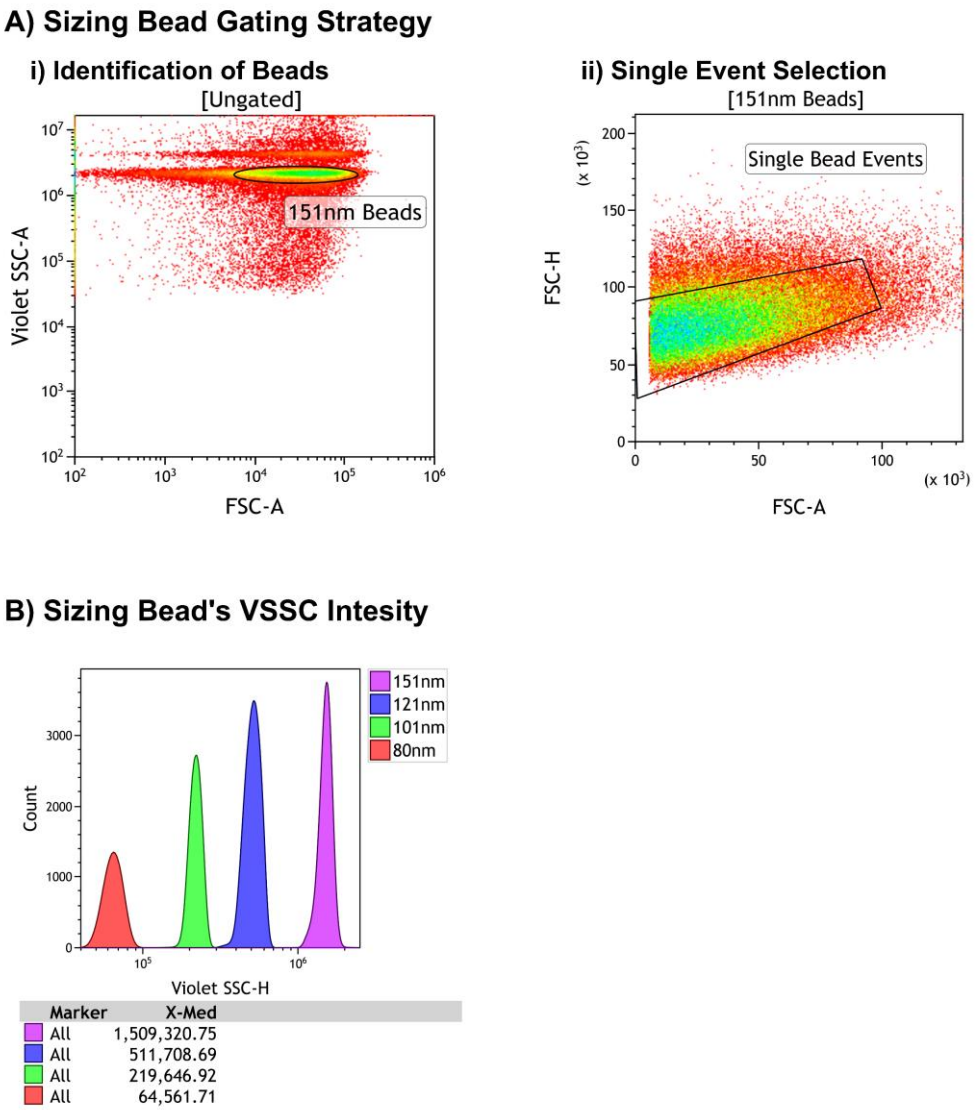

Figure 6.2. Flow Cytometric analysis of NIST beads of 80, 101, 121 and 151nm. A) Initial gating strategy for the **A)** identification of beads and the **B)** isolation of single events. **B)** Histogram overlay of the VSSC intensity.

Further analysis of this data using FCMpass software allowed for the input of median VSSC scatter intensities for each bead population, as well as their known refractive indexes. FCMpass utilises Mie theory, which models how light scatters off spherical objects to create scatter-diameter curves, as well as scatter-refractive index curves. These curves allow for the interpolation of the minimum size a polystyrene bead needs to be to generate a detectable signal on the machine (Figure 6.3). Figure 6.3 shows the FCMpass output for the CytoFLEX using data above. Minimum bead size detectable was identified as 74.8nm. However, VSSC sizing sensitivity of 74.8nm for polystyrene does

not directly translate to the minimum size of EV detectable due to differences in refractive indices. Application of Mie theory also allows for comparison of objects with different refractive indexes. Figure 6.3 shows the translation of these differences, allowing for both the identification of the minimum EV size detectable by the CytoFLEX, which was identified as 143.1nm and the interpolation of VSSC scatter intensity into EV size nm for analysis. However, a threshold of 143.1nm further emphasised the unsuitability of the CytoFLEX for the analysis of small EVs.

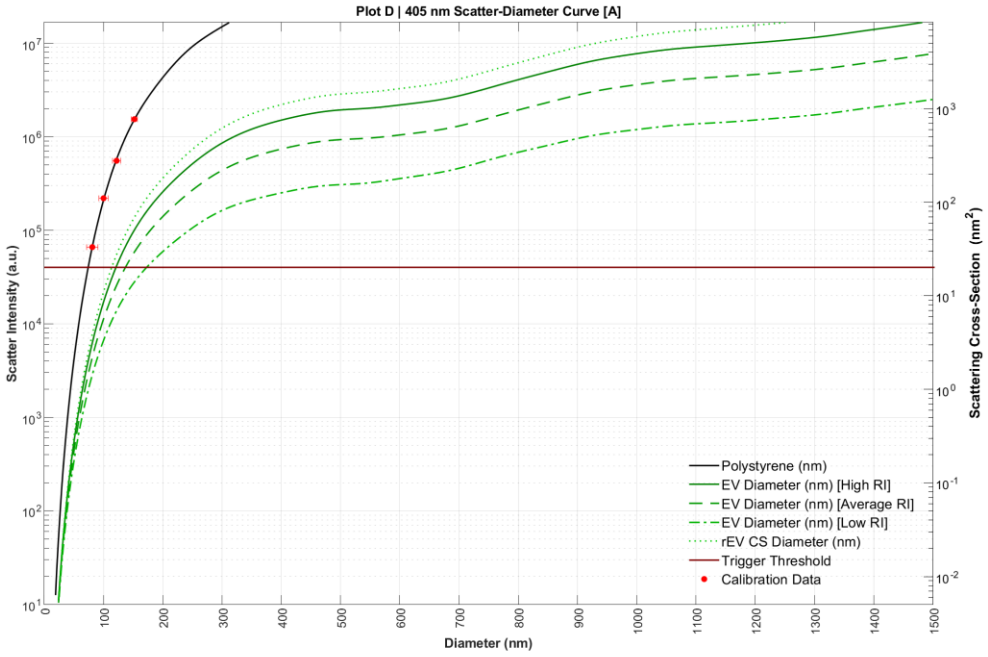

Figure 6.3. FCMpass Generated Curve for Interpolation of VSSC into EV Diameter (nm). Mie theory curve plotted using the known VSSC and refractive index of standardised NIST beads of 80, 101, 121 and 151nm **.**

6.3.2.2. ImageStream X MKII Sizing Sensitivity

Having established a sizing LoD of 74.8nm for polystyrene beads and 143.1nm for EVs, the sizing LoD on the ISX was assessed. Individual NIST bead populations of 60, 80, 101, 121 and 151nm were run through the machine using High Gain mode and VSSC. Additionally, lasers were set to max strength to ensure the machine was configured for maximum sensitivity. Figure 6.4A shows the gating strategy used to identify bead populations (Figure 6.4Ai). The ISX does not utilise forward scatter and instead uses a brightfield microscope. Consequently, isolation of individual events was

performed using a spot count, which is able to isolate events based on the number of objects in captured images. Spot counts were performed on VSSC channel signals to isolate individual scatter events (Figure 6.4Aii). As can be seen in Figure 6.4B, the ISX was able to detect and distinguish between all five bead populations. Currently, it is not possible to utilise FCMpass with ISX acquired data and so the interpolation and translation of LoDs for polystyrene beads and EVs could not be done. However, as the cytometer was able to distinguish 60nm beads, its greater sensitivity was evident.

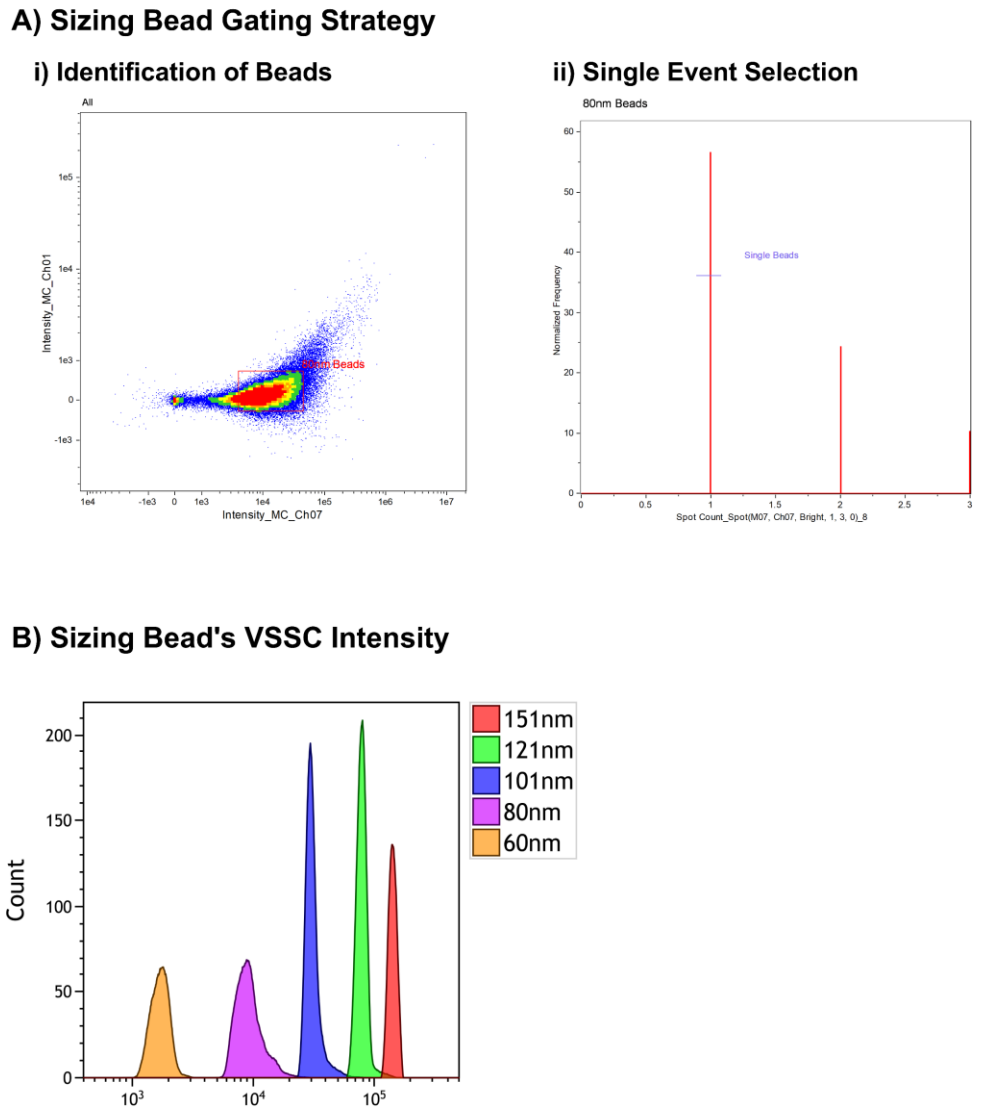

Figure 6.4. Flow Cytometric analysis of NIST beads of 80, 101, 121 and 151nm Run on the ImageStream X MKII. A) Initial gating strategy for the **A)** identification of beads and the **B)** isolation of single events using a spot count. **B)** Histogram overlay of the VSSC intensity.

To better quantify the sizing LoD for EVs on the ISX, a vFC™ EV analysis kit was utilised. This allowed for the interpolation of size through the comparison of vFRed-stained nanoRainbow beads (80-140nm) with fluorescent intensity (Figure 6.5A). This data can be calibrated using FCSexpress and the manufacturer's analysis templates to give a limit of detection. Additionally, staining of SEC isolated EVs with vFRed allows for the interpolation of individual EV sizes (Figure 6.5B). Sizing LoD using this method was 55nm for EVs, further emphasising the suitability of the ISX for small EV quantification and characterization. Consequently, the ISX was utilised moving forward.

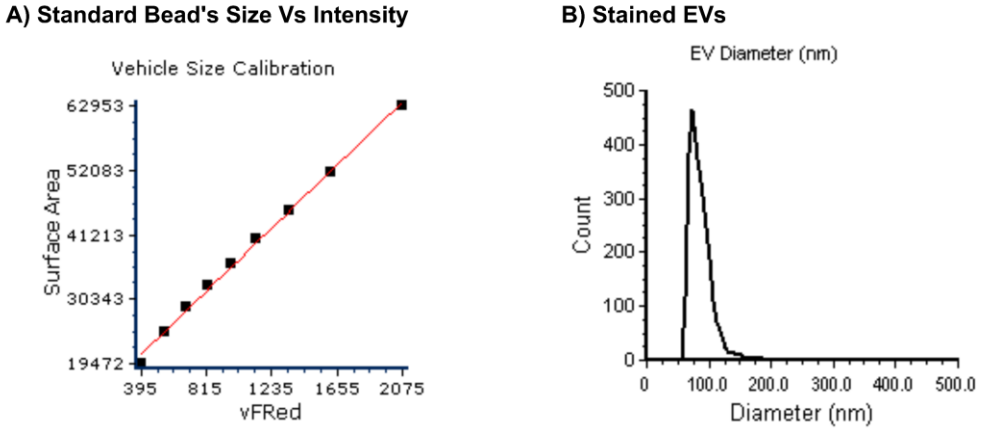

Figure 6.5. Flow Cytometric analysis of the ImageStream X MKII Sizing LoD using vFC™ . A) Standard beads size vs vFRed dye fluorescent intensity **B)** Histogram of interpolated sizes of SEC isolated EVs.

6.3.3. Optimisation of Quantification

Having profiled and identified a suitable machine for the analysis of small EVs, fluorescent staining of EVs themselves needed to be optimised. The cytoplasmic dye calcein-AM (FITC) was selected due to its functionality, which allowed for the selective staining of intact EVs. Having selected this dye, it was important to optimise EV staining concentrations to ensure staining saturation was achieved to allow for accurate quantification of samples.

Figure 6.6 outlines the gating strategy developed for the identification of single EV events. Figure 6.6A shows the localisation of 151nm beads on a plot of SSC against fluorescent intensity (488nm). 151nm NIST polystyrene beads were chosen for the localisation of the Small EV gate as the Mie theory interpolated data observed on the CytoFLEX indicated that this would gate for an equivalent of a 300nm EVs. Figure 6.6B shows a calcein-stained EV sample with the gating location identified in Figure 6.6A. After gating of the small EVs based on size, a spot count was performed on brightfield images. Samples are acquired on High Gain mode with the slowest flow rate. Acquisition of samples this way gives the brightfield channel an optical resolution of 330nm/pixel. Spot counts performed on the brightfield to exclude any events of 1 pixel or larger (objects ≥330nm) (Figure 6.6C). These sub-330nm populations were then taken forward, and an additional spot count was performed that selected single positive FITC fluorescent events (intact small EVs) (Figure 6.6D).

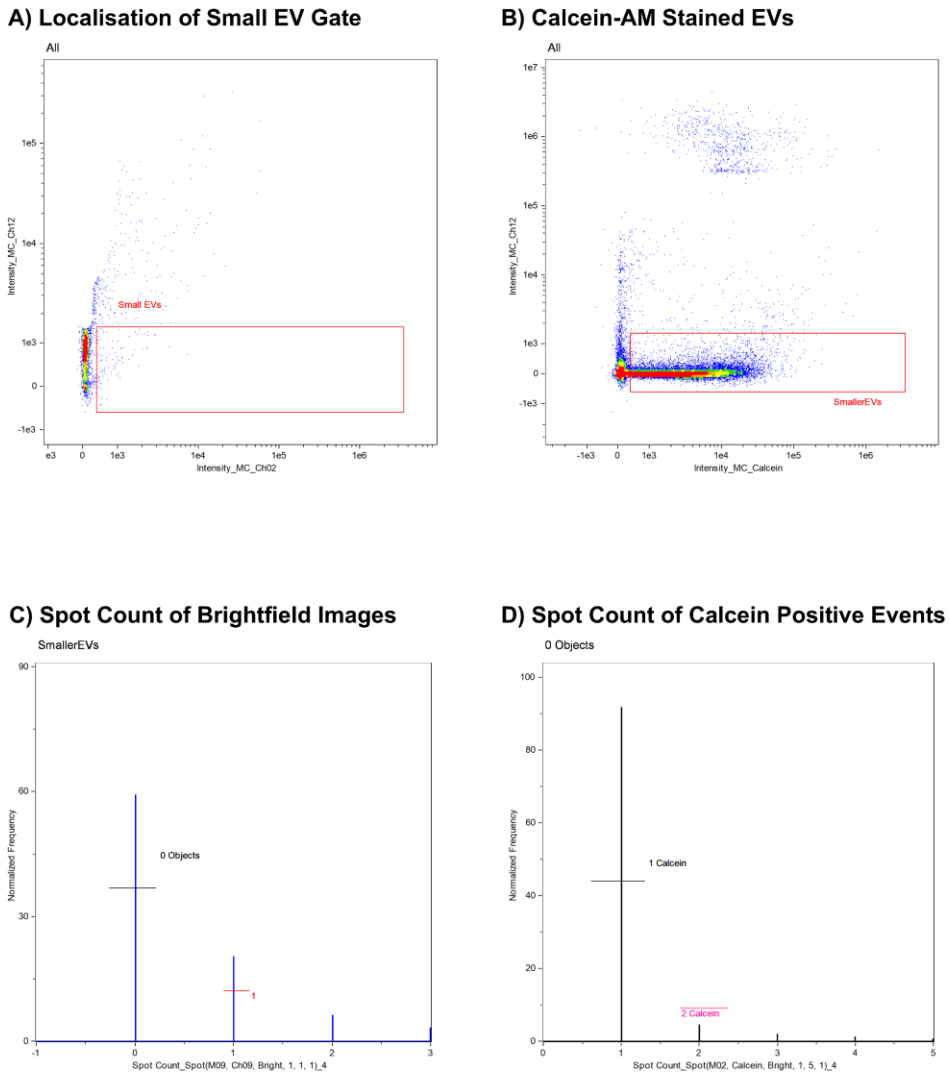

Figure 6.6. Gating Strategy for the isolation of single small EV events. A) Localisation of small EV gate relative to 151nm polystyrene NIST beads. **B)** Optimally Stained EV sample showing EVs isolated by Small EV Gate. **C)** Brightfield spot count of Small EV population, selecting for 0 detectable events (Events below 330nm). **D)** Spot count to isolate single positive fluorescent events.

Gating of samples with this strategy allows for the identification of calcein-AM-stained single positive intact EVs and their quantification in terms of EVs/ml.

To optimise the calcein-AM staining concentration, 30µl of basal media from epithelial ALI cultures was stained in triplicate with either 0.1, 0.2, 1, 2, 10, 20, 100 or 200µM of Calcein-AM. Additionally, 30µl of PBS were stained in triplicate with the same concentrations. Average counts for PBS samples were subtracted from culture samples to compensate for any background fluorescence. Samples were analysed using the gating strategy outlined in Figure 6.6. As can be seen in Figure 6.7 a saturation point was not met with these concentrations, so greater concentrations were assessed, but these concentrations caused the ISX to crash (Data not shown).

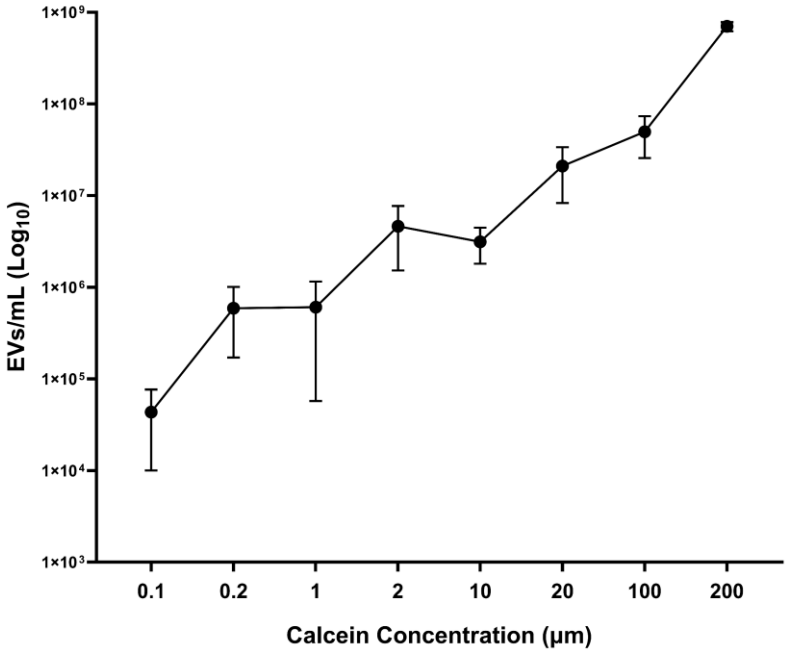

Figure 6.7. **Assessment of Calcein-AM Concentrations on the ISX.** EVs samples stained with different calcein-AM concentrations and the number of EVs measured was calculated (EVs/ml).

While it was not possible to identify a saturation point for calcein staining on the ISX, an in-parallel study was conducted on the CytoFLEX as part of a publication and a saturation point was identified. Samples or PBS were stained with either 0.1, 0.2, 1, 2, 10, 20, 100 or 200µm of Calcein-AM and run on the CytoFLEX. Before analysis could be undertaken, FCS files were put into FCMpass to translate VSSC signal into the size (nm) using Mie theory. Figure 6.8 shows the subsequent gating strategy used to analyse samples. A histogram of size was initially plotted, and a gate was placed

selecting for objects of 330nm and smaller (Figure 6.8A). This sub-330nm population was then plotted on a scatter plot of VSSC-area by VSSC-height to select for single events (Figure 6.8B). These single event populations where then plotted on scatter graphs of calcein-AM fluorescent intensity by VSSC-height (Figure 6.8C&D). The gate for positive events was set using a PBS control which was stained with the equivalent concentration of calcein-AM as the samples.

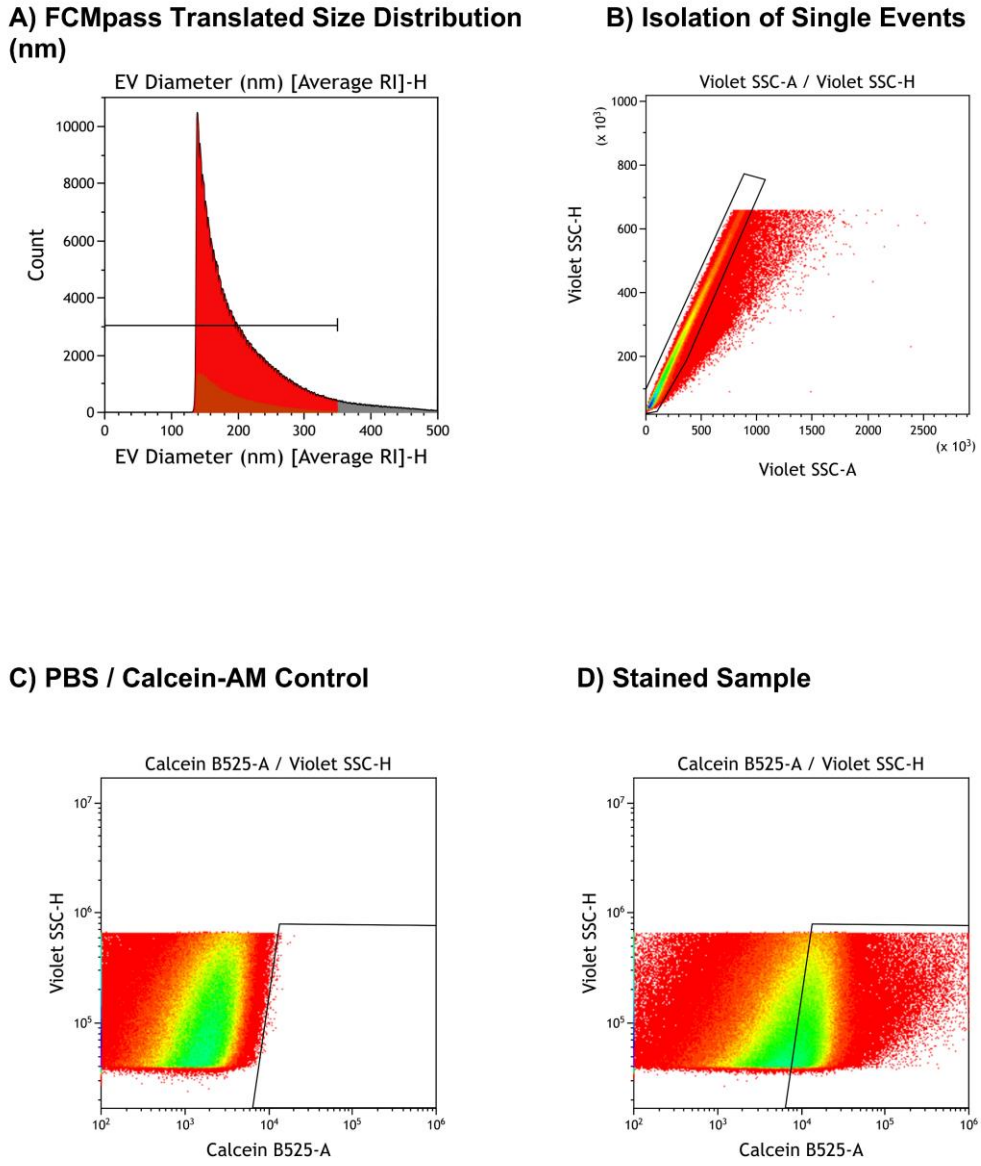

Figure 6.8. Gating of Small EVs on the CytoFLEX. A) A histogram of size distribution was used to isolate events 330nm and below. **B)** Single events were gated for using a VSSC-H / VSSC-A scatter plot. **C)** Calcein stained PBS was used to situate gate for positive events. **D)** Sample stained and analysed using gating strategy.

Initial increases in calcein-AM concentration from 0.1μM to 1μM saw increases in the number of EVs/ml detected, with an almost 10-fold increase in the number of EVs detected (Figure 6.9A). Subsequent staining concentrations saw a plateau in the number of EVs/ml measured, suggesting a saturation point had been reached. A stain index was also calculated to show the separation of the median fluorescence intensity of stained samples and their PBS staining equivalents (Figure 6.9B). While initial plateauing was seen at 1μM of calcein, a staining concentration of 10μM was identified as the most suitable, having the highest staining index and providing enough inbuilt redundancy to compensate for more concentrated samples. Finally, serial dilutions of sample (Neat, 1:2, 1:4 and 1:8) were stained with the identified 10μM concentration to assess both the functionality of staining and to assess any potential swarming at high concentrations of sample. As can be seen in Figure 6.9C, the average number of detected EVs/ml showed a linear decrease, halving with each 1:2 dilution, suggesting that staining was optimal and no swarming was conflating counts. Consequently, moving forward, a concentration of 10μM was used to stain samples.

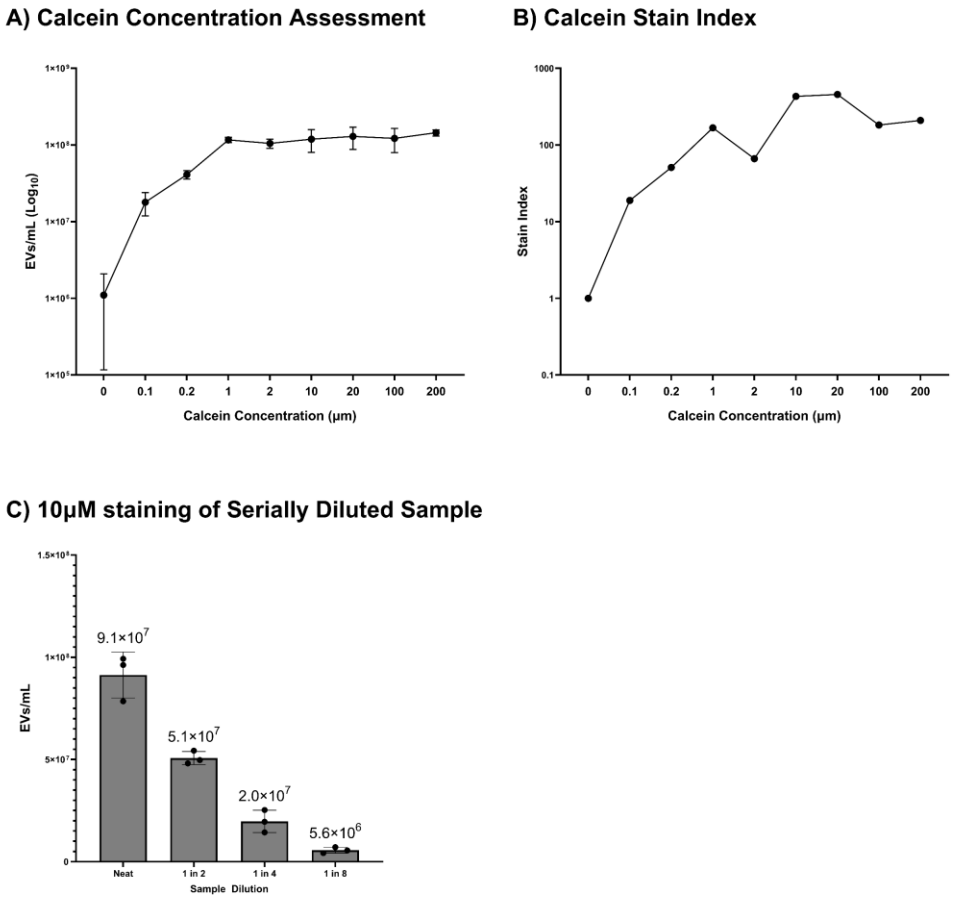

Figure 6.9. Assessment of Calcein Concentrations on the CytoFLEX. A) Number of EVs/ml stained in samples stained with different concentration of calcein-AM. **B)** Staining Index for samples and PBS-stained different concentrations of calcein-AM. **C)** Serial dilution of samples each stained with 10µM of calcein-AM. (N=3)

Lastly, to follow MISEV guidelines, a detergent control would also be used to confirm that positive events are membrane-bound lipid vesicles as opposed to protein complexes from the culture. Degradation of vesicles should result in the reduction of signal without the destruction of the proteins. Three detergents, SDS, Tween-20 and Triton-X, were assessed at different concentrations. Samples were stained with 10µM calcein-AM and treated with detergents after staining protocols were completed (Section 2.2.5). Figure 6.10 shows the effect on EV counts of each detergent. SDS was the only detergent which significantly depleted EV counts. Consequently, a concentration of 10% SDS was selected for the detergent control moving forward.

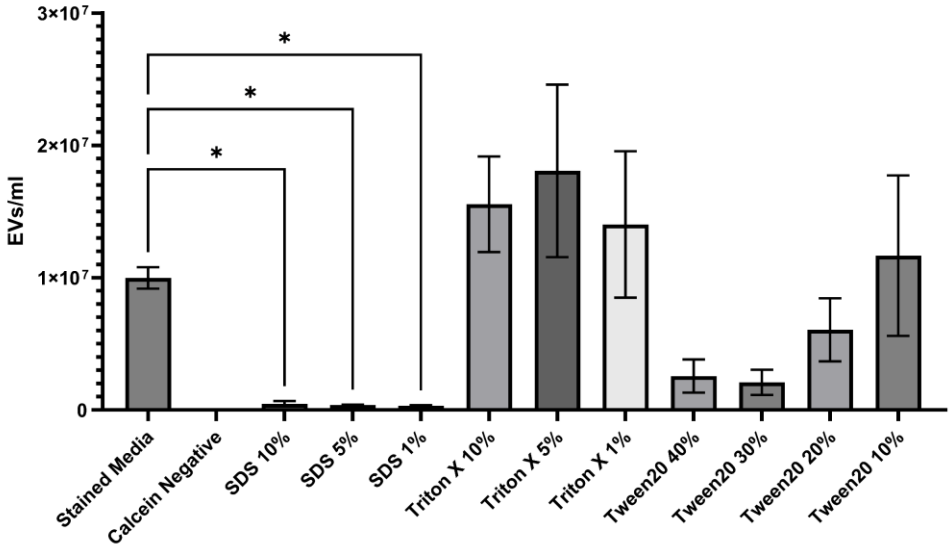

Figure 6.10. Assessment of Detergents on 10µM Stained EV Samples. The effect of different detergents on the depletion of airway epithelial derived EVs stained with 10µM calcein-AM. One-way ANOVA with Dunnett's multiple comparison test compared stained samples to detergent treated samples. *p≤0.05, (N=3)

6.3.4. ImageStream X MKII Fluorescent Limit of Detection

In addition to the quantification of EVs, flow cytometry will also be used to assess the expression of tetraspanin and cell origin markers. Initially, the sensitivity of the ISX to fluorescent signals was assessed to allow for the identification of optimal fluorophores for characterisation panels. Fluorophores PE-Cy5, PE-Cy7, PE, APC and PE-Vio615 were chosen for assessment due to their high brightness. To assess the LoDs in a comparable way, sensitivity to fluorophores was measured in terms of antibody binding capacity (ABC). Analysis this way allowed for the assessment of the minimum number of antibody binding events for positive detection (LoD). ABC was measured using Quantum^{TM} Simply Cellular Beads; these beads are divided into 4 populations with different known numbers of FC binding sites. This allows for the plotting of binding sites against average fluorescent intensity for each population using the manufacturer's analysis template. The fluorescent value for a blank bead population is then interpolated by the template and defined as the LoD.

ISX's lasers were set to maximum strength (mW) so the cytometer was configured for the highest sensitivity. Figure 6.11A shows the gating strategy used to analyse individual bead populations. Beads were identified using a scatter plot of the relevant fluorophore's channel against size (SSC) (Figure 6.11Ai). This selection was taken forward and a spot count was performed on the brightfield channel images, selecting for only single object events (Figure 6.11Aii). The single object populations were exported as FCS files and analysed in Kaluza 2.1. Figure 6.11B shows overlays of fluorescent histograms for each population stained with PE-Cy7-conjugated antibody and the average fluorescent intensity of each population.

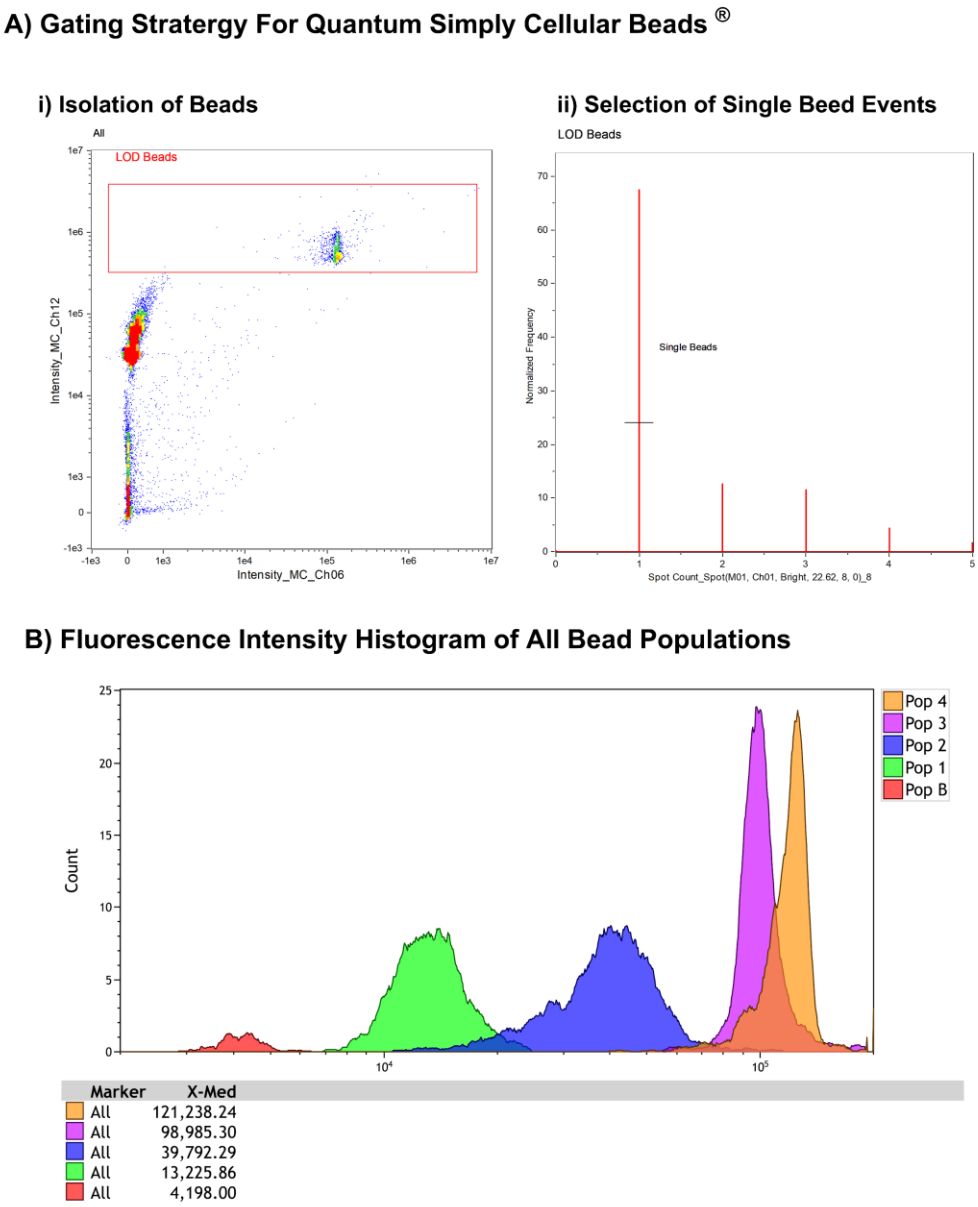

Figure 6.11. Flow Cytometric Analysis of Quantum Simply Cellular Beads® Used to Determine Fluorescent LoD on the ImageStream X MKII. A) Gating of beads first isolated using **Ai)** scatter plots of size (SSC) Vs fluorescent intensity before **Aii)** Isolation of single bead events using a spot count. **B)** Overlay histogram of all bead populations with different ABCs stained with PE-Cy7 and each population median fluorescent intensity.

These intensity values were then input into the manufacturer's analysis template to generate a logarithmic regression curve to interpolate the LoD in terms of ABC for each fluorophore. Table 6.2 shows the LoD of fluorophores assessed, as well as the regression coefficient (r^2). Fluorophores APC, PE and PE-Cy7 were identified as potential fluorophores due to their high sensitivities

and the commercial availability of relevant antibodies with the appropriate fluorophores conjugated.

Table 6.2 LoD of fluorophores assessed using the ISX and the R coefficients of curves used.

Fluorophores	LoD (ABC)	R Coefficient
PE-Cy5	24	0.9995
APC	46	0.9673
PE-Vio615	638	0.9991
PE	954	0.9985
PE-Cy7	1183	0.9973

Having selected these fluorophores, it was subsequently identified that staining of EV samples with APC crashed the ISX due to the detector being overwhelmed with signal. To compensate for this, the LoD of APC was assessed at different 642nm laser strengths to determine if it was possible to reduce the sensitivity of the machine to APC enough that samples could run without losing APC's high sensitivity. Beads were run at 4 different laser strengths, 150mW (Maximum strength), 100mW, 50mW and 2mW (minimum strength). Reduction of the laser's strength was observed to lower the LoD of APC on the ISX (Table 6.3). A laser strength of 2mW was identified as suitable, as this allowed for samples to run, while still being more sensitive than other identified fluorophores (PE and PE-Cy7) (Table 6.2) Additionally, a reduction of 642nm laser strength to 2mW, facilitates more relevant downstream comparison of markers as the LoDs are closer together. Consequently, all EV analysis performed with the ISX moving forward was conducted with the 642nm red laser set to 2mW.

Table 6.3 LoD of APC on ISX with 642nm laser set to different strengths and the R coefficients of curves used.

Laser strength (mW)	LoD (ABC)	R Coefficient
150	46	0.9673
100	47	0.9718
50	49	0.9774
2	259	0.9843

6.3.5. Optimisation of Tetraspanin Staining

Having identified fluorophores, two different types of fluorescently conjugated antibodies were assessed to see if the use of REAffinity antibodies or conventional mouse monoclonal antibodies would improve EV biomarker staining. REAffinity antibodies have a high purity as well as a mutated FC region, which eliminates background compared to conventional mouse monoclonal antibodies. EVs were stained with 10μM calcein and for tetraspanins (CD9, CD63 and CD81) using 2.5μg/ml (concentration identified from literature) of either a mixed fluorophore panel containing previously identified fluorophores PE, PE-Cy7 and APC or a pan-APC panel (APC was selected as it had the lowest LoD and commercially available antibodies for all targets). This was done for both REAffitniy and conventional antibodies and staining was compared. Staining with both the REAffinity mixed and APC panels showed better staining than with conventional antibodies (Figure 6.12). This was particularly emphasised in CD81 staining in the mixed panels, which showed a 10% increase in the detected expression on EVs when stained with REAffinity antibodies (Figure 6.12B). Consequently, characterisation of EVs was performed with REAffinity antibodies moving forward.

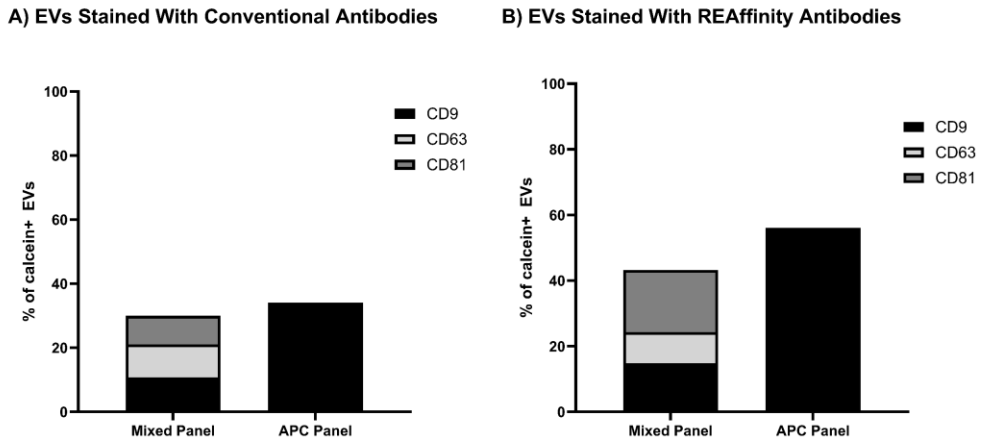

Figure 6.12. Comparison of Conventional and REAffinity Tetraspanin Staining . EVs stained with either a mixed fluorophore or pan- APC panel of **A)** Conventional mouse monoclonal or **B)** REAffinity antibodies (N=1).

In addition to looking at individual markers we also wanted to evaluate the potential of looking at multiple markers on individual EVs within a population. To achieve this, an additional gating strategy using EV populations identified using the strategy in Figure 6.6 was developed to allow for the profiling of multiple biomarkers on small intact EVs. Figure 6.13A shows the initial gating of the RMS_Gradient of FITC-positive EVs that allows for the selection of only in-focus images. Subsequent gates were situated using isotype controls. Figure 6.13B shows the individual gating for each EV marker stained using the panel previously identified. Figure 6.13C shows the quadrant gating used to identify EVs positive for 2 biomarkers. Finally, gating for EVs positive for all 3 biomarkers (Figure 6.13D) was done through the gating of EVs double positive for APC and PE (Figure 6.13Ci), these double positive populations were then gated using single positive PE-Vio615 gating (Figure 6.13Biii). Tetraspanin and origin cell biomarker expression can then be calculated as a percentage of the total in focus population to allow for comparison between samples.

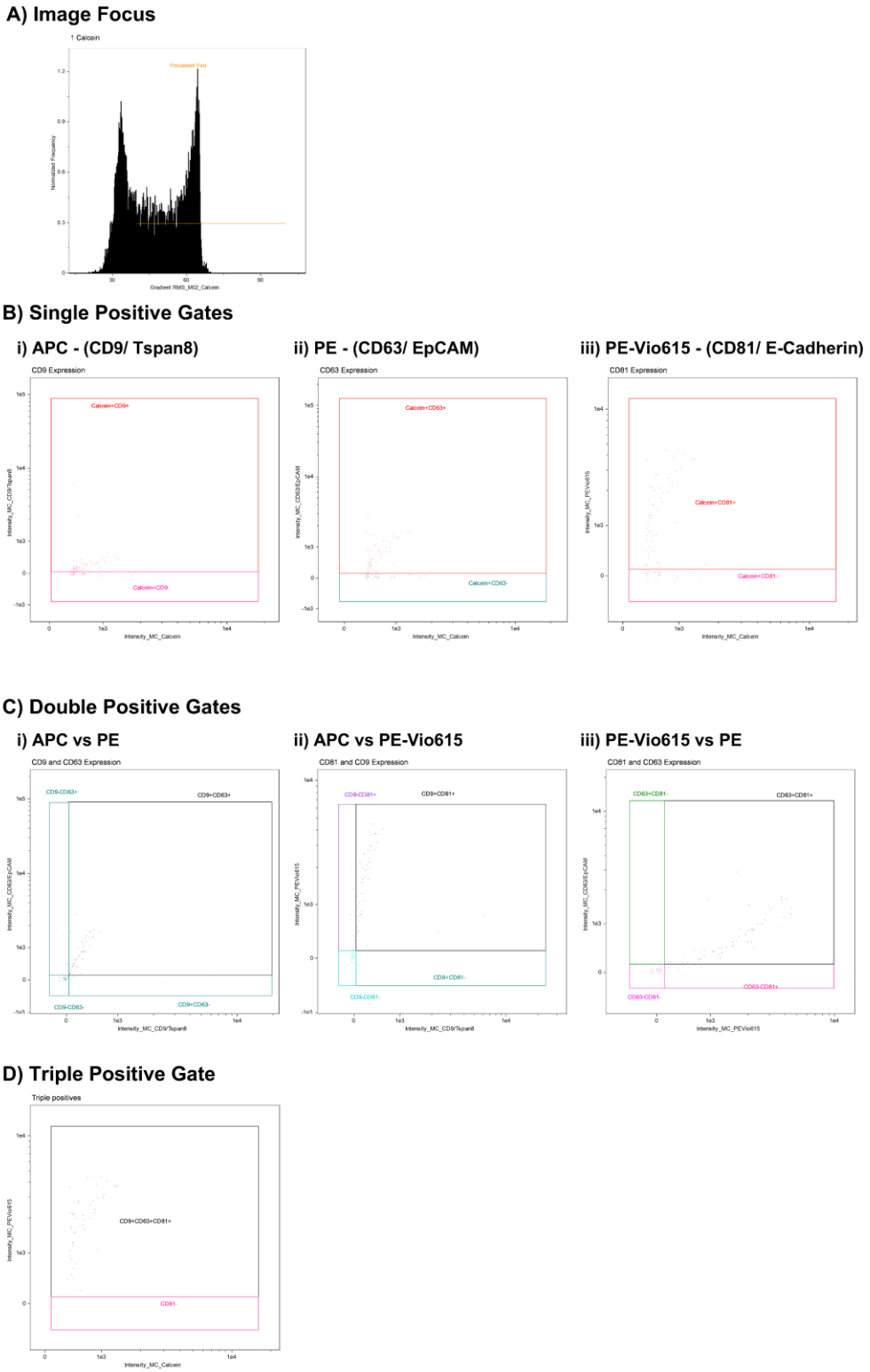

Figure 6.13. Gating Strategy for the characterisation of tetraspanin markers on small EVs. A) Selection of in focus calcein positive events**. B)** Gating for single positive events for **Bi)** APC, **Bii)** PE and **Biii)** PE-Vio615. **C)** Gating of events positive for either **Ci)** APC and PE, **Cii)** APC and PE-Vio615 and **Ciii**) PE-Vio615 and PE (Events bellow 330nm). **D)** Gating of events positive for all antibodies.

Figure 6.14 shows examples of EVs positive for each individual marker (CD9, CD63 and CD81) as well as double and triple positive EVs, identified using the ISX gating strategy and optimised calcein-AM and tetraspanin antibodies.

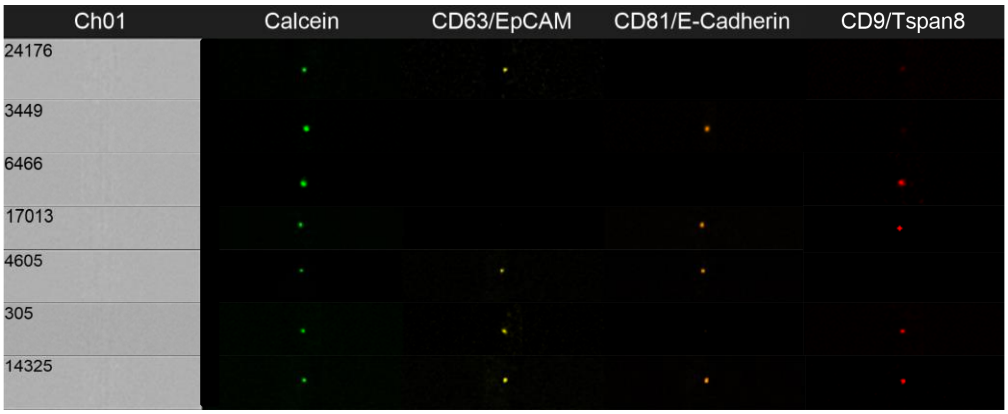

Figure 6.14. Epithelial Derived EV positive for CD9, CD63, and CD81. Basal supernatant taken from ALI culture and stained with 10μM calcein-AM and CD9, CD63 and CD81 REAffiniy antibodies.

6.3.6. Co-Factor Controls EV Response

In Chapter 5 (Section 5.3.6.) co-factors which will be added to Der p 1 to both activate (5mM L-Cysteines) and inactivate (10μM E-64) were assessed to see if they had a stimulatory effect on cytokine production. As a part of this initial assessment, the effect of co-factors on EV secretion was also assessed using the previously optimised staining. Inserts were either exposed to nebulise PBS (unstimulated controls), 5mM L-Cysteine or 10μM E-64 for 24 or 48 hours.

Comparison of apical response after 24 hours showed no significant change in response relative to unstimulated controls (Figure 6.15A). This lack of significance was again observed at 48 hours (Figure 6.15A). Basally, there was no significant change in EV numbers as a result of 24- or 48-hour exposure to co-factors and no significant increase in response was observed with increased exposure (Figure 6.15B). Interestingly there was a difference in total EV numbers observed between apical and basal samples with apical EV/ml counts averaging $7.5x10^8$ compared to an average basal response of $5.1x10^6$.

This further confirmed that co-factors added to Der p 1 samples do not influence ALI culture's responses.

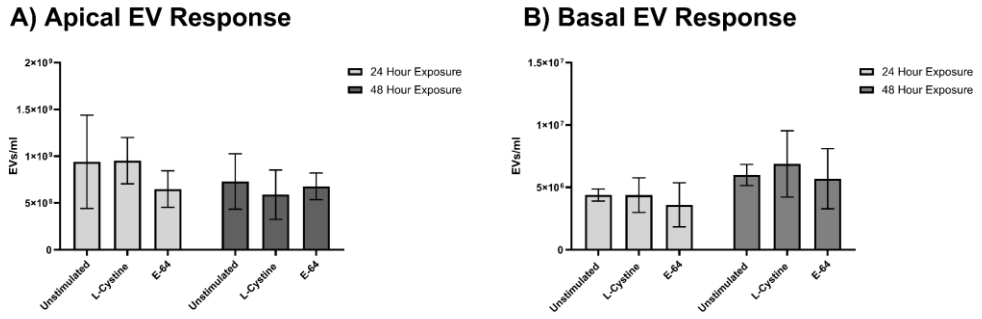

Figure 6.15. EV response of Airway Epithelial ALI Cultures to 24- and 48-hour exposure of either Nebulised; PBS, 5mM L-Cysteine or 10µM E-64. A) Apical EV response to 24- and 48-hour exposure to co-factors. **B)** Basal EV response to 24- and 48-hour exposure to co-factors. Columns represent mean and error bars represent standard deviation. Two-way ANOVAs with Sidak's multiple comparison test was used to compare 24- and 48-hour responses*p≤0.05, **p≤0.01, ***p≤0.001, ****p≤0.0001. (N=5).

6.4. Discussion

The use of flow cytometry for the characterisation and quantification of EVs provides a potentially more accurate method of EV quantification, as well as a high-throughput method for the characterisation of individual EV marker expression without the need for the isolation of EVs. The aim of this chapter was to identify a suitable flow cytometer for analysis, as well as optimise EV staining.

Initial isolation and profiling of EVs using TEM and NTA, confirmed the presence of EVs in cultures and EVs were observed to range in size from 50-300nm and presented with a cup-shaped morphology consistent with the literature (Kurtjak *et al.,* 2022). While NTA is currently considered the gold standard for EV quantification, its lack of specificity means it is unable to distinguish between individual and aggregated EVs, as well as potential contaminants, such as membrane fragments, resulting in conflated counts. The use of flow cytometry provides a potential alternative method for more selective and robust quantification. Consequently, two different flow cytometers (CytoFLEXs and ImageStream X MKII) were assessed for their suitability to profile small EVs.

Initial profiling of the sizing sensitivity of the two flow cytometers, using NIST beads ranging from 60-151nm, showed that the ISX had a greater sensitivity, detecting all bead populations, while the CytoFLEX was unable to detect the 60nm population. Subsequent translation of the CytoFLEX data using FCMpass (Welsh *et al.,* 2020) showed its LoD to be 74.8nm, which is the equivalent to a 143.1nm EV when adjusted for using Mie theory. While Mie theory adjustment was not possible for the ISX, the use of fluorescent sizing showed the cytometer could detected EVs as small as 55nm, suggesting this was a more suitable machine for small EV analysis.

Once a cytometer was identified, the cytoplasmic dye calcein-AM was assessed to find a suitable staining concentration. Calcein-AM allows for the selective staining of intact lipid vesicles (Chuo *et al.,* 2018, L. Miles *et al.,* 2015). EV samples were stained with concentrations ranging from 0.1-200μM and quantified, looking for a saturation point. A concentration of 10μM was

identified, using the CytoFLEX, as optimal as it both saturated samples and had the highest stain index.

Additionally, a detergent control was examined to demonstrate successful staining of lipid-bound plasma membrane as opposed to contaminant protein complex (Osteikoetxea *et al.,* 2015). Stained EV samples were treated with different concentrations of three detergents; SDS, tween-20 and tritonX, and 10% SDS was identified as a suitable detergent for the depletion of EVs.

Having optimised calcein-AM staining, it was then possible to optimise the characterisation of EVs using fluorescently-conjugated antibodies. Different fluorophores with high brightness were compared by measuring their LoDs in terms of ABC to identify a fluorophore panel for analysis. APC, PE and PE-Vio615 were identified due to having low LoDs that were close together, as well as commercial antibodies available for relevant targets. Antibodies were used at 2.5µg/ml, based on previous literature (Woud *et al.,* 2022, Lucchetti *et al.,* 2020).

Additionally, conventional monoclonal antibodies were compared with REAffintiy antibodies to assess which gave the highest staining. Samples were stained with either a mixed or pan-fluorophore panel (CD9, CD63 and CD81) for both conventional and REAffintiy antibodies. REAaffiniy antibodies were observed to stain more positive EVs with both panels and consequently were used moving forward.

Lastly, before final stimulations the effect of co-factors L-Cysteine and E-64 on EV responses were assessed to ensure these factors did not induce changes in secretion. No changes were observed in EV response to either co-factor at both 24 and 48 hours, this coupled with their lack of cytokine induction (Section 5.3.6) reaffirmed that any potential responses induce in active and inactive Der p 1 exposed inserts would be due to the allergen. Additionally, profiling of the proteolytic activity of Der p 1 confirmed the allergen was functional and that addition of E-64 significantly reduced its activity.

These experiments address the necessary considerations for the initial selection of a cytometer for small EV analysis, as well as the optimisation of EV staining for subsequent quantification and characterisation of biomarkers. Chapter 7 utilised these optimised techniques to enable the profiling of the small EV responses in 3D epithelial cultures exposed to allergens.

These experiments address the necessary considerations for the initial selection of a cytometer for small EV analysis, as well as the optimisation of EV staining for subsequent quantification and characterisation of biomarkers. Chapter 7 utilised these optimised techniques to enable the profiling of the small EV responses in 3D epithelial cultures exposed to allergens.

Chapter 7: Exposure of 3D Airway Epithelial Cultures to Nebulised Allergens

7.1. Introduction

Indoor allergens and their link to the development of type 1 hypersensitivity disorders are well established. Common sources of these allergens are house dust mites (HDMs), dogs, cats, rodents and cockroaches (Beheshti *et al.,* 2025). HDM are one of the most prominent sources of indoor allergens and as a consequence are a significant etiologic factor in the development of numerous allergic disorders, including AR, allergic asthma and atopic dermatitis (Imoto *et al.,* 2024, Li *et al.,* 2022, Hu *et al.,* 2022). Currently, it is estimated that allergy to HDMs and their associated proteins affects 4-6% of the global population (Jurkiewicz *et al.,* 2025). Sensitisation to HDM proteins has been established to occur early in life, with 68.3% of children with HDM induced AR developing symptoms before the age of 6. Furthermore, it's estimated that 53.5% of children aged 0-3 years with allergic asthma are HDM sensitised, with this jumping to 80.2% of allergic asthma cases in children aged 8-12 years (Jurkiewicz *et al.,* 2025).

The HDM species *Dermatophagoides pteronyssinus* is one of the most common to be associated with sensitisation, with a high prevalence in western cultures, particularly Europe, where it is the most common HDM species (Waldron *et al.,* 2019). To date, 40 major HDM allergens have been identified, all differing in their biological structure, function and ability to elicit allergic responses (Huang *et al.,* 2023). Of these 40 proteins, Der p 1 has been identified as one of the most clinically relevant to type 1 hypersensitivity, due to its high immunogenicity, its strong association with the induction of specific IgE antibodies and it's IgE reactivity (Jurkiewicz *et al.,* 2025). Der p 1 is a proteolytic enzyme from the cysteine protease family, and the most profuse allergenic protein found in HDM faecal pellets (Chevigné and Jacquet, 2018, Gough *et al.,* 1999). This proteolytic activity is induced by cysteine in a thiol-dependent manner, which results in the reduction of disulphide bonds in the active side of the enzyme allowing for the release of its inhibitory peptide

(Kalsheker et al., 1996). Inhalation of HDM faecal pellets is a major route for allergen exposure. Upon inhalation, the proteolytic activity of Der p 1 can induce barrier dysfunction through cleaving tight junction proteins, such as claudin, occludin and ZO-1 (Soh *et al.,* 2023, Ogi *et al.,* 2021). Barrier dysfunction facilities allergen penetration, inducing the secretion of alarmins IL-25, IL-33 and TSLP which in turn promote Th2 polarisation and sensitisation (Meng *et al.,* 2025). In addition to its proteolytic cleaving of tight junctions, Der p 1 also interacts with protease-activated receptors (PARs) and TLR-4 on epithelial cells. This facilitates the recruitment of ILC2s, dendritic cells and mast cells, further promoting allergic sensitisation (Abu Khweek *et al.,* 2020).

In addition to HDM, pets such as dogs and cats are a prominent source of indoor allergens. In the USA it's estimated that 70% of households have a cat or dog (Torres-Borrego and Sánchez-Solís, 2023). Currently there are seven distinct dog allergens, termed *Canis familiaris* 1-7 (Can f 1 – Can f 7). Exposure to these dog derived allergens are a significant risk factor in the development of type 1 hypersensitivity (Yamamoto *et al.,* 2019). The frequency of cat and dog allergies is around 10% in developed countries, with 50% of allergic individuals owning a pet. The sensitisation profiles against Can f proteins are diverse, consequently, there is currently no recognised predominant allergen, like Der p 1 in HDM (Torres-Borrego and Sánchez-Solís, 2023). However, IgE reactivity prevalence to Can f 1 has been reported to range from 49-75% depending on the populations studied (Caraballo *et al.,* 2020). Can f 1 is a lipocalin derived from dog saliva, which acts as a transporter ligand for steroids, retinol and pheromones (Torres-Borrego and Sánchez-Solís, 2023). Most mammals typically express exogenous lipocalins in their saliva, skin and urine, however humans have endogenous lipocalins. The mechanism through which Can f 1 sensitises an individual is not well understood. However, given the homology of mammalian and human lipocalins, the immune system inhibits T cell responses to mammalian lipocalins to prevent the creation of an auto immune response. It is currently hypothesized that it is this inhibition of T cell responses that favours the

development of Th2 responses to prevent potential autoimmunity (Virtanen *et al.,* 2012).

Previously, we have shown the development of both a biologically relevant 3D airway epithelial model comprised of differentiated airway epithelial cells and tight junctions and a mechanism for its successful stimulation through the use of nebulised stimulants. We have also shown the optimisation of an imaging flow cytometric method for the quantification and individual characterisation of airway epithelial EVs. Thus, this chapter aims to evaluate and profile changes in 3D airway epithelial culture cytokine and EV responses after exposure to indoor allergens, namely proteolytically active and inactive Der p 1, as well as the lipocalin Can f 1.

7.2. Materials and Methods

The proteolytic activity of Der p 1 was assessed using a cysteine protease activity kit (Calibiochem®, UK), full method is outlined in Section 2.2.12. 10µg/ml Der p 1 was assessed either alone or supplemented with 5mM L-Cysteine or 5mM L-Cysteine and 10µM E-64 to confirm the allergen was both activated and inhibited.

7.2.1. Exposure of 3D Airway Epithelial Cultures

3D airway epithelial cultures were generated through the culture of Calu-3 cells at ALI (Sections 2.2.1.1 and 2.2.1.4). After culture, inserts were washed with warmed PBS (37°C) and prepared for stimulation two days prior to nebulisation as outlined in Section (2.2.1.5). Inserts were subsequently exposed to either nebulised Der p 1 activated with 5mM L-Cysteine (Active), Der p 1 inhibited with E-64 (Inactive), Can f 1, Poly(I:C) or PBS (unstimulated control). Der p 1 was activated or inhibited as previous through the addition of L-cysteine or E-64 respectively 20 minutes prior to nebulisation (Section 2.2.1.5). Table 7.1 outlines volume and concentration of reagents added to the nebuliser, as well as the deposition after 35% adjustment.

Table 7.1. Concentration and volume of stimulants added to the nebuliser as well as the deposition of stimulant deposited into each insert after 35% deposition adjustment.

Stimulant	Concentration added to Nebuliser (mg/ml)	Vneb (ml)	Deposition (µg/cm^2)
PBS (Unstimulated)	Neat	0.3	-
Poly(I:C)	2.0	0.3	1.0
Active Der P 1 (Der P 1 and L-Cysteine)	1.0	0.2	0.35
Inactive Der P 1 (Der p 1 and E-64)	1.0	0.2	0.35
Can F 1	1.0	0.2	0.35

Nebulisations were conducted as specified in Section 2.2.1.5 and samples were profiled after 24 and 48 hours of nebulised exposure (N=6).

7.2.2. Profiling of Nebulised Exposure Responses

After 24- and 48-hour exposure, basal and apical supernatant were isolated from samples as outline in Section 2.2.1.4. In brief, apical samples were washed twice for 3 minutes with 200µl of warmed PBS (37ºC) and the supernatant was collected. This was subsequently topped up with an additional 100µl of PBS to allow for direct comparison of the apical and the 500µl basal samples.

7.2.2.1. Viability of Samples

The viability of samples was assessed using a Promega RealTime-Glo™ Lactate Dehydrogenase assay (LDH). LDH concentrations of basal samples were assessed as per Section 2.2.10.2 and percentage viability was calculated as a percentage relative to a 10% tritonX control.

$$Percentage\ Viability = 100 - \left(100 \times \frac{Sample\ LDH\ Comcentration}{TritonX\ LDH\ Concentration}\right)$$

7.2.2.2. Cytokine Responses

The apical and basal cytokine responses of airway epithelial cultures were assessed using ELISAs for cytokines; IL-1β, IL-6, IL-8, IL-25, IL-33 and TSLP (Section 2.2.11). Cytokines IL-1β, IL-6, IL-25, IL-33 and TSLP were assessed using neat sample and run in duplicates, while IL-8 samples were run at a 1:10 dilution and assessed in quadruplets.

7.2.2.3. Quantification and Characterisation of EVs

Apical and basal EV responses were quantified using imaging flow cytometry. Samples were stained as outline in Section 2.2.5 with 10µM of Calcein-AM. In addition to this, basal samples were profiled for tetraspanin and origin cell marker expression. Two sets of basal samples were stained for either CD9, CD63 and CD81 or Tspan8, EpCAM and E-Cadherin. Table 7.2 shows the antibodies and their fluorophores used in each panel, all were used at a concentration of 2.5µg/mL.

Table 7.2 Antibodies used for EV characterisation, listing: target, fluorophore, brightness, manufacturer, category number and staining concentration used.

Antibody	Fluorophore	Brightness	Manufacturer	Cat.no.
CD9	APC	4	Miltenyi	130-118-808
CD63	PE	5	Miltenyi	130-118-077
CD81	PE-Vio615	5	Miltenyi	130-131-387
EpCAM	PE	5	Miltenyi	130-110-999
E-Cadherin	PE-Vio615	5	Miltenyi	130-125-732
Tspan8	APC	4	Miltenyi	130-128-391
REA Control Antibody Human IgG1	APC	4	Miltenyi	130-113-434
REA Control Antibody Human IgG1	PE	5	Miltenyi	130-113-450
REA Control Antibody Human IgG1	PE-Vio615	5	Miltenyi	130-113-439

7.2.2.4. Microscopy of 3D Cultures

Inserts were imaged after 24- and 48-hour exposures using fluorescent confocal microscopy and SEM. Samples were prepared for confocal as per Section 2.2.2.1 and stained with 5µg/ml of fluorescent antibodies for tight junction proteins occludin (Alexa488) and ZO-1 (Alexa647). Samples were analysed using a Zeiss LSM900 with AiryScan; Objective: Plan-Apochromat 20x, Numerical Aperture: 0.8, Lasers used: AlexaFluor647, AlexaFluor488, Pixel size: 0.074µm x 0.074µm Z-Step size: 0.7µm.

Samples were prepared for SEM as outlined in Section 2.2.2.2. and samples were analysed using a JEOL JSM IT-200 LV SEM using a voltage of 5 kV and a working distance of 10 mm.

7.2.2.5. Transcriptomic Analysis

Samples were first prepared for transcriptomic analysis as outlined in Section 2.2.14. In brief, 70µl of 48 hour exposed basal samples were collected (N=6) and combined in pairs to make a total volume of 140µl (N=3). These samples were isolated and concentrated using SEC, as outlined in Section 2.2.7. These samples were stored at -80 before shipping to TAmiRNA for

analysis. The sample's RNA was isolated from EVs using TAmiRNA's extraction protocol and sequenced (Section 2.2.14.1 & 2.2.14.2). Data was subsequently analysed using the miND® pipeline outlined in Section 2.2.14.3. and the analysis was sent back for relevant interpretation.

7.3. Results

7.3.1. Proteolytic Activity of Der p 1

Before 3D cultures were exposed to nebulised Der p 1, its proteolytic activity was assessed using a FTC-casein protease activity test to ensure the allergen was functional. 10µg/ml of Der p 1 was assessed with and without 5mM of its activator L-cysteine, as well as with L-cysteine and 10µM of the protease inhibitor E-64, and a 10µg/ml Trypsin positive control was also run. Figure 7.1 showed that when L-Cysteine was added to Der p 1 there was a significant increase in proteolytic activity relative to Der p 1 on its own. Furthermore, the addition E-64 significantly reduced proteolytic activity, though this was significantly higher than Der p 1 on its own. This indicated that Der p 1 stocks were functional and suitable for use moving forward.

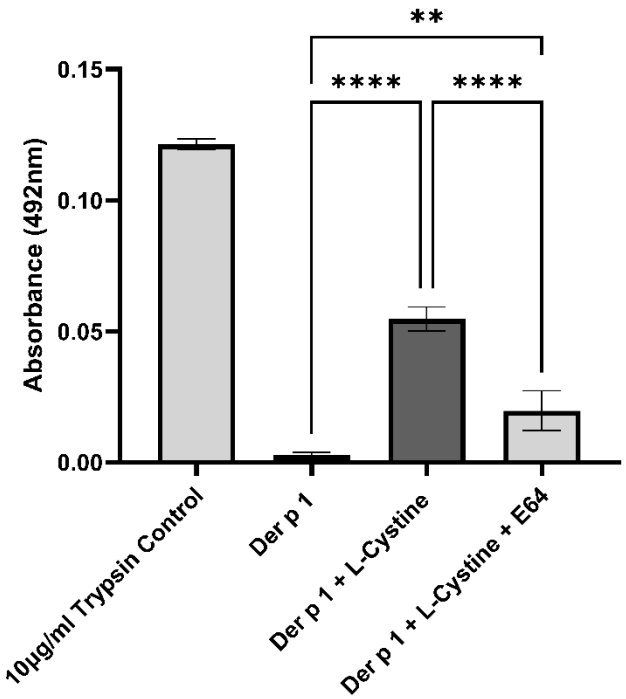

Figure 7.1 Proteolytic Activity of Inactive, Active and Inhibited Der p 1. 10µg/ml concentrations of Der p 1 had proteolytic activity assessed using an FTC-casein absorbance assay. Der p 1 was assessed in its inactive form (Der p 1), active form (Der p 1 + L-Cysteine) and in an inhibited form (Der p 1 + L-Cysteine + E-64). 10µg/ml Trypsin was used as a positive control. A One-way ANOVA with Sidak's multiple comparison test was used to compare Der p 1 conditions. *p≤0.05, **p≤0.01, ***p≤0.001, ****p≤0.0001. (N=3)

7.3.2. Exposure of 3D Airway Epithelial Cultures to Nebulised Allergens

Having confirmed Der p 1 was proteolytically active, it was possible to assess the effect of nebulised allergens on 3D airway epithelial culture cytokine and EV responses using the previously outlined optimised methodologies (See Chapters 5 and 6). Cultures were exposed to 0.35μg/cm^2 of either Der p 1 and 5mM L-Cysteine (Active Der p 1), Der p 1 and 10μM E-64 (Inactive Der p 1) or Can f 1. Nebulised PBS was used as an unstimulated control and 1.0μg/cm^2 Poly(I:C) was used as a positive control. Cultures were exposed for either 24 or 48 hours to stimulants (N=6) and apical and basal cytokine and EV responses were profiled. Inserts were also assessed with confocal staining and SEM to assess epithelial tight junctions and microstructure, as well as cell viability by LDH.

7.3.2.1. LDH Viability of Airway Epithelial Cultures After Exposure to Nebulised Allergen

Viability of epithelial cultures was assessed after 24- and 48-hours exposure in duplicate using LDH luminescence assays. Percentage viability was calculated relative to 10% tritonX treated insert controls as previously described. After 24 hours, unstimulated controls had the lowest viability of all conditions, with an average sample viability of 94% (Figure 7.2Ai). After 48-hour exposure, viability remained high, with the active Der p 1 having the lowest viability at 93% (Figure 7.2Aii). Evaluation of viability over time, showed viability for inserts exposed to active Der p 1, decreased from 96% to 94% (Figure 7.2B).

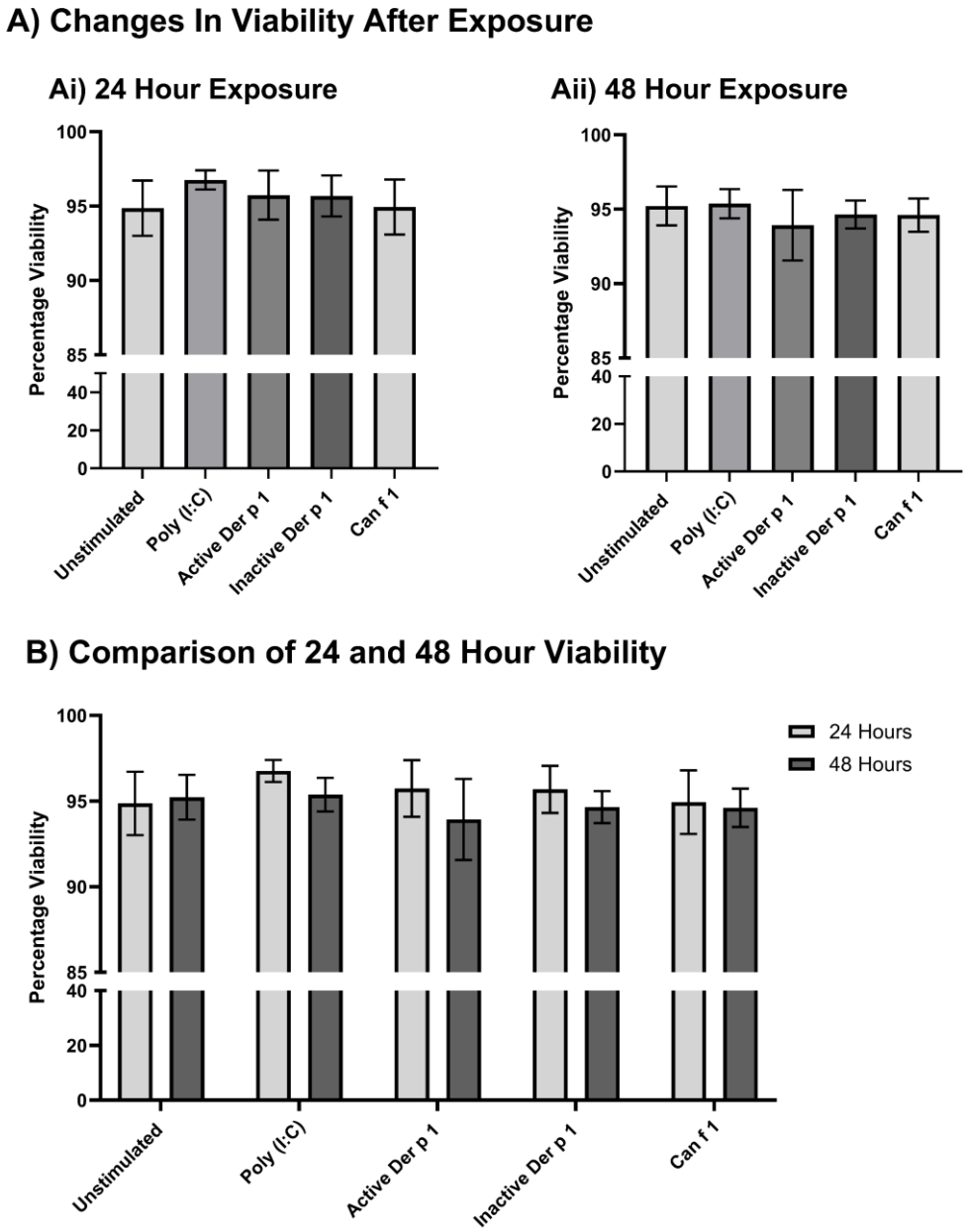

Figure 7.2. Viability of Airway epithelial Cultures After 24- and 48-Hour Exposure to Nebulised 1.0µg/cm^2 Poly(I:C) or 0.35µg/cm^2 of Active Der p 1 , Inactive Der p 1 or Can f 1. A) Percentage Viability of samples relative to 10% TritonX controls after **Ai)** 24-Hour Exposure and **Ai)** 48- Hour Exposure. **B)** Comparison of 24- and 48-hour post exposure viability. (N=12).

7.3.2.2. Tight Junction Staining

The effect of 24- and 48-hour exposure of nebulised allergens was also profiled, using confocal microscopy and fluorescent staining of occludin (Alexa488) and ZO-1 (Alexa647). Strong occludin and ZO-1 expression was observed in unstimulated samples (Figure 7.3Ai&ii). Combined staining shows the presence of tight junctions (7.3iii). Poly(I:C) samples were hard to image due to high levels of mucus, however, exposed samples also had tight junctions detected, with this expression diminished in comparison to unstimulated samples (Figure 7.3Biii). While occludin staining was consistent with unstimulated samples (Figure 7.3Bi), ZO-1 staining was weaker, suggesting a diminished level of ZO-1(Figure 7.3Bii). Tight junction staining of 24 hour exposed active Der p 1 also appeared to have diminished ZO-1 expression compared to inactive Der p 1 (Figure 7.3Cii) with no noticeable changes on occludin expression (Figure 7.3Ci). Evaluation of combined staining images indicated a reduced expression of tight junctions relative to unstimulated controls, similar to Poly(I:C). This diminished expression is further emphasised by comparison with samples exposed to inactive Der p 1, which had a higher expression of tight junctions (7.3Diii). Expression of both occludin and ZO-1 was high and similar to unstimulated samples, suggesting no barrier dysregulation due to inactive Der p 1 (Figure 7.3Di&Dii). Can f 1 exposed samples also had strong occludin and ZO-1 staining consistent with unstimulated samples (Figure 7.3Ei&Eii) and by extension strong tight junction staining, indicating no dysregulation of the epithelial barrier after 24-hour exposure (Figure 7.3Eiii).

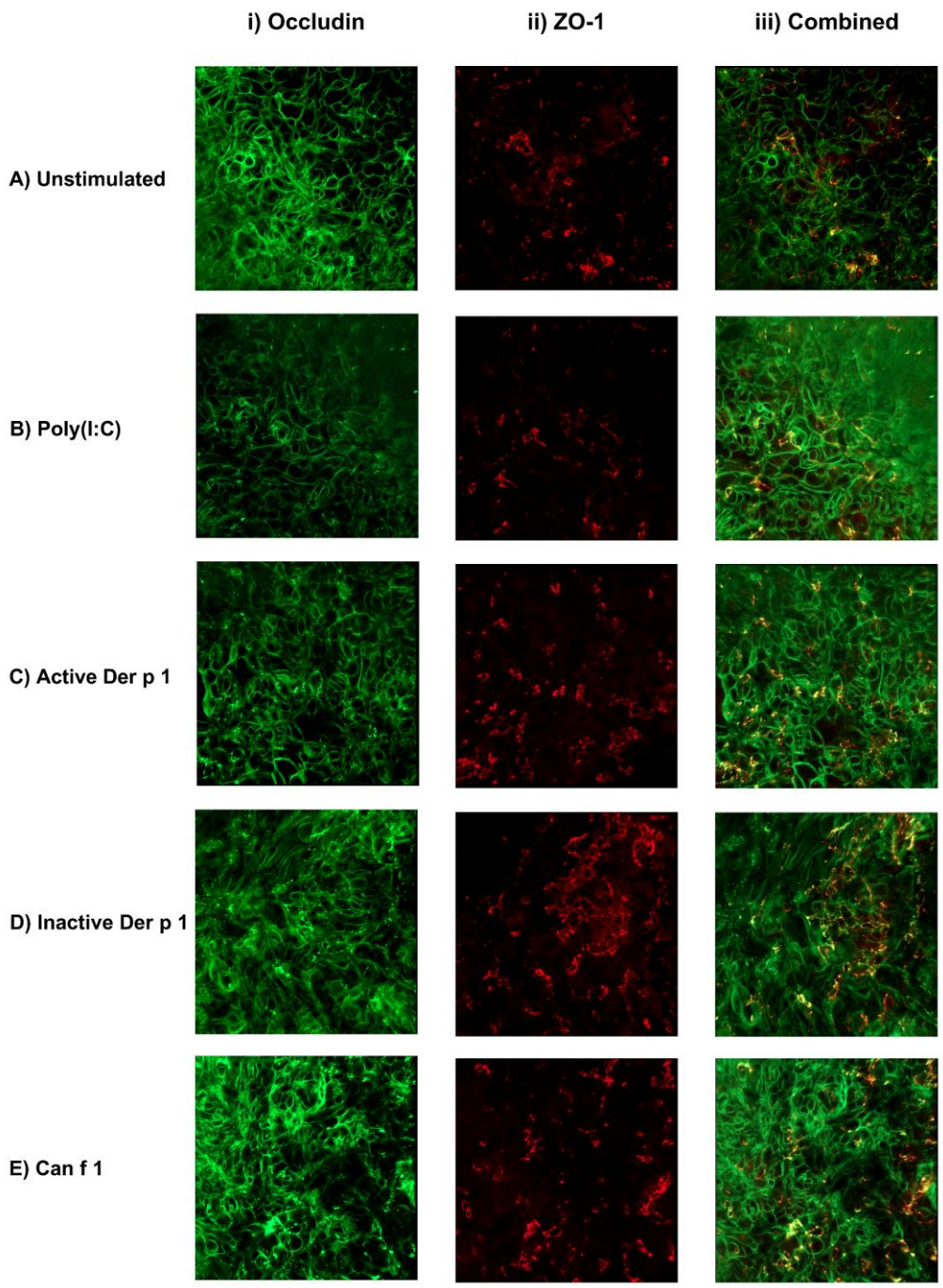

Figure 7.3. Airway epithelial tight junction expression after 24-hour exposure to Allergens. A) Unstimulated sample's **Ai)** Occludin, **Aii)** ZO-1 and **Aiii)** Combined expression. **B)** 0.5µg/cm^2 Poly(I:C) exposure **Bi)** Occludin, **Bii)** ZO-1 and **Biii)** Combined expression. **C)** 0.35µg/cm^2 Active Der P 1 exposure **Ci)** Occludin, **Cii)** ZO-1 and **Ciii)** Combined expression. **D)** 0.35µg/cm^2 Inactive Der p 1 exposure **Di)** Occludin, **Dii)** ZO-1 and **Diii)** Combined expression. **E)** 0.35µg/cm^2 Can f 1 exposure **Ei)** Occludin, **Eii)** ZO-1 and **Eiii)** Combined expression. Microscope: Zeiss LSM900 with AiryScan, Objective: Plan-Apochromat 20x, Numerical Aperture: 0.8 Lasers used: AlexaFluor647, AlexaFluor488, Pixel size: 0.074µm x 0.074µm Z-Step size: 0.7µm.

After 48-hour exposure unstimulated samples remained consistent with 24-hour exposure samples, with high expression of occludin (Figure 7.4Ai) and ZO-1 (Figure 7.4Aii), as well strong tight junction expression (Figure 7.4Aiii). Poly(I:C) exposed samples maintained high occludin expression (Figure 7.4Bi). However, as previously observed ZO-1 expression was reduced compared to unstimulated samples (Figure 7.4Bii), consequently there was reduced expression of tight junctions (Figure 7.4Biii). The reduction in ZO-1 observed after 24 hours exposure to active Der p 1 was more pronounced after 48 hours, with very weak ZO-1 expression observed indicating greater barrier dysregulation (Figure 7.4Cii), with fewer tight junctions stained (Figure 7.4Ciii). Occludin expression, however, remained consistent with both 24-hour samples and unstimulated samples (Figure 7.4Ci). Inactive Der p 1 samples appeared to have a slight decrease in ZO-1 relative to 24 hour and unstimulated 48 hour samples, with occludin expression remaining high (Figure 7.4Di&Dii) and strong tight junction expression (Figure 7.4Diii). 48 hour Can f 1 exposure also appeared to have no effect on barrier function, with strong expression of both occludin and ZO-1 and high tight junction expression (Figure 7.4E).

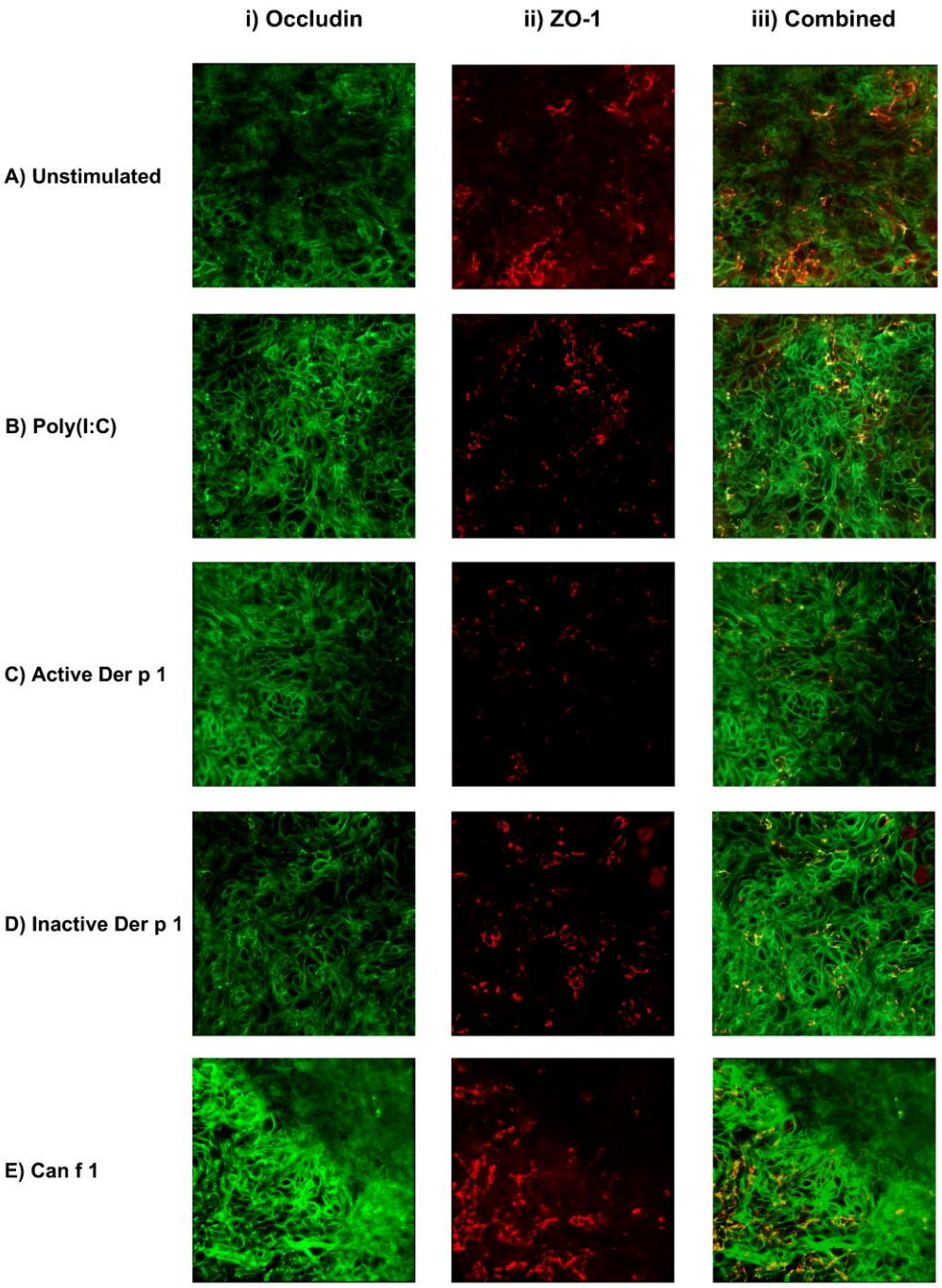

Figure 7.4. Airway epithelial tight junction expression after 48-hour exposure to Allergens. A) Unstimulated sample's **Ai)** Occludin, **Aii)** ZO-1 and **Aiii)** Combined expression. **B)** 0.5µg/cm^2 Poly(I:C) exposure **Bi)** Occludin, **Bii)** ZO-1 and **Biii)** Combined expression. **C)** 0.35µg/cm^2 Active Der P 1 exposure **Ci)** Occludin, **Cii)** ZO-1 and **Ciii)** Combined expression. **D)** 0.35µg/cm^2 Inactive Der p 1 exposure **Di)** Occludin, **Dii)** ZO-1 and **Diii)** Combined expression. **E)** 0.35µg/cm^2 Can f 1 exposure **Ei)** Occludin, **Eii)** ZO-1 and **Eiii)** Combined expression. Microscope: Zeiss LSM900 with AiryScan, Objective: Plan-Apochromat 20x, Numerical Aperture: 0.8 Lasers used: AlexaFluor647, AlexaFluor488, Pixel size: 0.074µm x 0.074µm Z-Step size: 0.7µm.

7.3.2.3. Scanning Electron Microscopy

In addition to confocal analysis of stained tight junctions, stimulated ALI cultures were also profiled using SEM. Inserts were processed and imaged after 24- and 48-hour exposure to stimulants using a JEOL JSM IT-200 LV SEM using a voltage of 5 kV and a working distance of 10 mm (N=1). Figure 7.5 shows ALI SEM images taken at 300x and 2.5kx magnification of inserts after 24-hour exposure. As can be seen in Figures 7.5C-E, samples stimulated with both active and inactive Der p 1 and Can f 1 were more mucus covered than the unstimulated control, which had more discernible cell populations. This increase in mucus cover is more noticeable in 2.5Kx magnified images. Despite this high mucus cover, cilia like structures were still identifiable on all three inserts exposed to nebulised allergen (Figure 7.5Ci-Ei). Poly(I:C) was noticeably different to unstimulated controls and allergen exposed samples, with even higher mucus cover, with it being hard to image areas with cellular structures exposed (Figure 7.5Bi). This was emphasised at 2.5Kx magnification where individual microstructures were not distinguishable (Figure 7.5Bii).

A) Unstimulated

Ai) 300x

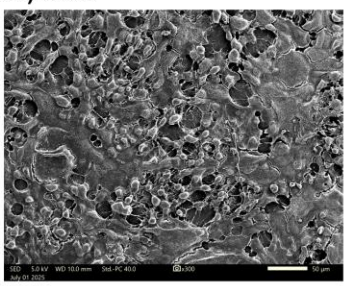

Aii) 2.5Kx

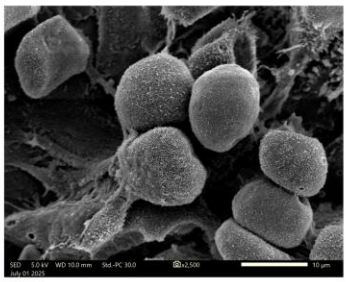

B) Poly (I:C)

Bi) 300x

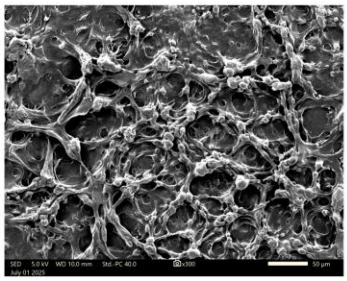

Bii) 2.5Kx

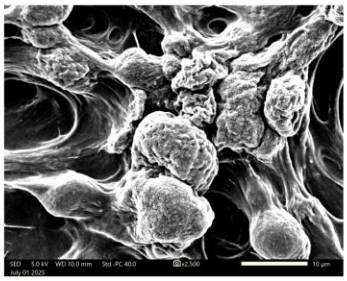

C) Active Der p 1

Ci) 300x

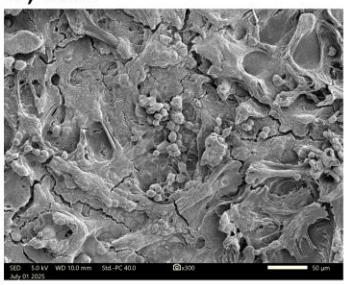

Cii) 2.5Kx

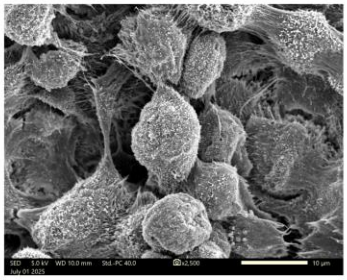

D) Inactive Der p 1

Di) 300x

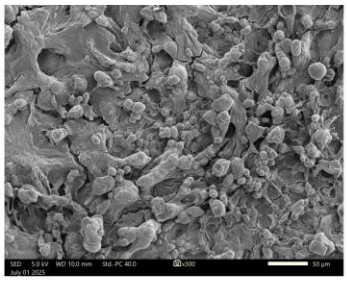

Dii) 2.5Kx

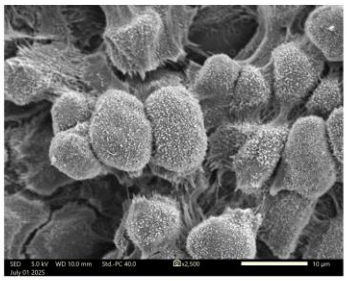

E) Can f 1

Ei) 300x

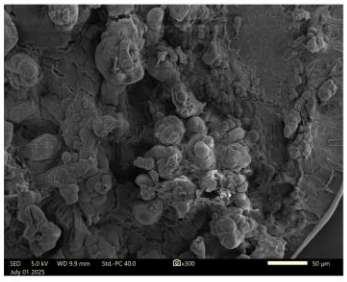

Eii) 2.5Kx

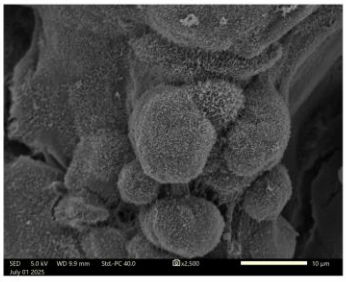

Figure 7.5 Scanning Electron Microscopy Images of 3D Airway Epithelial Cultures After 24- Hour to Nebulised Allergens (300x and 2.5kx Magnification). A) Unstimulated samples imaged at **Ai)** 300x and **Aii)** 2.5Kx. **B)** Poly(I:C) exposed samples imaged at **Ai)** 300x and **Aii)** 2.5kx. **C)** Active Der p 1 exposed samples imaged at **Ci)**300x and **Cii)** 2.5Kx. **D)** Inactive Der p 1 exposed samples imaged at **Di)** 300x and **Dii)** 2.5Kx. **E)** Can f 1 exposed samples imaged at **Ei)** 300x and **Eii)**2.5Kx magnification. Samples analysed using a JEOL JSM IT-200 LV SEM using a voltage of 5 kV and a working distance of 10 mm.

After 48-hour exposure, mucus cover was high on all samples making it challenging to discern cells (Figure 7.6) Images taken at 300x magnification highlight this with samples looking flat and smooth, with small peaks of cells protruding from the mucus. Mucus density appeared to be lower on samples exposed to Can f 1 and inactive Der p 1, however, microstructure was hard to image. Cilia were seen on inserts exposed to inactive Der p 1 and Can f 1 (Figure 7.6Di&Ei). Furthermore, it was possible to identify goblet cells on Can f 1 (Figure 7.6Ei).

A) Unstimulated

Ai) 300x

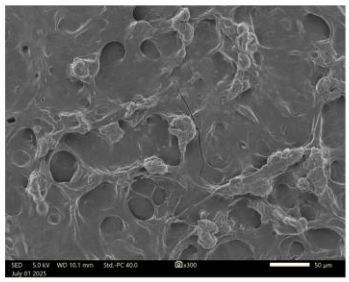

Aii) 2.5Kx

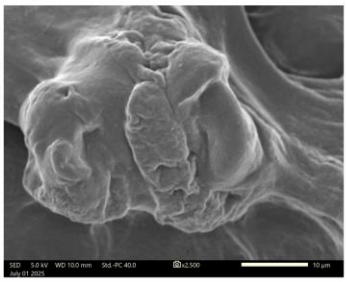

B) Poly (I:C)

Bi) 300x

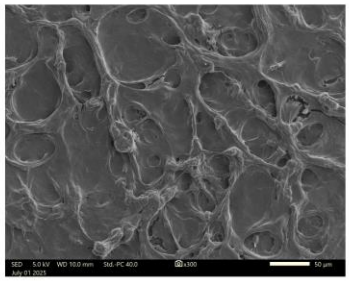

Bii) 2.5Kx

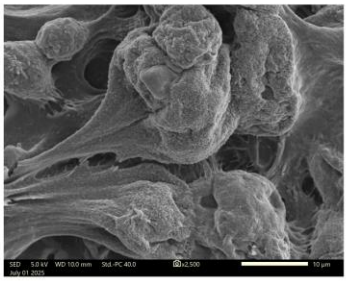

C) Active Der p 1

Ci) 300x

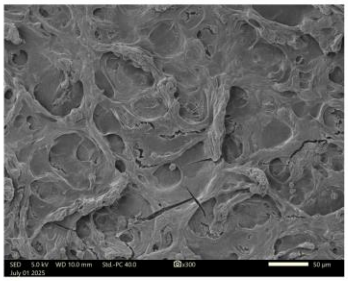

Cii) 2.5Kx

D) Inactive Der p 1

Di) 300x

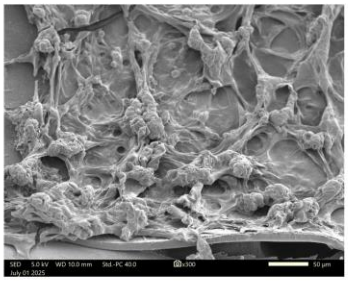

Dii) 2.5Kx

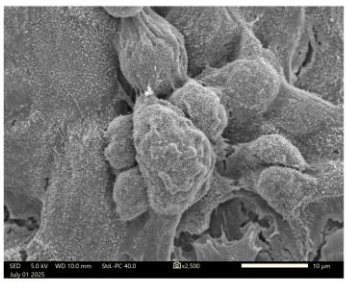

E) Can f 1

Ei) 300x

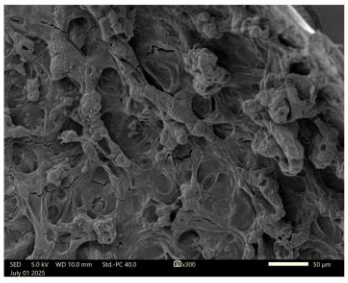

Eii) 2.5Kx

Figure 7.6 Scanning Electron Microscopy Images of 3D Airway Epithelial Cultures After 48- Hour to Nebulised Allergens (300x and 2.5kx Magnification). A) Unstimulated samples imaged at **Ai)** 300x and **Aii)** 2.5Kx. **B)** Poly(I:C) exposed samples imaged at **Ai)** 300x and **Aii)** 2.5kx. **C)** Active Der p 1 exposed samples imaged at **Ci)**300x and **Cii)** 2.5Kx. **D)** Inactive Der p 1 exposed samples imaged at **Di)** 300x and **Dii)** 2.5Kx. **E)** Can f 1 exposed samples imaged at **Ei)** 300x and **Eii)**2.5Kx magnification. Samples analysed using a JEOL JSM IT-200 LV SEM using a voltage of 5 kV and a working distance of 10 mm.

7.3.2.4. Cytokine Response of 3D Airway Epithelial Cultures After Exposure to Nebulised Allergen

The changes in cytokine responses of IL-1β, IL-6, IL-8, IL-17E, IL-33 and TSLP were also measured after 24- and 48-hours exposure by ELISAs. ELISAs for IL-1β, IL-17E, IL-33 and TSLP did not detect measurable levels of cytokine (data not shown). After 24-hour exposure apical IL-8 concentrations significantly increased in samples stimulated with 0.35µg/cm^2 Can f 1, with average concentrations increasing to 950.5pg/ml relative to 481.8pg/ml in unstimulated controls (Figure 7.7Ai). This Can f 1 induced increase in apical IL-8 concentration was not observed after 48-hour exposure, however, a significant increase in apical IL-8 was observed in samples exposed to 0.35µg/cm^2 of active Der p 1 (Figure 7.7Aii). Comparison of 24- and 48-hour apical responses saw significant increases in IL-8 responses for all conditions (Figure 7.7Aiii).

Basal IL-8 concentrations significantly increased in samples exposed to 0.35µg/cm^2 active Der p 1 for 24 hours, increasing from an unstimulated average of 1058.3pg/ml to 2496.6pg/ml (Figure 7.7Bi). This significant increase in response was also observed after 48-hour exposure, with samples increasing to an average concentration of 4966.5pg/ml for active Der p 1 relative to unstimulated controls (2449.2pg/ml) (Figure 7.7Bii). Additionally, significant increases in basal cytokine responses to inactive Der p 1 and Can f 1 were observed, with concentrations increasing to 4159.2pg/ml and 4355.8pg/ml respectively (Figure 7.7Bii). Comparison of 24- and 48-hour

responses again saw significant increases in IL-8 concentration for all conditions (Figure 7.7Biii).

IL-6 was not detected basally for any stimulation condition after exposure for both 24 and 48 hours. Additionally, there were no IL-6 responses detected apically after 24-hour exposure. There was, however, IL-6 apically detected after 48 hours for all conditions. These concentrations were low and there was no significant variation observed in the responses (Figure 7.7C).

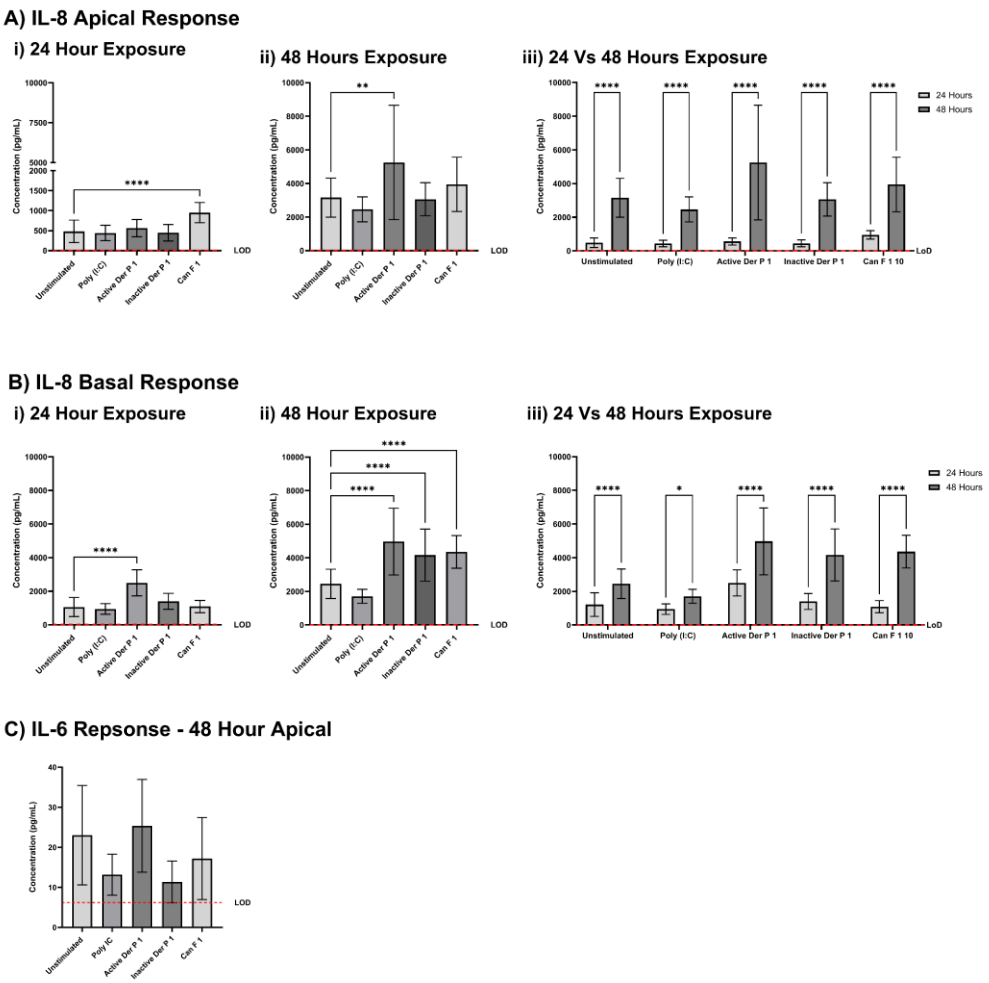

Figure 7.7. Airway Epithelial Cell Responses to 24- and 48-hour exposure to either 1.0µg/cm^2 Poly(I:C) or 0.35µg/cm^2 of Active Der p 1 , Inactive Der p 1 or Can f 1. A) Apical IL-8 responses to nebulised allergens after **Ai)** 24 hour and **Aii)** 48 hour exposure. **Aiii)** comparison of 24- and 48-hour apical responses. **B)** Basal IL-8 responses to nebulised allergens after **Bi)** 24 hour and **Bii)** 48 hour exposure. **Biii)** comparison of 24- and 48-hour apical responses. **C)** 48 hour Apical IL-6 responses. Columns represent means and error bars represent standard deviation. A One-way ANOVA with Dunnetts's comparison test was used to compare stimulated and unstimulated conditions. *p≤0.05, **p≤0.01, ***p≤0.001, ****p≤0.0001. (IL-8, N=24) (IL-6, N=12).

7.3.2.5. EV Response of 3D Airway Epithelial Cultures After Exposure to Nebulised Allergen

Changes in numbers of apical and basal EV were profiled using imaging flow cytometry. No significant changes in apical EV numbers were observed after 24- and 48-hour exposure to stimulants when compared with unstimulated controls (Figure 7.8Ai&Aii). Additionally, there was no significant difference in apical EV numbers when comparing 24- and 48-hour responses (Figure 7.8Aiii). However, significant changes in basal EV secretion were observed in samples exposed to 0.35μg/cm^2 of Can f 1 and inactive Der p 1, increasing from an average of 1.1x10^6 EVs/ml in unstimulated samples to an average of 1.85x10^6 and 1.8 x10^6 EVs/ml, respectively (Figure 7.8Bi). These significant changes were not observed after 48-hour exposure with no stimulation conditions showing a significant response (Figure 7.8Bii). Comparison of 24- and 48-hour responses did see a significant increase in samples stimulated with 1μg/cm^2 of Poly(I:C), increasing from an average of 1.15 x10^6 EVs/ml with 24-hour exposure to an average of 1.9x10^6 EVs/ml after 48-hour (Figure 7.8Biii). Figure 7.8C shows the counts of stained media (3x10^5 EVs/ml) and PBS (7.6 x10^4 EVs/ml) to indicate potential EV contaminant and fluorescent background respectively. Additionally, an apical unstimulated sample depleted with 10% SDS sample (1.2x10^5 EVs/ml) confirmed EV staining.

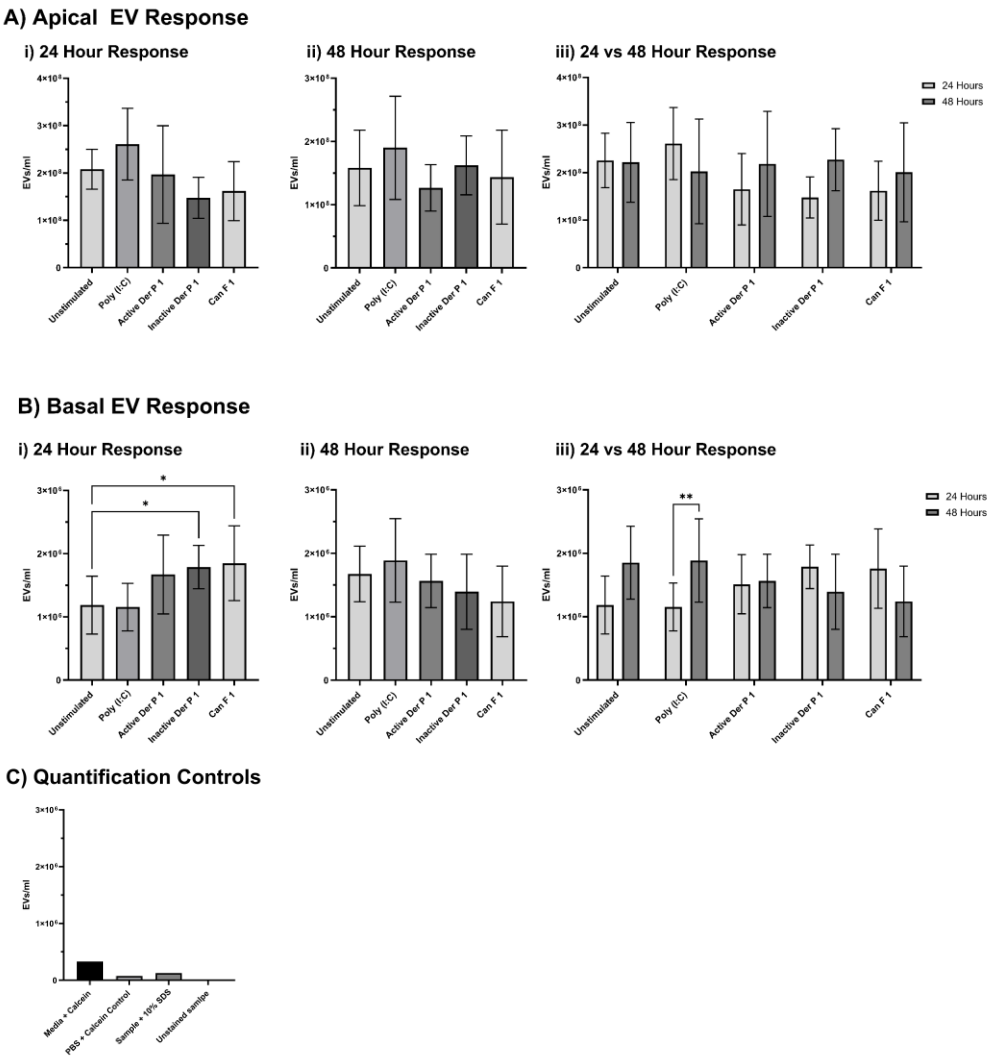

Figure 7.8. Airway Epithelial Cell EV Responses (EVs/ml) to 24- and 48-Hour Exposure to Either 1.0µg/cm^2 Poly(I:C) or 0.35µg/cm^2 of Active Der p 1 , Inactive Der p 1 or Can f 1. A) Apical EV responses to nebulised allergens after **Ai)** 24 hour and **Aii)** 48 hour exposure. **Aiii)** Comparison of 24- and 48-hour apical responses. **B)** Basal EV responses to nebulised allergens after **Bi)** 24 hour and **Bii)** 48 hour exposure. **Biii)** comparison of 24- and 48-hour apical responses. **C)** EV quantification controls (N=1); stained media, stained PBS, 10% SDS depleted apical sample and unstained sample. Columns represent means and error bars represent standard deviation. A One-way ANOVA with Dunnetts's comparison test was used to compare stimulated and unstimulated conditions. Two-way ANOVAs with Sidak's multiple comparison test was used to compare 24- and 48-hour responses*p≤0.05, **p≤0.01, ***p≤0.001, ****p≤0.0001. (Apical, N=6) (Basal, N=12).

In addition to quantifying EV numbers to stimuli, expression of tetraspanins; CD9, CD63 and CD81 and epithelial markers; Tspan8, EpCAM and E-Cadherin were also profiled on basal EVs after 24- and 48-hour exposure. Tetraspanins CD9, CD63 and CD81 were detected on EV populations isolated from all conditions. After 24-hour exposure to stimulants there was no significant change in the percentage of EVs expressing tetraspanins CD9, CD63 and CD81 (Figure 7.9A-C). However, the average percentage of EVs expressing CD81 was observed to be higher than CD9 and CD63, with an average expression of 30% relative to 20% and 22%, respectively. Despite no significant changes in the individual expression of markers, there was a significant change in the distribution of tetraspanin expression. This was characterised by a significant increase in the percentage of CD9 and CD63 double positive EVs in samples stimulated with 0.35μg/cm^2 of active Der p 1, increasing from 11% in unstimulated samples to 20% (Figure 7.9D). This significance was also observed in active Der p 1's triple positive population, with 19% of EVs positive for all three markers, indicating that 95% of the double positive population were triple positive (Figure 7.9G).

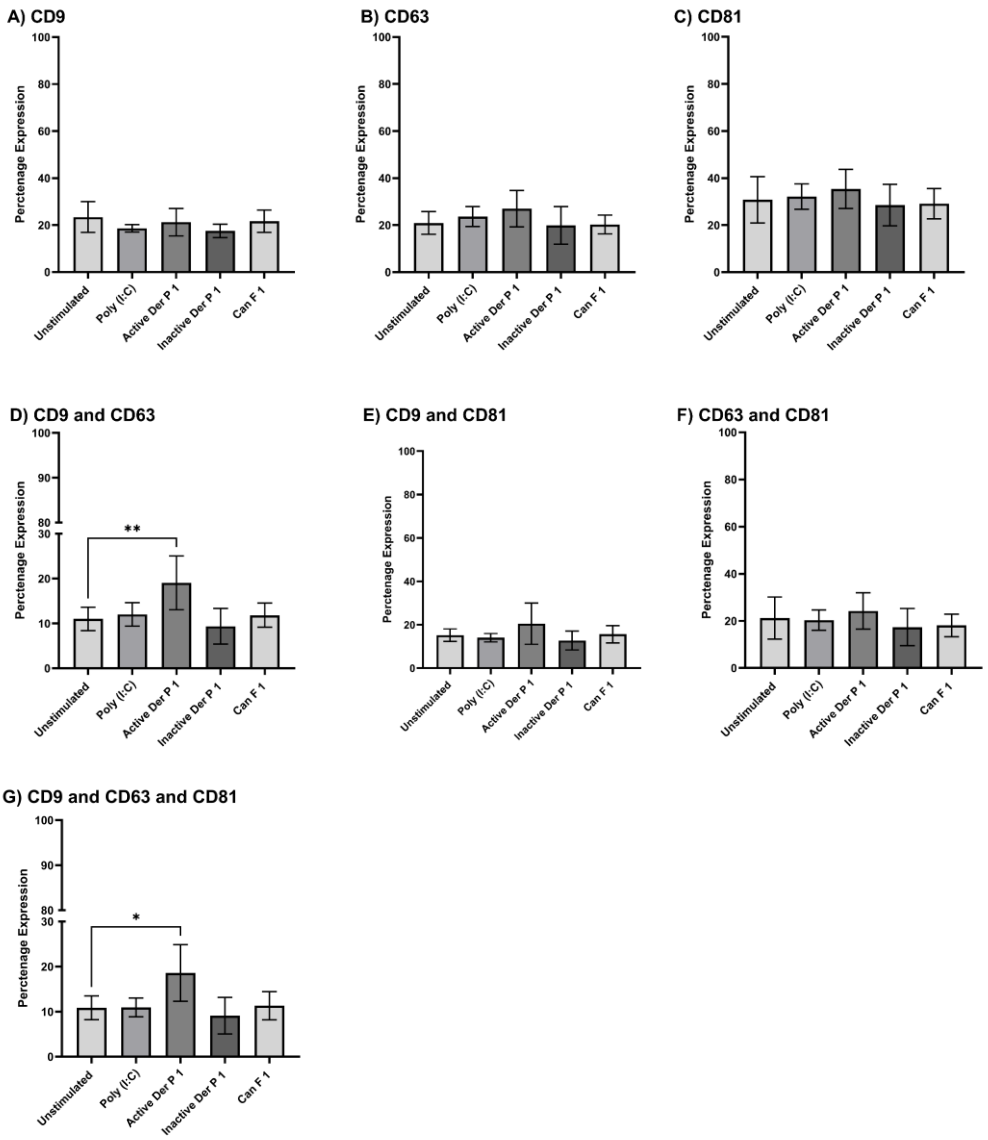

Figure 7.9. Changes in the Percentage Expression of Tetraspanin Markers After 24 Hour Exposure to Allergens. Changes in the percentage of EVs positive for **A)** CD9, **B)** CD63, **C)** CD81, **D)** CD9 and CD63, **E)** CD9 and CD81, **F)** CD63 and CD81 and **G)** CD9, CD63 and CD81. Columns represent means and error bars represent standard deviation. A One-way ANOVA with Dunnetts's comparison test was used to compare stimulated and unstimulated conditions. *p≤0.05, **p≤0.01, (N=6).

Profiling of changes in tetraspanin expression after 48-hour exposure showed no significant changes in the percentage of EVs expressing tetraspanins or in the distribution of tetraspanins within EV populations (Figure 7.10). Average expression of tetraspanins on EV populations saw the same pattern as previously, with the highest percentage of EVs expressing CD81, with an average of 67%, compared to 56% and 58% for CD9 and CD63, respectively (Figure 7.10A-C).

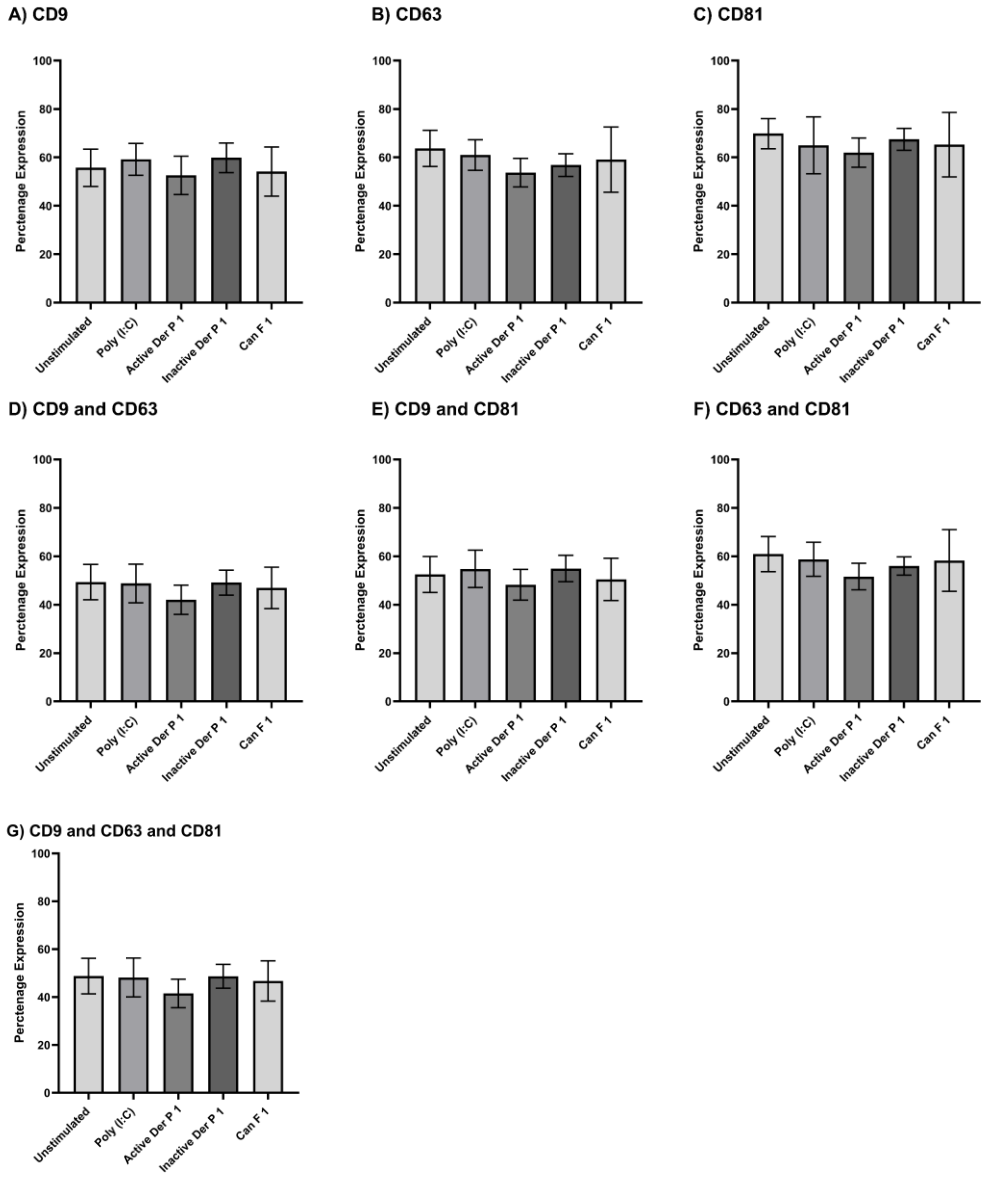

Figure 7.10. Changes in the Percentage Expression of Tetraspanin Markers After 48 Hour Exposure to Allergens. Changes in the percentage of EVs positive for **A)** CD9, **B)** CD63, **C)** CD81, **D)** CD9 and CD63, **E)** CD9 and CD81, **F)** CD63 and CD81 and **G)** CD9, CD63 and CD81. Columns represent means and error bars represent standard deviation. A One-way ANOVA with Dunnetts's comparison test was used to compare stimulated and unstimulated conditions. *p≤0.05, **p≤0.01, (N=6).

Comparison of the expression of tetraspanins after 24- and 48-hour exposure to allergens showed significant increases in the percentage of EVs expressing all tetraspanins and consequently significant increases in all combinations of tetraspanin expression (Figure 7.11).

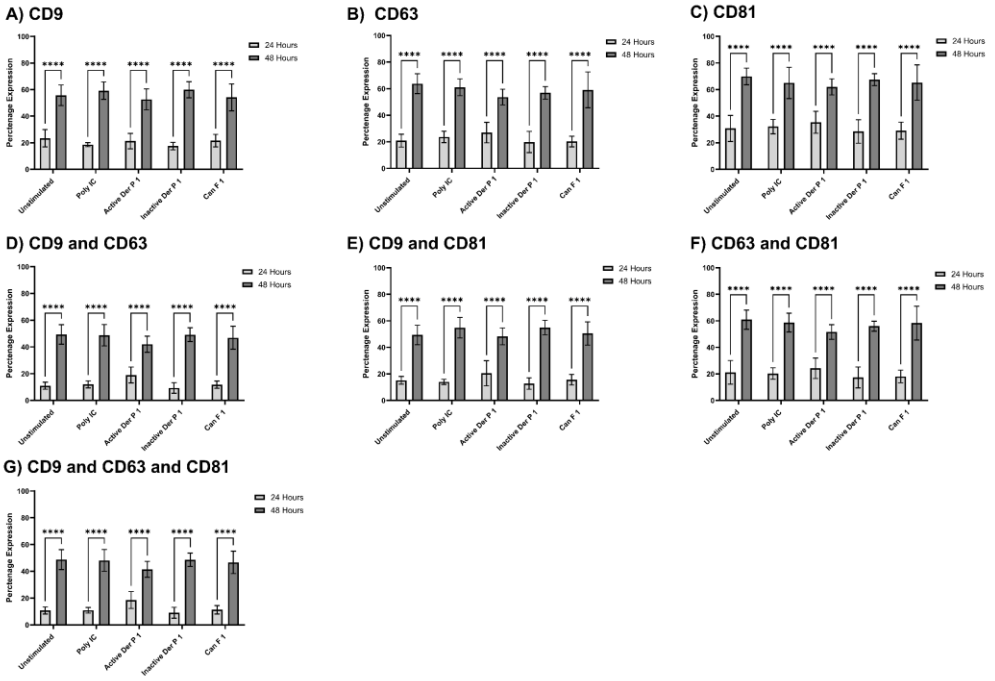

Figure 7.11. Comparison of Tetraspanin Marker Expression After 24- and 48-Hour Exposure to Allergens. Changes in the percentage of EVs positive for **A)** CD9, **B)** CD63, **C)** CD81, **D)** CD9 and CD63, **E)** CD9 and CD81, **F)** CD63 and CD81 and **G)** CD9, CD63 and CD81. Columns represent means and error bars represent standard deviation. Two-way ANOVAs with Sidak's multiple comparison test was used to compare 24- and 48-hour responses*p≤0.05, **p≤0.01, ***p≤0.001, ****p≤0.0001. (N=6).

All isolated EV populations had positive expression of epithelial cell markers, with the highest percentage of EVs expressing EpCAM and E-Cadherin. EVs were also positive for Tspan8, however, its expression within small EV population was lower than that of other markers with an average expression of 19% (Figure 7.12A) across all conditions, compared to 41% expression of EpCAM (Figure 7.12B). Comparison of both Tspan8 and EpCAM expression after 24-hour exposure saw no significant change, however, percentage of EVs expressing E-Cadherin was observed to significantly increase in samples exposed to active and inactive Der p 1 (Figure 7.12C). This percentage of EVs expressing E-Cadherin increased from an average of 40% in unstimulated samples to 51% and 53% in active and inactive samples, respectively. Additionally, while the increase was not significant ($p=0.08$) there was an increase in the percentage of EVs expressing E-Cadherin in the Can f 1 stimulated samples, increasing to 49%.

While there was a significant increase in the percentage of EVs expressing E-Cadherin within Der p 1 stimulated samples, there was no significant change in the distribution of origin cell markers, with no changes being observed in the expression of two or three markers (Figure 7.12D-G).

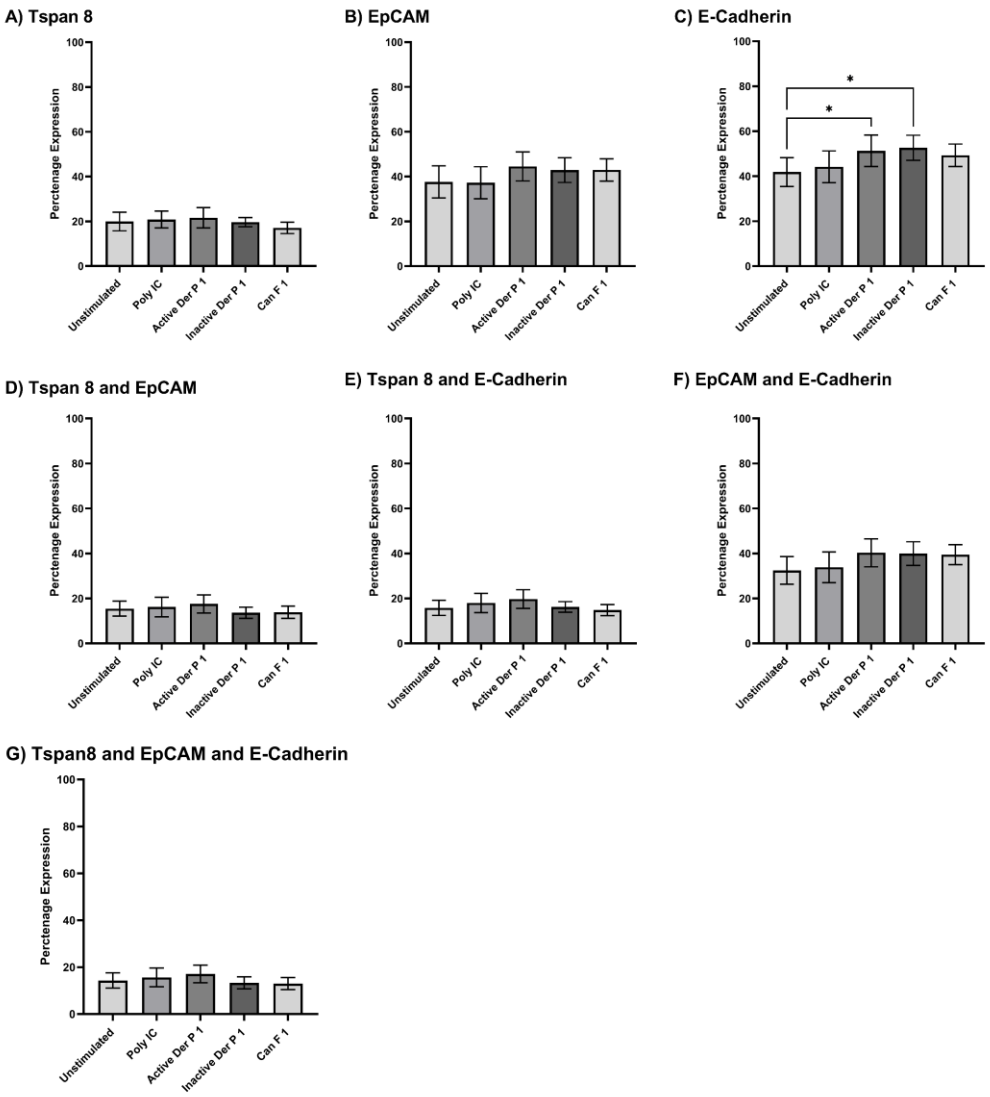

Figure 7.12. Changes in the Percentage Expression of Origin Cell Markers After 24 Hour Exposure to Allergens. Changes in the percentage of EVs positive for **A)** Tspan8, **B)** EpCAM, **C)** E-Cadherin, **D)** Tspan8 and EpCAM, **E)** Tspan8 and E-Cadherin, **F)** EpCAM and E-Cadherin and **G)** Tspan8, EpCAM and E-Cadherin. Columns represent means and error bars represent standard deviation. A One-way ANOVA with Dunnetts's comparison test was used to compare stimulated and unstimulated conditions. *$p \leq 0.05$, (N=6).

Evaluation of origin cell markers expression after 48-hour exposure showed high percentage of EVs expressing all markers. As with tetraspanin expression, the observed pattern was the same as after 24-hour exposure, with Tspan8 still lowest, with an average of 50% expression (Figure 7.13A). The percentage of EVs expressing EpCAM's was 58% and the percentage of EVs expressing E-Cadherin's remained the highest, with an average of 70% expression (Figure 7.13B&C). Comparison of marker expression after 48-hour exposure saw no significant change in the percentage of EVs expressing Tspan8 and E-Cadherin after stimulation, relative to unstimulated controls. However, a significant decrease in percentage of EVs expressing EpCAM was observed in samples exposed to inactive Der p 1 for 48 hours (Figure 7.13B). Furthermore, distribution of origin cell markers saw a significant change in percentage of EVs expressing EpCAM and E-Cadherin, with double positive expression significantly decreasing after 48-hour inactive Der p 1 exposure (Figure 7.13F). This significant decrease was not observed in EpCAM and Tspan8 double positive populations or triple positive populations (Figure 7.13D&G).

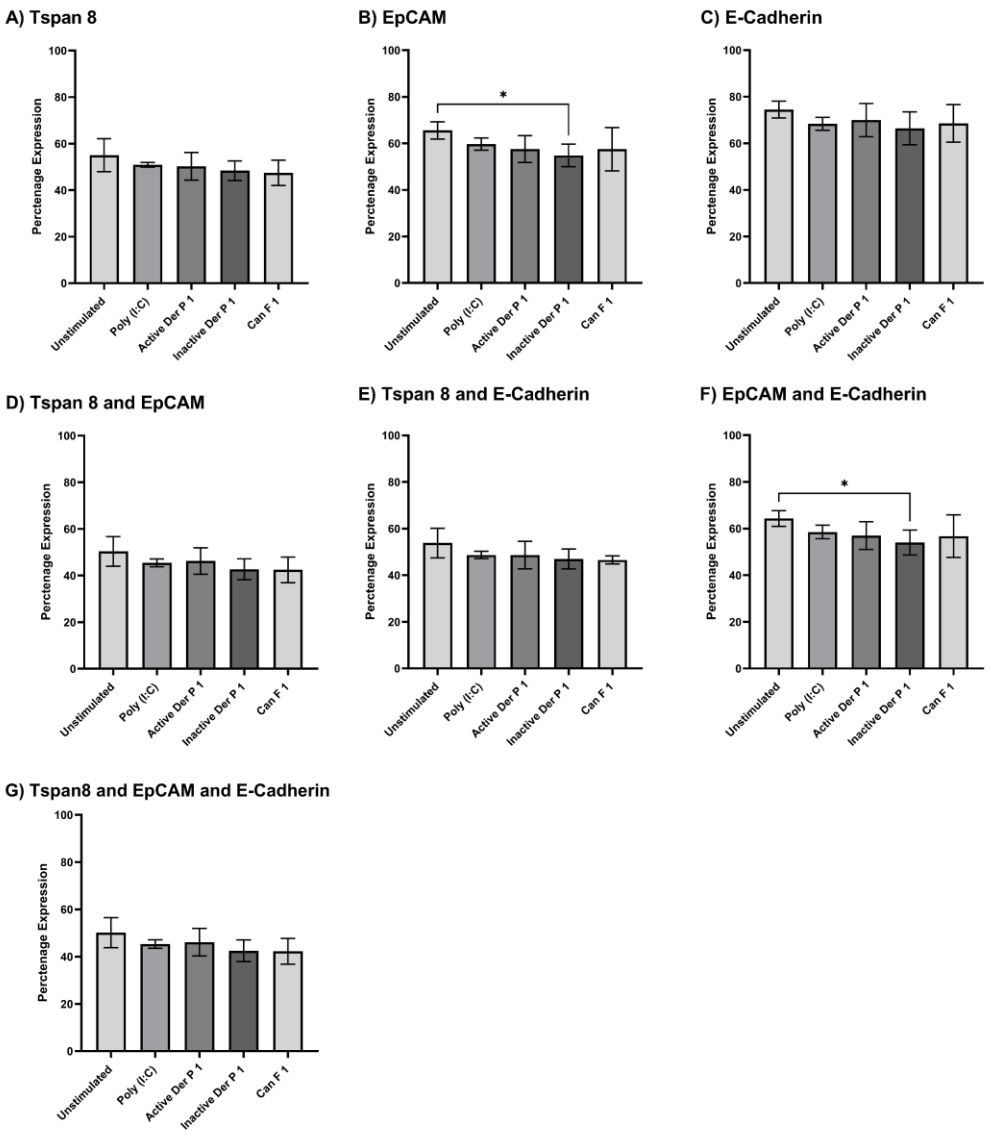

Figure 7.13. Changes in the Percentage Expression of Origin Cell Markers After 48 Hour Exposure to Allergens. Changes in the percentage of EVs positive for **A)** Tspan8, **B)** EpCAM, **C)** E-Cadherin, **D)** Tspan8 and EpCAM, **E)** Tspan8 and E-Cadherin, **F)** EpCAM and E-Cadherin and **G)** Tspan8, EpCAM and E-Cadherin. Columns represent means and error bars represent standard deviation. A One-way ANOVA with Dunnetts's comparison test was used to compare stimulated and unstimulated conditions. *p≤0.05, (N=6).

Comparison of 24- and 48-hour response expression saw significant increases in percentage of EVs expressing all marker combinations with increased exposure duration for all conditions (Figure 7.14). While all conditions saw significant increases in expression of markers, this increase was less pronounced in EpCAM expression after exposure to both active and inactive Der p 1 as well as Can f 1 (Figure 7.14B).

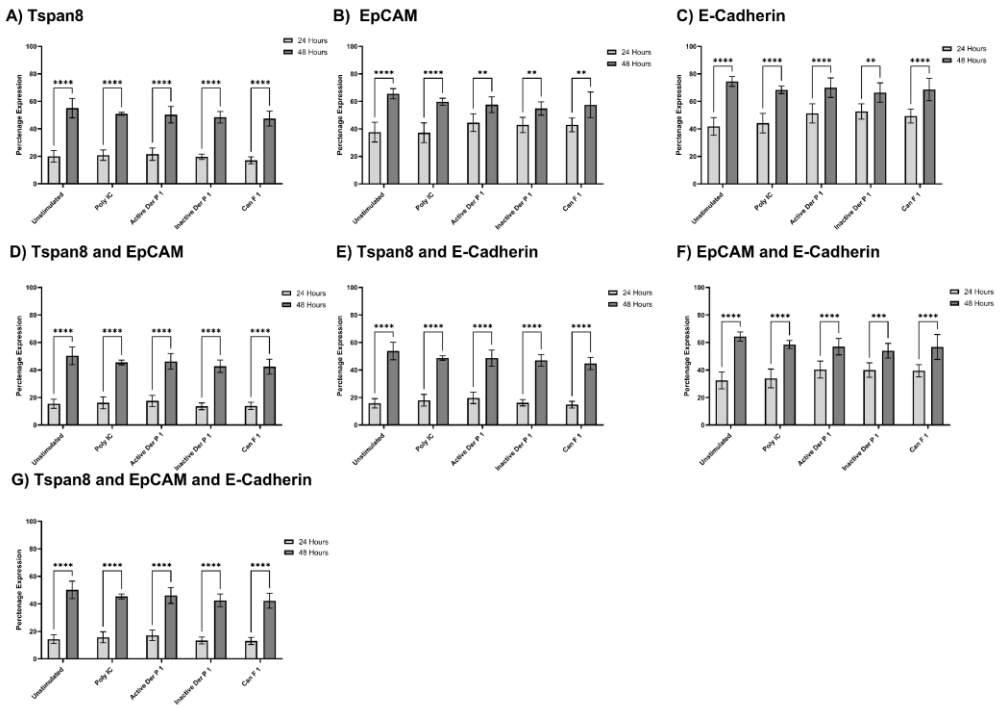

Figure 7.14. Comparison of Origin Cell Marker Expression After 24- and 48-Hour Exposure to Allergens. Changes in the percentage of EVs positive for **A)** Tspan8, **B)** EpCAM, **C)** E-Cadherin, **D)** Tspan8 and EpCAM, **E)** Tspan8 and E-Cadherin, **F)** EpCAM and E-Cadherin and **G)** Tspan8, EpCAM and E-Cadherin. Columns represent means and error bars represent standard deviation. Two-way ANOVAs with Sidak's multiple comparison test was used to compare 24- and 48-hour responses*p≤0.05, **p≤0.01, ***p≤0.001, ****p≤0.0001. (N=6).

7.3.3. Airway Epithelial-Derived EV Transcriptomic Analysis

Changes in EV cargo was also evaluated through transcriptomic analysis. 48-hour exposed basal EVs were isolated and sent for transcriptomic analysis (TAmiRNA, Austria). Analysis was performed using the miND® analysis pipeline. A false discovery rate of 0.2 was used as a cut off, to capture some less significant miRNAs, due to limited sample available for analysis. Data was normalised to replicates per million (RPM) to facilitate comparison. Initially, miRNA's identified in Chapter 3 were reviewed to see if previously identified miRNAs; miR34a-5p, miR92b-3p, miR146a-5p and miR210-3p showed any differential expression in samples. No significant changes in regulation were observed for any of the identified miRNAs (Figure 7.15). However, miR-92b-3p did show upregulation in both Can f 1 and active Der p 1 samples after 48-hour exposure (Figure 7.15B), relative to unstimulated controls. Furthermore, miR210-3p was observed to be upregulated in samples exposed to Poly(I:C) for 48 hours (Figure 7.15D).

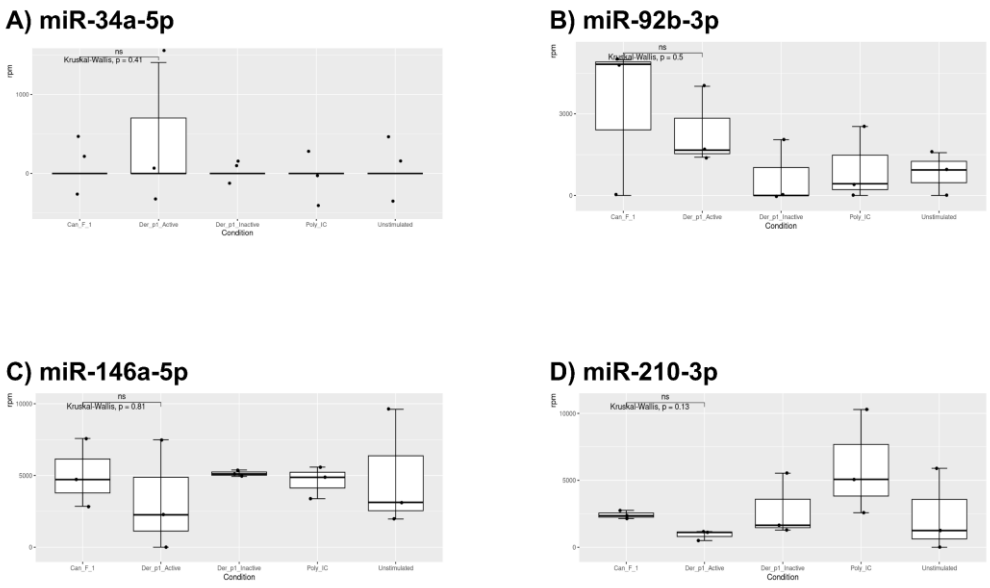

Figure 7.15. Evaluation of the Expression of miRNAs identified Through Systematic Review of the literature (Chapter 3). Replicates per million for identified miRNAs **A)** miR34a-5p, **B)** miR92b-3p, **C)** miR146a-5p and **D)** miR210-3p. Within each box horizontal lines denote media values and boxes extend to 25th and 75th percentiles of each group's distribution, vertical bars denote adjacent values. Global comparison of groups was performed using a Kruskal-Wallis test follows by a Wilcoxon test. *p≤0.05 (N=3)

In addition to evaluating previously identified miRNAs, TAmiRNA's analysis also identified numerous variably expressed mRNAs. Due to time limitations, it was not possible to extensively analyse this data set. However, a preliminary assessment of differentially expressed miRNAs allowed for the identification of some immunologically interesting miRNAs. Figure 7.16 shows the RPM expression of these miRNAs. Expression of miR101-3p and miR224-5p were observed to be elevated in samples exposed to Can f 1, active Der p 1 and Poly(I:C), while remaining low in inactive Der p 1 and unstimulated samples, however, global comparison showed no significance (Figure 7.16A&E). Additionally, miR107 and miR103-3p, were observed to have higher replicates per million in all allergen containing conditions, with RPM remaining low in Poly(I:C) and unstimulated controls (Figure 7.16B&C). Finally, miR148a-5p, saw a slight increase in RPM in active Der p 1 containing samples relative to unstimulated controls, however global comparisons saw no significant changes (Figure 7.16B).

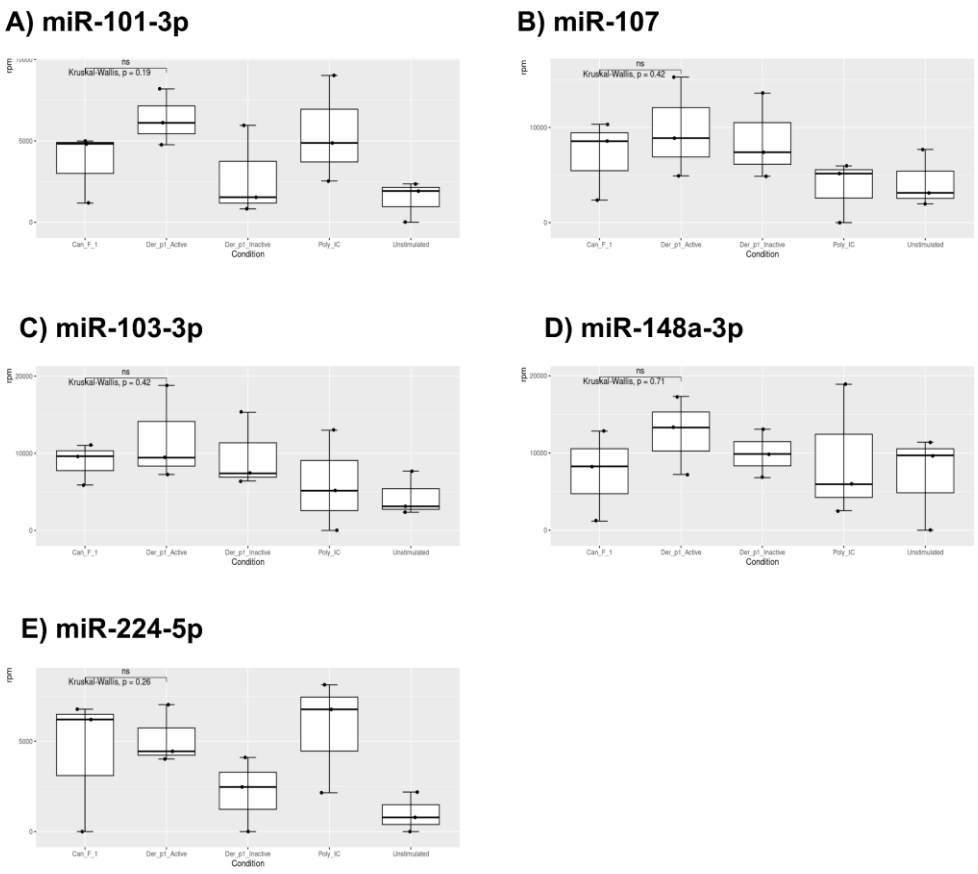

Figure 7.16. Evaluation of the Expression of miRNAs identified Through TAmiRNA's miND® Pipeline. Replicates per million for identified miRNAs **A)** miR101-3p, **B)** miR107, **C)** miR103-3p and **D)** miR148a-3p and **E)** miR224-5p. Within each box horizontal lines denote media values and boxes extend to 25th and 75th percentiles of each group's distribution, vertical bars denote adjacent values. Global comparison of groups was performed using a Kruskal-Wallis test follows by a Wilcoxon

7.4. Discussion

A better understanding of epithelial immune cross talk and the processes through which it communicates could provide greater insight into the mechanisms that underpin allergic sensitisation. Here, we have developed an *in vitro* 3D culture model of the airway epithelium, to investigate the role that epithelial-derived EVs play in allergic sensitisation. 3D cultures were exposed to nebulised indoor allergens, Der p 1 and Can f 1, and their responses were assessed to determine any potential influence on sensitisation. It was hypothesised that exposure of 3D epithelial cultures to nebulised allergens would induce changes in EV responses, either increasing their secretion or changing their cargo to facilitate the promotion of Th2 polarisation. The profiling of EV responses using imaging flow cytometry and transcriptomic analysis, coupled with cytokine responses, would be used to indicate how the allergens could drive allergic sensitisation. The data presented here indicates that exposure of 3D cultures to Der p 1 and Can f 1 induces changes in EV secretion and composition, as well as inducing changes in cargo.

The viability of cultures after 24 and 48 hours was assessed, as substantial reductions in culture viability can result in the release of apoptotic bodies and apoptosmes by cells which can influence the quantification and transcriptomic analysis of EVs (Théry *et al.,* 2018). No changes in viability were observed between conditions at either time point, however, active Der p 1 samples had a 2% decrease in viability at 48 hours compared to 24 hours, from 96%-94%.

Having determined there was no change in viability relative to unstimulated controls, the structure of the epithelial was assessed by SEM and confocal microscopy. Analysis of epithelial tight junctions showed downregulation of ZO-1 in samples exposed to Poly(I:C) for 24 and 48 hours. This was consistent with the literature, which indicates that Poly(I:C) exposure induces barrier dysfunction through inducing ZO-1 dissociation (Comstock *et al.,* 2011). Additionally, active Der p 1 was observed to influence ZO-1 expression, with noticeably reduced expression after both 24- and 48-hour

exposure when compared with inactive Der p 1. Degradation of tight junctions as a result of active Der p 1 exposure is well established in the literature (Ogi *et al.,* 2021, Wan *et al.,* 1999).

SEM analysis showed 24-hour exposure of 3D cultured to nebulised stimulants increased mucus secretion relative to unstimulated controls. This was more pronounced in Poly(I:C) samples, which is consistent with studies that have shown Poly(I:C) can upregulate the expression of MUC5A and MUC5B enhancing mucus secretion (Lever *et al.,* 2015). After 48 hours mucus cover was too high to image cells.

The cytokine responses of cultures was then assessed. Alarmins IL-17E (IL-25) IL-33 and TSLP were assessed as there is evidence in the literature that the proteolytic cleaving of tight junctions by Der p 1 induces their secretion (Meng *et al.,* 2025). Contrary to the literature, exposure of 3D cultures to active Der p 1 did not induce any significant alarmin response, with no measurable cytokine detected. Profiling of proinflammatory cytokines IL-1β and IL-6 showed no significant changes in response to allergen exposure, with no detectable IL-1β and a low apical IL-6 response observed after 48 hours. This again contradicted the literature, which suggested that the Der p 1 potently induces IL-1β and IL-6 in 2D epithelial cultures (Wong, 2006). Der p 1 exposure has also been shown to induce IL-1β in mice (Wang *et al.,* 2024). Can f 1 also did not induce significant changes in the levels of IL-1β, IL-6, IL-17E, IL-33 and TSLP. The context of this is unclear as the literature for Can f 1 induced epithelial cytokine responses is highly limited.

Analysis of IL-8 responses showed 24-hour exposure to Can f 1 induced significant apical IL-8 secretion. This was a directional response, with no significant basal response. After 48-hour exposure this significance was no longer observed, however there was a significant increase in response to active Der p 1. Basally, after 24-hour exposure, active Der p 1 induced a significant IL-8 response which was observed again after 48-hour exposure, along with significant increase in response to inactive Der p 1 and Can f 1. Increases in response to active Der p 1 and Can f 1 confirmed successful stimulation of cultures. The induction of a response by inactive Der p 1 after 48 hours,

suggests that the protein itself is immunogenic, which is supported by the literature (Kauffman *et al.,* 2006).

Quantification of EV responses after 24-hour exposure showed significant basal changes in samples stimulated with inactive Der p 1 and Can f 1, with this significant change being lost after 48-hour exposure. Apically, no significant changes in EV numbers were observed, suggesting a polarised EV response. Subsequent analysis of EV tetraspanin expression revealed no significant changes of each individual tetraspanins (CD9, CD63 and CD81). However, evaluation of multiple marker expression on individual EVs showed significant changes in the distribution of tetraspanins, with samples exposed to active Der p 1 for 24 hours expressing higher levels of CD9 and CD63 in combination as well as significantly higher levels of all 3 tetraspanins in combination. After 48-hour exposure, no significant changes in tetraspanin expression or distribution were observed, however, the percentage of tetraspanin expressing EVs were higher at 48 hours.

Profiling of origin cell markers on EVs to confirm epithelial origin showed no significant changes in EpCAM and Tspan8 after 24 hour exposure. However, percentage of E-Cadherin expressing EVs was seen to significantly increase from samples exposed to active and inactive Der p 1 for 24 hours. Despite this significant increase in E-Cadherin there was no significant change in the distribution of markers, with no variation in the expression of double and triple positive EVs between conditions. After 48 hours a significant decrease in the percentage of EpCAM expressing EVs was observed in samples exposed to inactive Der p 1. This significant decrease was also observed in EVs positive for both EpCAM and E-Cadherin.

Transcriptomic analysis of EVs showed upregulation of one miRNA identified in the systematic review, miR92b-3p (Browne *et al.,* 2025). This miRNA was also identified in airway epithelial derived EVs where it was suggested that it may play an important role in the early development of a Th2 responses (Bartel *et al.,* 2020). Additionally, the literature suggests it may participate in eosinophilic inflammation and airway remodelling associated with asthma (Zhang *et al.,* 2021a). Preliminary analysis identified a further

five miRNA which were upregulated following allergen exposure compared to unstimulated EVs which could play a role in allergic sensitisation (miR101-3p, miR103-3p, miR107, miR148a-3p and miR224a-5p). Each of these miRNAs is implicated in the induction and polarisation of Th2 responses. miR101-3p has been identified as a differential miRNA in individuals with allergic asthma relative to healthy controls and has been linked to TLR2 expression (Huang *et al.,* 2020). miR103-3p has been shown to have higher expression in the EVs of patients with atopic dermatitis compared to healthy controls, with EVs from mast cells containing miR103-3p enhancing IL-5 secretion in ILC2 cells (Toyoshima *et al.,* 2021). miR107 has been found to be associated with IgE levels and eosinophil counts in HDM sensitised individuals (Kim *et al.,* 2025a). miR148a-3p has been shown to play a role in M1/M2 macrophage polarisation, promoting M1 macrophages and potentially inducing tolerance (Huang *et al.,* 2017). miR224-5p has been shown to play a role in the Th1/Th2 polarisation, with its overexpression being linked to reduced development of AR and its symptoms (Li *et al.,* 2024a).

Overall, the data presented here shows the successful stimulation of a 3D airway epithelial model with nebulised active and inactive Der p 1 and Can f 1. We showed that active Der p 1 exposure induced a basal IL-8 response after both 24 and 48 hours, as well as inducing significant changes in EV marker expression and also changes in EV cargo. The lack of significance observed in cargo changes is likely due to the low sample volume sent for analysis, resulting in low detected miRNA RPM, as well as the statistical corrections for the global comparison of conditions. Future research could focus on a more comprehensive evaluation of the miRNA data acquired, including pathway analysis to further understand the downstream role these miRNAs may have in allergic sensitisation.

Chapter 8: General Discussion

The aim of this PhD was to assess the potential role of airway epithelial-derived EVs in allergic sensitisation, through the development and use of a 3D bronchial epithelial model and the subsequent flow cytometric and transcriptomic analysis of EVs. This 3D model, and a method for the quantification and characterisation of EVs using imaging flow cytometry, were initially optimised before stimulation with the indoor allergens Der p 1 and Can f 1.

To first develop a model of the airway epithelium, preliminary work was conducted in a 2D culture model, to facilitate the use of the cell line, Calu-3. However, due to the lack of cellular diversity and relevant tissue structures, it was felt that a 2D model lacked biological relevance. 3D airway epithelial models are rapidly becoming the gold standard for the profiling of lung responses (Wallace *et al.,* 2025, Lee *et al.,* 2023, Fang and Eglen, 2017). This is due to their diverse cellular composition and the formation of key microstructures, such as tight junctions, giving them a better homology with the tissues they aim to model (Wallace *et al.,* 2025, Lee *et al.,* 2023). Furthermore, a recent systematic review identified a significant gap in the literature, with only one study looking into the role of epithelial-derived EVs in allergic sensitisation using a 3D culture model (Browne *et al.,* 2025, Bartel *et al.,* 2020). The use of Calu-3 in ALI models is further supported in the literature, with them being shown to differentiate into mucus secreting cells and form tight junctions as part of forming apical junction complexes (Wallace *et al.,* 2025).

Having identified and optimised a 3D culture model, it was crucial to evaluate a mechanism for its stimulation. Commonly, Calu-3 stimulation in 3D has been conducted via submersion (De Ávila *et al.,* 2025, Ogi *et al.,* 2021). However, our results showed that stimulation in this way made it difficult to distinguish between the cellular response induced by stimuli and the background submersion induced response. Additionally, the submersion of ALI cultures undermines the relevance of the model as it does not reflect natural inhaled exposure. While stimulation of ALI via the addition of

stimulant to the basal chamber overcame the submerged background issue consistent with the literature (Chen *et al.,* 2019), it did not reflect natural exposure. The concurrence of these issues has led to the recent development and adoption of nebulised exposures (De Ávila *et al.,* 2025, Sengupta *et al.,* 2023). This, facilitates the exposure of 3D cultures to aerosolised stimulants, more closely modelling natural exposure and allowing for more robust interrogation of 3D airway epithelial models. When considering aerosolised exposure, it is important to consider the droplet size induced by nebulisers. Smaller droplet sizes can sheer and damage peptides, disrupting their functionality (Matthews *et al.,* 2020, Bodier-Montagutelli *et al.,* 2020). Therefore, before exposure of ALI cultures to nebulised stimulants, it was important to first establish that nebulisation did not impact protein function. Additionally, due to logistical complications, it was not possible to use the nebuliser in its optimal configuration, having to place culture plates within the chamber. Consequently, it was important to assess the potential impairment to its ability to deliver nebulised proteins. Deposition was observed to be 45% lower relative to optimal configuration. This was potentially due to the introduction of plastic into the chamber, which would be consistent with current *in vivo* literature which suggests that electrostatic charges in plastic spaces reduce lung dose delivery in children by more than two-fold (Anhøj *et al.,* 1999).

Following the development of a 3D model and the optimised exposure system, this project aimed to further develop a selective method for the quantification of EVs. The current gold standard techniques for EV quantification, such as TEM and NTA, require initial isolation of EVs and are low throughput techniques which lack specificity, resulting in conflated and potentially exaggerated EV counts. Consequently, this project aimed to develop a selective high throughput method, without the need for isolation, to quantify and characterise EVs. While the use of flow cytometry to profile EVs is well established in the literature (Morales-Kastresana and Jones, 2017, Welsh *et al.,* 2023), the logistics underpinning its suitability have only recently started to be explored (Welsh *et al.,* 2020, Van Der Pol *et al.,* 2018). The data we present here attempts to highlight the initial considerations for adapting

flow cytometry for small EV characterisation and quantification. Here we show that the initial profiling of the CytoFLEX and ImageStreamX MKII's (ISX) ability to detect small particles using different sizes of standardised NIST beads, differed between machines, with conventional cytometry being the least sensitive. The observed unsuitability of conventional cytometry for the profiling of small EVs is in concordance with previous literature (Lucchetti *et al.,* 2020). These differences in the ability of cytometers and cytometry techniques to detect small particles highlights the importance of this profiling prior to analysis, ultimately facilitating the selection of a cytometer capable of detecting the EV populations of interest. Furthermore, the subsequent translation of this information into a biological context further emphasises the importance of this consideration. Adjustment for the variance in refractive index of biologic (EVs) and non-biologic (Polystyrene NIST beads) using Mie theory further contextualises the suitability of machines for small particle analysis. Currently there is a tendency in the literature to use polystyrene beads to position gates for analysis without this context, often implicating that 80nm beads are equivalent to 80nm EVs (Brennan *et al.,* 2022), which has been shown both in the literature (Welsh *et al.,* 2020, Van Der Pol *et al.,* 2018), and in the data presented here, not to be the case. Additionally, it is important to consider the method through which individual cytometers acquire data. Cytometers have a trigger threshold which can be set for side scatter (object size), or fluorescence, which allows it to filter out low end electronic noise. While the CytoFLEX has a higher trigger threshold than the ISX making it unsuitable for small particle detection, this reduced electronic noise can also be a strength, as observed in experiments aimed at identifying a calcein-AM staining concentration. The removal of increasing fluorescent background noise associated with higher concentrations of stain allowed for plateauing of staining, which was not possible with the ISX, potentially due to its lower trigger threshold. The use of calcein-AM for the staining of EVs has been previously reported in the literature (Tertel *et al.,* 2022, Gray *et al.,* 2015, de Rond *et al.,* 2018, Calderón-Peláez *et al.,* 2025). However, here we present an optimised method for the detection and quantification of intact calcein positive single EVs using imaging flow cytometry.

Having optimised a method for the quantification of single intact EV events, the characterisation of these events needed to be optimised. The characterisation and profiling of tetraspanin expression on the surface of EVs is a standardised practice within the field of EV research and is a requirement of MISEV (Mizenko *et al.,* 2021, Welsh *et al.,* 2024). While tetraspanin expression on EVs is not fully understood, they represent an important biomarker with highly varied expression that can be an indicator of both an EV's cellular origin, as well as its potential function (Kugeratski *et al.,* 2021, Nazarenko *et al.,* 2010, Okada-Tsuchioka *et al.,* 2022, Welsh *et al.,* 2024). While there are a variety of ways to profile the expression of these markers, such as RTq- PCR and western blot analysis, flow cytometry provides an exciting and potentially more refined approach to characterising tetraspanins on EVs. The use of imaging flow cytometry does not just provide an indication of a marker's presence, but also the individual and combined expressions of theses markers on single EVs, as well as across a whole population. While the potential for flow cytometry as a tool for EV characterisation presents an interesting and powerful prospect, the transition from its initial optimised purpose of characterising cellular populations to EV populations requires a variety of considerations to be effectively implemented at the small particle scale, particularly for tetraspanin characterisation.

A key consideration regarding the characterisation of EVs with flow cytometry is the sensitivity of the cytometer to specific fluorophores. At the cellular level, the literature suggests that tetraspanins are expressed at about 30,000-100,000 copies per cell (Hemler, 2003), ultimately providing adequate binding sites for enough antibodies to create a detectable signal for the cytometer. While the heterogeneous and varied nature of tetraspanin expression on EVs is established in the literature (Kugeratski *et al.,* 2021, Okada-Tsuchioka *et al.,* 2022, Mizenko *et al.,* 2021), how this relates to copy numbers on an EV is unknown. Due to the varied biogenesis, such as budding from the cell, and their significant difference in size, it is reasonable to assume a reduced copy number relative to its cell of origin. Consequently, to avoid potential false negative profiling as a result of lower copy numbers, the LoD of the assay was measured to give context to analysis. To assess this in a way

that is translatable to EVs, the LoD of different fluorophores were measured on ISX in terms of antibody binding capacity (ABC). Understanding LoDs in the context of a minimum number of bound antibodies required to trigger a detectable event, or ABC provides a platform for a more practical assessment of a fluorophore's suitability for small particle tetraspanin analysis and characterisation as it can be related to potential copy numbers on EVs.

Here we highlight not just the importance of traditional fluorophore selection based on colour separation, but also on the cytometer being used, as well as the intended application. For example, on the ISX the LoDs ranged from 24 – 1183 depending on the fluorophore. While a LoD of 1183 would be more than adequate for the profiling of cells with 30,000 or more copies, how this relates to EVs is less clear and should be taken into consideration. Consequently, identifying and using fluorophores with low LoDs, such as APC and PE-Cy5, would be preferable for the confirmation of individual marker expression and reporting of the LoD can lend further weight to the relevance of data presented. However, the variation observed between LoDs of different fluorophores could present an issue when characterising the expressions of multiple tetraspanins simultaneously within a population, with potential observed changes in the expression of markers relative to others being the result in differences in fluorophore sensitivity rather than a significant change in expression. Consequently, selections of fluorophores with not just low, but also similar LoDs, is preferable. Considering these logistics, the presented data identified the use of APC, PE-Vio615 and PE as the optimal panel for this analysis.

It is important to highlight that LoDs for fluorophores will vary between different machines of the same make and optimal fluorophores on one machine might not be the same as on others. In addition, the LoDs presented here are calculated from the autofluorescence measured from the blank bead population provided. The increased size of the beads relative to EVs could mean that LoD values quoted here are potentially an overestimate and could be lower than quoted. Consequently, LoDs could be measured using

the autofluorescence of the unstained samples to provide lower and more accurate LoDs for EV analysis.

Having optimised a 3D epithelial culture model, a suitable mechanism for its stimulation and the characterisation and quantification of EVs using imaging flow cytometry, it was possible to assess the effect of two allergens, Der p 1 and Can f 1, on epithelial-derived EV responses. We believe this is the first study which examines the effect of both nebulised Der p 1 (both active and inactive) and Can f 1 on 3D airway epithelial culture in any capacity. The data presented here shows the effect of allergen 24- and 48-hour exposure on microstructures, such as tight junctions and cilia, as well as their effect on cytokine and EV responses. Here we assessed the expression of tight junction proteins occludin and ZO-1, where ZO-1 was observed to decrease with prolonged expose to active Der p 1. This is supported by the literature, with the ability of Der p 1 to promote epithelial barrier dysfunction through the proteolytic cleaving of tight junction proteins such as claudin, occludin and ZO-1 being extensively reported (Jurkiewicz *et al.,* 2025, Nur Husna *et al.,* 2021b, Zhang *et al.,* 2017). Additionally, because Poly(I:C) and Der p 1 are known to promote the secretion of mucus (Piñeiro-Hermida *et al.,* 2017, Lever *et al.,* 2015), SEM was used to profile changes to the epithelial barrier microstructure, as well as assess mucus coverage. The novel data presented here showed that 24-hour exposure of cells to nebulised active Der p 1 did promote mucus secretion relative to proteolytically inactive Der p 1, which has not been previously reported. After 48 hours, mucus density was too high in all samples to properly ascertain the effect of stimuli. Additionally, nebulised Can f 1 was observed to increase mucus production in 3D cultures which has also not been reported previously in the literature.

The link between epithelial barrier disruption and alarmin cytokine response is well established (Wenger *et al.,* 2023). Exposure of our model to nebulised allergens was observed to induce no measurable level of alarmin cytokine response. While this appears to significantly contradict the literature regarding epithelial cell responses, the reporting on alarmin production by Calu-3 cells is poor, particularly in ALI culture. A study by Melnikova *et al.,*

did show that Bet v 1 and Aln g 1 allergen exposure of Calu-3 cells cultured at ALI did induce a significant increase in IL-33 and TSLP response, however, this looked at gene expression, rather than cytokine secretion (Melnikova *et al.,* 2025). Additionally, secretion of IL-25 in ALI Calu-3 has not been previously reported. The secretion of inflammatory cytokines, such as IL-1β, IL-6 and IL-8 in response to allergen stimulation is also well established in the literature (Naso *et al.,* 2025, Chung, 2001, Bachert *et al.,* 1995). While Melnikova *et al.* also reported a significant increase in IL-1β gene expression with allergen exposure, a study by He *et al.,* showed that nebulised exposure of Calu-3 to LPS induced no detectable level of IL-1β in concordance with our findings (He *et al.,* 2021). The lack of observed IL-6 secretion contradicts literature regarding epithelial responses (Naso *et al.,* 2025, Ogi *et al.,* 2021), however, information regarding nebulised responses of Calu-3 is limited, with one study showing that nebulised LPS exposure of Calu-3 induced apical IL-6 secretion (Braakhuis *et al.,* 2023). Notably, the lack of IL-6 secretion observed after 24-hour exposure of ALI inserts to Der p 1 conflicts with the literature, with a study by Ogi *et al.,* showing significant basal secretion of IL-6 after Der p 1 exposure of ALI cultured primary nasal epithelial cells (Ogi *et al.,* 2021) . This difference in observation could be the result of the method of stimulation, with Ogi *et al.,* performing submerged stimulations which were noted to induce IL-6 secretion in the presented submerged stimulations.

Here we show that exposure of 3D cultured Calu-3 epithelial cultures to nebulised allergens can induce significant changes in IL-8 secretion. Exposure of cultures to Can f 1 for 24 hours induced a significant polarised apical cytokine response, which transitioned into a polarised basal response after prolonged exposed, consistent with preliminary stimulation in Chapter 5. There is currently no literature regarding the nebulised exposure of Can f 1 in culture. Additionally, we showed that 24-hour exposure to active Der p 1 induced a significant polarised basal response, which became systematic after 48-hour exposure, being secreted both apically and basally. Der p 1 induced IL-8 secretion has been observed in 2D culture models (Shi *et al.,* 2010, Adam *et al.,* 2006), however, 3D culture literature is sparce. Polarised epithelial cytokine responses in 3D epithelial cultures, particularly IL-8, are being

increasingly reported in the literature (Barnett *et al.,* 2023, Chen *et al.,* 2019, Rossi *et al.,* 2013, Chow *et al.,* 2010). Additionally, these observations are consistent with *in vivo* observations with luminal IL-8 being associated with allergic phenotypes such as AR (Cergan *et al.,* 2025, Gosset *et al.,* 1997). Secretion of IL-8 is highly associated with the promotion of allergic phenotypes through the recruitment of immune cells, such as neutrophils, mast cells and basophils promoting the generation of inflammation at the site of allergen challenge (Ghrairi and Elhechmi, 2025, Cergan *et al.,* 2025). The directionality of observed cytokine responses could serve to recruit immune cells to facilitate allergen clearance at sites of epithelial barrier dysfunction and penetration. Additionally, it has been suggested that the luminal secretion of IL-8 could be an autocrine signal. Rossi *et al.* have shown the apical IL-8 secretion promoted intestinal epithelial differentiation, potentially acting as a mechanism to restore the epithelial barrier function after it is compromised (Rossi *et al.,* 2013). This would support observations here which saw a significant apical IL-8 response to Der p 1 alongside a pronounced decrease in tight junction presence. Additionally, this apical restorative function could further explain the lack of apical responses observed in inactive Der p 1, with basal IL-8 secretion being induced through interaction with cells, as opposed to damage induced secretion.

The effect of Der p 1 and Can f 1 on epithelial EVs is poorly explored in the literature, with a recent systematic review identifying just one paper looking at Der p 1 (Qiu *et al.,* 2011) and two papers looking at the broader HDM extract (Gon *et al.,* 2017, Zhang *et al.,* 2021b). Furthermore, no literature was identified looking at the effect of the aeroallergen Can f 1 on EV response. Here we show, 24-hour exposure of nebulised Can f 1 induced a significant EV response, promoting the secretion of EVs basally. Furthermore, we show that exposure of inserts to active and inactive Der p 1 increased EV secretion, with this increase being significant in proteolytically inactive samples. This suggests that the Der p 1 protein itself plays an important role in the induction of EV responses. While this observation in EV response is unique, it is corroborated by other reports in the literature and cytokine data presented here which suggests that the peptide itself is immunogenic

(Kauffman *et al.,* 2006). While inactive Der p 1 and Can f 1 exposure induced significant increases in EV secretion after 24-hour exposure, they did not significantly alter tetraspanin expression or distribution. Here we show that active Der p 1 stimulation of epithelial cells can induce a significant change in the distribution of tetraspanins on EVs, significantly upregulating the percentage of CD9 and CD63 EVs as well as the number of CD9, CD63 and CD81 positive EVs. Tetraspanins play a diverse role in the context of EVs being associated with the early biogenesis of exosomes, facilitating the recruitment of ubiquitinated cargo to MVBs as part of the ESCRT pathway. Consequently, observed changes in tetraspanin distribution on EVs could be a potential indicator of cargo change as a result of stimulation. Tetraspanins, such as CD9, have been shown to regulate the internalisation of MHC class II in DCs as well as enhance epidermal growth factor internalisation (Toribio and Yáñez-Mó, 2022, Rocha-Perugini *et al.,* 2017, Murayama *et al.,* 2008). Additionally, this change in distribution could also indicate a change in signal target. Tetraspanins CD9 and CD81 have been shown to be involved in the targeting and uptake of exosomes by DCs (Jankovičová *et al.,* 2020, Fanaei *et al.,* 2011). In the context of allergy this is further supported by a study conducted by Zhang *et al* which showed that HDM-induced airway epithelial EVs were able to facilitate the recruitment, migration and activation of monocyte derived DCs (Zhang *et al.,* 2021b). In addition to changes in tetraspanin distribution, we also showed that 24 hour nebulised active and inactive Der p 1 exposure induced significance in the percentage of EVs positive for E-Cadherin. A study by Takahashi *et.al*. saw similar results to the data presented, seeing a significant increase in E-Cadherin expressing EVs from nasal epithelial cells as a result of epithelial injury, as well as no significant change in EpCAM expression (Takahashi *et al.,* 2020). In their study they speculated that this change in E-Cadherin expression may reflect the loss of adherent junctions which is consistent with tight junction staining data for active Der p 1 (Takahashi and Schleimer, 2021). Additionally, E-Cadherin has been shown to improve the structural stability of EVs, enhancing their ability to signal over longer distances (Bänfer *et al.,* 2022).

Transcriptomic analysis of EV cargo showed upregulation of the previously identified miR92b-3p in samples treated with active Der p 1 and Can f 1. A study conducted by Bartel *et al.,* initially saw upregulation of this miRNA in a 3D "asthma like" model, with their pathway analysis suggesting that this miRNA could facilitate the polarisation of Th2 cells by DCs (Bartel *et al.,* 2020). Consequently, upregulation of miR92b-3p in allergen exposed samples relative to unstimulated controls potentially demonstrates a mechanism through which allergen-epithelial cell interactions could induce EVs which can promote Th2 skewing and the promotion of sensitisation. In addition, assessing the expression of previously identified miRNAs, the data presented here identifies some additional miRNAs which could further influence Th2 polarisation; miR101-3p, mir103-3p, miR107, miR148a and miR224a-5p.

A recent study by Kim *et al.,* profiled 304 miRNAs in children with asthma, separated by their sensitisation to HDM status. In this study they identified a strong association between the expression of miR107 and HDM sensitisation, with there being a link between miR107 expression and more severe asthma phenotypes, including higher peripheral blood eosinophils and total IgE levels (Kim *et al.,* 2025a). miR107 expression has been previously associated with TLR4 activation in other metabolic diseases (Foley and O'Neill, 2012), which could explain its up regulation in active and inactive Der p 1 samples. The association of this miR107 with HDM sensitised individuals, and its upregulation in EVs after allergen exposure, could provide an avenue for further understanding the role epithelial EVs can play in the promotion of allergic sensitisation.

Upregulated expansion of miR103a-3p was observed in all allergen containing exposures. The miRNA miR103a-3p has been previously shown to be expressed in primed mast cells, where it was able to enhance IL-5 secretion of ILC2s in the presence of IL-33 (Toyoshima *et al.,* 2021). ILC2s play a central role in allergic sensitisation and the generation of Th2 responses, activating and facilitating the induction of pro Th2 DCs (Zheng *et al.,* 2021, Bartemes and Kita, 2021). The presence of upregulated miR103-3p in epithelial-derived EVs could perform a similar role to that observed in mast

cell EVs, further activating and promoting ILC2 cytokine response, alongside the secretion of IL-33, ultimately promoting allergic sensitisation.

Here we show an upregulation of miR148a-3p after exposure to active Der p 1. Currently miR148a-3p had been shown to play an important role in Notch signalling which promotes the activation and polarisation of M1 macrophages. M1 macrophages produce pro-inflammatory cytokines such as TNF-α, IL-6 and IL-1β and have been shown to be capable of inducing sustained hyper reactive inflammation in response to HDM (Cergan *et al.,* 2025, Dunbar *et al.,* 2024). The ability of epithelial derived EVs to promote M1 macrophage phenotypes is well established in the literature (Yu *et al.,* 2021, Kulshreshtha *et al.,* 2013, Shin *et al.,* 2010), and was recently identified in a recent systematic review as a key mechanism through which epithelial EVs can promote allergic sensitisation (Browne *et al.,* 2025). Conversely, active Der p 1 and Can f 1 exposed samples also showed upregulated miR101-3p. This has been previously reported to down regulate the expression of inflammatory cytokines in proinflammatory macrophages, through the inhibition of TLR2 pathways (Huang *et al.,* 2020). This suggests that epithelial-derived EVs could also promote allergic tolerance through macrophages, as well as promote sensitisation. The ability of airway epithelial derived EVs to promote tolerance as a result of allergen exposure has been previously reported in the literature (Prado *et al.,* 2010, Prado *et al.,* 2008).

In addition to the promotion of tolerance through the suppression of M1 macrophages, epithelial-derived EVs could also promote tolerance through the upregulation of miR224-5p. Upregulation of miR224-5p was observed in samples exposed to Can f 1 and active Der p 1, as well in Poly(I:C) stimulated cells. A study Li *et al.,* showed that miR224-5p plays an important role in the modulation of Th1/Th2 responses, where miR224-5p promoted Th1 differentiation and consequently suppressed Th2 induction through GATA3 (Li *et al.,* 2024a). Over expression of miR224-5p was also shown to reduce AR development, as well as attenuate symptoms, suggesting its presence in allergen stimulated epithelial-derived EVs could act to prevent sensitisation and promote tolerance.

While the data presented here indicates the potential roles of airway epithelial-derived EVs in allergic sensitisation, there are limitations with this study. A major limitation of this study was that only a preliminary examination of the transcriptomic data was feasible. Data only became available in the second week of September 2025, around two weeks prior to thesis submission. A more robust and extensive analysis of this data, as well as pathway analysis of identified miRNAs, could provide additional insight and more robust understanding of the role EVs play in allergic sensitisation. Furthermore, due to limited sample availability, replicates had to be combined to create samples concentrated enough for miRNA analysis. The reduction in sample size from n=6 to n=3, and the limited amount of sample in combined replicates, reduced the power of miRNA analysis. Consequently, future work could focus specifically on this output, generating samples solely for transcriptomic analysis, lending the analysis greater statistical strength.

Additionally, while the cell line Calu-3 identified for this model was suitable for the development of a 3D model, their varied cytokine responses, particularly the reports of upregulated alarmin cytokine gene expression with no downstream protein observed in this study, and the literature suggests that their cytokine machinery does not function properly (Melnikova *et al.,* 2025, He *et al.,* 2021). Additionally, Calu-3 are known to be a high mucus secretion cell line when cultured at ALI (Sonntag *et al.,* 2022). This provides many technical challenges regarding the dosing of inserts, and can impact analysis as was seen in this study with SEM analysis after 48 hours. Transformed cell lines are a useful and accessible tool for the studying of disease pathogenesis, however, as culture methods are further developed to better represent the tissues they aim to model, the use of primary cells could further enhance the biological relevance of models. Consequently, future work could focus on the implementation of this and the profiling of cytokine and EV responses after allergen exposure.

The robustness of the flow cytometric analysis could have been further enhanced through the addition of EV negative markers. These could supplement the selective Calcein-AM and cellular origin staining confirming EVs are of cellular origin as opposed to potential contaminants (such as EVs

of mitochondrial origin (MitoEVs)). The addition of antibodies for MitoEVs markers such as VDAC or COX-IV would further emphasis the epithelial origin of EVs (Zhou et al., 2023). However, this was not possible due to limited panel space and the commercial availability of antibodies with optimal fluorophores.

The final limitation of this study was the configuration of the Vitrocell. While the nebuliser functioned as intended and stimulation of cells was possible, the reduced deposition of stimulant as a result of adding plastic plates to the chamber meant it was not possible to profile different allergen concentrations. Due to the lack of literature regarding nebulised Der p 1 and Can f 1 there was no recognised dose and as such allergens were used neat. The profiling of different concentrations of allergen could allow for more close modelling of the natural day to day exposure to allergens, giving the model greater robustness.

Overall, the work presented here outlines the potential role airway epithelial-derived EVs can have to both promote and prevent allergic sensitisation. Through the development of a 3D airway epithelial model and mechanism for its exposure, we were able to more accurately mimic the exposure of the airway epithelium to common indoor allergens Der p 1 and Can f 1. This facilitated the subsequent profiling of the EV responses, through the development of novel imaging flow cytometric staining and analysis. This analysis allowed for the profiling of tetraspanins and epithelial markers on individual EVs, as well as across a whole population. Despite the lack of significance observed in transcriptomic data, the upregulation of miRNAs; miR101-3p, miR103-3p, miR107, miR148a and miR224a-5p were observed to influence sensitisation, in mechanisms similar to that previously reported in the literature (Browne *et al.,* 2025). While the data presented provides a potential avenue for the better understanding of the mechanisms underpinning allergic sensitisation, more research is still required to understand the full scope of the role airway epithelial-derived EVs play in the regulation of allergic sensitisation.

References

ABELS, E. R. & BREAKEFIELD, X. O. 2016. Introduction to Extracellular Vesicles: Biogenesis, RNA Cargo Selection, Content, Release, and Uptake. *Cellular and Molecular Neurobiology,* 36**,** 301-312.

ABU KHWEEK, A., KIM, E., JOLDRICHSEN, M. R., AMER, A. O. & BOYAKA, P. N. 2020. Insights Into Mucosal Innate Immune Responses in House Dust Mite-Mediated Allergic Asthma. *Frontiers in Immunology,* 11**,** 534501.

ADAM, E., HANSEN, K. K., ASTUDILLO, O. F., COULON, L., BEX, F., DUHANT, X., JAUMOTTE, E., HOLLENBERG, M. D. & JACQUET, A. 2006. The House Dust Mite Allergen Der p 1, Unlike Der p 3, Stimulates the Expression of Interleukin-8 in Human Airway Epithelial Cells via a Proteinase-activated Receptor-2-independent Mechanism. *Journal of Biological Chemistry,* 281**,** 6910-6923.

ADMYRE, C., BOHLE, B., JOHANSSON, S. M., FOCKE-TEJKL, M., VALENTA, R., SCHEYNIUS, A. & GABRIELSSON, S. 2007. B cell–derived exosomes can present allergen peptides and activate allergen-specific T cells to proliferate and produce TH2-like cytokines. *Journal of Allergy and Clinical Immunology,* 120**,** 1418-1424.

AKDIS, C. A. 2021. Does the epithelial barrier hypothesis explain the increase in allergy, autoimmunity and other chronic conditions? *Nature Reviews Immunology,* 21**,** 739-751.

ALLAKHVERDI, Z., COMEAU, M. R., JESSUP, H. K., YOON, B.-R. P., BREWER, A., CHARTIER, S., PAQUETTE, N., ZIEGLER, S. F., SARFATI, M. & DELESPESSE, G. 2007. Thymic stromal lymphopoietin is released by human epithelial cells in response to microbes, trauma, or inflammation and potently activates mast cells. *The Journal of Experimental Medicine,* 204**,** 253-258.

ANDREWS, S. 2010. *FastQC: A quality control tool for high throughput sequence data* [Online]. Available: https://www.bioinformatics.babraham.ac.uk/projects/fastqc/ [Accessed].

ANHØJ, J., BISGAARD, H. & LIPWORTH, B. J. 1999. Effect of electrostatic charge in plastic spacers on the lung delivery of HFA-salbutamol in children. *British Journal of Clinical Pharmacology,* 47**,** 333-336.

ARNAU-SOLER, A., TREMBLAY, B. L., SUN, Y., MADORE, A. M., SIMARD, M., KERSTEN, E. T. G., GHAURI, A., MARENHOLZ, I., EIWEGGER, T., SIMONS, E., CHAN, E. S., NADEAU, K., SAMPATH, V., MAZER, B. D., ELLIOTT, S., HAMPSON, C., SOLLER, L., SANDFORD, A., BEGIN, P., HUI, J., WILKEN, B. F., GERDTS, J., BOURKAS, A., ELLIS, A. K., VASILEVA, D., CLARKE, A., ESLAMI, A., BEN-SHOSHAN, M., MARTINO, D., DALEY, D., KOPPELMAN, G. H., LAPRISE, C., LEE, Y. A. & ASAI, Y. 2025. Food Allergy Genetics and Epigenetics: A Review of Genome-Wide Association Studies. *Allergy,* 80**,** 106-131.

ASADIRAD, A., GHADIRI, A. A., AMARI, A., GHASEMI DEHCHESHMEH, M., SADEGHI, M. & DEHNAVI, S. 2023. Sublingual prophylactic administration of OVA-loaded MSC-derived exosomes to prevent allergic sensitization. *International Immunopharmacology,* 120**,** 110405.

ASANO, K., HIROSE, S., NARITA, K., SUBSOMWONG, P., KAWAI, N., SUKCHAWALIT, R. & NAKANE, A. 2021. Extracellular vesicles from methicillin resistant

Staphylococcus aureus stimulate proinflammatory cytokine production and trigger IgE-mediated hypersensitivity. *Emerging Microbes & Infections,* 10**,** 2000-2009.

AUN, M., BONAMICHI-SANTOS, R., ARANTES-COSTA, F. M., KALIL, J. & GIAVINA-BIANCHI, P. 2017. Animal models of asthma: utility and limitations. *Journal of Asthma and Allergy,* Volume10**,** 293-301.

AYRE, D. C., ELSTNER, M., SMITH, N. C., MOORES, E. S., HOGAN, A. M. & CHRISTIAN, S. L. 2015. Dynamic regulation of CD24 expression and release of CD24 containing microvesicles in immature B cells in response to CD24 engagement. *Immunology,* 146**,** 217-233.

BACHERT, C., HAUSER, U., PREM, B., RUDACK, C. & GANZER, U. 1995. Proinflammatory cytokines in allergic rhinitis. *European Archives of Oto-Rhino-Laryngology,* 252**,** S44-S49.

BADAOUI, M. & CHANSON, M. 2023. Intercellular Communication in Airway Epithelial Cell Regeneration: Potential Roles of Connexins and Pannexins. *International Journal of Molecular Sciences,* 24**,** 16160.

BALAN, S. & BHARDWAJ, N. 2020. Cross-Presentation of Tumor Antigens Is Ruled by Synaptic Transfer of Vesicles among Dendritic Cell Subsets. *Cancer Cell,* 37**,** 751-753.

BALDO, B. A. & PHAM, N. H. 2013. Mechanisms of Hypersensitivity. *Drug Allergy.* Springer New York.

BALLANTYNE, S. J., BARLOW, J. L., JOLIN, H. E., NATH, P., WILLIAMS, A. S., CHUNG, K. F., STURTON, G., WONG, S. H. & MCKENZIE, A. N. J. 2007. Blocking IL-25 prevents airway hyperresponsiveness in allergic asthma. *Journal of Allergy and Clinical Immunology,* 120**,** 1324-1331.

BÄNFER, S., KUTSCHER, S., FLECK, F., DIENST, M., PREUßER, C., POGGE VON STRANDMANN, E. & JACOB, R. 2022. Late domain dependent E-cadherin recruitment into extracellular vesicles. *Frontiers in Cell and Developmental Biology,* 10**,** 878620.

BARNETT, K. C., XIE, Y., ASAKURA, T., SONG, D., LIANG, K., TAFT-BENZ, S. A., GUO, H., YANG, S., OKUDA, K., GILMORE, R. C., LOOME, J. F., OGUIN III, T. H., SEMPOWSKI, G. D., RANDELL, S. H., HEISE, M. T., LEI, Y. L., BOUCHER, R. C. & TING, J. P. Y. 2023. An epithelial-immune circuit amplifies inflammasome and IL-6 responses to SARS-CoV-2. *Cell Host & Microbe,* 31**,** 243-259.e6.

BARTEL, S., LA GRUTTA, S., CILLUFFO, G., PERCONTI, G., BONGIOVANNI, A., GIALLONGO, A., BEHRENDS, J., KRUPPA, J., HERMANN, S., CHIANG, D., PFAFFL, M. W. & KRAUSS-ETSCHMANN, S. 2020. Human airway epithelial extracellular vesicle miRNA signature is altered upon asthma development. *Allergy,* 75**,** 346-356.

BARTEMES, K. R. & KITA, H. 2021. Roles of innate lymphoid cells (ILCs) in allergic diseases: The 10-year anniversary for ILC2s. *Journal of Allergy and Clinical Immunology,* 147**,** 1531-1547.

BASCOM, R., PIPKORN, U., LICHTENSTEIN, L. M. & NACLERIO, R. M. 1988. The Influx of Inflammatory Cells into Nasal Washings during the Late Response to Antigen Challenge: Effect of Systemic Steroid Pretreatment. *American Review of Respiratory Disease,* 138**,** 406-412.

BASIL, M. C., KATZEN, J., ENGLER, A. E., GUO, M., HERRIGES, M. J., KATHIRIYA, J. J., WINDMUELLER, R., YSASI, A. B., ZACHARIAS, W. J., CHAPMAN, H. A., KOTTON, D. N., ROCK, J. R., SNOECK, H.-W., VUNJAK-NOVAKOVIC, G., WHITSETT, J. A. & MORRISEY, E. E. 2020. The Cellular and Physiological Basis for Lung Repair and Regeneration: Past, Present, and Future. *Cell Stem Cell,* 26**,** 482-502.

BATTAGLIA, M., GIANFRANI, C., GREGORI, S. & RONCAROLOA, M. G. 2004. IL-10-Producing T Regulatory Type 1 Cells and Oral Tolerance. *Annals of the New York Academy of Sciences,* 1029**,** 142-153.

BAX, H. J., KEEBLE, A. H. & GOULD, H. J. 2012. Cytokinergic IgE Action in Mast Cell Activation. *Frontiers in Immunology,* 3**,** 229.

BEAVITT, S.-J. E., HARDER, K. W., KEMP, J. M., JONES, J., QUILICI, C., CASAGRANDA, F., LAM, E., TURNER, D., BRENNAN, S., SLY, P. D., TARLINTON, D. M., ANDERSON, G. P. & HIBBS, M. L. 2005. Lyn-Deficient Mice Develop Severe, Persistent Asthma: Lyn Is a Critical Negative Regulator of Th2 Immunity. *The Journal of Immunology,* 175**,** 1867-1875.

BEBELMAN, M. P., SMIT, M. J., PEGTEL, D. M. & BAGLIO, S. R. 2018. Biogenesis and function of extracellular vesicles in cancer. *Pharmacology & Therapeutics,* 188**,** 1-11.

BEBO, B. F., YONG, T., ORR, E. L. & LINTHICUM, D. S. 1996. Hypothesis: a possible role for mast cells and their inflammatory mediators in the pathogenesis of autoimmune encephalomyelitis. *Journal of Neuroscience Research,* 45**,** 340-348.

BEHESHTI, R., GRANT, T. L. & WOOD, R. A. 2025. Minimizing Indoor Allergen Exposure: What Works? *Current Allergy and Asthma Reports,* 25**,** 3.

BELOT, N. 2017. Adaptation of the KeratinoSens™ skin sensitization test to animal-product-free cell culture. *ALTEX,* 34**,** 560-564.

BODIER-MONTAGUTELLI, E., RESPAUD, R., PERRET, G., BAPTISTA, L., DUQUENNE, P., HEUZÉ-VOURC'H, N. & VECELLIO, L. 2020. Protein stability during nebulization: Mind the collection step! *European Journal of Pharmaceutics and Biopharmaceutics,* 152**,** 23-34.

BOILARD, E. 2018. Thematic Review Series: Exosomes and Microvesicles: Lipids as Key Components of their Biogenesis and Functions Extracellular vesicles and their content in bioactive lipid mediators: more than a sack of microRNA. *Journal of Lipid Research,* 59**,** 2037-2046.

BRAAKHUIS, H. M., GREMMER, E. R., BANNUSCHER, A., DRASLER, B., KESHAVAN, S., ROTHEN-RUTISHAUSER, B., BIRK, B., VERLOHNER, A., LANDSIEDEL, R., MELDRUM, K., DOAK, S. H., CLIFT, M. J. D., ERDEM, J. S., FOSS, O. A. H., ZIENOLDDINY-NARUI, S., SERCHI, T., MOSCHINI, E., WEBER, P., BURLA, S., KUMAR, P., SCHMID, O., ZWART, E., VERMEULEN, J. P. & VANDEBRIEL, R. J. 2023. Transferability and reproducibility of exposed air-liquid interface co-culture lung models. *NanoImpact,* 31**,** 100466.

BRENNAN, K., IVERSEN, K. F., BLANCO-FERNÁNDEZ, A., LUND, T., PLESNER, T. & MC GEE, M. M. 2022. Extracellular Vesicles Isolated from Plasma of Multiple Myeloma Patients Treated with Daratumumab Express CD38, PD-L1, and the Complement Inhibitory Proteins CD55 and CD59. *Cells,* 11**,** 3365.

BROUGH, H. A., SIMPSON, A., MAKINSON, K., HANKINSON, J., BROWN, S., DOUIRI, A., BELGRAVE, D. C. M., PENAGOS, M., STEPHENS, A. C., MCLEAN, W. H. I., TURCANU, V., NICOLAOU, N., CUSTOVIC, A. & LACK, G. 2014. Peanut allergy: Effect of environmental peanut exposure in children with filaggrin loss-of-function mutations. *Journal of Allergy and Clinical Immunology,* 134**,** 867-875.e1.

BROWNE, W., HOPKINS, G., COCHRANE, S., JAMES, V., ONION, D. & FAIRCLOUGH, L. C. 2025. The Role of Epithelial-Derived Extracellular Vesicles in Allergic Sensitisation: A Systematic Review. *International Journal of Molecular Sciences,* 26**,** 5791.

BRÜSER, L. & BOGDAN, S. 2017. Adherens Junctions on the Move—Membrane Trafficking of E-Cadherin. *Cold Spring Harbor Perspectives in Biology,* 9**,** a029140.

BURGER, D., TURNER, M., XIAO, F., MUNKONDA, M. N., AKBARI, S. & BURNS, K. D. 2017. High glucose increases the formation and pro-oxidative activity of endothelial microparticles. *Diabetologia,* 60**,** 1791-1800.

BUSCHOW, S. I., NOLTE-'T HOEN, E. N. M., VAN NIEL, G., POLS, M. S., TEN BROEKE, T., LAUWEN, M., OSSENDORP, F., MELIEF, C. J. M., RAPOSO, G., WUBBOLTS, R., WAUBEN, M. H. M. & STOORVOGEL, W. 2009. MHC II in Dendritic Cells is Targeted to Lysosomes or T Cell-Induced Exosomes Via Distinct Multivesicular Body Pathways. *Traffic,* 10**,** 1528-1542.

BUZAS, E. I. 2023. The roles of extracellular vesicles in the immune system. *Nature Reviews Immunology,* 23**,** 236-250.

CALABRESE, E. J., BARNES, R., STANEK, E. J., PASTIDES, H., GILBERT, C. E., VENEMAN, P., WANG, X., LASZTITY, A. & KOSTECKI, P. T. 1989. How much soil do young children ingest: An epidemiologic study. *Regulatory Toxicology and Pharmacology,* 10**,** 123-137.

CALDERÓN-PELÁEZ, M. A., CASTELLANOS, J. E. & VELANDIA-ROMERO, M. L. 2025. A protocol for loading Calcein-AM into extracellular vesicles from mammalian cells for clear visualization with a fluorescence microscope coupled to a deconvolution system. *PLoS One,* 20**,** e0317689.

CAMPBELL, A. M., VACHIER, I., CHANEZ, P., VIGNOLA, A. M., LEBEL, B., KOCHAN, J., GODARD, P. & BOUSQUET, J. 1998. Expression of the High-affinity Receptor for IgE on Bronchial Epithelial Cells of Asthmatics. *American Journal of Respiratory Cell and Molecular Biology,* 19**,** 92-97.

CAMPBELL, A. M., VIGNOLA, A. M., CHANEZ, P., GODARD, P. & BOUSQUET, J. 1994. Low-affinity receptor for IgE on human bronchial epithelial cells in asthma. *Immunology,* 82**,** 506-8.

CAMPBELL, H. K., MAIERS, J. L. & DEMALI, K. A. 2017. Interplay between tight junctions & adherens junctions. *Experimental Cell Research,* 358**,** 39-44.

CARABALLO, L., VALENTA, R., PUERTA, L., POMÉS, A., ZAKZUK, J., FERNANDEZ-CALDAS, E., ACEVEDO, N., SANCHEZ-BORGES, M., ANSOTEGUI, I., ZHANG, L., VAN HAGE, M., ABEL-FERNÁNDEZ, E., KARLA ARRUDA, L., VRTALA, S., CURIN, M., GRONLUND, H., KARSONOVA, A., KILIMAJER, J., RIABOVA, K., TRIFONOVA, D. & KARAULOV, A. 2020. The allergenic activity and clinical impact of individual IgE-antibody binding molecules from indoor allergen sources. *World Allergy Organization Journal,* 13**,** 100118.

CERGAN, R., BERGHI, O., DUMITRU, M., VRINCEANU, D., MANOLE, F., MUSAT, G. C., OANCEA, A. L. A. & SERBOIU, C. 2025. Interleukin 8 Molecular Interplay in Allergic Rhinitis and Chronic Rhinosinusitis with Nasal Polyps: A Scoping Review. *Life,* 15**,** 469.

CHEN, R., SMITH, S. G., SALTER, B., EL-GAMMAL, A., OLIVERIA, J. P., OBMINSKI, C., WATSON, R., O'BYRNE, P. M., GAUVREAU, G. M. & SEHMI, R. 2017. Allergen-induced Increases in Sputum Levels of Group 2 Innate Lymphoid Cells in Subjects with Asthma. *American Journal of Respiratory and Critical Care Medicine,* 196**,** 700-712.

CHEN, X., SONG, C. H., FENG, B. S., LI, T. L., LI, P., ZHENG, P. Y., CHEN, X. M., XING, Z. & YANG, P. C. 2011. Intestinal epithelial cell-derived integrin αβ6 plays an important role in the induction of regulatory T cells and inhibits an antigen-specific Th2 response. *Journal of Leukocyte Biology,* 90**,** 751-759.

CHEN, Y., KUMAR, R. K., THOMAS, P. S. & HERBERT, C. 2019. Th1/17-Biased Inflammatory Environment Associated with COPD Alters the Response of Airway Epithelial Cells to Viral and Bacterial Stimuli. *Mediators of Inflammation,* 2019**,** 1-12.

CHENG, D., XUE, Z., YI, L., SHI, H., ZHANG, K., HUO, X., BONSER, L. R., ZHAO, J., XU, Y., ERLE, D. J. & ZHEN, G. 2014. Epithelial Interleukin-25 Is a Key Mediator in Th2-High, Corticosteroid-Responsive Asthma. *American Journal of Respiratory and Critical Care Medicine,* 190**,** 639-648.

CHEVIGNÉ, A. & JACQUET, A. 2018. Emerging roles of the protease allergen Der p 1 in house dust mite–induced airway inflammation. *Journal of Allergy and Clinical Immunology,* 142**,** 398-400.

CHOW, A. W.-M., LIANG, J. F.-T., WONG, J. S.-C., FU, Y., TANG, N. L.-S. & KO, W.-H. 2010. Polarized Secretion of Interleukin (IL)-6 and IL-8 by Human Airway Epithelia 16HBE14o- Cells in Response to Cationic Polypeptide Challenge. *PLoS ONE,* 5**,** e12091.

CHUNG, F. 2001. Anti-inflammatory cytokines in asthma and allergy: interleukin-10, interleukin-12, interferon-γ. *Mediators of Inflammation,* 10**,** 51-59.

CHUO, S. T.-Y., CHIEN, J. C.-Y. & LAI, C. P.-K. 2018. Imaging extracellular vesicles: current and emerging methods. *Journal of Biomedical Science,* 25**,** 91.

CHURCH, M. & LEVISCHAFFER, F. 1997. The human mast cell. *Journal of Allergy and Clinical Immunology,* 99**,** 155-160.

CITI, S., FROMM, M., FURUSE, M., GONZÁLEZ-MARISCAL, L., NUSRAT, A., TSUKITA, S. & TURNER, J. R. 2024. A short guide to the tight junction. *Journal of Cell Science,* 137.

COMSTOCK, A. T., GANESAN, S., CHATTORAJ, A., FARIS, A. N., MARGOLIS, B. L., HERSHENSON, M. B. & SAJJAN, U. S. 2011. Rhinovirus-Induced Barrier Dysfunction in Polarized Airway Epithelial Cells Is Mediated by NADPH Oxidase 1. *Journal of Virology,* 85**,** 6795-6808.

COOKE, R. A. & VEER, A. V. 1916. Human Sensitization. *The Journal of Immunology,* 1**,** 201-305.

COOMBS, R. R. A. & GELL, P. G. H. 1968. *Clinical aspects of immunology,* Oxford.

CUSTOVIC, A. 2015. To what extent is allergen exposure a risk factor for the development of allergic disease? *Clinical & Experimental Allergy,* 45**,** 54-62.

D'SOUZA-SCHOREY, C. & CLANCY, J. W. 2012. Tumor-derived microvesicles: shedding light on novel microenvironment modulators and prospective cancer biomarkers. *Genes & Development,* 26**,** 1287-1299.

DE ÁVILA, R. I., MÜLLER, I., BARLOW, H., MIDDLETON, A. M., THEIVENTHRAN, M., BASILI, D., BOWDEN, A. M., SAIB, O., ENGI, P., PIETRENKO, T., WALLACE, J., BODA, B., CONSTANT, S., BEHRSING, H. P., PATEL, V. & BALTAZAR, M. T. 2025. Evaluation of a non-animal toolbox informed by adverse outcome pathways for human inhalation safety. *Frontiers in Toxicology,* 7**,** 1426132.

DE ROND, L., VAN DER POL, E., HAU, C. M., VARGA, Z., STURK, A., VAN LEEUWEN, T. G., NIEUWLAND, R. & COUMANS, F. A. W. 2018. Comparison of Generic Fluorescent Markers for Detection of Extracellular Vesicles by Flow Cytometry. *Clin Chem,* 64**,** 680-689.

DEL CONDE, I., SHRIMPTON, C. N., THIAGARAJAN, P. & LÓPEZ, J. A. 2005. Tissue-factor–bearing microvesicles arise from lipid rafts and fuse with activated platelets to initiate coagulation. *Blood,* 106**,** 1604-1611.

DEMKOW, U. & STELMASZCZYK-EMMEL, A. 2021. Extracellular Vesicles in Allergic Rhinitis and Asthma and Laboratory Possibilities for Their Assessment. *International Journal of Molecular Sciences,* 22**,** 2273.

DEPREZ, M., ZARAGOSI, L.-E., TRUCHI, M., BECAVIN, C., RUIZ GARCÍA, S., ARGUEL, M.-J., PLAISANT, M., MAGNONE, V., LEBRIGAND, K., ABELANET, S., BRAU, F., PAQUET, A., PE'ER, D., MARQUETTE, C.-H., LEROY, S. & BARBRY, P. 2020. A Single-Cell Atlas of the Human Healthy Airways. *American Journal of Respiratory and Critical Care Medicine,* 202**,** 1636-1645.

DIENDORFER, A., KHAMINA, K., PULTAR, M. & HACKL, M. 2022. miND (miRNA NGS Discovery pipeline): a small RNA-seq analysis pipeline and report generator for microRNA biomarker discovery studies. *F1000Research,* 11**,** 233.

DINARELLO, C. A. 2018. Overview of the IL-1 family in innate inflammation and acquired immunity. *Immunological Reviews,* 281**,** 8-27.

DOMINGO, C., BUSSE, W. W., HANANIA, N. A., ERTUGRUL, M., MILLETTE, L. A., MAIO-TWOFOOT, T., JAUMONT, X. & PALOMARES, O. 2025. The Direct and Indirect Role of IgE on Airway Epithelium in Asthma. *Allergy,* 80**,** 919-931.

DONG, H., HU, Y., LIU, L., ZOU, M., HUANG, C., LUO, L., YU, C., WAN, X., ZHAO, H., CHEN, J., XIE, Z., LE, Y., ZOU, F. & CAI, S. 2016. Distinct roles of short and long thymic stromal lymphopoietin isoforms in house dust mite-induced asthmatic airway epithelial barrier disruption. *Scientific Reports,* 6**,** 39559.

DOUWES, J. & PEARCE, N. 2002. Asthma and the westernization 'package'. *International Journal of Epidemiology,* 31**,** 1098-1102.

DOYLE, L. & WANG, M. 2019. Overview of Extracellular Vesicles, Their Origin, Composition, Purpose, and Methods for Exosome Isolation and Analysis. *Cells,* 8**,** 727.

DRAKE, L. Y. & KITA, H. 2017. IL-33: biological properties, functions, and roles in airway disease. *Immunological Reviews,* 278**,** 173-184.

DU TOIT, G., SAMPSON, H. A., PLAUT, M., BURKS, A. W., AKDIS, C. A. & LACK, G. 2018. Food allergy: Update on prevention and tolerance. *Journal of Allergy and Clinical Immunology,* 141**,** 30-40.

DUNBAR, H., HAWTHORNE, I. J., MCNAMEE, E. N., ARMSTRONG, M. E., DONNELLY, S. C. & ENGLISH, K. 2024. The human MIF polymorphism CATT7 enhances pro-inflammatory macrophage polarization in a clinically relevant model of allergic airway inflammation. *The FASEB Journal,* 38**,** e23576.

EDER, W., KLIMECKI, W., YU, L., VON MUTIUS, E., RIEDLER, J., BRAUN-FAHRLÄNDER, C., NOWAK, D. & MARTINEZ, F. D. 2004. Toll-like receptor 2 as a major gene for asthma in children of European farmers. *Journal of Allergy and Clinical Immunology,* 113**,** 482-488.

EL ANDALOUSSI, S., MÄGER, I., BREAKEFIELD, X. O. & WOOD, M. J. A. 2013. Extracellular vesicles: biology and emerging therapeutic opportunities. *Nature Reviews Drug Discovery,* 12**,** 347-357.

ESSER, J., GEHRMANN, U., D'ALEXANDRI, F. L., HIDALGO-ESTÉVEZ, A. M., WHEELOCK, C. E., SCHEYNIUS, A., GABRIELSSON, S. & RÅDMARK, O. 2010. Exosomes from human macrophages and dendritic cells contain enzymes for leukotriene biosynthesis and promote granulocyte migration. *Journal of Allergy and Clinical Immunology,* 126**,** 1032-1040.e4.

EWELS, P., MAGNUSSON, M., LUNDIN, S. & KÄLLER, M. 2016. MultiQC: summarize analysis results for multiple tools and samples in a single report. *Bioinformatics,* 32**,** 3047-3048.

FANAEI, M., PETER & LYNDA 2011. The role of tetraspanins in fusion. *Biochemical Society Transactions,* 39**,** 524-528.

FANG, S.-B., ZHOU, Z.-R., PENG, Y.-Q., LIU, X.-Q., HE, B.-X., CHEN, D.-H., CHEN, D. & FU, Q.-L. 2021. Plasma EVs Display Antigen-Presenting Characteristics in Patients With Allergic Rhinitis and Promote Differentiation of Th2 Cells. *Frontiers in Immunology,* 12**,** 710372.

FANG, Y. & EGLEN, R. M. 2017. Three-Dimensional Cell Cultures in Drug Discovery and Development. *SLAS Discovery,* 22**,** 456-472.

FOLEY, N. H. & O'NEILL, L. A. 2012. miR-107: a Toll-like receptor-regulated miRNA dysregulated in obesity and type II diabetes. *Journal of Leukocyte Biology,* 92**,** 521-527.

FORT, M. M., CHEUNG, J., YEN, D., LI, J., ZURAWSKI, S. M., LO, S., MENON, S., CLIFFORD, T., HUNTE, B., LESLEY, R., MUCHAMUEL, T., HURST, S. D., ZURAWSKI, G., LEACH, M. W., GORMAN, D. M. & RENNICK, D. M. 2001. IL-25 Induces IL-4, IL-5, and IL-13 and Th2-Associated Pathologies In Vivo. *Immunity,* 15**,** 985-995.

FREDERICK, B. A., HELFRICH, B. A., COLDREN, C. D., ZHENG, D., CHAN, D., BUNN, P. A. & RABEN, D. 2007. Epithelial to mesenchymal transition predicts gefitinib resistance in cell lines of head and neck squamous cell carcinoma and non–small cell lung carcinoma. *Molecular Cancer Therapeutics,* 6**,** 1683-1691.

FRIEDLÄNDER, M. R., MACKOWIAK, S. D., LI, N., CHEN, W. & RAJEWSKY, N. 2012. miRDeep2 accurately identifies known and hundreds of novel microRNA genes in seven animal clades. *Nucleic Acids Research,* 40**,** 37-52.

FROIDURE, A., SHEN, C., GRAS, D., VAN SNICK, J., CHANEZ, P. & PILETTE, C. 2014. Myeloid dendritic cells are primed in allergic asthma for thymic stromal

lymphopoietin-mediated induction of Th2 and Th9 responses. *Allergy,* 69**,** 1068-1076.

GALLAY, P., BARRAS, C., TOBIAS, P. S., CALANDRA, T., GLAUSER, M. P. & HEUMANN, D. 1994. Lipopolysaccharide (LPS)-Binding Protein In Human Serum Determines The Tumor Necrosis Factor Response Of Monocytes To LPS. *Journal of Infectious Diseases,* 170**,** 1319-1322.

GATTI, S., BRUNO, S., DEREGIBUS, M. C., SORDI, A., CANTALUPPI, V., TETTA, C. & CAMUSSI, G. 2011. Microvesicles derived from human adult mesenchymal stem cells protect against ischaemia-reperfusion-induced acute and chronic kidney injury. *Nephrology Dialysis Transplantation,* 26**,** 1474-1483.

GEORAS, S. N. & REZAEE, F. 2014. Epithelial barrier function: At the front line of asthma immunology and allergic airway inflammation. *Journal of Allergy and Clinical Immunology,* 134**,** 509-520.

GHRAIRI, N. & ELHECHMI, Y. Z. 2025. Physiopathology of Allergic Asthma: A Comprehensive Review. *Scandinavian Journal of Immunology,* 101**,** e70032.

GILLES, S., AKDIS, C., LAUENER, R., SCHMID-GRENDELMEIER, P., BIEBER, T., SCHÄPPI, G. & TRAIDL-HOFFMANN, C. 2018. The role of environmental factors in allergy: A critical reappraisal. *Experimental Dermatology,* 27**,** 1193-1200.

GON, Y., MARUOKA, S., INOUE, T., KURODA, K., YAMAGISHI, K., KOZU, Y., SHIKANO, S., SODA, K., LÖTVALL, J. & HASHIMOTO, S. 2017. Selective release of miRNAs via extracellular vesicles is associated with house-dust mite allergen-induced airway inflammation. *Clinical and Experimental Allergy,* 47**,** 1586-1598.

GOSSET, P., TILLIE-LEBLOND, I., MALAQUIN, F., DURIEU, J., WALLAERT, B. & TONNEL, A. B. 1997. Interleukin-8 secretion in patients with allergic rhinitis after an allergen challenge: interleukin-8 is not the main chemotactic factor present in nasal lavages. *Clinical & Experimental Allergy,* 27**,** 379-388.

GOUGH, L., SCHULZ, O., SEWELL, H. F. & SHAKIB, F. 1999. The Cysteine Protease Activity of the Major Dust Mite Allergen Der P 1 Selectively Enhances the Immunoglobulin E Antibody Response. *The Journal of Experimental Medicine,* 190**,** 1897-1902.

GOULD, H. J. & SUTTON, B. J. 2008. IgE in allergy and asthma today. *Nature Reviews Immunology,* 8**,** 205-217.

GOULD, H. J., TAKHAR, P., HARRIES, H. E., CHEVRETTON, E. & SUTTON, B. J. 2007. The Allergic March from Staphylococcus aureus Superantigens to Immunoglobulin E. KARGER.

GRAY, W. D., MITCHELL, A. J. & SEARLES, C. D. 2015. An accurate, precise method for general labeling of extracellular vesicles. *MethodsX,* 2**,** 360-367.

GRIFFITHS-JONES, S. 2004. The microRNA Registry. *Nucleic Acids Research,* 32**,** 109D-111.

GROTENBOER, N. S., KETELAAR, M. E., KOPPELMAN, G. H. & NAWIJN, M. C. 2013. Decoding asthma: Translating genetic variation in IL33 and IL1RL1 into disease pathophysiology. *Journal of Allergy and Clinical Immunology,* 131**,** 856-865.e9.

GUL, B., SYED, F., KHAN, S., IQBAL, A. & AHMAD, I. 2022. Characterization of extracellular vesicles by flow cytometry: Challenges and promises. *Micron,* 161**,** 103341.

GUTOWSKA-ŚLESIK, J., SAMOLIŃSKI, B. & KRZYCH-FAŁTA, E. 2023. The increase in allergic conditions based on a review of literature. *Advances in Dermatology and Allergology,* 40**,** 1-7.

HADIS, U., WAHL, B., SCHULZ, O., HARDTKE-WOLENSKI, M., SCHIPPERS, A., WAGNER, N., MÜLLER, W., SPARWASSER, T., FÖRSTER, R. & PABST, O. 2011. Intestinal Tolerance Requires Gut Homing and Expansion of FoxP3+ Regulatory T Cells in the Lamina Propria. *Immunity,* 34**,** 237-246.

HAN, M., RAJPUT, C., HONG, J. Y., LEI, J., HINDE, J. L., WU, Q., BENTLEY, J. K. & HERSHENSON, M. B. 2017. The Innate Cytokines IL-25, IL-33, and TSLP Cooperate in the Induction of Type 2 Innate Lymphoid Cell Expansion and Mucous Metaplasia in Rhinovirus-Infected Immature Mice. *The Journal of Immunology,* 199**,** 1308-1318.

HAN, X., NA, T., WU, T. & YUAN, B.-Z. 2020. Human lung epithelial BEAS-2B cells exhibit characteristics of mesenchymal stem cells. *PLOS ONE,* 15**,** e0227174.

HANSEN, I., KLIMEK, L., MÖSGES, R. & HÖRMANN, K. 2004. Mediators of inflammation in the early and the late phase of allergic rhinitis. *Current Opinion in Allergy and Clinical Immunology,* 4**,** 159-163.

HARVEY-SEUTCHEU, C., HOPKINS, G. & FAIRCLOUGH, L. C. 2024. The Role of Extracellular Vesicles in Atopic Dermatitis. *Int J Mol Sci,* 25.

HAYAKAWA, H., HAYAKAWA, M., KUME, A. & TOMINAGA, S.-I. 2007. Soluble ST2 Blocks Interleukin-33 Signaling in Allergic Airway Inflammation. *Journal of Biological Chemistry,* 282**,** 26369-26380.

HE, R.-W., BRAAKHUIS, H. M., VANDEBRIEL, R. J., STAAL, Y. C. M., GREMMER, E. R., FOKKENS, P. H. B., KEMP, C., VERMEULEN, J., WESTERINK, R. H. S. & CASSEE, F. R. 2021. Optimization of an air-liquid interface in vitro cell co-culture model to estimate the hazard of aerosol exposures. *Journal of Aerosol Science,* 153**,** 105703.

HE, R., OYOSHI, M. K., GARIBYAN, L., KUMAR, L., ZIEGLER, S. F. & GEHA, R. S. 2008. TSLP acts on infiltrating effector T cells to drive allergic skin inflammation. *Proceedings of the National Academy of Sciences,* 105**,** 11875-11880.

HELLINGS, P. W. & STEELANT, B. 2020. Epithelial barriers in allergy and asthma. *Journal of Allergy and Clinical Immunology,* 145**,** 1499-1509.

HEMLER, M. E. 2003. Tetraspanin Proteins Mediate Cellular Penetration, Invasion, and Fusion Events and Define a Novel Type of Membrane Microdomain. *Annual Review of Cell and Developmental Biology,* 19**,** 397-422.

HERBERT, C., DO, K., CHIU, V., GARTHWAITE, L., CHEN, Y., PAUL, TRAINI, D. & RAKESH 2017. Allergic environment enhances airway epithelial pro-inflammatory responses to rhinovirus infection. *Clinical Science,* 131**,** 499-509.

HEWITT, R. J. & LLOYD, C. M. 2021. Regulation of immune responses by the airway epithelial cell landscape. *Nature Reviews Immunology,* 21**,** 347-362.

HEYDENREICH, B., BELLINGHAUSEN, I., KÖNIG, B., BECKER, W. M., GRABBE, S., PETERSEN, A. & SALOGA, J. 2012. Gram-positive bacteria on grass pollen exhibit adjuvant activity inducing inflammatory T cell responses. *Clinical & Experimental Allergy,* 42**,** 76-84.

HILS, M., WÖLBING, F., HILGER, C., FISCHER, J., HOFFARD, N. & BIEDERMANN, T. 2020. The History of Carbohydrates in Type I Allergy. *Frontiers in Immunology,* 11**,** 586924.

HONG, S.-W., CHOI, E.-B., MIN, T.-K., KIM, J.-H., KIM, M.-H., JEON, S. G., LEE, B.-J., GHO, Y. S., JEE, Y.-K., PYUN, B.-Y. & KIM, Y.-K. 2014. An Important Role of α-Hemolysin in Extracellular Vesicles on the Development of Atopic Dermatitis Induced by Staphylococcus aureus. *PLoS ONE,* 9**,** e100499.

HONG, S. W., KIM, M. R., LEE, E. Y., KIM, J. H., KIM, Y. S., JEON, S. G., YANG, J. M., LEE, B. J., PYUN, B. Y., GHO, Y. S. & KIM, Y. K. 2011. Extracellular vesicles derived from Staphylococcus aureus induce atopic dermatitis-like skin inflammation. *Allergy,* 66**,** 351-359.

HOPKINS, G. V., COCHRANE, S., ONION, D. & FAIRCLOUGH, L. C. 2022. The Role of Lipids in Allergic Sensitization: A Systematic Review. *Frontiers in Molecular Biosciences,* 9**,** 832330.

HOPKINS, G. V., COCHRANE, S., ONION, D. & FAIRCLOUGH, L. C. 2023. Invariant NKT cells are more abundant in peanut-allergic adults and a subset of CD8+ iNKT cells are depleted after peanut oil exposure. *Frontiers in Immunology,* 14**,** 1293158.

HOVHANNISYAN, L., CZECHOWSKA, E. & GUTOWSKA-OWSIAK, D. 2021. The Role of Non-Immune Cell-Derived Extracellular Vesicles in Allergy. *Frontiers in Immunology,* 12**,** 702381.

HU, R.-H., WU, C.-T., WU, T.-S., YU, F.-Y., KO, J.-L., LUE, K.-H. & LIU, Y.-F. 2022. Systematic Characterization of the Group 2 House Dust Mite Allergen in Dermatophagoides microceras. *Frontiers in Cellular and Infection Microbiology,* 11**,** 793559.

HUANG, F., ZHAO, J.-L., WANG, L., GAO, C.-C., LIANG, S.-Q., AN, D.-J., BAI, J., CHEN, Y., HAN, H. & QIN, H.-Y. 2017. miR-148a-3p Mediates Notch Signaling to Promote the Differentiation and M1 Activation of Macrophages. *Frontiers in Immunology,* 8**,** 1327.

HUANG, H.-J., SARZSINSZKY, E. & VRTALA, S. 2023. House dust mite allergy: The importance of house dust mite allergens for diagnosis and immunotherapy. *Molecular Immunology,* 158**,** 54-67.

HUANG, L., ZHANG, X., WANG, M., CHEN, Z., YAN, Y., GU, W., TAN, J., JIANG, W. & JI, W. 2019. Exosomes from Thymic Stromal Lymphopoietin-Activated Dendritic Cells Promote Th2 Differentiation through the OX40 Ligand. *Pathobiology,* 86**,** 111-117.

HUANG, T., YANG, J., ZHANG, J., KE, W., ZOU, F., WAN, C., WANG, L., ZHANG, X., LIANG, F., MEI, S., ZHANG, Q., RONG, Z., YANG, B. & ZHENG, H. 2020. MicroRNA-101-3p Downregulates TLR2 Expression, Leading to Reduction in Cytokine Production by Treponema pallidum–Stimulated Macrophages. *Journal of Investigative Dermatology,* 140**,** 1566-1575.e1.

HUVENNE, W., CALLEBAUT, I., PLANTINGA, M., VANOIRBEEK, J. A. J., KRYSKO, O., BULLENS, D. M. A., GEVAERT, P., VAN CAUWENBERGE, P., LAMBRECHT, B. N., CEUPPENS, J. L., BACHERT, C. & HELLINGS, P. W. 2010. *Staphylococcus aureus* enterotoxin B facilitates allergic sensitization in experimental asthma. *Clinical & Experimental Allergy,* 40**,** 1079-1090.

IGEA, J. M. 2013. The history of the idea of allergy. *Allergy,* 68**,** 966-973.

IMOTO, Y., SAKASHITA, M., TOKUNAGA, T., KANNO, M., SAITO, K., SHIMIZU, A., MAEGAWA, A. & FUJIEDA, S. 2024. Recent prevalence of allergic rhinitis caused by house dust mites among the pediatric population in Fukui, Japan. *World Allergy Organization Journal,* 17**,** 100932.

INEICHEN, B. V., FURRER, E., GRÜNINGER, S. L., ZÜRRER, W. E. & MACLEOD, M. R. 2024. Analysis of animal-to-human translation shows that only 5% of animal-tested therapeutic interventions obtain regulatory approval for human applications. *PLOS Biology,* 22**,** e3002667.

ISLAM, M. A., ALBARRACIN, L., TOMOKIYO, M., VALDEZ, J. C., SACUR, J., VIZOSO-PINTO, M. G., ANDRADE, B. G. N., CUADRAT, R. R. C., KITAZAWA, H. & VILLENA, J. 2021. Immunobiotic Lactobacilli Improve Resistance of Respiratory Epithelial Cells to SARS-CoV-2 Infection. *Pathogens,* 10**,** 1197.

JAKWERTH, C. A., ORDOVAS-MONTANES, J., BLANK, S., SCHMIDT-WEBER, C. B. & ZISSLER, U. M. 2022. Role of Respiratory Epithelial Cells in Allergic Diseases. *Cells,* 11**,** 1387.

JANKOVIČOVÁ, J., SEČOVÁ, P., MICHALKOVÁ, K. & ANTALÍKOVÁ, J. 2020. Tetraspanins, More than Markers of Extracellular Vesicles in Reproduction. *International Journal of Molecular Sciences,* 21**,** 7568.

JANSSEN, R., DE KLEER, J. W. M., HEMING, B., BASTIAAN-NET, S., GARSSEN, J., WILLEMSEN, L. E. M. & MASEREEUW, R. 2024. Food allergen sensitization on a chip: the gut–immune–skin axis. *Trends in Biotechnology,* 42**,** 119-134.

JENEROWICZ, D., SILNY, W., DAŃCZAK-PAZDROWSKA, A., POLAŃSKA, A., OSMOLA-MAŃKOWSKA, A. & OLEK-HRAB, K. 2012. Environmental factors and allergic diseases. *Annals of Agricultural and Environmental Medicine,* 19**,** 475-481.

JEPPESEN, D. K., FENIX, A. M., FRANKLIN, J. L., HIGGINBOTHAM, J. N., ZHANG, Q., ZIMMERMAN, L. J., LIEBLER, D. C., PING, J., LIU, Q., EVANS, R., FISSELL, W. H., PATTON, J. G., ROME, L. H., BURNETTE, D. T. & COFFEY, R. J. 2019. Reassessment of Exosome Composition. *Cell,* 177**,** 428-445.e18.

JOHNSON, S. M., BANYARD, A., SMITH, C., MIRONOV, A. & MCCABE, M. G. 2020. Large Extracellular Vesicles Can be Characterised by Multiplex Labelling Using Imaging Flow Cytometry. *International Journal of Molecular Sciences,* 21**,** 8723.

JOURNEAY, W. S., SURI, S. S., MORALEZ, J. G., FENNIRI, H. & SINGH, B. 2008. Low Inflammatory Activation by Self-Assembling Rosette Nanotubes in Human Calu-3 Pulmonary Epithelial Cells. *Small,* 4**,** 817-823.

JURKIEWICZ, K., JUTEL, M. & SMOLINSKA, S. 2025. Update on HDM Allergy: Principal Changes over the Years. *International Journal of Molecular Sciences,* 26**,** 5660.

KALSHEKER, N. A., DEAM, S., CHAMBERS, L., SREEDHARAN, S., BROCKLEHURST, K. & LOMAS, D. A. 1996. The House Dust Mite AllergenDer p1 Catalytically Inactivates α1-Antitrypsin by Specific Reactive Centre Loop Cleavage: A Mechanism That Promotes Airway Inflammation and Asthma. *Biochemical and Biophysical Research Communications,* 221**,** 59-61.

KAUFFMAN, H. F., TAMM, M., TIMMERMAN, J. A. B. & BORGER, P. 2006. House dust mite major allergens Der p 1 and Der p 5 activate human airway-derived epithelial cells by protease-dependent and protease-independent mechanisms. *Clinical and Molecular Allergy,* 4**,** 5.

KAUFMANN, S. H. E. 2019. Immunology's Coming of Age. *Frontiers in Immunology,* 10**,** 684.

KERYAKOUS, M. M. S., HASHEM, M. A. M., HASAN, E. I., HAFEZ, S. M. N. A. & HASAN, D. M. A. 2022. Interleukin 6 as a Novel Biomarker for Differentiating Drowning from Postmortem Submersion. *NeuroQuantology: An Interdisciplinary Journal of Neuroscience and Quantum Physics,* 20**,** 3467+.

KEUMATIO DOUNGSTOP, B. C., VAN VLIET, S. J., VAN REE, R., DE JONG, E. C. & VAN KOOYK, Y. 2021. Carbohydrates in allergy: from disease to novel immunotherapies. *Trends in Immunology,* 42**,** 635-648.

KHAMINA, K., DIENDORFER, A. B., SKALICKY, S., WEIGL, M., PULTAR, M., KRAMMER, T. L., FOURNIER, C. A., SCHOFIELD, A. L., OTTO, C., SMITH, A. T., BUCHTELE, N., SCHOERGENHOFER, C., JILMA, B., FRANK, B. J. H., HOFSTAETTER, J. G., GRILLARI, R., GRILLARI, J., RUPRECHT, K., GOLDRING, C. E., REHRAUER, H., GLAAB, W. E. & HACKL, M. 2022. A MicroRNA Next-Generation-Sequencing Discovery Assay (miND) for Genome-Scale Analysis and Absolute Quantitation of Circulating MicroRNA Biomarkers. *International Journal of Molecular Sciences,* 23**,** 1226.

KIM, B. K., YANG, M. S., SRIVASTAVA, U., PIPARIA, S., SHARMA, R., TIWARI, A., KHO, A., WONG, R., CELEDÓN, J. C., WEISS, S. T., MCGEACHIE, M. & TANTISIRA, K. 2025a. MiR-107 and Its Association With House Dust Mite Sensitisation: Implications for Asthma. *Clinical & Experimental Allergy,* 55**,** 67-74.

KIM, K. A., JUNG, J. H., KANG, I. G., CHOI, Y. S. & KIM, S. T. 2018. ROS Is Involved in Disruption of Tight Junctions of Human Nasal Epithelial Cells Induced by HRV16. *The Laryngoscope,* 128**,** E393-E401.

KIM, S.-Y., KERR, G. H., VAN DONKELAAR, A., MARTIN, R. V., WEST, J. J. & ANENBERG, S. C. 2025b. Tracking air pollution and CO2 emissions in 13,189 urban areas worldwide using large geospatial datasets. *Communications Earth & Environment,* 6**,** 311.

KOLONICS, F., SZEIFERT, V., TIMÁR, C. I., LIGETI, E. & LŐRINCZ, Á. M. 2020. The Functional Heterogeneity of Neutrophil-Derived Extracellular Vesicles Reflects the Status of the Parent Cell. *Cells,* 9**,** 2718.

KORTEKAAS KROHN, I., SEYS, S. F., LUND, G., JONCKHEERE, A. C., DIERCKX DE CASTERLÉ, I., CEUPPENS, J. L., STEELANT, B. & HELLINGS, P. W. 2020. Nasal epithelial barrier dysfunction increases sensitization and mast cell degranulation in the absence of allergic inflammation. *Allergy,* 75**,** 1155-1164.

KRIEGER, S. M., BOVERHOF, D. R., WOOLHISER, M. R. & HOTCHKISS, J. A. 2013. Assessment of the respiratory sensitization potential of proteins using an enhanced mouse intranasal test (MINT). *Food and Chemical Toxicology,* 59**,** 165-176.

KRISHNAMURTHY, P. & KAPLAN, M. H. 2016. STAT6 and PARP Family Members in the Development of T Cell-dependent Allergic Inflammation. *Immune Network,* 16**,** 201.

KUGERATSKI, F. G., HODGE, K., LILLA, S., MCANDREWS, K. M., ZHOU, X., HWANG, R. F., ZANIVAN, S. & KALLURI, R. 2021. Quantitative proteomics identifies the core proteome of exosomes with syntenin-1 as the highest abundant protein and a putative universal biomarker. *Nature Cell Biology,* 23**,** 631-641.

KULIS, M. D., SMEEKENS, J. M., IMMORMINO, R. M. & MORAN, T. P. 2021. The airway as a route of sensitization to peanut: An update to the dual allergen exposure hypothesis. *Journal of Allergy and Clinical Immunology,* 148**,** 689-693.

KULSHRESHTHA, A., AHMAD, T., AGRAWAL, A. & GHOSH, B. 2013. Proinflammatory role of epithelial cell-derived exosomes in allergic airway inflammation. *Journal of Allergy and Clinical Immunology,* 131(4)**,** 1194-1203.e14.

KURTJAK, M., KEREÏCHE, S., KLEPAC, D., KRIŽAN, H., PERČIĆ, M., KRUŠIĆ ALIĆ, V., LAVRIN, T., LENASSI, M., WECHTERSBACH, K., KOJC, N., VUKOMANOVIĆ, M., ZRNA, S., BIBERIĆ, M., DOMITROVIĆ, R., GRABUŠIĆ, K. & MALENICA, M. 2022. Unveiling the Native Morphology of Extracellular Vesicles from Human Cerebrospinal Fluid by Atomic Force and Cryogenic Electron Microscopy. *Biomedicines,* 10**,** 1251.

L. MILES, F., E. LYNCH, J. & A. SIKES, R. 2015. Cell-based assays using calcein acetoxymethyl ester show variation in fluorescence with treatment conditions. *Journal of Biological Methods,* 2**,** 1.

LAM, T., QUACH, H. T., HALL, L., ABOU CHAKRA, M. & WONG, A. P. 2025. A multidisciplinary approach towards modeling of a virtual human lung. *npj Systems Biology and Applications,* 11**,** 38.

LAMBRING, C. B., SIRAJ, S., PATEL, K., SANKPAL, U. T., MATHEW, S. & BASHA, R. 2019. Impact of the Microbiome on the Immune System. *Critical Reviews in Immunology,* 39**,** 313-328.

LAMIABLE, O., MAYER, J. U., MUNOZ-ERAZO, L. & RONCHESE, F. 2020. Dendritic cells in Th2 immune responses and allergic sensitization. *Immunology & Cell Biology,* 98**,** 807-818.

LANGMEAD, B., TRAPNELL, C., POP, M. & SALZBERG, S. L. 2009. Ultrafast and memory-efficient alignment of short DNA sequences to the human genome. *Genome Biology,* 10**,** R25.

LEE, R. E., REIDEL, B., NELSON, M. R., MACDONALD, J. K., KESIMER, M. & RANDELL, S. H. 2023. Air-Liquid interface cultures to model drug delivery through the mucociliary epithelial barrier. *Advanced Drug Delivery Reviews,* 198**,** 114866.

LEVER, A. R., PARK, H., MULHERN, T. J., JACKSON, G. R., COMOLLI, J. C., BORENSTEIN, J. T., HAYDEN, P. J. & PRANTIL-BAUN, R. 2015. Comprehensive evaluation of poly(I:C) induced inflammatory response in an airway epithelial model. *Physiological Reports,* 3**,** e12334.

LI, H., WANG, Y. M. & HAN, X. L. 2023. ESP-B4 promotes nasal epithelial cell-derived extracellular vesicles containing miR-146a-5p to modulate Smad3/GATA-3 thus relieving allergic rhinitis ESP-B4/miR-146a-5p in AR. *Phytomedicine,* 108**,** 13.

LI, Y., AN, R., WU, M., HE, J. & HE, X. 2024a. miR-224-5p Attenuates Allergic Responses in Mice with Allergic Rhinitis by Modulating the Th1/Th2 Response. *Analytical Cellular Pathology,* 2024**,** 1-13.

LI, Y., ZHU, L., WEI, J., WU, C., ZHAO, Z., NORBÄCK, D., ZHANG, X., LU, C., YU, W., WANG, T., ZHENG, X., ZHANG, L. & ZHANG, Y. 2024b. Intrauterine and early postnatal exposures to submicron particulate matter and childhood allergic rhinitis: A multicity cross-sectional study in China. *Environmental Research,* 247**,** 118165.

LI, Z., ZHENG, N., AN, Q., LI, X., SUN, S., ZHANG, W., JI, Y., WANG, S. & LI, P. 2022. Impact of environmental factors and bacterial interactions on dust mite allergens in different indoor dust. *Science of The Total Environment,* 844**,** 157177.

LICHTERMAN, J. N. & REDDY, S. M. 2021. Mast Cells: A New Frontier for Cancer Immunotherapy. *Cells,* 10**,** 1270.

LIEW, F. Y., GIRARD, J.-P. & TURNQUIST, H. R. 2016. Interleukin-33 in health and disease. *Nature Reviews Immunology,* 16**,** 676-689.

LIU, A. H. 2002. Endotoxin exposure in allergy and asthma: Reconciling a paradox. *Journal of Allergy and Clinical Immunology,* 109**,** 379-392.

LÖTVALL, J., HILL, A. F., HOCHBERG, F., BUZÁS, E. I., DI VIZIO, D., GARDINER, C., GHO, Y. S., KUROCHKIN, I. V., MATHIVANAN, S., QUESENBERRY, P., SAHOO, S., TAHARA, H., WAUBEN, M. H., WITWER, K. W. & THÉRY, C. 2014. Minimal experimental requirements for definition of extracellular vesicles and their functions: a position statement from the International Society for Extracellular Vesicles. *Journal of Extracellular Vesicles,* 3**,** 26913.

LOVE, M. I., HUBER, W. & ANDERS, S. 2014. Moderated estimation of fold change and dispersion for RNA-seq data with DESeq2. *Genome Biology,* 15**,** 550.

LUCCHETTI, D., BATTAGLIA, A., RICCIARDI-TENORE, C., COLELLA, F., PERELLI, L., DE MARIA, R., SCAMBIA, G., SGAMBATO, A. & FATTOROSSI, A. 2020. Measuring Extracellular Vesicles by Conventional Flow Cytometry: Dream or Reality? *International Journal of Molecular Sciences,* 21**,** 6257.

LUNDEQUIST, A. & PEJLER, G. 2011. Biological implications of preformed mast cell mediators. *Cellular and Molecular Life Sciences,* 68**,** 965-975.

LUO, S., LIN, H., WU, C., ZHU, L., HUA, Q., WENG, Y., WANG, L., FAN, X., ZHAO, K.-B., LIU, G., WANG, Y., CHEN, H.-T., XU, L. & ZHENG, L. 2024. Cholinergic macrophages promote the resolution of peritoneal inflammation. *Proceedings of the National Academy of Sciences,* 121**,** e2402143121.

LUO, X., HAN, M. M., LIU, J. Q., WANG, Y., LUO, X. Q., ZHENG, J., WANG, S., LIU, Z. G., LIU, D. B., YANG, P. C. & LI, H. B. 2015. Epithelial cell-derived micro RNA-146a generates interleukin-10-producing monocytes to inhibit nasal allergy. *Scientific Reports,* 5**,** 10.

MAEDA, K., CALDEZ, M. J. & AKIRA, S. 2019. Innate immunity in allergy. *Allergy,* 74**,** 1660-1674.

MARTIN, M. 2011. Cutadapt removes adapter sequences from high-throughput sequencing reads. *EMBnet.journal,* 17**,** 10.

MARTIN, R. A., ATHER, J. L., LUNDBLAD, L. K. A., SURATT, B. T., BOYSON, J. E., BUDD, R. C., ALCORN, J. F., FLAVELL, R. A., EISENBARTH, S. C. & POYNTER, M. E. 2013. Interleukin-1 Receptor and Caspase-1 Are Required for the Th17 Response in Nitrogen Dioxide–Promoted Allergic Airway Disease. *American Journal of Respiratory Cell and Molecular Biology,* 48**,** 655-664.

MATTHEWS, A. A., EE, P. L. R. & GE, R. 2020. Developing inhaled protein therapeutics for lung diseases. *Molecular Biomedicine,* 1**,** 11.

MCALEES, J. W., WHITEHEAD, G. S., HARLEY, I. T., CAPPELLETTI, M., REWERTS, C. L., HOLDCROFT, A. M., DIVANOVIC, S., WILLS-KARP, M., FINKELMAN, F. D., KARP, C. L. & COOK, D. N. 2015. Distinct Tlr4-expressing cell compartments control

neutrophilic and eosinophilic airway inflammation. *Mucosal Immunology,* 8**,** 863-873.

MCCLURE, R. & MASSARI, P. 2014. TLR-Dependent Human Mucosal Epithelial Cell Responses to Microbial Pathogens. *Frontiers in Immunology,* 5**,** 386.

MCKINNON, K. M. 2018. Flow Cytometry: An Overview. *Current Protocols in Immunology,* 120**,** 5 1 1-5 1 11.

MEDZHITOV, R., PRESTON-HURLBURT, P. & JANEWAY, C. A. 1997. A human homologue of the Drosophila Toll protein signals activation of adaptive immunity. *Nature,* 388**,** 394-397.

MEIER, K., LEHR, C.-M. & DAUM, N. 2009. Differentiation potential of human pancreatic stem cells for epithelial- and endothelial-like cell types. *Annals of Anatomy - Anatomischer Anzeiger,* 191**,** 70-82.

MELNIKOVA, D. N., POTAPOV, A. E., OVCHINNIKOVA, T. V. & BOGDANOV, I. V. 2025. Modeling Human Airway Epithelial Barrier Penetration Using Birch Bet v 1 and Alder Aln g 1 Pollen Allergens During Sensitization Process. *International Journal of Molecular Sciences,* 26**,** 5169.

MENG, J., XIAO, H., XU, F., SHE, X., LIU, C. & CANONICA, G. W. 2025. Systemic barrier dysfunction in type 2 inflammation diseases: perspective in the skin, airways, and gastrointestinal tract. *Immunologic Research,* 73**,** 60.

MESTAS, J. & HUGHES, C. C. W. 2004. Of Mice and Not Men: Differences between Mouse and Human Immunology. *The Journal of Immunology,* 172**,** 2731-2738.

MICHAUDEL, C., MACKOWIAK, C., MAILLET, I., FAUCONNIER, L., AKDIS, C. A., SOKOLOWSKA, M., DREHER, A., TAN, H.-T. T., QUESNIAUX, V. F., RYFFEL, B. & TOGBE, D. 2018. Ozone exposure induces respiratory barrier biphasic injury and inflammation controlled by IL-33. *Journal of Allergy and Clinical Immunology,* 142**,** 942-958.

MILLER, A. J. & SPENCE, J. R. 2017. In Vitro Models to Study Human Lung Development, Disease and Homeostasis. *Physiology,* 32**,** 246-260.

MIMASAKA, S., HASHIYADA, M., NATA, M. & FUNAYAMA, M. 2001. Correlation between Serum IL-6 Levels and Death: Usefulness in Diagnosis of "Traumatic Shock"? *The Tohoku Journal of Experimental Medicine,* 193**,** 319-324.

MIRANDA-WALDETARIO, M. C. G. & MARIA, A. 2024. Oral tolerance to dietary antigens and Foxp3⁺ regulatory T cells. *Immunological Reviews,* 326**,** 8-16.

MIYABARA, Y., TAKANO, H., ICHINOSE, T., LIM, H.-B. & SAGAI, M. 1998. Diesel Exhaust Enhances Allergic Airway Inflammation and Hyperresponsiveness in Mice. *American Journal of Respiratory and Critical Care Medicine,* 157**,** 1138-1144.

MIYATA, M., HATSUSHIKA, K., ANDO, T., SHIMOKAWA, N., OHNUMA, Y., KATOH, R., SUTO, H., OGAWA, H., MASUYAMA, K. & NAKAO, A. 2008. Mast cell regulation of epithelial TSLP expression plays an important role in the development of allergic rhinitis. *European Journal of Immunology,* 38**,** 1487-1492.

MIZENKO, R. R., BROSTOFF, T., ROJALIN, T., KOSTER, H. J., SWINDELL, H. S., LEISEROWITZ, G. S., WANG, A. & CARNEY, R. P. 2021. Tetraspanins are

unevenly distributed across single extracellular vesicles and bias sensitivity to multiplexed cancer biomarkers. *Journal of Nanobiotechnology,* 19**,** 250.

MOHAMMADIPOOR, A., HERSHFIELD, M. R., LINSENBARDT, H. R., SMITH, J., MACK, J., NATESAN, S., AVERITT, D. L., STARK, T. R. & SOSANYA, N. M. 2023. Biological function of Extracellular Vesicles (EVs): a review of the field. *Molecular Biology Reports,* 50**,** 8639-8651.

MOMTAZMANESH, S. & REZAEI, N. 2022. Hypersensitivity. *Encyclopedia of Infection and Immunity.* Elsevier.

MORALES-KASTRESANA, A. & JONES, J. C. 2017. Flow Cytometric Analysis of Extracellular Vesicles. Springer New York.

MORITA, I. 2002. Distinct functions of COX-1 and COX-2. *Prostaglandins & Other Lipid Mediators,* 68-69**,** 165-175.

MOWEN, K. A. & GLIMCHER, L. H. 2004. Signaling pathways in Th2 development. *Immunological Reviews,* 202**,** 203-222.

MUCIDA, D. 2005. Oral tolerance in the absence of naturally occurring Tregs. *Journal of Clinical Investigation,* 115**,** 1923-1933.

MURAYAMA, Y., SHINOMURA, Y., ORITANI, K., MIYAGAWA, J. I., YOSHIDA, H., NISHIDA, M., KATSUBE, F., SHIRAGA, M., MIYAZAKI, T., NAKAMOTO, T., TSUTSUI, S., TAMURA, S., HIGASHIYAMA, S., SHIMOMURA, I. & HAYASHI, N. 2008. The tetraspanin CD9 modulates epidermal growth factor receptor signaling in cancer cells. *Journal of Cellular Physiology,* 216**,** 135-143.

MURPHY, K., WEAVER, C., LESLIEBERG & BARTON, G. 2022. *Janeway's Immunobiology,* New York, W.W. Norton and Company.

NABHAN, J. F., HU, R., OH, R. S., COHEN, S. N. & LU, Q. 2012. Formation and release of arrestin domain-containing protein 1-mediated microvesicles (ARMMs) at plasma membrane by recruitment of TSG101 protein. *Proceedings of the National Academy of Sciences,* 109**,** 4146-4151.

NABIPUR, L., MOUAWAD, M. & K. AGRAWAL, D. 2025. Bioaerosols and Airway Diseases: Mechanisms of Epithelial Dysfunction, Immune Activation, and Strategies for Exposure Mitigation. *Archives of Internal Medicine Research,* 8**,** 178-191.

NACLERIO, R. M., PROUD, D., TOGIAS, A. G., ADKINSON, N. F., MEYERS, D. A., KAGEY-SOBOTKA, A., PLAUT, M., NORMAN, P. S. & LICHTENSTEIN, L. M. 1985. Inflammatory Mediators in Late Antigen-Induced Rhinitis. *New England Journal of Medicine,* 313**,** 65-70.

NASO, M., TRINCIANTI, C., TOSCA, M. A. & CIPRANDI, G. 2025. Quercetin and Its Lecithin-Based Formulation: Potential Applications for Allergic Diseases Based on a Narrative Review. *Nutrients,* 17**,** 1476.

NAZARENKO, I., RANA, S., BAUMANN, A., MCALEAR, J., HELLWIG, A., TRENDELENBURG, M., LOCHNIT, G., PREISSNER, K. T. & ZÖLLER, M. 2010. Cell Surface Tetraspanin Tspan8 Contributes to Molecular Pathways of Exosome-Induced Endothelial Cell Activation. *Cancer Research,* 70**,** 1668-1678.

NÉMETH, A., ORGOVAN, N., SÓDAR, B. W., OSTEIKOETXEA, X., PÁLÓCZI, K., SZABÓ-TAYLOR, K. É., VUKMAN, K. V., KITTEL, Á., TURIÁK, L., WIENER, Z., TÓTH, S., DRAHOS, L., VÉKEY, K., HORVATH, R. & BUZÁS, E. I. 2017. Antibiotic-induced

release of small extracellular vesicles (exosomes) with surface-associated DNA. *Scientific Reports,* 7**,** 8202.

NICHOLS, J. E., NILES, J. A., VEGA, S. P., ARGUETA, L. B., EASTAWAY, A. & CORTIELLA, J. 2014. Modeling the lung: Design and development of tissue engineered macro- and micro-physiologic lung models for research use. *Experimental Biology and Medicine,* 239**,** 1135-1169.

NUR HUSNA, S. M., SITI SARAH, C. O., TAN, H.-T. T., MD. SHUKRI, N., MOHD ASHARI, N. S. & WONG, K. K. 2021a. Reduced occludin and claudin-7 expression is associated with urban locations and exposure to second-hand smoke in allergic rhinitis patients. *Scientific Reports,* 11**,** 1245.

NUR HUSNA, S. M., TAN, H.-T. T., MD SHUKRI, N., MOHD ASHARI, N. S. & WONG, K. K. 2021b. Nasal Epithelial Barrier Integrity and Tight Junctions Disruption in Allergic Rhinitis: Overview and Pathogenic Insights. *Frontiers in Immunology,* 12**,** 663626.

OBER, C., SPERLING, A. I., VON MUTIUS, E. & VERCELLI, D. 2017. Immune development and environment: lessons from Amish and Hutterite children. *Current Opinion in Immunology,* 48**,** 51-60.

OBER, C. & YAO, T. C. 2011. The genetics of asthma and allergic disease: a 21st century perspective. *Immunological Reviews,* 242**,** 10-30.

OBERSTEINER, A., GILLES, S., FRANK, U., BECK, I., HÄRING, F., ERNST, D., ROTHBALLER, M., HARTMANN, A., TRAIDL-HOFFMANN, C. & SCHMID, M. 2016. Pollen-Associated Microbiome Correlates with Pollution Parameters and the Allergenicity of Pollen. *PLOS ONE,* 11**,** e0149545.

OGI, K., RAMEZANPOUR, M., LIU, S., FERDOUSH TULI, J., BENNETT, C., SUZUKI, M., FUJIEDA, S., PSALTIS, A. J., WORMALD, P.-J. & VREUGDE, S. 2021. Der p 1 Disrupts the Epithelial Barrier and Induces IL-6 Production in Patients With House Dust Mite Allergic Rhinitis. *Frontiers in Allergy,* 2**,** 692049.

OKADA-TSUCHIOKA, M., KAJITANI, N., OMORI, W., KURASHIGE, T., BOKU, S. & TAKEBAYASHI, M. 2022. Tetraspanin heterogeneity of small extracellular vesicles in human biofluids and brain tissue. *Biochem Biophys Res Commun,* 627**,** 146-151.

OKADA, H., KUHN, C., FEILLET, H. & BACH, J. F. 2010. The 'hygiene hypothesis' for autoimmune and allergic diseases: an update. *Clinical and Experimental Immunology,* 160**,** 1-9.

OLIVEIRA-NASCIMENTO, L., MASSARI, P. & WETZLER, L. M. 2012. The Role of TLR2 in Infection and Immunity. *Frontiers in Immunology,* 3**,** 79.

OSKERITZIAN, C. A., ZHAO, W., MIN, H.-K., XIA, H.-Z., POZEZ, A., KIEV, J. & SCHWARTZ, L. B. 2005. Surface CD88 functionally distinguishes the MCTC from the MCT type of human lung mast cell. *Journal of Allergy and Clinical Immunology,* 115**,** 1162-1168.

OSTEIKOETXEA, X., SÓDAR, B., NÉMETH, A., SZABÓ-TAYLOR, K., PÁLÓCZI, K., VUKMAN, K. V., TAMÁSI, V., BALOGH, A., KITTEL, Á., PÁLLINGER, É. & BUZÁS, E. I. 2015. Differential detergent sensitivity of extracellular vesicle subpopulations. *Organic & Biomolecular Chemistry,* 13**,** 9775-9782.

OUYANG, W., LÖHNING, M., GAO, Z., ASSENMACHER, M., RANGANATH, S., RADBRUCH, A. & MURPHY, K. M. 2000. Stat6-Independent GATA-3

Autoactivation Directs IL-4-Independent Th2 Development and Commitment. *Immunity,* 12**,** 27-37.

PALANIYANDI, S., TOMEI, E., LI, Z., CONRAD, D. H. & ZHU, X. 2011. CD23-Dependent Transcytosis of IgE and Immune Complex across the Polarized Human Respiratory Epithelial Cells. *The Journal of Immunology,* 186**,** 3484-3496.

PARK, M., LEE, J. S. & PARK, M. K. 2019. The Effects of Air Pollutants on the Prevalence of Common Ear, Nose, and Throat Diseases in South Korea: A National Population-Based Study. *Clinical and Experimental Otorhinolaryngology,* 12**,** 294-300.

PASTWIŃSKA, J., AGIER, J., DASTYCH, J. & BRZEZIŃSKA-BŁASZCZYK, E. 2017. Mast cells as the strength of the inflammatory process. *Polish Journal of Pathology,* 68**,** 187-196.

PAWANKAR, R. 2014. Allergic diseases and asthma: a global public health concern and a call to action. *World Allergy Organ J,* 7**,** 12.

PENG, Y. Q., WU, Z. C., XU, Z. B., FANG, S. B., CHEN, D. H., ZHANG, H. Y., LIU, X. Q., HE, B. X., CHEN, D., AKDIS, C. A. & FU, Q. L. 2022. Mesenchymal stromal cells-derived small extracellular vesicles modulate DC function to suppress Th2 responses via IL-10 in patients with allergic rhinitis. *European Journal of Immunology,* 52**,** 1129-1140.

PETERS, R. L., SORIANO, V. X., ALLEN, K. J., TANG, M. L. K., PERRETT, K. P., LOWE, A. J., WIJESURIYA, R., PARKER, K. M., LOKE, P., DHARMAGE, S. C. & KOPLIN, J. J. 2024. The Prevalence of IgE-Mediated Food Allergy and Other Allergic Diseases in the First 10 Years: The Population-Based, Longitudinal HealthNuts Study. *The Journal of Allergy and Clinical Immunology: In Practice,* 12**,** 1819-1830.e3.

PFEFFERLE, P. I., KEBER, C. U., COHEN, R. M. & GARN, H. 2021. The Hygiene Hypothesis – Learning From but Not Living in the Past. *Frontiers in Immunology,* 12**,** 635935.

PIÑEIRO-HERMIDA, S., GREGORY, J. A., LÓPEZ, I. P., TORRENS, R., RUÍZ-MARTÍNEZ, C., ADNER, M. & PICHEL, J. G. 2017. Attenuated airway hyperresponsiveness and mucus secretion in <scp>HDM</scp>-exposed Igf1r-deficient mice. *Allergy,* 72**,** 1317-1326.

PIRQUET, C. V. 1906. Allergie. *Münchener Medizinische Wochenschrift,* 53**,** 1457.

POLAK, D., HAFNER, C., BRIZA, P., KITZMÜLLER, C., ELBE-BÜRGER, A., SAMADI, N., GSCHWANDTNER, M., PFÜTZNER, W., ZLABINGER, G. J., JAHN-SCHMID, B. & BOHLE, B. 2019. A novel role for neutrophils in IgE-mediated allergy: Evidence for antigen presentation in late-phase reactions. *Journal of Allergy and Clinical Immunology,* 143**,** 1143-1152.e4.

PORTELLI, M. A., HODGE, E. & SAYERS, I. 2015. Genetic risk factors for the development of allergic disease identified by genome-wide association. *Clinical & Experimental Allergy,* 45**,** 21-31.

POTHOVEN, K. L. & SCHLEIMER, R. P. 2017. The barrier hypothesis and Oncostatin M: Restoration of epithelial barrier function as a novel therapeutic strategy for the treatment of type 2 inflammatory disease. *Tissue Barriers,* 5**,** e1341367.

PRADO, N., CAÑAMERO, M., VILLALBA, M., RODRÍGUEZ, R. & BATANERO, E. 2010. Bystander suppression to unrelated allergen sensitization through intranasal

administration of tolerogenic exosomes in mouse. *Mol Immunol,* 47**,** 2148-51.

PRADO, N., DE LINARES, C., SANZ, M. L., GAMBOA, P., VILLALBA, M., RODRÍGUEZ, R. & BATANERO, E. 2015. Pollensomes as Natural Vehicles for Pollen Allergens. *The Journal of Immunology,* 195**,** 445-449.

PRADO, N., MARAZUELA, E. G., SEGURA, E., FERNÁNDEZ-GARCÍA, H., VILLALBA, M., THÉRY, C., RODRÍGUEZ, R. & BATANERO, E. 2008. Exosomes from bronchoalveolar fluid of tolerized mice prevent allergic reaction. *Journal of Immunology,* 181**,** 1519-1525.

PRESCOTT, S. L., MACAUBAS, C., SMALLACOMBE, T., HOLT, B. J., SLY, P. D. & HOLT, P. G. 1999. Development of allergen-specific T-cell memory in atopic and normal children. *The Lancet,* 353**,** 196-200.

QIU, S., DU, Y., DUAN, X., GENG, X., XIE, J., GAO, H. & YANG, P. C. 2011. Cytotoxic T lymphocytes mediate chronic inflammation of the nasal mucosa of patients with atypical allergic rhinitis. *N Am J Med Sci,* 3**,** 378-83.

QIU, S. Q., DUAN, X. B., GENG, X. R., XIE, J. X. & GAO, H. 2012. Antigen-specific activities of CD8+T cells in the nasal mucosa of patients with nasal allergy. *Asian Pacific Journal of Allergy and Immunology,* 30**,** 107-113.

RAMU, S., AKBARSHAHI, H., MOGREN, S., BERLIN, F., CERPS, S., MENZEL, M., HVIDTFELDT, M., PORSBJERG, C., ULLER, L. & ANDERSSON, C. K. 2021. Direct effects of mast cell proteases, tryptase and chymase, on bronchial epithelial integrity proteins and anti-viral responses. *BMC Immunology,* 22**,** 35.

RAPOSO, G., NIJMAN, H. W., STOORVOGEL, W., LIEJENDEKKER, R., HARDING, C. V., MELIEF, C. J. & GEUZE, H. J. 1996. B lymphocytes secrete antigen-presenting vesicles. *The Journal of experimental medicine,* 183**,** 1161-1172.

RAUTAVA, S., RUUSKANEN, O., OUWEHAND, A., SALMINEN, S. & ISOLAURI, E. 2004. The Hygiene Hypothesis of Atopic Disease—An Extended Version. *Journal of Pediatric Gastroenterology and Nutrition,* 38**,** 378-388.

REES, P., SUMMERS, H. D., FILBY, A., CARPENTER, A. E. & DOAN, M. 2022. Imaging flow cytometry. *Nature Reviews Methods Primers,* 2.

REGUEIRO, V. N., MORANTA, D., CAMPOS, M. A., MARGARETO, J., GARMENDIA, J. & BENGOECHEA, J. A. 2009. Klebsiella pneumoniae Increases the Levels of Toll-Like Receptors 2 and 4 in Human Airway Epithelial Cells. *Infection and Immunity,* 77**,** 714-724.

ROBINSON, M. D., MCCARTHY, D. J. & SMYTH, G. K. 2010. <tt>edgeR</tt>: a Bioconductor package for differential expression analysis of digital gene expression data. *Bioinformatics,* 26**,** 139-140.

ROCHA-PERUGINI, V., MARTÍNEZ DEL HOYO, G., GONZÁLEZ-GRANADO, J. M., RAMÍREZ-HUESCA, M., ZORITA, V., RUBINSTEIN, E., BOUCHEIX, C. & SÁNCHEZ-MADRID, F. 2017. CD9 Regulates Major Histocompatibility Complex Class II Trafficking in Monocyte-Derived Dendritic Cells. *Molecular and Cellular Biology,* 37**,** MCB.00202-17.

RODUIT, C., FREI, R., DEPNER, M., SCHAUB, B., LOSS, G., GENUNEIT, J., PFEFFERLE, P., HYVÄRINEN, A., KARVONEN, A. M., RIEDLER, J., DALPHIN, J.-C., PEKKANEN, J., VON MUTIUS, E., BRAUN-FAHRLÄNDER, C. & LAUENER, R. 2014. Increased food diversity in the first year of life is inversely associated with allergic diseases. *Journal of Allergy and Clinical Immunology,* 133**,** 1056-1064.e7.

ROSSI, O., KARCZEWSKI, J., STOLTE, E. H., BRUMMER, R. J. M., VAN NIEUWENHOVEN, M. A., MEIJERINK, M., VAN NEERVEN, J. R. J., VAN IJZENDOORN, S. C. D., VAN BAARLEN, P. & WELLS, J. M. 2013. Vectorial secretion of interleukin-8 mediates autocrine signalling in intestinal epithelial cells via apically located CXCR1. *BMC Research Notes,* 6**,** 431.

ROYER, P.-J., EMARA, M., YANG, C., AL-GHOULEH, A., TIGHE, P., JONES, N., SEWELL, H. F., SHAKIB, F., MARTINEZ-POMARES, L. & GHAEMMAGHAMI, A. M. 2010. The Mannose Receptor Mediates the Uptake of Diverse Native Allergens by Dendritic Cells and Determines Allergen-Induced T Cell Polarization through Modulation of IDO Activity. *The Journal of Immunology,* 185**,** 1522-1531.

RUIZ GARCÍA, S., DEPREZ, M., LEBRIGAND, K., CAVARD, A., PAQUET, A., ARGUEL, M.-J., MAGNONE, V., TRUCHI, M., CABALLERO, I., LEROY, S., MARQUETTE, C.-H., MARCET, B., BARBRY, P. & ZARAGOSI, L.-E. 2019. Novel dynamics of human mucociliary differentiation revealed by single-cell RNA sequencing of nasal epithelial cultures. *Development,* 146**,** dev.177428.

RUTKOWSKI, K., SOWA, P., RUTKOWSKA-TALIPSKA, J., SULKOWSKI, S. & RUTKOWSKI, R. 2014. Allergic diseases: the price of civilisational progress. *Advances in Dermatology and Allergology,* 2**,** 77-83.

SANGAPHUNCHAI, P., TODD, I. & FAIRCLOUGH, L. C. 2020. Extracellular vesicles and asthma: A review of the literature. *Clinical & Experimental Allergy,* 50**,** 291-307.

SCHAUBERGER, E., PEINHAUPT, M., CAZARES, T. & LINDSLEY, A. W. 2016. Lipid Mediators of Allergic Disease: Pathways, Treatments, and Emerging Therapeutic Targets. *Current Allergy and Asthma Reports,* 16**,** 48.

SCHULZ, C., FARKAS, L., WOLF, K., KRÄTZEL, K., EISSNER, G. & PFEIFER, M. 2002. Differences in LPS-Induced Activation of Bronchial Epithelial Cells (BEAS-2B) and Type II-Like Pneumocytes (A-549). *Scandinavian Journal of Immunology,* 56**,** 294-302.

SEDGWICK, A. E. & D'SOUZA-SCHOREY, C. 2018. The biology of extracellular microvesicles. *Traffic,* 19**,** 319-327.

SENGUPTA, A., DORN, A., JAMSHIDI, M., SCHWOB, M., HASSAN, W., DE MADDALENA, L. L., HUGI, A., STUCKI, A. O., DORN, P., MARTI, T. M., WISSER, O., STUCKI, J. D., KREBS, T., HOBI, N. & GUENAT, O. T. 2023. A multiplex inhalation platform to model in situ like aerosol delivery in a breathing lung-on-chip. *Frontiers in Pharmacology,* 14**,** 1114739.

SHAIK-DASTHAGIRISAHEB, Y. B., VARVARA, G., MURMURA, G., SAGGINI, A., POTALIVO, G., CARAFFA, A., ANTINOLFI, P., TETÈ, S., TRIPODI, D., CONTI, F., CIANCHETTI, E., TONIATO, E., ROSATI, M., CONTI, P., SPERANZA, L., PANTALONE, A., SAGGINI, R., THEOHARIDES, T. C. & PANDOLFI, F. 2013. Vascular Endothelial Growth Factor (VEGF), Mast Cells and Inflammation. *International Journal of Immunopathology and Pharmacology,* 26**,** 327-335.

SHETA, M., TAHA, E. A., LU, Y. & EGUCHI, T. 2023. Extracellular Vesicles: New Classification and Tumor Immunosuppression. *Biology,* 12**,** 110.

SHI, J., LUO, Q., CHEN, F., CHEN, D., XU, G. & LI, H. 2010. Induction of IL-6 and IL-8 by House Dust Mite Allergen Der p1 in Cultured Human Nasal Epithelial Cells Is Associated with PAR/PI3K/NFκB Signaling. *ORL,* 72**,** 256-265.

SHIN, T. S., KIM, J. H., KIM, Y. S., JEON, S. G., ZHU, Z., GHO, Y. S. & KIM, Y. K. 2010. Extracellular vesicles are key intercellular mediators in the development of immune dysfunction to allergens in the airways. *Allergy,* 65**,** 1256-65.

SHIN, T. S., PARK, J. Y., KIM, Y. K. & KIM, J. G. 2022. Extracellular vesicles derived from small intestinal lamina propria reduce antigen-specific immune response. *Korean J Intern Med,* 37**,** 85-95.

SHLOMOVITZ, I., ERLICH, Z., ARAD, G., EDRY-BOTZER, L., ZARGARIAN, S., COHEN, H., MANKO, T., OFIR-BIRIN, Y., COOKS, T., REGEV-RUDZKI, N. & GERLIC, M. 2021. Proteomic analysis of necroptotic extracellular vesicles. *Cell Death & Disease,* 12**,** 1059.

SHULMAN, S. T. 2016. Clemens von Pirquet: A Remarkable Life and Career. *Journal of the Pediatric Infectious Diseases Society,* 6**,** piw063.

SICHERER, S. H., FURLONG, T. J., MAES, H. H., DESNICK, R. J., SAMPSON, H. A. & GELB, B. D. 2000. Genetics of peanut allergy: A twin study. *Journal of Allergy and Clinical Immunology,* 106**,** 53-56.

SIMMONS, J. & GALLO, R. L. 2024. The Central Roles of Keratinocytes in Coordinating Skin Immunity. *Journal of Investigative Dermatology,* 144**,** 2377-2398.

SIMONS, F. E. R. & SIMONS, K. J. 2011. Histamine and H1-antihistamines: Celebrating a century of progress. *Journal of Allergy and Clinical Immunology,* 128**,** 1139-1150.e4.

SKOGBERG, G., LUNDBERG, V., BERGLUND, M., GUDMUNDSDOTTIR, J., TELEMO, E., LINDGREN, S. & EKWALL, O. 2015. Human thymic epithelial primary cells produce exosomes carrying tissue-restricted antigens. *Immunology & Cell Biology,* 93**,** 727-734.

SMEEKENS, J. M., IMMORMINO, R. M., BALOGH, P. A., RANDELL, S. H., KULIS, M. D. & MORAN, T. P. 2019. Indoor dust acts as an adjuvant to promote sensitization to peanut through the airway. *Clinical & Experimental Allergy,* 49**,** 1500-1511.

SMYTH, L. A., RATNASOTHY, K., TSANG, J. Y. S., BOARDMAN, D., WARLEY, A., LECHLER, R. & LOMBARDI, G. 2013. CD73 expression on extracellular vesicles derived from $CD4^+$ $CD25^+$ $Foxp3^+$ T cells contributes to their regulatory function. *European Journal of Immunology,* 43**,** 2430-2440.

SOH, W. T., ZHANG, J., HOLLENBERG, M. D., VLIAGOFTIS, H., ROTHENBERG, M. E., SOKOL, C. L., ROBINSON, C. & JACQUET, A. 2023. Protease allergens as initiators–regulators of allergic inflammation. *Allergy,* 78**,** 1148-1168.

SONNTAG, T., RAPP, M., DIDIER, P., LEBEAU, L., PONS, F. & CASSET, A. 2022. Mucus-producing epithelial models for investigating the activity of gene delivery systems in the lung. *International Journal of Pharmaceutics,* 614**,** 121423.

STEELANT, B., SEYS, S. F., VAN GERVEN, L., VAN WOENSEL, M., FARRÉ, R., WAWRZYNIAK, P., KORTEKAAS KROHN, I., BULLENS, D. M., TALAVERA, K., RAAP, U., BOON, L., AKDIS, C. A., BOECKXSTAENS, G., CEUPPENS, J. L. & HELLINGS, P. W. 2018. Histamine and T helper cytokine–driven epithelial barrier dysfunction in allergic rhinitis. *Journal of Allergy and Clinical Immunology,* 141**,** 951-963.e8.

STEWART, C. E., TORR, E. E., MOHD JAMILI, N. H., BOSQUILLON, C. & SAYERS, I. 2012. Evaluation of Differentiated Human Bronchial Epithelial Cell Culture Systems for Asthma Research. *Journal of Allergy,* 2012**,** 1-11.

STRACHAN, D. P. 1989. Hay fever, hygiene, and household size. *BMJ,* 299**,** 1259-1260.

SUGITA, K. & KABASHIMA, K. 2020. Tight junctions in the development of asthma, chronic rhinosinusitis, atopic dermatitis, eosinophilic esophagitis, and inflammatory bowel diseases. *Journal of Leukocyte Biology,* 107**,** 749-762.

SWEENEY, B. A., PETROV, A. I., BURKOV, B., FINN, R. D., BATEMAN, A., SZYMANSKI, M., KARLOWSKI, W. M., GORODKIN, J., SEEMANN, S. E., CANNONE, J. J., GUTELL, R. R., FEY, P., BASU, S., KAY, S., COCHRANE, G., BILLIS, K., EMMERT, D., MARYGOLD, S. J., HUNTLEY, R. P., LOVERING, R. C., FRANKISH, A., CHAN, P. P., LOWE, T. M., BRUFORD, E., SEAL, R., VANDESOMPELE, J., VOLDERS, P.-J., PARASKEVOPOULOU, M., MA, L., ZHANG, Z., GRIFFITHS-JONES, S., BUJNICKI, J. M., BOCCALETTO, P., BLAKE, J. A., BULT, C. J., CHEN, R., ZHAO, Y., WOOD, V., RUTHERFORD, K., RIVAS, E., COLE, J., LAULEDERKIND, S. J. F., SHIMOYAMA, M., GILLESPIE, M. E., ORLIC-MILACIC, M., KALVARI, I., NAWROCKI, E., ENGEL, S. R., CHERRY, J. M., TEAM, S., BERARDINI, T. Z., HATZIGEORGIOU, A., KARAGKOUNI, D., HOWE, K., DAVIS, P., DINGER, M., HE, S., YOSHIHAMA, M., KENMOCHI, N., STADLER, P. F. & WILLIAMS, K. P. 2019. RNAcentral: a hub of information for non-coding RNA sequences. *Nucleic Acids Research,* 47**,** D221-D229.

SZEIFERT, V., KOLONICS, F., BARTOS, B., KHAMARI, D., VÁGI, P., BARNA, L., LIGETI, E. & LŐRINCZ, Á. M. 2021. Mac-1 Receptor Clustering Initiates Production of Pro-Inflammatory, Antibacterial Extracellular Vesicles From Neutrophils. *Frontiers in Immunology,* 12**,** 671995.

TAKAHASHI, T., KATO, A., SUH, L. A., CARTER, R. G., STEVENS, W. W., PRICE, C. P. E., NORTON, J. E., WEIBMAN, A. R., HARRIS, K. E., PETERS, A. T., GRAMMER, L. C., WELCH, K., SHINTANI-SMITH, S., CONLEY, D. B., BERDNIKOVS, S., TAN, B. K., KERN, R. C. & SCHLEIMER, R. P. 2020. Integrin β6 microparticles in nasal lavage fluids; potential new biomarkers for basal cell activation in chronic rhinosinusitis. *Allergy,* 75**,** 3261-3264.

TAKAHASHI, T. & SCHLEIMER, R. P. 2021. Epithelial-Cell-Derived Extracellular Vesicles in Pathophysiology of Epithelial Injury and Repair in Chronic Rhinosinusitis: Connecting Immunology in Research Lab to Biomarkers in Clinics. *International Journal of Molecular Sciences,* 22**,** 11709.

TAKANO, K.-I., KOJIMA, T., GO, M., MURATA, M., ICHIMIYA, S., HIMI, T. & SAWADA, N. 2005. HLA-DR- and CD11c-positive Dendritic Cells Penetrate beyond Well-developed Epithelial Tight Junctions in Human Nasal Mucosa of Allergic Rhinitis. *Journal of Histochemistry & Cytochemistry,* 53**,** 611-619.

TENG, Z.-X., ZHOU, X.-C., XU, R.-T., ZHU, F.-Y., BING, X., GUO, N., SHI, L., QI, W.-W., LIU, C.-C. & XIA, M. 2022. Tfh Exosomes Derived from Allergic Rhinitis Promote DC Maturation Through miR-142-5p/CDK5/STAT3 Pathway. *Journal of Inflammation Research,* Volume 15**,** 3187-3205.

TERTEL, T., SCHOPPET, M., STAMBOULI, O., AL-JIPOURI, A., JAMES, P. F. & GIEBEL, B. 2022. Imaging flow cytometry challenges the usefulness of classically used extracellular vesicle labeling dyes and qualifies the novel dye Exoria for the labeling of mesenchymal stromal cell–extracellular vesicle preparations. *Cytotherapy,* 24**,** 619-628.

THÉRY, C., WITWER, K. W., AIKAWA, E., ALCARAZ, M. J., ANDERSON, J. D., ANDRIANTSITOHAINA, R., ANTONIOU, A., ARAB, T., ARCHER, F., ATKIN-SMITH, G. K., AYRE, D. C., BACH, J. M., BACHURSKI, D., BAHARVAND, H.,

BALAJ, L., BALDACCHINO, S., BAUER, N. N., BAXTER, A. A., BEBAWY, M., BECKHAM, C., BEDINA ZAVEC, A., BENMOUSSA, A., BERARDI, A. C., BERGESE, P., BIELSKA, E., BLENKIRON, C., BOBIS-WOZOWICZ, S., BOILARD, E., BOIREAU, W., BONGIOVANNI, A., BORRÀS, F. E., BOSCH, S., BOULANGER, C. M., BREAKEFIELD, X., BREGLIO, A. M., BRENNAN, M. Á., BRIGSTOCK, D. R., BRISSON, A., BROEKMAN, M. L., BROMBERG, J. F., BRYL-GÓRECKA, P., BUCH, S., BUCK, A. H., BURGER, D., BUSATTO, S., BUSCHMANN, D., BUSSOLATI, B., BUZÁS, E. I., BYRD, J. B., CAMUSSI, G., CARTER, D. R., CARUSO, S., CHAMLEY, L. W., CHANG, Y. T., CHEN, C., CHEN, S., CHENG, L., CHIN, A. R., CLAYTON, A., CLERICI, S. P., COCKS, A., COCUCCI, E., COFFEY, R. J., CORDEIRO-DA-SILVA, A., COUCH, Y., COUMANS, F. A., COYLE, B., CRESCITELLI, R., CRIADO, M. F., D'SOUZA-SCHOREY, C., DAS, S., DATTA CHAUDHURI, A., DE CANDIA, P., DE SANTANA, E. F., DE WEVER, O., DEL PORTILLO, H. A., DEMARET, T., DEVILLE, S., DEVITT, A., DHONDT, B., DI VIZIO, D., DIETERICH, L. C., DOLO, V., DOMINGUEZ RUBIO, A. P., DOMINICI, M., DOURADO, M. R., DRIEDONKS, T. A., DUARTE, F. V., DUNCAN, H. M., EICHENBERGER, R. M., EKSTRÖM, K., EL ANDALOUSSI, S., ELIE-CAILLE, C., ERDBRÜGGER, U., FALCÓN-PÉREZ, J. M., FATIMA, F., FISH, J. E., FLORES-BELLVER, M., FÖRSÖNITS, A., FRELET-BARRAND, A., et al. 2018. Minimal information for studies of extracellular vesicles 2018 (MISEV2018): a position statement of the International Society for Extracellular Vesicles and update of the MISEV2014 guidelines. *Journal of Extracellular Vesicles,* 7**,** 1535750.

TORDESILLAS, L., CUBELLS-BAEZA, N., GÓMEZ-CASADO, C., BERIN, C., ESTEBAN, V., BARCIK, W., O'MAHONY, L., RAMIREZ, C., PACIOS, L. F., GARRIDO-ARANDIA, M. & DÍAZ-PERALES, A. 2017. Mechanisms underlying induction of allergic sensitization by Pru p 3. *Clinical & Experimental Allergy,* 47**,** 1398-1408.

TORIBIO, V. & YÁÑEZ-MÓ, M. 2022. Tetraspanins interweave EV secretion, endosomal network dynamics and cellular metabolism. *European Journal of Cell Biology,* 101**,** 151229.

TORRES-BORREGO, J. & SÁNCHEZ-SOLÍS, M. 2023. Dissecting Airborne Allergens. *Journal of Clinical Medicine,* 12**,** 5856.

TOYOSHIMA, S., SAKAMOTO-SASAKI, T., KUROSAWA, Y., HAYAMA, K., MATSUDA, A., WATANABE, Y., TERUI, T., GON, Y., MATSUMOTO, K. & OKAYAMA, Y. 2021. miR103a-3p in extracellular vesicles from FcεRI-aggregated human mast cells enhances IL-5 production by group 2 innate lymphoid cells. *Journal of Allergy and Clinical Immunology,* 147**,** 1878-1891.

TRAJKOVIC, K., HSU, C., CHIANTIA, S., RAJENDRAN, L., WENZEL, D., WIELAND, F., SCHWILLE, P., BRÜGGER, B. & SIMONS, M. 2008. Ceramide Triggers Budding of Exosome Vesicles into Multivesicular Endosomes. *Science,* 319**,** 1244-1247.

TRICARICO, C., CLANCY, J. & D'SOUZA-SCHOREY, C. 2017. Biology and biogenesis of shed microvesicles. *Small GTPases,* 8**,** 220-232.

TRIVEDI, B., VALERIO, C. & SLATER, J. E. 2003. Endotoxin content of standardized allergen vaccines. *J Allergy Clin Immunol,* 111**,** 777-83.

TROMPETTE, A., DIVANOVIC, S., VISINTIN, A., BLANCHARD, C., HEGDE, R. S., MADAN, R., THORNE, P. S., WILLS-KARP, M., GIOANNINI, T. L., WEISS, J. P. & KARP, C. L. 2009. Allergenicity resulting from functional mimicry of a Toll-like receptor complex protein. *Nature,* 457**,** 585-588.

TRZPIS, M., MCLAUGHLIN, P. M. J., DE LEIJ, L. M. F. H. & HARMSEN, M. C. 2007. Epithelial Cell Adhesion Molecule. *The American Journal of Pathology,* 171**,** 386-395.

TUCIS, D., HOPKINS, G., BROWNE, W., JAMES, V., ONION, D. & FAIRCLOUGH, L. C. 2024. The Role of Extracellular Vesicles in Allergic Sensitization: A Systematic Review. *International Journal of Molecular Sciences,* 25**,** 4492.

TUNG, S. L., BOARDMAN, D. A., SEN, M., LETIZIA, M., PENG, Q., CIANCI, N., DIONI, L., CARLIN, L. M., LECHLER, R., BOLLATI, V., LOMBARDI, G. & SMYTH, L. A. 2018. Regulatory T cell-derived extracellular vesicles modify dendritic cell function. *Scientific Reports,* 8**,** 6065.

UZZAMAN, A. & CHO, S. H. 2012. Chapter 28: Classification of hypersensitivity reactions. *Allergy and Asthma Proceedings,* 33**,** 96-99.

VALLHOV, H., GUTZEIT, C., HULTENBY, K., VALENTA, R., GRÖNLUND, H. & SCHEYNIUS, A. 2015. Dendritic cell-derived exosomes carry the major cat allergen Fel d 1 and induce an allergic immune response. *Allergy,* 70**,** 1651-1655.

VAN DER POL, E., STURK, A., VAN LEEUWEN, T., NIEUWLAND, R., COUMANS, F., MOBARREZ, F., ARKESTEIJN, G., WAUBEN, M., SILJANDER, P. R. M., SÁNCHEZ-LÓPEZ, V., OTERO-CANDELERA, R., RAMÓN, L. A., DOLZ, S., VILA, V., MACKMAN, N., GEDDINGS, J., MULLIER, F., BAILLY, N., HAN, J. Y., KWAAN, H. C., WEISS, I. M., BUZÁS, E. I., PÁLLINGER, E., HARRISON, P., KRAAN, J., HEDLEY, B. D., LAZOLANGNER, A., ENJETI, A., NORRIS, P. J., PARIS, C., SUSEN, S., BONNEFOY, A., DELORME, I., CHANDLER, W. L., HAU, C., AASS, H. C. D., CONNOR, D., WU, X., DRAGOVIC, R., UOTILA, L. M., LACROIX, R. & ROBERT, S. 2018. Standardization of extracellular vesicle measurements by flow cytometry through vesicle diameter approximation. *Journal of Thrombosis and Haemostasis,* 16**,** 1236-1245.

VAN DEUN, J., MESTDAGH, P., AGOSTINIS, P., AKAY, Ö., ANAND, S., ANCKAERT, J., MARTINEZ, Z. A., BAETENS, T., BEGHEIN, E., BERTIER, L., BERX, G., BOERE, J., BOUKOURIS, S., BREMER, M., BUSCHMANN, D., BYRD, J. B., CASERT, C., CHENG, L., CMOCH, A., DAVELOOSE, D., DE SMEDT, E., DEMIRSOY, S., DEPOORTER, V., DHONDT, B., DRIEDONKS, T. A. P., DUDEK, A., ELSHARAWY, A., FLORIS, I., FOERS, A. D., GÄRTNER, K., GARG, A. D., GEEURICKX, E., GETTEMANS, J., GHAZAVI, F., GIEBEL, B., KORMELINK, T. G., HANCOCK, G., HELSMOORTEL, H., HILL, A. F., HYENNE, V., KALRA, H., KIM, D., KOWAL, J., KRAEMER, S., LEIDINGER, P., LEONELLI, C., LIANG, Y., LIPPENS, L., LIU, S., LO CICERO, A., MARTIN, S., MATHIVANAN, S., MATHIYALAGAN, P., MATUSEK, T., MILANI, G., MONGUIÓ-TORTAJADA, M., MUS, L. M., MUTH, D. C., NÉMETH, A., NOLTE-'T HOEN, E. N. M., O'DRISCOLL, L., PALMULLI, R., PFAFFL, M. W., PRIMDAL-BENGTSON, B., ROMANO, E., ROUSSEAU, Q., SAHOO, S., SAMPAIO, N., SAMUEL, M., SCICLUNA, B., SOEN, B., STEELS, A., SWINNEN, J. V., TAKATALO, M., THAMINY, S., THÉRY, C., TULKENS, J., VAN AUDENHOVE, I., VAN DER GREIN, S., VAN GOETHEM, A., VAN HERWIJNEN, M. J., VAN NIEL, G., VAN ROY, N., VAN VLIET, A. R., VANDAMME, N., VANHAUWAERT, S., VERGAUWEN, G., VERWEIJ, F., WALLAERT, A., WAUBEN, M., WITWER, K. W., ZONNEVELD, M. I., DE WEVER, O., VANDESOMPELE, J. & HENDRIX, A. 2017. EV-TRACK: transparent reporting and centralizing knowledge in extracellular vesicle research. *Nature Methods,* 14**,** 228-232.

VIEIRA BRAGA, F. A., KAR, G., BERG, M., CARPAIJ, O. A., POLANSKI, K., SIMON, L. M., BROUWER, S., GOMES, T., HESSE, L., JIANG, J., FASOULI, E. S., EFREMOVA, M.,

VENTO-TORMO, R., TALAVERA-LÓPEZ, C., JONKER, M. R., AFFLECK, K., PALIT, S., STRZELECKA, P. M., FIRTH, H. V., MAHBUBANI, K. T., CVEJIC, A., MEYER, K. B., SAEB-PARSY, K., LUINGE, M., BRANDSMA, C.-A., TIMENS, W., ANGELIDIS, I., STRUNZ, M., KOPPELMAN, G. H., VAN OOSTERHOUT, A. J., SCHILLER, H. B., THEIS, F. J., VAN DEN BERGE, M., NAWIJN, M. C. & TEICHMANN, S. A. 2019. A cellular census of human lungs identifies novel cell states in health and in asthma. *Nature Medicine,* 25**,** 1153-1163.

VIRTANEN, T., KINNUNEN, T. & RYTKÖNEN-NISSINEN, M. 2012. Mammalian lipocalin allergens – insights into their enigmatic allergenicity. *Clinical & Experimental Allergy,* 42**,** 494-504.

WAERN, I., LUNDEQUIST, A., PEJLER, G. & WERNERSSON, S. 2013. Mast cell chymase modulates IL-33 levels and controls allergic sensitization in dust-mite induced airway inflammation. *Mucosal Immunology,* 6**,** 911-920.

WAHLUND, C. J. E., GÜCLÜLER, G., HILTBRUNNER, S., VEERMAN, R. E., NÄSLUND, T. I. & GABRIELSSON, S. 2017. Exosomes from antigen-pulsed dendritic cells induce stronger antigen-specific immune responses than microvesicles in vivo. *Scientific Reports,* 7**,** 17095.

WALDRON, R., MCGOWAN, J., GORDON, N., MCCARTHY, C., MITCHELL, E. B. & FITZPATRICK, D. A. 2019. Proteome and allergenome of the European house dust mite Dermatophagoides pteronyssinus. *PLOS ONE,* 14**,** e0216171.

WALLACE, J., MCELROY, M. C., KLAUSNER, M., CORLEY, R. & AYEHUNIE, S. 2025. Two- and Three-Dimensional Culture Systems: Respiratory In Vitro Tissue Models for Chemical Screening and Risk-Based Decision Making. *Pharmaceuticals,* 18**,** 113.

WAN, H., WINTON, H. L., SOELLER, C., TOVEY, E. R., GRUENERT, D. C., THOMPSON, P. J., STEWART, G. A., TAYLOR, G. W., GARROD, D. R., CANNELL, M. B. & ROBINSON, C. 1999. Der p 1 facilitates transepithelial allergen delivery by disruption of tight junctions. *Journal of Clinical Investigation,* 104**,** 123-133.

WANG, H., SONG, X., WANG, Y., YANG, T., LIU, W., MOU, Y., REN, C. & SONG, X. 2024. Interleukin 1β Mediates the Pathogenesis of Nasal Mucosal Epithelial Barrier Dysfunction in Allergic Rhinitis. *Journal of Inflammation Research,* Volume 17**,** 9071-9085.

WANG, N., YAO, Y., LIU, Y. H., ZENG, M. & LIU, Z. 2025a. Allergic Rhinitis in China: Trends, Challenges and Implications Over the Past Two Decades. *Clin Exp Allergy,* 55**,** 648-658.

WANG, T., CAI, W., WU, Q., CHEN, D., WANG, P. & XU, Z. 2021. Exosomal lncRNA Nuclear Paraspeckle Assembly Transcript 1 (NEAT1)contributes to the progression of allergic rhinitis via modulating microRNA-511/Nuclear Receptor Subfamily 4 Group A Member 2 (NR4A2) axis. *Bioengineered,* 12**,** 8067-8079.

WANG, W., QIAO, S., KONG, X., ZHANG, G. & CAI, Z. 2025b. The role of exosomes in immunopathology and potential therapeutic implications. *Cellular & Molecular Immunology,* 22**,** 975-995.

WANG, Y.-H., ITO, T., WANG, Y.-H., HOMEY, B., WATANABE, N., MARTIN, R., BARNES, C. J., MCINTYRE, B. W., GILLIET, M., KUMAR, R., YAO, Z. & LIU, Y.-J. 2006. Maintenance and Polarization of Human TH2 Central Memory T Cells by

Thymic Stromal Lymphopoietin-Activated Dendritic Cells. *Immunity,* 24**,** 827-838.

WARREN, C. M., JIANG, J. & GUPTA, R. S. 2020. Epidemiology and Burden of Food Allergy. *Current Allergy and Asthma Reports,* 20**,** 6.

WATANABE, N., HANABUCHI, S., SOUMELIS, V., YUAN, W., HO, S., DE WAAL MALEFYT, R. & LIU, Y.-J. 2004. Human thymic stromal lymphopoietin promotes dendritic cell–mediated CD4+ T cell homeostatic expansion. *Nature Immunology,* 5**,** 426-434.

WELSH, J. A., ARKESTEIJN, G. J. A., BREMER, M., CIMORELLI, M., DIGNAT-GEORGE, F., GIEBEL, B., GÖRGENS, A., HENDRIX, A., KUIPER, M., LACROIX, R., LANNIGAN, J., VAN LEEUWEN, T. G., LOZANO-ANDRÉS, E., RAO, S., ROBERT, S., DE ROND, L., TANG, V. A., TERTEL, T., YAN, X., WAUBEN, M. H. M., NOLAN, J. P., JONES, J. C., NIEUWLAND, R. & VAN DER POL, E. 2023. A compendium of single extracellular vesicle flow cytometry. *Journal of Extracellular Vesicles,* 12**,** e12299.

WELSH, J. A., GOBERDHAN, D. C. I., O'DRISCOLL, L., BUZAS, E. I., BLENKIRON, C., BUSSOLATI, B., CAI, H., DI VIZIO, D., DRIEDONKS, T. A. P., ERDBRÜGGER, U., FALCON-PEREZ, J. M., FU, Q. L., HILL, A. F., LENASSI, M., LIM, S. K., MAHONEY, M. G., MOHANTY, S., MÖLLER, A., NIEUWLAND, R., OCHIYA, T., SAHOO, S., TORRECILHAS, A. C., ZHENG, L., ZIJLSTRA, A., ABUELREICH, S., BAGABAS, R., BERGESE, P., BRIDGES, E. M., BRUCALE, M., BURGER, D., CARNEY, R. P., COCUCCI, E., CRESCITELLI, R., HANSER, E., HARRIS, A. L., HAUGHEY, N. J., HENDRIX, A., IVANOV, A. R., JOVANOVIC-TALISMAN, T., KRUH-GARCIA, N. A., KU'ULEI-LYN FAUSTINO, V., KYBURZ, D., LÄSSER, C., LENNON, K. M., LÖTVALL, J., MADDOX, A. L., MARTENS-UZUNOVA, E. S., MIZENKO, R. R., NEWMAN, L. A., RIDOLFI, A., ROHDE, E., ROJALIN, T., ROWLAND, A., SAFTICS, A., SANDAU, U. S., SAUGSTAD, J. A., SHEKARI, F., SWIFT, S., TER-OVANESYAN, D., TOSAR, J. P., USECKAITE, Z., VALLE, F., VARGA, Z., VAN DER POL, E., VAN HERWIJNEN, M. J. C., WAUBEN, M. H. M., WEHMAN, A. M., WILLIAMS, S., ZENDRINI, A., ZIMMERMAN, A. J., THÉRY, C. & WITWER, K. W. 2024. Minimal information for studies of extracellular vesicles (MISEV2023): From basic to advanced approaches. *Journal of Extracellular Vesicles,* 13**,** e12404.

WELSH, J. A., HORAK, P., WILKINSON, J. S., FORD, V. J., JONES, J. C., SMITH, D., HOLLOWAY, J. A. & ENGLYST, N. A. 2020. FCM_{PASS} Software Aids Extracellular Vesicle Light Scatter Standardization. *Cytometry Part A,* 97**,** 569-581.

WENG, C.-M., LEE, M.-J., CHAO, W., LIN, Y.-R., CHOU, C.-J., CHEN, M.-C., CHOU, C.-L., TSAI, I. L., LIN, C.-H., FAN CHUNG, K. & KUO, H.-P. 2023. Airway epithelium IgE-FcεRI cross-link induces epithelial barrier disruption in severe T2-high asthma. *Mucosal Immunology,* 16**,** 685-698.

WENGER, M., GROSSE-KATHOEFER, S., KRAIEM, A., PELAMATTI, E., NUNES, N., POINTNER, L. & AGLAS, L. 2023. When the allergy alarm bells toll: The role of Toll-like receptors in allergic diseases and treatment. *Frontiers in Molecular Biosciences,* 10**,** 1204025.

WHETSTONE, C. E., RANJBAR, M., OMER, H., CUSACK, R. P. & GAUVREAU, G. M. 2022. The Role of Airway Epithelial Cell Alarmins in Asthma. *Cells,* 11**,** 1105.

WIDDICOMBE, J. H. 2019. Early studies on the surface epithelium of mammalian airways. *American Journal of Physiology-Lung Cellular and Molecular Physiology,* 317**,** L486-L495.

WONG, C. K. 2006. House dust mite allergen Der p 1 elevates the release of inflammatory cytokines and expression of adhesion molecules in co-culture of human eosinophils and bronchial epithelial cells. *International Immunology,* 18**,** 1327-1335.

WONG, G. W.-K. 2024. Food allergies around the world. *Frontiers in Nutrition,* 11**,** 1373110.

WOUD, W. W., VAN DER POL, E., MUL, E., HOOGDUIJN, M. J., BAAN, C. C., BOER, K. & MERINO, A. 2022. An imaging flow cytometry-based methodology for the analysis of single extracellular vesicles in unprocessed human plasma. *Communications Biology,* 5**,** 633.

WU, G., YANG, G., ZHANG, R., XU, G., ZHANG, L., WEN, W., LU, J., LIU, J. & YU, Y. 2015. Altered microRNA Expression Profiles of Extracellular Vesicles in Nasal Mucus From Patients With Allergic Rhinitis. *Allergy Asthma Immunol Res,* 7**,** 449-57.

WU, Z., MEHRABI NASAB, E., ARORA, P. & ATHARI, S. S. 2022. Study effect of probiotics and prebiotics on treatment of OVA-LPS-induced of allergic asthma inflammation and pneumonia by regulating the TLR4/NF-kB signaling pathway. *Journal of Translational Medicine,* 20**,** 130.

XU, X., YU, R., YANG, Z., LI, C., XIONG, H. & LI, C. 2025. Toll-like receptor-mediated immune imbalance in asthma: controversies, breakthroughs, and future directions. *Frontiers in Immunology,* 16**,** 1605185.

YAGAMI, A., ORIHARA, K., MORITA, H., FUTAMURA, K., HASHIMOTO, N., MATSUMOTO, K., SAITO, H. & MATSUDA, A. 2010. IL-33 Mediates Inflammatory Responses in Human Lung Tissue Cells. *The Journal of Immunology,* 185**,** 5743-5750.

YAMAMOTO, K., ISHIBASHI, O., SUGIURA, K., UBATANI, M., SAKAGUCHI, M., NAKATSUJI, M., SHIMAMOTO, S., NODA, M., UCHIYAMA, S., FUKUTOMI, Y., NISHIMURA, S. & INUI, T. 2019. Crystal structure of the dog allergen Can f 6 and structure-based implications of its cross-reactivity with the cat allergen Fel d 4. *Scientific Reports,* 9**,** 1503.

YÁÑEZ-MÓ, M., SILJANDER, P. R. M., ANDREU, Z., BEDINA ZAVEC, A., BORRÀS, F. E., BUZAS, E. I., BUZAS, K., CASAL, E., CAPPELLO, F., CARVALHO, J., COLÁS, E., CORDEIRO-DA SILVA, A., FAIS, S., FALCON-PEREZ, J. M., GHOBRIAL, I. M., GIEBEL, B., GIMONA, M., GRANER, M., GURSEL, I., GURSEL, M., HEEGAARD, N. H. H., HENDRIX, A., KIERULF, P., KOKUBUN, K., KOSANOVIC, M., KRALJ-IGLIC, V., KRÄMER-ALBERS, E. M., LAITINEN, S., LÄSSER, C., LENER, T., LIGETI, E., LINĒ, A., LIPPS, G., LLORENTE, A., LÖTVALL, J., MANČEK-KEBER, M., MARCILLA, A., MITTELBRUNN, M., NAZARENKO, I., NOLTE-'T HOEN, E. N. M., NYMAN, T. A., O'DRISCOLL, L., OLIVAN, M., OLIVEIRA, C., PÁLLINGER, É., DEL PORTILLO, H. A., REVENTÓS, J., RIGAU, M., ROHDE, E., SAMMAR, M., SÁNCHEZ-MADRID, F., SANTARÉM, N., SCHALLMOSER, K., STAMPE OSTENFELD, M., STOORVOGEL, W., STUKELJ, R., VAN DER GREIN, S. G., HELENA VASCONCELOS, M., WAUBEN, M. H. M. & DE WEVER, O. 2015. Biological properties of extracellular vesicles and their physiological functions. *Journal of Extracellular Vesicles,* 4**,** 27066.

YU, D., LIU, J. Q., MO, L. H., LUO, X. Q., LIU, Z. Q., WU, G. H., YANG, L. T., LIU, D. B., WANG, S., LIU, Z. G. & YANG, P. C. 2020. Specific antigen-guiding exosomes inhibit food allergies by inducing regulatory T cells. *Immunology & Cell Biology,* 98**,** 639-649.

YU, Y., ZHOU, Y., DI, C., ZHAO, C., CHEN, J., SU, W., WU, Q., WU, M., SU, X. & XIA, Z. 2021. Increased airway epithelial cell-derived exosomes activate macrophage-mediated allergic inflammation via CD100 shedding. *Journal of Cellular and Molecular Medicine,* 25(18)**,** 8850-8862.

ZENG, F., PANG, G., HU, L., SUN, Y., PENG, W., CHEN, Y., XU, D., XIA, Q., ZHAO, L., LI, Y. & HE, M. 2024. Subway Fine Particles ($PM_{2.5}$)-Induced Pro-Inflammatory Response Triggers Airway Epithelial Barrier Damage Through the TLRs NFκB Dependent Pathway In Vitro. *Environmental Toxicology,* 39**,** 5296-5308.

ZENG, H. T., LIU, J. Q., ZHAO, M., YU, D., YANG, G., MO, L. H., LIU, Z. Q., WANG, S., LIU, Z. G. & YANG, P. C. 2020. Exosomes carry IL-10 and antigen/MHC II complexes to induce antigen-specific oral tolerance. *Cytokine,* 133**,** 9.

ZERBINO, D. R., ACHUTHAN, P., AKANNI, W., BARRELL, D., BHAI, J., BILLIS, K., CUMMINS, C., GALL, A., GIRÓN, C. G., GIL, L., GORDON, L., HAGGERTY, L., HASKELL, E., HOURLIER, T., IZUOGU, O. G., JANACEK, S. H., JUETTEMANN, T., TO, J. K., LAIRD, M. R., LAVIDAS, I., LIU, Z., LOVELAND, J. E., MAUREL, T., MCLAREN, W., MOORE, B., MUDGE, J., MURPHY, D. N., NEWMAN, V., NUHN, M., OGEH, D., ONG, C. K., PARKER, A., PATRICIO, M., RIAT, H. S., SCHUILENBURG, H., SHEPPARD, D., SPARROW, H., TAYLOR, K., THORMANN, A., VULLO, A., WALTS, B., ZADISSA, A., FRANKISH, A., HUNT, S. E., KOSTADIMA, M., LANGRIDGE, N., MARTIN, F. J., MUFFATO, M., PERRY, E., RUFFIER, M., STAINES, D. M., TREVANION, S. J., AKEN, B. L., CUNNINGHAM, F., YATES, A. & FLICEK, P. 2018. Ensembl 2018. *Nucleic Acids Research,* 46**,** D754-D761.

ZHANG, J., WANG, Z., ZHANG, D., PAN, Y., LIU, X., QIAO, X., CUI, W. & DONG, L. 2021a. Integrative Analysis Reveals a miRNA-mRNA Regulatory Network and Potential Causative Agents in the Asthmatic Airway Epithelium. *Journal of Asthma and Allergy,* Volume 14**,** 1307-1321.

ZHANG, M., YU, Q. Y., TANG, W., WU, Y. J., LV, J. J., SUN, L., SHI, G. C., WU, M., QU, J. M., DI, C. X. & XIA, Z. W. 2021b. Epithelial exosomal contactin-1 promotes monocyte-derived dendritic cell-dominant T-cell responses in asthma. *Journal of Allergy and Clinical Immunology,* 148**,** 1545-1558.

ZHANG, R., DONG, H., ZHAO, H., ZHOU, L., ZOU, F. & CAI, S. 2017. 1,25-Dihydroxyvitamin D3 targeting VEGF pathway alleviates house dust mite (HDM)-induced airway epithelial barrier dysfunction. *Cellular Immunology,* 312**,** 15-24.

ZHAO, F. & KLIMECKI, W. T. 2015. Culture conditions profoundly impact phenotype in BEAS-2B, a human pulmonary epithelial model. *Journal of Applied Toxicology,* 35**,** 945-951.

ZHAO, R., GUO, Z., ZHANG, R., DENG, C., XU, J., DONG, W., HONG, Z., YU, H., SITU, H., LIU, C. & ZHUANG, G. 2018. Nasal epithelial barrier disruption by particulate matter ≤2.5 μm via tight junction protein degradation. *Journal of Applied Toxicology,* 38**,** 678-687.

ZHAO, X. O., SOMMERHOFF, C. P., PAIVANDY, A. & PEJLER, G. 2022. Mast cell chymase regulates extracellular matrix remodeling-related events in primary human small airway epithelial cells. *Journal of Allergy and Clinical Immunology,* 150**,** 1534-1544.

ZHENG, H., ZHANG, Y., PAN, J., LIU, N., QIN, Y., QIU, L., LIU, M. & WANG, T. 2021. The Role of Type 2 Innate Lymphoid Cells in Allergic Diseases. *Frontiers in Immunology,* 12**,** 586078.

ZHOU, J., LU, Y., WU, W. & FENG, Y. 2021. HMSC-Derived Exosome Inhibited Th2 Cell Differentiation via Regulating miR-146a-5p/SERPINB2 Pathway. *Journal of Immunology Research,* 2021**,** 1-11.

ZHOU, X., LIU, S., LU, Y., WAN, M., CHENG, J. & LIU, J. 2023. MitoEVs: A new player in multiple disease pathology and treatment. *Journal of Extracellular Vesicles,* 12.

ZHOU, X., ZHANG, W., YAO, Q., ZHANG, H., DONG, G., ZHANG, M., LIU, Y., CHEN, J.-K. & DONG, Z. 2017. Exosome production and its regulation of EGFR during wound healing in renal tubular cells. *American Journal of Physiology-Renal Physiology,* 312**,** F963-F970.

ZHU, X., WANG, X., WANG, Y. & ZHAO, Y. 2020. Exosomal long non-coding RNA GAS5 suppresses Th1 differentiation and promotes Th2 differentiation via downregulating EZH2 and T-bet in allergic rhinitis. *Mol Immunol,* 118**,** 30-39.

ZIEGLER, S. F. 2012. Thymic stromal lymphopoietin and allergic disease. *Journal of Allergy and Clinical Immunology,* 130**,** 845-852.